DURBAN UNIVERSITY OF TECHNOLOGY
INYUVESI YASETHEKWINI YEZOBUCHWEPHESHE

Biochemical characterization of selected carbohydrases from *Beauveria bassiana* and their potential applications

Ayodeji Emmanuel Amobonye
21750827

Submitted in fulfilment of the requirements for the degree of Doctor of Philosophy (PhD): Biotechnology in the Department of Biotechnology and Food Science, Faculty of Applied Sciences, Durban University of Technology, Durban, South Africa

Supervisor: Prof. S.K. Pillai
Co-supervisor: Prof. S. Singh

July 2021

DECLARATION

I, Ayodeji Emmanuel Amobonye, hereby declare that this thesis entitled "Biochemical characterization of selected carbohydrases from *Beauveria bassiana* and their potential applications", handed in for Doctor of Philosophy (PhD): Biotechnology in the Department of Biotechnology and Food Science, Faculty of Applied Sciences, Durban University of Technology, Durban, South Africa, has not been submitted in any form to any other academic institution. This study presents original work by the author and all sources used or quoted have been duly acknowledged in the text. The research described in this thesis was carried out in the Biotechnology and Food Science Department, Faculty of Applied Sciences, Durban University of Technology, South Africa, under the supervision of Prof. S.K. Pillai and Prof. S. Singh.

As the candidate's supervisors we agree to the submission of this thesis

DEDICATION

To Jehovah, for his mercies.

To my parents, Mr Olatunji & Mrs Ololade Amobonye

To my wife and dream-maker, Olufunke Amobonye

To my kids, Ms Ololade Amobonye (Jnr) & Ms Omotola Amobonye

To my cousin, Mr Olasunkanmi Ogunyemi.

ACKNOWLEDGEMENT

Firstly, I am deeply grateful for the support given to me by my supervisor, Prof. S.K. Pillai, right from the time he accepted to be my supervisor until the end of my Ph.D. study. His tutelage, his patience and his faith in me have seen me through this study. I would also like to appreciate my co-supervisor, Prof S. Singh, without his assistance and dedicated involvement, this thesis would not be possible. My sincere gratitude to my senior colleague turned brother, Dr P.K. Bhagwat, for his immense scientific contribution and ever available motivation, I am forever indebted to you. May I also use this opportunity to acknowledge the National Research Foundation (NRF) of South Africa as well as the Durban University of Technology for funding my study and ensuring my subsistence right from the beginning to the end. I also profusely grateful to Prof. F. O. Shode, Prof. S. Kumari, Mrs S. Juglal and Mrs S. Beekrum, who have all contributed in one way or the other to ensure the success of my program.

I also acknowledge with a deep sense of gratitude the contribution of all the faculty members and administrative staff members of the Biotechnology and Food Science Department as well as the staff of the Institute for Water and Wastewater Technology (IWWT), both of the Durban University of Technology. Specifically, I acknowledge the contribution of the lab technicians, the lab assistants, the cleaners, Postdoctoral fellows as well as my fellow students in the department, whose contribution I cannot overestimate. A million “thank yous” to my lovely parents Mr Olatunji and Mrs Ololade Amobonye, my wife, best friend, and soulmate, Olufunke Amobonye, and my daughters, Ololade and Omotola as well as my sisters, Oluwakemi and Dolapo, you are everything to me. Lastly, I cannot forget my friends and colleagues at NAFDAC, particularly my “bro” Adetunji Gbolagade, who has always been there for me and my “sis” Mrs Olufunke Ojo. This degree would not have been completed without you all. God bless you all.

TABLE OF CONTENT

LIST OF FIGURES

LIST OF TABLES

LIST OF ABBREVIATIONS

3D: Three dimensional

ANOVA: Analysis of variance

BEA: Beauvericin

BC: Banana corm extract

BSA: Bovine serum albumin

bp: Base pair

BLAST: Basic local alignment search tool

BME: β-mercaptoethanol

BP: Biological Process

CASTp: Computed Atlas of Surface Topography of proteins3D3D

CAZymes: Carbohydrate active enzymes

cDNA: Complementary Deoxyribonucleic acid

CC: Cellular Component

CCD: Central Composite Design

CMC: Carboxymethyl cellulose

DEGs: Differentially expressed genes

DNA: Deoxyribonucleic acid

DNS: 3, 5-dinitrosalicylic acid

DPPH: 2,2-diphenyl-1-picrylhydrazyl

DTT: dithiothreitol

EDTA: Ethylenediamine tetra-acetic acid

FASTA: Fast Adaptive Shrinkage Threshold Algorithm

FDRs: False discovery rates

FRAP: Ferric reducing ability of plasma

FTIR: Fourier transformed infrared

Gb: Gigabyte

GRAVY: Grand average of hydropathicity

GO Gene ontology

INT: Iodonitrotetrazolium violet

ITS: Internal transcribed spacer

k_{cat}: Enzyme turnover number

$K_{m:}$ Michaelis constant

ODA: Oatmeal dodine agar

MPD: Mannitol-1-phosphate dehydrogenase

mRNA: Messenger Ribonucleic acid

MF: Molecular Function

NCBI: National Centre for Biotechnology Information

NICD: National Institute for Communicable Diseases

PBD: Plackett-Burman design

PCA: Principal Component Analysis

PCR: Polymerase chain reaction

PDA: Potato dextrose agar

PDB: Potato dextrose broth

PDB: Protein Data Bank

PMSF: Phenylmethylsulphonyl fluoride

rDNA: Ribosomal DNA

RNA: Ribonucleic acid

RNA-Seq: Ribonucleic acid sequencing

SB: Sugarcane bagasse

SD: Standard deviation

SDS: Sodium dodecyl sulphate

SDS-PAGE: Sodium dodecyl (lauryl) -polyacrylamide gel electrophoresis.

SEM: Scanning Electron Microscopy

SOD: Superoxide dismutases

SOPMA: Self-Optimized Prediction Method with Alignment

TFC total flavonoid content

TMHMM: Transmembrane helices; Hidden Markov Model

WB: Wheat bran

PUBLICATIONS AND CONFERENCES

Publications

1. Amobonye, A., Bhagwat, P., Pandey, A., Singh, S., Pillai, S. 2020. Biotechnological potential of *Beauveria bassiana* as a source of novel biocatalysts and metabolites. *Critical Reviews in Biotechnology* 40:1019-1034.
2. Amobonye, A., Bhagwat, P., Singh, S. and Pillai, S. 2021. Enhanced xylanase and endoglucanase production from *Beauveria bassiana* SAN01, an entomopathogenic fungal endophyte. *Fungal Biology* 125: 39-48.
3. *Bhagwat, P., *Amobonye, A., Singh, S. and Pillai, S. 2021. A comparative analysis of GH18 chitinases and their isoforms from *Beauveria bassiana*: An *in-silico* approach. *Process Biochemistry* 100: 207-216.
   *Bhagwat, P. and Amobonye, A contributed equally to this work as first authors.

Publications under preparation

1. Amobonye, A., Bhagwat, P., Singh, S., Pillai, S. 2021. Effective pear juice clarification by *Beauveria bassiana* SAN01 amylase-polygalacturonase cocktail.
2. Amobonye, A., Bhagwat, P., Singh, S., Pillai, S. 2021. Optimized production of *Beauveria bassiana* SAN01 amylase-polygalacturonase using response surface methodology.
3. Amobonye, A., Bhagwat, P., Arshad, I., Kwenda, S., Singh, S., Pillai, S. 2021. Comparative transcriptome of *Beauveria bassiana* SAN01 under endophytic and fermentation conditions.

Conference

Amobonye, A., Bhagwat, P., Singh, S., Pillai, S. 2020. *Beauveria bassiana* xylanase: a biomass degrading enzyme from an entomopathogen. Federation of European Microbiological Societies Online Conference on Microbiology 2020, 28 -31 October 2020.

ABSTRACT

Different filamentous fungi have continued to attract scientific interests as novel sources of enzymes and other important bioproducts. *Beauveria bassiana*, a well-known entomopathogenic fungi has long been valued for its biotechnological application as a biocontrol agent in its entomopathogenic state and as a plant-growth promoter in its endophytic state. The fungus has also been proven to be safe for human health, as studies have shown *B. bassiana* strains to be non-pathogenic to humans, other animals and plants. Furthermore, its ability to utilize various agro-residues for its growth and the concomitant production of important bioproducts have been well demonstrated. However, despite all of these, there has been no appreciable attempt at exploring this remarkable fungus for the production of industrially important enzymes, especially in its saprophytic state. Recently, a filamentous fungus was isolated in its endophytic state from onion leaves, in our laboratory. It was confirmed by rDNA ITS sequencing to be a *B. bassiana* strain and was subsequently designated as *B. bassiana* SAN01. Preliminary experiments revealed the remarkable ability of this novel strain to utilize lignocellulosic biomass for its metabolism while secreting various biomass-degrading enzymes in the process. Hence, carbohydrases from *B. bassiana* SAN01 were considered worthy of investigation because of the established safety of the source organism, as well as the probable low production cost of the enzymes using readily available plant biomass. Besides, it was also observed that there has been no significant investigation into the biochemical properties of lignocellulolytic enzymes from *B. bassiana*, which has probably hindered their industrial applicability.

Hence, this Ph.D. research was focused on investigating the production, the biochemical properties, as well as the potential applicability of selected biomass-degrading enzymes, *viz*., amylase, cellulase (endoglucanase), pectinase (polygalacturonase) and xylanase from *B. bassiana* SAN01. To achieve these, the phylogenetic relationship of the fungal strain was established, and its carbon utilization profile was annotated using phenotypic microarray technology. Furthermore, to understand the dynamics surrounding its lignocellulosic biomass utilization and its carbohydrase-production capabilities, comparative transcriptomics analysis was carried out *B. bassiana* SAN01 under three different simulated conditions i.e., endophytic, fermentation and lab control conditions. In addition, to fully explore the carbohydrase production potential of the fungus, the production of the selected carbohydrases was optimized using response surface

methodology; subsequently, all the selected enzymes were purified to enhance the evaluation of their biochemical properties as well as their potential industrial applications.

The proclivity of *B. bassiana* SAN01 for polyols, pentoses, N-acetyl-D-glucosamine and some other carbon sources was demonstrated by the phenotype microarray profiling. While the comparative genome-wide transcriptome analyses revealed a clear distinction between the fungus under the different trophic conditions investigated. It was observed that 4-5% of the 10,365 *B. bassiana* SAN01 genes were differentially expressed between these conditions, and a significant proportion of the genes were found to be involved in lignocellulose deconstruction. The annotation of CAZymes from the *B. bassiana* SAN01 transcriptome under fermentation (saprophytic) conditions confirmed the upregulation of biomass-degrading enzymes such as amylases, cellulases, chitinases, glucanases, laccases, lignases, pectinases and xylanases. The subsequent optimization of the production parameters of *B. bassiana* SAN01 amylase, endoglucanase, polygalacturonase and xylanase led to heightened yields of 34.82 UmL^{-1}, 23.03 UmL^{-1}, 51.05 UmL^{-1}, and 1061 $UmL^{-1,}$ respectively. These were estimated to be 1.79-, 1.35-, 1.87- and 3.44- folds higher than unoptimized production levels and are also the highest ever production levels recorded for these enzymes from any *B. bassiana* strain.

Further in the study, the xylanase from *B. bassiana* SAN01 was purified to homogeneity while the other three enzymes were partially purified. The purified xylanase was demonstrated to have a molecular mass of ~37 kDa and performed optimally at pH 6.0 and 45ºC. However, the optimum pH of the partially purified amylase, endoglucanase, and polygalacturonase were found to be pHs 6.0, 6.0 and 7.0, while the optimum temperatures were observed to be 35ºC, 35ºC and 45ºC, respectively. Consequently, the purified *B. bassiana* SAN01 xylanase was demonstrated to be effective in deinking wastepaper with an optimized deinking rate of 106.72% relative to the control. In addition, the partially purified amylase-polygalacturonase from *B. bassiana* SAN01 was demonstrated to adequately clarify pear juice with a 1.37-fold improvement in clarity recorded under optimal conditions. Furthermore, results also showed that the enzymatic-assisted juice clarification was without any detrimental effect on some quality parameters of the juice. In the same vein, crude endoglucanase-xylanase from the fungus was shown to significantly hydrolyze sugarcane bagasse, releasing ~20% reducing sugars under optimal conditions.

Finally, to gain insights into the structure-function relationship of *B. bassiana* carbohydrases, the structural properties of *B. bassiana* chitinases and xylanases were elucidated for the first time using computational techniques. The *in silico* prediction revealed that the enzymes were generally hydrophilic, thermostable, negatively charged and extracellularly secreted. The modelled tertiary structures of *B. bassiana* chitinase and xylanase were validated by the presence of ~ 90% of their amino acid residues in the Ramachandran plot's favoured region. The findings from this study have thus created a strong framework for the prospective utilization of *B. bassiana* and its carbohydrases in alternative biotechnological processes.

CHAPTER ONE

Introduction and Literature Review

Part of this chapter has already been published: Amobonye, A., Bhagwat, P., Pandey, A., Singh, S., Pillai, S. 2020. Biotechnological potential of *Beauveria bassiana* as a source of novel biocatalysts and metabolites. *Critical Reviews in Biotechnology* 40:1019-1034.

CRITICAL REVIEWS IN BIOTECHNOLOGY
https://doi.org/10.1080/07388551.2020.1805403

Taylor & Francis
Taylor & Francis Group

REVIEW ARTICLE

Check for updates

Biotechnological potential of *Beauveria bassiana* as a source of novel biocatalysts and metabolites

Ayodeji Amobonye[a], Prashant Bhagwat[a], Ashok Pandey[b], Suren Singh[a] and Santhosh Pillai[a]

[a]Department of Biotechnology and Food Technology, Faculty of Applied Sciences, Durban University of Technology, Durban, South Africa; [b]Centre for Innovation and Translational Research, CSIR-Indian Institute of Toxicology Research, Lucknow, India

ABSTRACT

Beauveria bassiana though widely perceived as an entomopathogenic fungus has also been found in nature to be endophytic. As entomopathogens, the life cycle of different *B. bassiana* strains are organized and adapted as pathogens to their invertebrate hosts while as endophytes they maintain a symbiotic relationship with their plant hosts. To fulfill these aforementioned ecological roles, this fungus secretes an array of enzymes as well as secondary metabolites, which all have significant biological roles. Basically, chitinases, lipases and proteases are considered to be the most important of all the enzymes produced by *B. bassiana*. However, studies have also shown their ability to produce other vital enzymes which include amylase, asparaginase, cellulase, galactosidase etc. Previous reports on this filamentous fungus have laid more emphasis on its entomopathogenicity, its endophytism and its highly acclaimed application in the biological control of pests. This review, however, is the first to fully assess the enzyme-secreting potential of this entomopathogenic fungus and its use as a novel source of several industrial biocatalysts and other important biochemicals. This article highlights the inherent properties of the fungus to degrade various biopolymers as well as its relative safety for human use. Some of the important factors have raised the possibilities of exploitation for industrial production and as safe hosts for gene expression.

ARTICLE HISTORY
Received 23 December 2019
Revised 16 May 2020
Accepted 19 July 2020

KEYWORDS
Beauveria bassiana; entomopathogen; endophyte; enzyme; industrial potential; metabolite

Introduction

The ongoing search for novel enzymes suitable for diverse industrial applications has continually sustained interest in the enzyme profiles of fungal strains from diverse habitats hitherto unexplored. Entomopathogenic fungi are well-established biocontrol agents that are gradually replacing synthetic chemicals in pest control [1]. These fungi have the ability to infect hundreds of insects, other arthropods, as well as nematodes. The fungal penetration of the hosts' cuticle is typically initiated by the development of fungal germlings into appressorium on the host cuticular surface and finally ends in the development of blastopores in the hosts' hemocoel [2]. This physiological evolution during pathogenicity indicates that fungal germlings are constantly engaging in chemical conversations with their environment and are also continuously adapting in order to colonize their hosts' tissue as well as to counteract their hosts' defence systems [3]. In this regard, the pathogenicity of this group of fungi depends majorly on the ability of their enzymatic machinery to degrade insects' integument and also on the secretion of bioactive volatile organic compounds and antibiotics [4].

The natural ability of entomopathogenic fungi to produce a wide variety of enzymes is now being exploited in the industry to meet the ever-increasing demand for novel biocatalysts [5]. The rising adoption of entomopathogenic fungal enzymes in industry has also been ascribed to their appealing characteristics which includes high specificity of action, their natural origin, stability and generally safe nature [2,5,6]. As a result, many studies have been dedicated to the potential of various entomopathogenic fungi for the production of important enzymes and other important metabolites; these include: *Metarhizium anisopliae* [7], *Lecanicillium lecanii* [8], *Beauveria bassiana* [9], etc.

Another group of fungi with potential for enzyme mining are the endophytic fungi, which live asymptotically inside plant tissues. Interestingly, it has been shown in nature that some endophytic fungi also belong to the genera that encompass entomopathogenic fungi [10]. Very few fungi have been reported to possess this

CONTACT Santhosh Pillai santhoshk@dut.ac.za Department of Biotechnology and Food Technology, Faculty of Applied Sciences, Durban University of Technology, P O Box 1334, Durban, 4000, South Africa

Abstract

Beauveria bassiana though widely perceived as an entomopathogenic fungus has also been found in nature to be endophytic and facultatively saprophytic. As entomopathogens, the life cycle of different *B. bassiana* strains are organized and adapted as pathogens to their invertebrate hosts, while as endophytes, they maintain a symbiotic relationship with their plant hosts. To fulfil these aforementioned ecological roles, the fungus secretes an array of enzymes as well as secondary metabolites, which all have significant biological roles. Chitinases, lipases and proteases are considered the most important of all the enzymes produced by *B. bassiana,* however, studies have also shown their ability to produce other vital enzymes which include amylase, asparaginase, cellulase, galactosidase, glutaminase, etc. Previous reports on this filamentous fungus have laid more emphasis on its entomopathogenicity, its endophytism and its highly acclaimed application in the biological control of pests. In light of this, this chapter reviews current literature with a special focus on the enzyme-secreting potential of this entomopathogenic fungus and its use as a novel source of several industrial biocatalysts and other important biochemicals. It also discusses the inherent properties of the fungus to degrade various biopolymers as well as its relative safety for human use, being some of the critical factors that have raised the possibilities for their exploitation for industrial production and as safe hosts for gene expression.

1.1 Introduction

The perpetual search for novel enzymes suitable for diverse industrial applications has continually sustained interests in the enzyme profiles of fungal strains from diverse habitats hitherto unexplored. Entomopathogenic fungi are well-established biocontrol agents that are gradually replacing synthetic chemicals in pest control (Bara and Laing 2020). These fungi have the ability to infect hundreds of insects, other arthropods, as well as nematodes. The fungal penetration of the hosts' cuticle is typically initiated by the development of fungal germlings into appressorium on the host cuticular surface and finally ends in the development of blastopores in the hosts' haemocoel (Litwin, Nowak and Różalska 2020). This physiological evolution during pathogenicity indicates that fungal germlings are constantly engaging in chemical conversations with their environments and are also continuously adapting in order to colonize their hosts' tissue as well as counteract their hosts' defense systems (Keyhani 2018). In this regard, the pathogenicity of this group of fungi depends majorly on the ability of their enzymatic machinery to degrade insects' integument and also on the secretion of bioactive volatile organic compounds and antibiotics (Dhawan and Joshi 2017; Łopusiewicz *et al.,* 2020).

The natural ability of entomopathogenic fungi to produce a wide variety of enzymes is now being exploited in the industry to meet the ever-increasing demand for novel biocatalysts (Mondal *et al.,* 2016; Łopusiewicz *et al.,* 2020). The rising adoption of entomopathogenic fungal enzymes in the industry has also been ascribed to their appealing characteristics, including high specificity of action, their natural origin, stability, and generally safe nature (Mondal *et al.,* 2016; Shin, Bae and Woo 2016; Litwin, Nowak and Różalska 2020). As a result, many studies have been dedicated to the potentials of various entomopathogenic fungi for the production of important enzymes and other important metabolites; these include *Beauveria bassiana* (Liu *et al.,* 2020a), *Lecanicillium lecanii* (Rojas-Osnaya *et al.,* 2020), *Metarhizium anisopliae* (dos Reis *et al.,* 2018), etc. Another group of fungi with potential for enzyme mining is the endophytic fungi, which live asymptotically inside plant tissues. Interestingly, it has been shown in nature that some endophytic fungi also belong to the genera that encompass entomopathogenic fungi (Jaber and Ownley 2018; Mantzoukas and Eliopoulos 2020). Very few fungi have been reported to possess this dual biological role which has been shown by fungi such as *Lecanicillium* spp.*, Metarhizium robertsii* and our fungus of interest, *B. bassiana*. Similar to entomopathogens, endophytes employ a wide array of

enzymes in the process of colonizing their different plant hosts. Some of these enzymes are responsible for their attachment to hosts, while others are responsible for their ability to tap and utilize their hosts' nutrients, amongst other functions. *Cladosporium cladosporioides* (Vázquez-Montoya et al., 2020)*, Penicillium spp.* and *Aspergillus spp.* (Adhikari and Pandey 2019) are examples of endophytes that have been recently investigated as probable sources of industrial enzymes.

Beauveria bassiana is a filamentous fungus (Hypocreales) that can be considered both as an entomopathogen and an endophyte, hence the nomenclature entomopathogenic fungal endophyte and/or endophytic fungal entomopathogen. It is more popularly known for its use as a biopesticide for the biological control of insect pests (Bara and Laing 2020) and as an asymptomatic associate of plants (Nishi *et al.,* 2020). In fulfilling its dual biological role, *B. bassiana* secretes a wide variety of extracellular enzymes, which include chitinases, protease, lipases, amylases, laccases etc. Its inherent ability to secrete enzymes in copious quantities, its relative safety to human health, together with its well-characterized genome have made this fungus a potential mining site for industrial enzymes and other important biomolecules. Previous studies have focused primarily on *B. bassiana*'s enzymes as significant factors in their pathogenicity to arthropods (de Carolina Sánchez-Pérez *et al.,* 2014; Lovera *et al.,* 2020), in their endophytic colonization (Ownley *et al.,* 2008) and in their popular use as biocontrol agents (Mascarin and Jaronski 2016; Alves *et al.,* 2020).

B. bassiana has been observed to utilize different agricultural residues for its growth, especially during the cultivation for its much sought-after blastospores, which is being produced in commercial quantities (Jaronski and Mascarin 2017; Reddy and Bhardwaj 2020). However, though it is a well-studied fungus, there are relatively a few reports on biomass-degrading enzymes and carbohydrases from *B. bassiana*. Although the decomposition role in the ecosystem is mainly reserved for saprophytic fungi which warrants them to produce high levels of extracellular enzymes to digest the biomass (Liao *et al.,* 2018, Hage and Rosso 2021), some endophytic fungi have also been shown to participate in this role (Cline *et al.,* 2018; Gray and Kernaghan 2020). Interestingly, some studies have also demonstrated that *B. bassiana* could exist as a facultative saprophyte as well (Magara *et al.,* 2004; Wang *et al.,* 2018a; Punia *et al.,* 2019; Khonsanit *et al.,* 2020). However, the metabolic changes that prompt endophytic fungi to degrade plant biomass and secrete high levels of hydrolytic enzymes have not been well studied.

Therefore, this research intends to investigate the metabolic and physiological changes in *B. bassiana* during its transition from its prominent role as an endophytic fungus to a biomass-degrading fungus. The study will also focus on characterizing selected carbohydrate-active enzymes secreted by the fungus while degrading plant biomass for possible industrial applications.

1.2 *B. bassiana*, an entomopathogenic fungal endophyte

B. bassiana was named after Agostino Bassi, an Italian entomologist who discovered that the fungus was the causal agent of pebrine disease that turned thousands of Italy's silkworms into white mummies. Shortly after the discovery in 1835, the entomopathogenic fungus was used extensively to manage chinch bugs in the US Midwest (Lord 2005). *B. bassiana* has since been noted to be one of the most important and well-characterized entomopathogenic fungi, as it is highly regarded for its role in controlling various pests in agriculture. It is widely used as a biological control agent against a variety of insect pests, including agricultural and stored food products. Entomopathogens are microbes that are pathogenic to insects, but this definition has now been extended to include microbes that can attack spiders, mites, and ticks as well (Yang *et al.,* 2020). These group of organisms have been shown to include naturally occurring bacteria, fungi, nematodes, and viruses found in diverse ecosystems (Lacey 2017; da Silva *et al.,* 2020). *B. bassiana* has been observed to affect more than 200 different species of insect pests, primarily through contact with its conidia, which is now highly sought after as a biopesticide. Recent findings have also established the ability of the fungus to affect a wide variety of insects (Dhar *et al.,* 2019; Ramakuwela *et al.,* 2020) and other arthropods (Alagesan *et al.,* 2019; Canassa *et al.,* 2020), mostly plant pests. In addition, *B. bassiana* has also been shown to be capable of infecting other pests, such as nematodes (Niveditha *et al.,* 2019; Silva *et al.,* 2020).

The initial entomopathogenic process is divided into four steps which include the adsorption of *B. bassiana* cells to the cuticular surface, as well as the adhesion and consolidation of the interface between pre-germinant propagules and the insects' epicuticle. The germination/development occurs at the insect cuticular surface until the emergence of the appressorium, the penetration peg, which exerts physical pressure on the host body covering (Cytryńska, Wojda and Jakubowicz 2016). The high turgor of the appressorium provided by high glycerol content allows the fungus to force its way into the insect's body (Vertyporokh, Hułas-Stasiak and Wojda 2020). Furthermore, the

intrusion is also facilitated by the fungal extracellular enzymes, including chitinases, lipases, and proteases. These enzymes also degrade the various organic polymers in the host's tissues, using the degradation products as energy and nutrient sources (Mondal *et al.,* 2016; Sharma *et al.,* 2020). On entering the haemolymph, the fungus grows as blastospores, which are single yeast-like cells with a fragile cell wall. The shift to blastospores is believed to allow a reduction in the number of hosts' pathogen-associated molecular patterns (PAMPs), which has been noted to be important in minimizing the hosts' recognition and defence response mechanisms (Vertyporokh, Hułas-Stasiak and Wojda 2020). These blastospores proliferate hosts' organs by disseminating across the insect body through haemolymph circulation, which eventually results in mortality. After host mortality, the fungus shifts to facultative feeding as it initiates hyphal development outwards the integument, building a massive number of spores in this process. The conidiospores produced are utilized to establish new infestations. The typical infection cycle of *B. bassiana* on its insect hosts is depicted in Figure 1.1 while the physical manifestation of the infection is shown in Figure 1.2. Besides blastospores, *B. bassiana* also produces submerged conidia and aerospores. While blastospores and submerged conidia are produced in rich and poor liquid medium respectively, aerospores are produced in solid medium. Although these three types of cells differ in their physical properties, all of them are infectious (Holder and Keyhani 2005; Holder *et al.,* 2007). The pathogenicity of *B. bassiana* has also been shown to be attenuated by its secretion of mycotoxins including beauvericin, cyclodepsipeptide, destruxin and desmethyldestruxin, at the beginning of the infestations. These compounds have been implicated in host immune suppression, with subsequent destruction of the host's internal tissues as well as nutrient depletion, all leading to host death (Gibson *et al.,* 2014; Al Khoury *et al.,* 2019).

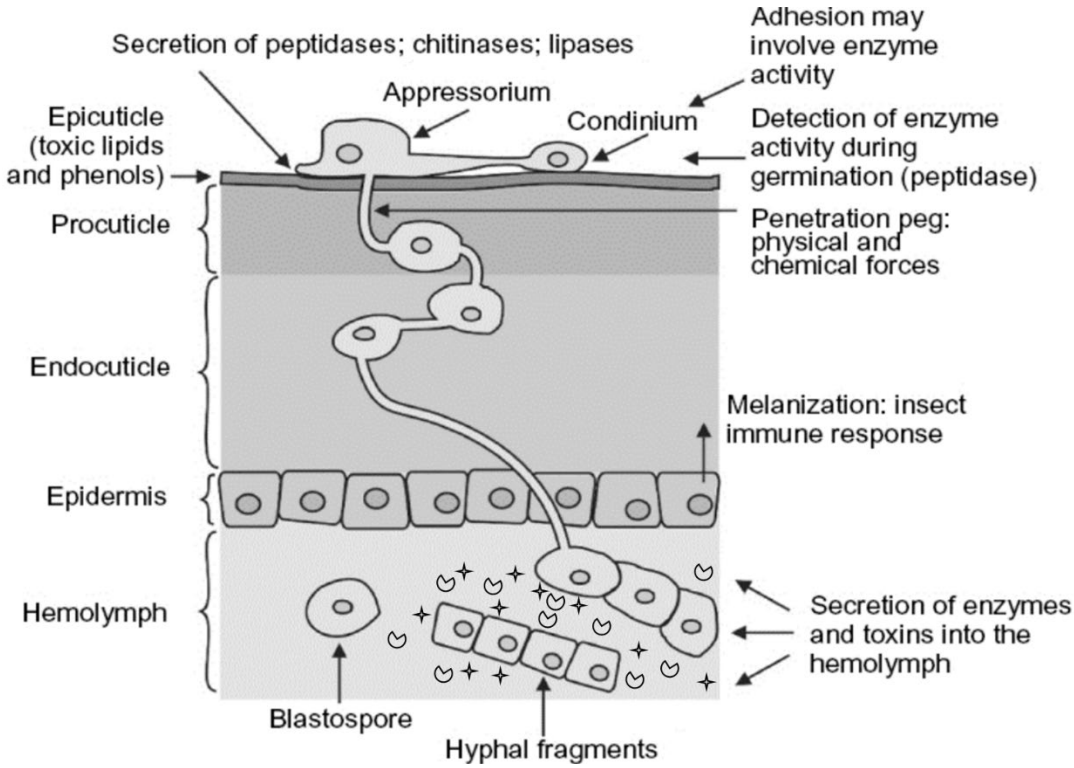

Figure 1.1: Overview of the infection cycle of *B. bassiana* during insect attack (Adapted from Singh, Raina and Singh 2017)

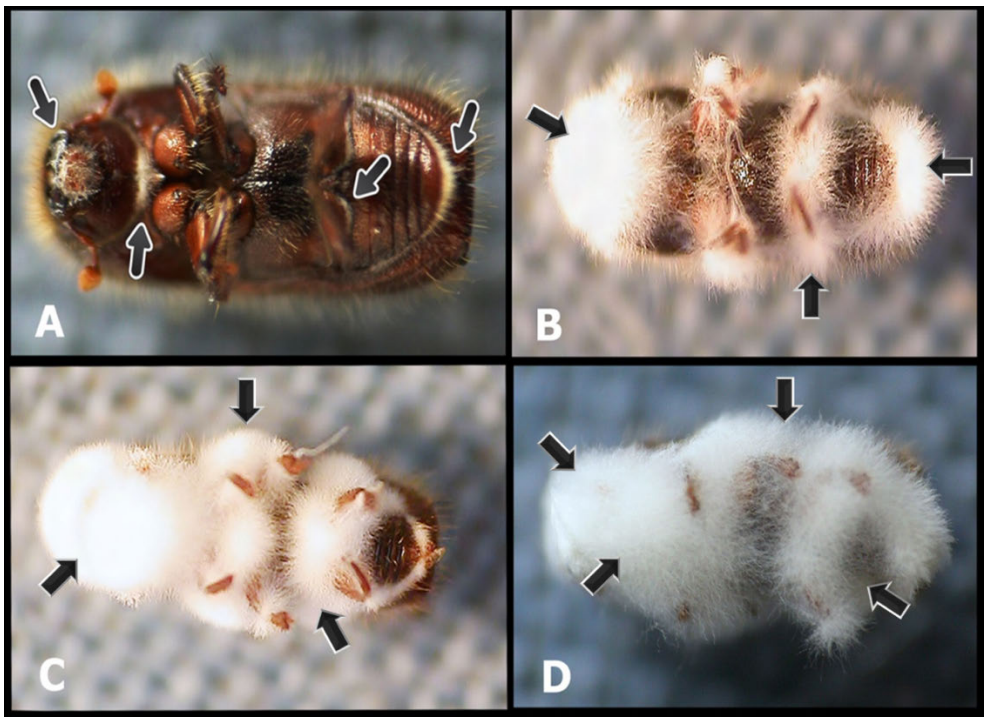

Figure 1.2: Physical manifestation of *B. bassiana* on insects **(**A) Primary infection (first signs of germination), (B) Secondary infection, (C–D) Severe infection (Adapted from Mudrončeková *et al.,* 2019).

As a result of the metabolic versatility and the adaptability of many entomopathogenic fungi, they have also been shown to exist in different environmental states and niches (Mondal *et al.,* 2016). *B. bassiana* has been discovered to be an endophytic colonist inhabiting several plant species, in addition to parasitizing insects. The fungus has also been shown to thrive saprophytically in the soil, colonizing plant rhizosphere (Zimmermann 2007; Bara and Laing 2020). Various studies have revealed the ability of *B. bassiana* to establish mutualistic associations with plants and pathogenic association with insects. These relationships can coexist simultaneously, with fungus colonising plant tissues and parasitising insects, forming a tripartite interaction (Branine *et al.,* 2019). Furthermore, *B*. *bassiana,* like many other microbes, has also been reported to be isolated in one environmental lifestyle and made to exist in another, hence they can shuffle between the entomopathogenic and endophytic states (Biswas *et al.,* 2012). The fungus has been found in its endophytic state inhabiting different crops asymptotically, these crops include wheat (Sánchez-Rodríguez *et al.,* 2018), grapes (Rondot and Reineke 2018), tomato (Silva *et al.,* 2020), lemon (Bamisile *et al.,* 2020), soybean (Russo *et al.,* 2019), banana (Akello *et al.,* 2008) and lot more. Hence, they are also classified into the broad group of fungal endophytes, where fungi live in plant tissues without causing symptoms or harm the host plant. In this regard, they have been shown to play important roles within the plants which include systemic protection of plants against herbivorous insects and plant pathogens (Rondot and Reineke 2018; Russo *et al.,* 2019; Bara and Laing 2020), as well as acting as growth promoters (Lopez and Sword 2015; Tall and Meyling 2018). Besides occurring as part of the natural endophytic community of different plants, the fungus has also been artificially inoculated and established as an endophyte in many plant species. Studies have shown that the establishment can be achieved through seed treatment (Jensen, Enkegaard and Steenberg 2019), soil application (Ramakuwela *et al.,* 2020), direct injection (Gaviria, Parra and Gonzales 2020) and/or roots drenching (Canassa *et al.,* 2020). Hence, exploring means of ensuring the effective endophytic establishment of *B. bassiana* strains in different crop plants is currently the focus of several studies to achieve a dual biocontrol strategy against insect pests and plant pathogens.

Different mechanisms have been proposed for their protective effects on plants during co-habitation. *B. bassiana*, like other endophytic fungal entomopathogens, can directly

suppress plant pathogens through competition for ecological niches and nutrition, mycoparasitism and also by the secretion of secondary metabolites (Espinoza *et al.,* 2019; Barra-Bucarei *et al.,* 2020a). Induced systemic resistance, a state observed to be elicited by beneficial microbes, has emerged as an important mechanism by which the whole plant is primed for enhanced defence against various plant pathogens and pests (Pieterse *et al.,* 2014). Evidence for this induced resistance is basically the reduction of disease symptoms in plant parts distant from the site where the inducing agent is active, which has been shown in cotton seedlings inoculated with *B. bassiana* (Ownley *et al.,* 2008). Plant growth promotion by the fungus has also been speculated to be a result of enhanced nutrient uptake as earlier shown by Sánchez-Rodríguez, Del Campillo and Quesada-Moraga (2015). In addition, *B. bassiana* has also been demonstrated to re-channel the insect-derived nitrogen to plants (Behie and Bidochka 2013). The synergy between endophytic fungal entomopathogens and other endophytes has also been shown to be beneficial to the plant hosts. Hence, different endophytic consortia have been studied for the dual control of plant pests and pathogens with the aim of increasing the variety of effective action mechanisms as well as the range of pests and pathogens that are negatively impacted by these consortia. This synergy has been observed between *B. bassiana* and *P. fluorescens* in reducing leaf miner damage and collar rot in groundnut (Senthilraja *et al.,* 2010). This has also been shown with *Rhizophagus intraradices* against beet armyworm in tomato plants (Shrivastava *et al.,* 2015).

1.3 *B. bassiana* genome

The ecological and industrial importance of *B. bassiana* has been highlighted by various efforts to sequence the genome as well as to understand the genome organization within different strains of the fungus (Viaud *et al.,* 1996; Xiao *et al.,* 2012; Valero-Jiménez *et al.,* 2016; Atzeni *et al.,* 2020). The complete genome sequence of *B. bassiana* has been noted to be typically between 32-45 megabytes (Xiao *et al.,* 2012; Lee *et al.,* 2018). Comparative genomics at the intraspecific level has also shown a high level of genetic diversity between different strains of *B. bassiana*, which enabled the strains to be classified into two distinct phylogenetic clusters according to their genome. In addition, a detailed study of the karyotype profiles of different *B. bassiana* strains also indicated remarkable flexibility in their chromosomal organization, which was observed to be a function of their origins (Viaud *et al.,* 1996). The analysis of some of these strains revealed that the typical core genome consists of 7,341 orthologous gene clusters, while

the pan-genome consists of 13,068 orthologous gene clusters. It was thus suggested that *B. bassiana* has an open pan-genome, which is highly expected for dynamic species which have the ability to naturally colonize diverse environments (Valero-Jimenez *et al.,* 2016). This is significant as the fungus has been well known to colonize different insects, arachnidal and nematodal hosts, in addition to its ability to colonize different species of plants. Currently, a significant portion of the open reading frames (ORFs) in each of these genomes has been assigned to different biological functions. In this regard, expressed sequence tag analyses, gene functional studies and insertion mutagenesis have been instrumental in the identification of some of the genes involved in detoxification, fungal development, insect immune avoidance, stress responses and virulence (Tartar and Boucias 2004; Fan *et al.,* 2011; Kim *et al.,* 2016). The functional analysis of the annotated *B. bassiana* genome is illustrated in Figure 1.3. The shotgun genome sequencing of the well-studied *B. bassiana* ARSEF 2860 revealed a size of 33.7 Mb with a significantly compact genome structure when compared to some other pathogenic fungi. This genome was predicted to encode 10,366 protein genes which include genes for different proteases (23 trypsins, 43 subtilisins, 21 aspartic proteases, 52 carboxypeptidases, 47 cysteine peptidases, 20 threonine peptidases and 98 metallopeptidases) (Xiao *et al.,* 2012). The fungus was also noted to possess genes for 145 carbohydrate-active enzymes which include chitinases, cellulases, hemicellulases, ketolases etc. (Xiao *et al.,* 2012). More recently, the genome size of *B. bassiana* ATCC 74040 (commercial strain) was estimated to be 32.4 Mb in size and shown to contain 2,322 contigs, with an N50 value of 36,979 bp (Atzeni *et al.,* 2020). The 20,271 predicted genes in the strain were noted to be related to insecticidal activity: chitinases, proteases, as well as hydrophobins.

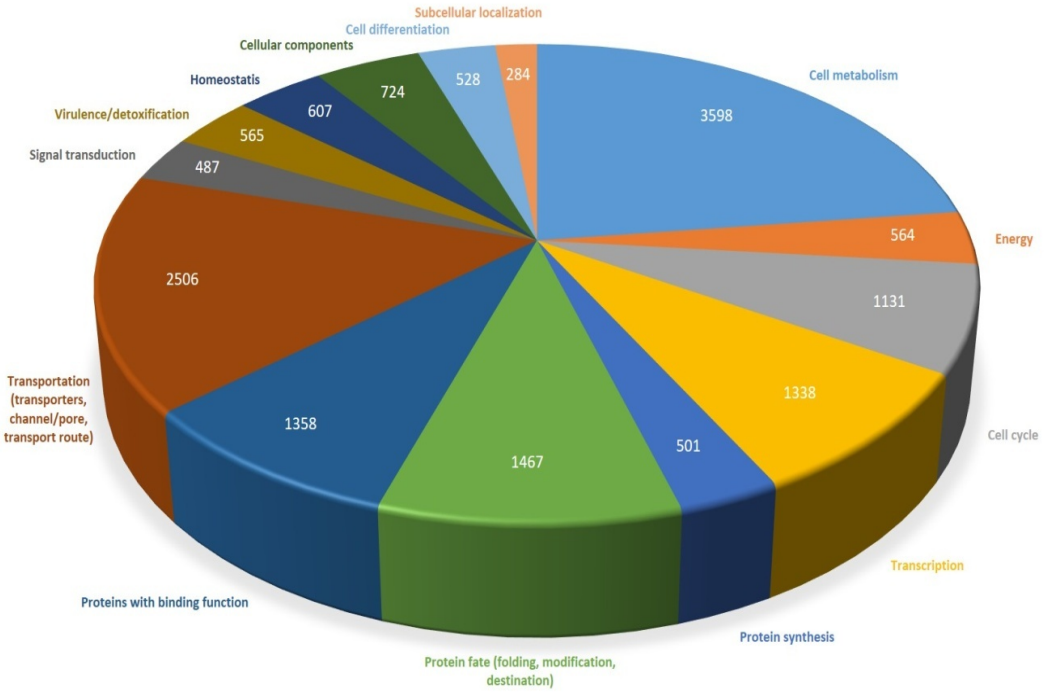

Figure 1.3: Genomics analysis and functional classification of *Beauveria bassiana* proteins. Each numerical value on the sectors denotes the relative fraction of genes represented in each category of the genome (Adapted from Xiao *et al.,* 2012).

1.4 *B. bassiana* transcriptome

A detailed understanding of the processes by which different genes are up- and down-regulated as well as the processes of protein secretion in a cell, are considered valuable. This is because the cell's ability to regulate these activities is important in its metabolism of extracellular substrates and its continued existence in its environment. In the long run, the understanding of the "protein secretion mechanism" will allow the application of different organisms as "cellular factories" for the production of commercially important proteins in significant quantities (Tjalsma *et al.,* 2000; Du and van Wezel 2018). In this regard, the "omics" tools, which include the secretomics, proteomics, transcriptomics etc., have been widely used in the identification and elucidation of the enzyme repertoire in different industrially important organisms including *B. bassiana* (Xie *et al.,* 2010; Alfaro *et al.,* 2016; Grosse-Holz *et al.,* 2018). The transcriptome of *B. bassiana* has also been well studied across different strains, environmental conditions, virulence efficiency, and insects' hosts especially with the goal of understanding *B. bassiana* host-pathogen interactions (Dong *et al.,* 2017; Lai *et al.,* 2017; Wang *et al.,* 2017b; Zhou *et al.,* 2019).

This has been achieved more effectively by the application of RNA-seq methods and validated by quantitative-PCR. These methods have been noted to be more effective than others in giving insights into the global gene expression on specific conditions due to high resolution (Gamba and Zenkin 2018). In addition, the previous elucidation of the *B. bassiana* genome has also provided a theoretical foundation and reference for analysing its transcriptomes under different conditions. For instance, different expression levels for genes encoding enzymes and proteins necessary for degrading various organic polymers, such as glycans and lipids, were observed in different strains of *B. bassiana* which suggests that the different strains employ distinct strategies or possess varying ability to obtain nutrition (Wang *et al.,* 2017b).

Regarding enzyme profiling of *B. bassiana*, transcriptome analysis of submerged *B. bassiana* conidia revealed a large number of depolymerases that include proteases, glycosidases, and lipases as well as many amino acid and carbohydrate transporters (Cho *et al.,* 2006). In this study on *B. bassiana* transcriptome, 2400 unique sequences were identified and 4360 were found to be clustered. These sequences are believed to indicate a large and versatile gene expression repository being available for the fungus' growth during different environmental and developmental conditions. Hence, translating into a large amount of data for gene discovery as well as genome annotation (Cho, Boucias and Keyhani 2006). The gene expression profile of *B. bassiana* in response to insect cuticles also showed a large array of transcripts that were not identified during *in vitro* growth conditions; these include enzymes such as peroxidases, trehalase, lipase, peptidase, phosphatase and lyase as well as other enzymes responsible for the degradation of specific cuticle substrates (Mantilla *et al.,* 2012). In recent studies, industrially important enzymes including β-1,3-glucanases, chitinolytic enzyme systems (Lai *et al.,* 2017), tyrosinases and reductases (Zhang *et al.,* 2019b) have been highlighted to be expressed at varying levels in *B. bassiana* during different metabolic conditions. Interestingly, the importance of alternative splicing in the metabolic responses and adaptation of *B. bassiana* was also highlighted, thus further unravelling the complexity of the transcriptome as well as the virulence of the entomopathogenic fungus (Dong *et al.,* 2017).

1.5 *B. bassiana* enzymes

Besides their well-established role as biological control agents, *B. bassiana* have also been widely used as whole-cell biological catalysts (Grogan and Holland 2000). The major enzymes that are produced spontaneously by the fungus are the chitinases, lipases and proteases. However, some other notable enzymes have also been shown to be produced by *B. bassiana* using both defined and non-defined media under solid-state (SSF) and submerged fermentation (SmF) conditions. The physicochemical properties of some characterized *B. bassiana* enzymes are summarized in Table 1.1.

Table 1.1: Properties of some *Beauveria bassiana* enzymes

Strain	Fermentation mode; Activity/ Molecular weight (kDa)	Optimum pH/ Temp (°C)	Substrate	Activator(s)	Inhibitor(s)	References
Amylase						
B. bassiana SG 8702	SmF; 1315.82 Umg^{-1}/ 37	4.0/ 40	Starch	NR	Cu^{2+}, Mn^{2+}, Na^{2+}, Hg^{2+}, Fe^{2+} and Mg^{2+}	(Feng and Ying, 2002)
B. bassiana MTCC-5184	SmF; 4.5 $IUmL^{-1}$, SSF; 50 $IUmL^{-1}$/ 36	6.0/ 45	Starch	NR	NR	(Ryali *et al.,* 2020)
Beta galactosidase						
B. bassiana (unidentified)	NR/290	6.8/ 50	Sucrose	Ca^{2+}, Zn^{2+} K^{+}, Galactose	2-mercaptoethanol	(MacPherson and Khachatourians 1991)

Beta glucosidase						
B. bassiana P1	SmF; 5.20 UmL^{-1}/ 400 - 600	5.0/ 55	Wheat bran	$CoSO_4$, $BaCl_2$	$CuCl_2$, Beta-mercaptoethanol, $ZnSO_4$, $MnSO_4$,	(Borgi and Gargouri 2016)
Cellulase						
B. bassiana B14532	SmF; 3.59 UmL^{-1}/ NR	NR/ NR	Carboxymethylcellulose	NR	NR	(Petlamul and Boukaew 2019)
Chitinase						
B. bassiana CG432	NR; NR/ 86	5.5/ 45	Colloidal chitin	NR	NR	(Sassá *et al.,* 2008)
B. bassiana 174	SSF; 126 $Ugds^{-1}$/ NR	5.0/ 48	Colloidal chitin	NR	NR	(Zhang *et al.,* 2004)
B. bassiana 0062	SmF; 97 UmL^{-1} / NR	5.0/ 40	Colloidal chitin	NR	NR	(Fan *et al.,* 2007a)
B. bassiana (unidentified)	SmF; 0.585 UmL^{-1} / NR	NR/ NR	Colloidal chitin	NR	NR	(Elawati, Pujiyanto and Kusdiyantini 2018)
B. bassiana B02	SmF; 449 UmL^{-1} / NR	NR/ NR	*Zabrotes subfasciatus*	NR	NR	(Mancillas-Paredes *et al.,* 2019)
Lipase						
B. bassiana MTCC-5184	SmF; 4.5 $IUmL^{-1}$, SSF; 10 IUg^{-1}/ 144	7.0/ 50	Olive oil and tributyrin	NR	NR	(Ryali *et al.,* 2020)
B. bassiana B1	SmF; 9.07 Uml^{-1} / 25	7.0/ 35	Tributyrin	Mg^{2+} and Zn^{2+} Ca^{2+}	NaCl	(Zibaee, Sadeghi-Sefidmazgi and Fazeli-Dinan 2011)
B. bassiana CFF7	SSF; 8.59 Umg^{-1} / 78	6.0/ 50	Tributyrin	Triton X-100, Tween 80,	NR	(Vici *et al.,* 2015)

				Tergitol and CTAB		
Protease						
B. bassiana MTCC-5184	SmF; 13.5 $IUmL^{-1}$, SSF; 47.5 IUg^{-1} / 28.2	9.0/ 50	Casein, haemoglobin and bovine serum albumin	EDTA	PMSF	(Ryali *et al.,* 2020)
B. bassiana 111892A	SmF; 15.6 UmL^{-1} /32	8.5/ 25	Azocoll, gelatin	Pepstatin	Leupeptin, PMSF	(Urtz and Rice 2000)
B. bassiana B1	SmF; 3.44 UmL^{-1}/ 47	8.0/ 45	*Eurygaster integriceps*	$CaCl_2$, $MgSO_4$, $ZnCl_2$	$MnSO_4$, NaCl, KCl	(Zibaee and Bandani 2009)
Trehalase						
B. bassiana ARSEF2860	NR; NR/ 84	7.0/ 55	Trehalose, galactose	$MnCl_2$ and $CaCl_2$	$CuCl_2$, ZnCl and EDTA	(Liu, Ying and Feng 2011)
Xylanase						
B. bassiana MTCC-5184	SmF; 4.75 $IUmL^{-1}$, SSF; 96.5 IUg^{-1}/ 28.2	6.0/ 50	Soluble xylan	EDTA	PMSF	(Ryali *et al.,* 2020)

*NR: Not recorded
*SmF: Submerged fermentation
*SSF: Solid-state fermentation
* CTAB: Cetyltrimethylammonium bromide
* PMSF: Phenylmethylsulfonyl fluoride
* EDTA: Ethylenediaminetetraacetic acid

1.5.1 Chitinase

Chitinases (EC 3.2.11.14) hydrolyze the β (1,4) linkage of chitin polymer into N-acetyl β-D-glucosamine monomers. This enzymatic reaction is considered very important as the substrate chitin is the second most ubiquitous natural polymer; thus, chitinases are a key focus to researchers as a result of their diverse applications in bioremediation, dye removal, fungicide, biosensing, drug delivery etc. (Rameshthangam *et al.,* 2018; Kidibule *et al.,* 2020). Being one of the most important enzymes needed to hydrolyze insect cuticle by entomopathogens, the production of chitinases in *B. bassiana* has been highlighted in different studies (Augustyniuk-Kram 2018; Mancillas-Paredes *et al.,* 2019; Schmaltz *et al.,* 2021). Experimentally, the fungus has been shown to produce extracellular chitinase at different levels during both SSF and SmF, usually using colloidal chitin as the carbon source (Beygmoradi *et al.,* 2018; Elawati, Pujiyanto and Kusdiyantini 2018). From the available literature, the highest production level recorded for chitinase in *B. bassiana* are 449 UmL^{-1} and 248 $Ugds^{-1}$ under SmF (Mancillas-Paredes *et al.,* 2019) and SSF (Beygmoradi *et al.,* 2018) respectively.

Some studies have shown that the optimum incubation period for the production of chitinase by *B. bassiana* is usually four or five days under SmF (Leopold and Samsˇinˇáková 1970; Elawati, Pujiyanto and Kusdiyantini 2018). It is also noted that the enzyme production is inducible by different chitooligosaccharides (Dhar and Kaur 2010; Mancillas-Paredes *et al.,* 2019). Furthermore, chitinase production has been observed under acidic (Sassá *et al.,* 2008), alkaline (Suresh and Chandrasekaran 1998) and neutral conditions (Elawati, Pujiyanto and Kusdiyantini 2018). Recently, ultrasound treatment was used to increase chitinase production from *B. bassiana* by almost 50% of the initial production level (Schmaltz *et al.,* 2021).

There are few reports on the characterization of different chitinases produced by *B. bassiana*. One such study has shown a *B. bassiana* chitinase that is moderately acidic with optimum pH between 5.5 and 6.0 (Sassá *et al.,* 2008). The optimum temperature of *B. bassiana* chitinases have also been shown to be between 30°C and 48°C, thus they can be said to be in the range of mesophilic to moderately thermophilic chitinases (Fan *et al.,* 2007a; Sassá *et al.,* 2008). Furthermore, studies have shown that chitinases from some *B. bassiana* strains are approximately 70 kDa (Dhar and Kaur 2010; ZHEN *et al.,* 2010).

In order to improve the enzyme production levels, chitinase genes from *B. bassiana* have been successfully cloned in different host systems, including *E. coli* (Fang *et al.,* 2005; Fan *et al.,* 2007a) and *Pichia pastoris* (Fan *et al.,* 2007b). The introduction of a constitutive promoter from *Aspergillus nidulans* into *B. bassiana* was shown to increase chitinase production level by approximately 20 folds (Fang *et al.,* 2005). Hybrid chitinases with higher activity have also been engineered by fusing *B. bassiana* chitinase with chitin-binding domains derived from other sources and expressing them in *P. pastoris* (Fan *et al.,* 2007a). Notably, *B. bassiana* was also used as a host for the expression of chitinase genes from another fungus, *Ophiocordyceps unilateralis* (Chantasingh *et al.,* 2011). The recent isolation of thermotolerant *B. bassiana* strains (Alali *et al.,* 2019) is expected to open a new vista for the production of thermostable chitinases which would be useful in many industrial applications that operate at high temperatures.

1.5.2 Lipases

Lipases (EC 3.1.1.3) are a class of enzymes that hydrolyze long-chain triglycerides to fatty acids and acylglycerols. These enzymes can catalyze both hydrolysis and synthesis reactions of esterification, interesterification and transesterification (Devi *et al.,* 2020), thus they constitute one of the most important groups of biocatalysts in biotechnology. Microbial lipases particularly have been found useful in industries such as agrochemicals, animal feed, biofuel, biocatalytic resolution, biosensor, bioremediation, cosmetic, dairy, food and beverage, cleaning, fine chemicals production, pharmaceuticals, perfumery and textile (Chandra, Singh and Arora 2020). The pivotal elements of the insect's cuticle are mainly the surface lipids as well as the long-chained, saturated, unsaturated, and branched hydrocarbons (Xu *et al.,* 2018). The specific biological roles of these cuticular lipids, especially in the epicuticle, include serving as barriers to pathogens, taxonomical markers, osmoregulation, and function in nestmate recognition (Barbero 2016; Wu *et al.,* 2020a). Hence, the secretion of lipases by entomopathogenic fungi is a crucial step in the cuticle-degrading sequence and pathways involved in phospholipid homeostasis and triglyceride metabolism which all contribute to their virulence and pathogenicity (Keyhani 2018). Lipases have been produced from different *B. bassiana* strains, although the production levels are difficult to be compared, due to the difference in enzyme activity assays and substrates used. However, on this account, the highest lipase activity reported for any *B. bassiana* strain is 906.7 U, which

was achieved using p-nitrophenyl butyrate as the substrate (Zibaee, Sadeghi-Sefidmazgi and Fazeli-Dinan 2011). In general, lipase production level in *B. bassiana* under SmF has been shown to be highest on the 6th or 7th day (Zibaee, Sadeghi-Sefidmazgi and Fazeli-Dinan 2011; Dhawan and Joshi 2017). As expected, lipase production in *B. bassiana* was shown to be inhibited by the addition of fatty acids, such as oleic, stearic etc. and enhanced by the addition of triacylglycerols. Studies have shown that lipases from *B. bassiana* perform optimally across a wide range of pH including acidic (Vici *et al.,* 2015), neutral and alkaline (Zibaee, Sadeghi-Sefidmazgi and Fazeli-Dinan 2011). Some *B. bassiana* lipases have been found to be mesophilic (Zibaee, Sadeghi-Sefidmazgi and Fazeli-Dinan 2011) while others were shown to be thermophilic (Vici *et al.,* 2015). It also appears that molecular weights of *B. bassiana* lipases vary from 25 kDa (Zibaee, Sadeghi-Sefidmazgi and Fazeli-Dinan 2011) to 60 kDa (Vici *et al.,* 2015). Heterologous production of *B. bassiana* lipase has been achieved by expressing the gene in *P. pastoris*. The recombinant lipase produced by cloning the lipase gene from *B. bassiana* CFF74 was also successfully immobilized by both anionic and hydrophobic interactions thus raising possibilities for important industrial applications (Vici *et al.,* 2015).

1.5.3 Proteases

Proteases (EC 3.4) constitute the largest single-family of industrial enzymes with a wide range of applications. Also referred to as peptidases or proteinases, they catalyze the proteolytic cleavage of proteins into smaller peptides or amino acids. They have been found very useful in the cosmetics, chemical, detergent, food, leather, pharmaceutical, silk degumming, silver recovery and wastewater treatment industries (Naveed *et al.,* 2020). The insects' epicuticle, which is the outermost cuticle layer, is principally made of proteins and lipids which are stabilized by various biopolymers (Lemoine, Engl and Kaltenpoth 2020). Proteases attack the cuticle prior to the attack on weakened microfibers by chitinolytic enzymes (Grizanova *et al.,* 2019).

A significant protease production level of 280.72 UmL^{-1} has been reported in *Beauveria* spp. after 7 days incubation (Rao *et al.,* 2006). However, a hyper-producing *B. bassiana* mutant strain was shown to have the highest protease production level (~ 2000 UmL^{-1}) ever recorded under liquid fermentation, hence, the *B. bassiana* P2 strain is being considered a top candidate in industrial protease production (Borgi *et al.,* 2016). Studies have shown most *B. bassiana* proteases to possess optimum activity at the

mesophilic range (Mishra, Kumar and Malik 2013; Firouzbakht *et al.,* 2015), however, *B. bassiana* proteases have been reported to be stable at 45°C (Zibaee and Bandani 2009) and 60°C (Shankar and Laxman 2015). Characterization of proteases from different strains of the fungus have shown the existence of both acidic (Mishra, Kumar and Malik 2013) and alkaline proteases, raising their application potential under these different conditions (Firouzbakht *et al.,* 2015). An alkaline protease from *Beauveria* sp. MTCC 5184 was shown to be thermostable and was successfully applied as an effective detergent (Shankar and Laxman 2015). Subsequently, an enzyme from the same strain was used efficiently for the degumming of silk and subsequent hydrolysis of sericin to low molecular weight peptides (More, Chavan and Prabhune 2018). There is a wide variation in the molecular weight of proteases from different *B. bassiana* strains, ranging from 32 kDa (Borgi *et al.,* 2016) to 105 kDa (Firouzbakht *et al.,* 2015). Furthermore, *B. bassiana* proteases have shown to exhibit proteolytic activities on a wide range of substrates from collagen, elastin (Urtz and Rice 2000), to haemoglobin (Shankar and Laxman 2015) etc. Such broad-spectrum activity of proteases increases their prospective applications especially in detergent manufacture, in peptide synthesis, and in basic analytical research.

1.5.4 Amylases

Amylases (EC 3.2.1.1.3) are key enzymes with diverse applications in the field of biotechnology which include breaking down of starch into smaller units for fuel-alcohol production and for starch-based food processing, desizing of fabrics in the textile industry, paper processing, etc. (Saini, Saini and Dahiya 2017; Bhatt, Trivedi and Patel 2020). Unlike lipases, proteases and chitinases, amylases are not categorized as pathogenic or virulence factors in entomopathogenic fungi. However, there are reports on the production of the enzyme by many fungi in general and endophytic organisms in particular (Toghueo *et al.,* 2017; Naik 2019). In endophytic microbes, the secretion of amylases is essential to degrade the different sugar polymers, especially starch, found in plants. Hence, being an endophyte*, B. bassiana* is also expected to produce amylase as well.

Extracellular amylase production by *B. bassiana* under different conditions while utilizing different media have been reported (Feng and Ying, 2002; Fernandes *et al.,* 2012; Martins, Pereira and Baptista 2014). *B. bassiana* SG 8702 was shown to produce an amylase under acidic fermentation conditions with optimal activity at 40°C and pH

4.0. Furthermore, the enzyme exhibited significant stability between pH 3.0-8.0, at 37°C, and also maintained significant activity between 40°C and 60°C, making it a potential candidate for industrial applications that involve varying reaction conditions (Feng and Ying, 2002). *Beauveria* sp. MTCC 5184 produced 4 $IUmL^{-1}$ and 50 IUg^{-1} of amylase under both SmF and SSF conditions, respectively (Ryali *et al.,* 2020). However, a higher activity of 1315.82 Umg^{-1} was achieved by *B. bassiana* SG8702 under SmF conditions (Feng and Ying, 2002).

1.5.5 Cellulases

Cellulases (3.2.1.4) are a group of enzymes which, acting together, hydrolyze the β-1,4 linkages of cellulose to yield glucose. The production of these enzymes is a necessary step in the cellulolytic biomass-to-ethanol conversion process for energy sustainability. Besides their main use in the production of biofuels, cellulases have found wide applications in the paper/pulp, textile, animal feed, food processing and agricultural industries, to mention but a few (Ahmed and Bibi 2018; Chandra and Yadav 2021). Similar to amylases, the secretion of cellulases has been found to be necessary for endophytic fungi such as *B. bassiana*. This is reinforced by the fact that the role of cellulases in endophytic colonization has been established by mutational analysis (Krause *et al.,* 2006). Furthermore, the expression of cellulase was identified *ad planta* at the main entry sites of *Azoarcus* spp. BH72, a well-studied endophyte (Reinhold-Hurek *et al.,* 2006). The earliest report on *B. bassiana* cellulase was provided by Leopold and Samšiňáková (Leopold and Samsˇinˇáková 1970). Recent investigations have further revealed the capacity of *B. bassiana* to produce cellulases under different fermentation conditions. For example, the ability of *B. bassiana* to utilize carboxymethylcellulose for its growth and extracellular cellulase enzyme production was shown by Petlamul *et al.,* (2017). Cellulase production in *B. bassiana* B14532 attained the highest level (3.89 UmL^{-1}) at an optimum pH of 6.5 and temperature of 80°C after 6 days of SmF (Petlamul and Boukaew 2019). It was also shown in this study that the enzyme retained more than 50% of its activity at 80°C, thus highlighting the significant thermostability of the enzyme. Recently, a *B. bassiana* strain was observed to produce 46.78 Ug^{-1} of exocellulase and 28.0 Ug^{-1} of endocellulase while utilizing different lignocellulosic biomass under solid-state fermentation conditions (Alves *et al.,* 2020).

1.5.6 Other enzymes

The potential of *B. bassiana* for the production of other industrially important enzymes besides lipases, proteases, chitinases, amylase and cellulase has not been extensively studied. These enzymes which can be considered as *B. bassiana* ancillary enzymes include asparaginase, chitosanase, β-1,3-glucanase, β-glucosidase, glutaminase, keratinase, mannitol-1-phosphate dehydrogenase, quercetinase, superoxide dismutase, trehalase, etc.

1.5.6.1 *Asparaginase*

Asparaginases (EC 3.5.1.1) are enzymes that deamidate asparagine to aspartic acid and ammonia. They have been found useful as anti-tumour agents, as biosensors, and in mitigating acrylamide levels in baked/fried foods (Chand *et al.,* 2020). *B. bassiana* SS18/41 and its different mutants have shown to produce asparaginase at significant levels under SmF (Kamala Kumari, Sankar and Prabhakar 2015). *B. bassiana* SS18/41 has also been shown to produce asparaginase under SSF achieving 90 $Ugds^{-1}$ using wheat bran as the main carbon source (Nageswara, Guntuku and Tadimalla 2014).

1.5.6.2 *Catalase*

Catalase (EC 1.11.1.6) regulates cellular hydrogen peroxide metabolism as it catalyses the breakdown of hydrogen peroxide into oxygen and water. It is an oxidoreductase that plays a crucial role as an antioxidant and protects the cell against oxidative stress. It has been found useful in many industrial applications such as treatment of bleach in bioremediation, quality control in the dairy industry, and in clinical diagnosis (Kaushal *et al.,* 2018). Two forms of the enzymes with molecular weights of 54.7 and 84.0 kDa have been sourced from a strain of *B. bassiana* (Pedrini *et al.,* 2006). While the *B. bassiana* peroxisomal catalase was sensitive to pH, heat and high concentration of the hydrogen peroxide substrate, the other form, the cytosolic isoform, was tolerant across a wide range of pH (6.0–10.0), thermostable at 55°C and was fully active at higher concentrations of hydrogen peroxide.

1.5.6.3 *Chitosanase*

Chitosanase (EC 3.2.1.132) is characterized by its ability to catalyze the hydrolytic cleavage of chitosan (Sinha, Chand and Tripathi 2016). Considering its biotechnological importance, especially in the bioconversion of marine crustacean biomaterials and as a

biocontrol agent, chitosanases have been well studied from various sources (Thadathil and Velappan 2014). A chitosanase like protein was isolated and purified from *B. bassiana* 618. However, the 28 kDa protein, which showed remarkable insecticidal activity, was found to be thermolabile (Fuguet, Théraud and Vey 2004). Subsequently, the cloning of a chitosanase gene from *B. bassiana* in *Pichia pastoris* resulted in the expression of a chitosanase which was stable between pH 2.0 and 8.0 and below 40°C, however, the mass of this chitosanase was estimated to be 33 kDa (Liu *et al.,* 2020a).

1.5.6.4 *Beta-1,3-glucanase*

β-(1,3)-glucanases (EC 3.2.1.6) are responsible for the hydrolysis of β-(1,3)-glycosidic bonds in β-(1,3)-glucans. β-(1,3)-glucans are the principal cell wall component in filamentous fungi, yeast callose (a structural polysaccharide in plants) and are also found in some bacterial exopolysaccharides (Zhou *et al.,* 2017). The enzymes have been found useful in malting, brewing (Sena *et al.,* 2011), vinification (Blättel *et al.,* 2011) and as antifungals (Confortin *et al.,* 2019). The production of this enzyme has been highlighted in some *B. bassiana* strains. β-(1,3)-glucanases production levels ranging from 0.46 Umg^{-1} to 18.04 Umg^{-1} were recorded with *B. bassiana* IBCB 66 while utilizing different plant biomass (Alves *et al.,* 2020). The effect of ultrasound treatment on the enzyme production in another *B. bassiana* strain has been shown with a 46% increase in yield observed after the treatment (Schmaltz *et al.,* 2021).

1.5.6.5 *Beta-glucosidase*

Beta-glucosidases (EC 3.2.1.21) are an important component of cellulose metabolizing enzymes (cellulase system) as they catalyze the terminal step in cellulose catabolism (Keller *et al.,* 2020). They have found applications in ethanol and biofuel production, synthesis of oligosaccharides, etc. (Ahmed, Batool and Bibi 2017). β-Glucosidases activity was detected in *B. bassiana* EAB 90/2-Dm which was isolated from locust (Quesada-Moraga and Alain 2004). The *B. bassiana P1 strain* was also shown to produce a thermostable β-glucosidase during submerged fermentation with wheat bran as the carbon source; the enzyme was also stable under acidic conditions (Borgi and Gargouri 2016).

1.5.6.6 *Glutaminase*

Glutaminase (EC 3.5.1.2) production has also been shown in *B. bassiana*. Glutaminases deamidate glutamine to glutamic acid and ammonia, a property that has made them useful

as potential anti-tumour agents, in the induction of umami taste in oriental foods, and as biosensors etc. (Amobonye, Singh and Pillai 2019). *Beauveria* sp. BTMF S10 produced extracellular L-glutaminase at production levels of 46.9 Uml^{-1} under SmF (Keerthi *et al.,* 1999). A significant production level of glutaminase by the fungus has also been achieved under SSF (Sabu *et al.,* 2000).

1.5.6.7 *Keratinase*

Keratinase (EC 3.4.4.25) is a special class of inducible *proteolytic* enzyme with the capability to degrade insoluble keratin substrates. They have been found useful in feather meal processing, fertilizers, cosmetics, animal feed production, etc. (Hassan *et al.,* 2020). *B. bassiana* was shown to achieve a keratinase production level estimated at 62.8 U (Marcondes *et al.,* 2008). Keratinase production has also been shown in *Beauveria* sp. MTCC 5184, though at a lower level, using chicken feather as the carbon source (Ryali *et al.,* 2020).

1.5.6.8 *Mannitol-1-phosphate dehydrogenase*

Mannitol-1-phosphate dehydrogenase (EC 1.1.1.17) catalyzes the reversible reduction of fructose 6-phosphate to mannitol 1-phosphate (Sand *et al.,* 2015). The mannitol-1-phosphate dehydrogenase (MPD) gene from *B. bassiana* 2860 was cloned and expressed in *E. coli* (Wang, Ying and Feng 2010). Characterization of the MPD revealed it possesses high catalytic efficiency and high specificity for D-fructose-6- phosphate. Optimum temperature and pH for the *B. bassiana* MPD were 37°C and pH 7.0, respectively.

1.5.6.9 *Quercetinase*

Quercetinases (EC 1.13.11.24) are metal-dependent dioxygenases that cleave the quercetin heterocyclic ring (Nianios *et al.,* 2015). The ability of *B. bassiana* to synthesize this enzyme has been reported with the strains *B. bassiana* ATCC 7159 and *B. bassiana* IP 11 showing the highest among the studied *B. bassiana* strains, with production levels of 29.6 and 27.5 $nmolml^{-1}min^{-1}$ respectively (Costa *et al.,* 2011). However, no *B. bassiana* quercetinase has been characterized to date.

1.5.6.10 *Superoxide dismutases*

Superoxide dismutases (SODs) (EC 1.15.1.1) are ubiquitous enzymes found in all organisms that live in the presence of oxygen (Wang *et al.,* 2018b; Stephenie *et al.,* 2020).

They are important enzymes that detoxify harmful superoxide radicals into molecular oxygen and hydrogen peroxide. Thus, the enzyme may be useful in the treatment of ailments including Alzheimer's disease, Parkinson's disease, rheumatoid arthritis and diabetes which have all been characterized by low SOD levels (Younus 2018). (Xie *et al.,* 2010) characterized a Cu/Zn-superoxide dismutase (SOD) from *B. bassiana* 2860 by cloning and expressing the gene in *E. coli* to produce an enzyme that showed significant similarity with other fungal Cu/Zn-SODs.

1.5.6.11 *Trehalase*

Trehalase (3.2.1.28) catalyzes the hydrolysis of trehalose into glucose molecules. It is a multiple stress-responsive enzyme involved in energy metabolism, antioxidation, thermotolerance, osmotolerance and barotolerance (Nardelli *et al.,* 2019). A neutral trehalase (NTH1) from *B. bassiana* ARSEF2860 was produced by cloning *B. bassiana* NTH1 gene in *E. coli*. The enzyme was shown to have a molecular mass of 84.4 kDa, an optimum pH of 7.0 and an optimum temperature of 55°C (Liu, Ying and Feng 2011).

1.5.6.12 *Xylanases*

Xylanases (EC 3.2.1.8) are enzymes that cleave the β-1, 4 backbone of the polysaccharide xylan and are found useful in biomass saccharification, biopulping, biobleaching, food processing, etc. (Sharma, Thakur and Goyal 2019; Malgas, Mafa and Pletschke 2020). *B. bassiana* MTCC 5184 was shown to produce extremophilic xylanase under SmF at 5 $IUmL^{-1}$ (Ryali *et al.,* 2020). The extremophilic xylanase was active over a wide range of pH (4.0-9.0) and temperature (30 - 70°C) with optimum activity at 50°C. Higher xylanase production level of 41.01 UmL^{-1} was however recorded in *B. bassiana* B14532 at pH 6.5 and 55°C (Petlamul and Boukaew 2019).

1.6 Other applications of *B. bassiana*

Although the main focus of this chapter is the enzyme-production potentials of *B. bassiana*, we cannot undermine its popular industrial use as a biopesticide and its other bioactive metabolites (Figure 1.4 and Table 1.2). Being active against a broad range of hosts (above 700 different insect species), *B. bassiana* has assumed an important role in the management of various agricultural and forest pests as well as many pests of veterinary importance (Zimmermann 2007; Alali *et al.,* 2019; Dannon *et al.,* 2020). The fungus is typically deployed in a mass release of aerial conidia in dry, emulsion or liquid preparations (Mascarin and Jaronski 2016). In the previous decade, it was estimated that

approximately two-fifth of the total mycoinsecticides were *Beauveria* based (de Faria and Wraight 2007). *B. bassiana* 's potential as a nematicide has also been shown in many studies; the microbe and its culture filtrate were active against a range of plant nematodes which include *Meloidogyne hapla* (Liu et al., 2008)*, Heterodera glycines* (Zhao *et al.,* 2013) and *Heterodera filipjevi* (Zhang et al., 2020). Furthermore, beauvericin (BEA), a metabolite produced by *B. bassiana* has been reported to possess nematicidal activity (Kepenekci *et al.,* 2017). Interestingly novel BEA derivatives also exhibited cytotoxicity as well as insecticidal activity (Xu *et al.,* 2007).

Apart from beauvericin, several other important secondary metabolites/toxins with different industrial significances have also been isolated from *B. bassiana*. These include bassianolide (Patocka 2016), beauvetetraones A-C, dipicolinic acid (Lee *et al.,* 2019), isoleucylisoleucyl anhydride (Strasser, Hutwimmer and Burgstaller 2011), oosporein (Fan *et al.,* 2017), etc. These metabolites have been shown to have potential in various agricultural, industrial, and pharmaceutical applications. Specifically, these applications include their use in analytical chemistry (Michalski 2018), as insecticides (Farooq and Freed 2018), as antibacterials, as antifungals (Sahab 2012), etc. Pyridovericin is another notable example of these metabolites; it was singled out of many metabolites isolated from *B. bassiana* mycelial extract for its significant cytotoxicity against four different cancer cell lines (Andrioli *et al.,* 2017). *B. bassiana* have long been noted to be useful in Chinese and Korean traditional medicines as the silk moth fungus (batryticated silkworms), as records have shown its folkloric use over the years in the treatments of stroke, urticaria and diabetes (Pemberton 1999; Lee *et al.,* 2019). However, unlike some other entomopathogenic fungi such as *Cordyceps chinensis* and *C. militaris* (Park *et al.,* 2018), there is currently no known scientific evidence about the use of *B. bassiana* in human medicine. However, recent experiments have shown the potentials of *B. bassiana* as a "plant probiotic", as its treatment was able to promote better growth in maize plants (Tall and Meyling 2018).

B. bassiana has also been reported to have a good biotransformation ability. Whole-cell *B. bassiana* has been used industrially to catalyze the ring hydroxylation reaction of (*R*)-2-phenoxypropionic acid, a necessary step in the synthesis of various agrochemicals (Carballeira *et al.,* 2009). *B. bassiana ATCC* 7159 mediated biotransformation of curcumin has also been shown to result in the formation of curcumin-8'-O-4"-O-methyl-β-D-glucopyranoside, which exhibited a 39,000-fold higher water solubility than its

precursor, thus increasing its potential use in medicine (Zeng *et al.,* 2010). Similarly, *B. bassiana* ATCC 7159 mediated biotransformation of anticancer compound piperlongumine to 5-hydroxylpiperlongumine was shown to improve its water solubility and biological activities (Zi, Gladstone and Zhan 2012). Considering these factors, much emphasis should be placed on exploring biotransformation potential of *B. bassiana* in the future.

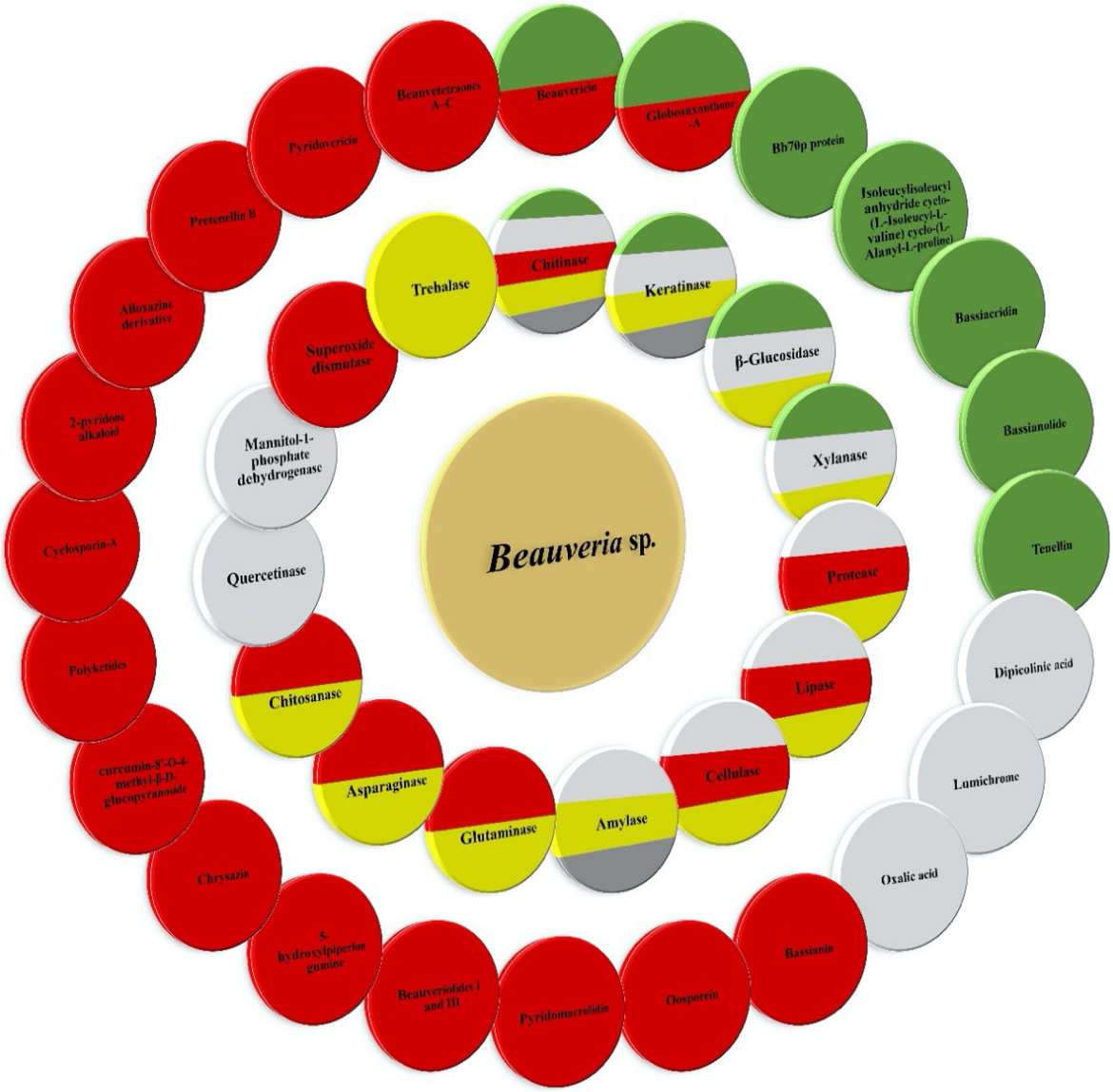

Figure 1.4: Potential of *Beauveria* sp. to produce various industrially important enzymes (inner circle) and metabolites (outer circle). Different colours represent applications in various industries (green: agriculture, yellow: nutritional biotechnology, red: medicine, white: industrial biotechnology, grey: environmental protection).

Table 1.2: Other industrially- important *Beauveria bassiana* metabolites

Metabolite	Bioactive properties	Reference
Beauvericin	Insecticidal, antitumor, antimicrobial, antiviral	(Hu, Li and Zhang 2016; Manyes *et al.,* 2018)
Isoleucylisoleucyl anhydride, cyclo-(L-Isoleucyl-L-valine), cyclo-(L-Alanyl-L-proline)	Insecticidal	(Strasser, Hutwimmer and Burgstaller 2011)
Novel beauvericin derivative (beauvericins G1–3, beauvericins H1–3)	Insecticidal, cytotoxic and antihaptotactic	(Xu *et al.,* 2007)
Bassianin	Erythrocyte membrane ATPase inhibition	(Jeffs and Khachatourians 1997)
Oosporein	Erythrocyte membrane ATPase inhibition, antiviral, antibacterial	(Jeffs and Khachatourians 1997)
Bassiacridin	Insecticidal	(Quesada-Moraga and Alain 2004)
Bassianolide	Insecticidal	(Patocka 2016)
Beauveriolides I and III	Antiatherosclerotic	(Namatame *et al.,* 2004; Ohshiro *et al.,* 2017)
5-hydroxylpiperlongumine	Anticancer	(Zi, Gladstone and Zhan 2012)
Chrysazin	Antifungal	(Yamazaki *et al.,* 2012)
Globosuxanthone A	Antifungal, anticancer	(Yamazaki *et al.,* 2012)
Pyridovericin	Anticancer	(Andrioli *et al.,* 2017)
Beauvetetraones A-C	Anticancer	(Lee *et al.,* 2019)
Dipicolinic acid	Insecticidal	(Singh, Son and Lee 2016)

1.7 Current commercial status of *B. bassiana*

Microbial pesticides have become more popular in recent years as the global attention has continued to shift towards environmentally friendly agricultural/industrial practices as well as minimizing spraying and control costs, which may be achieved by employing low-cost biologically effective insecticides (Dar, Lotfy and Moustafa 2020). The advantages of biopesticides include their short half-life, high degradability, and selectivity over certain species (Meena and Mishra 2020; Regnault-Roger 2020). Hence,

in many countries, especially in Europe and in North America, regulatory authorities are encouraging the approval and use of more biopesticides annually compared to conventional chemicals. *Beauveria* species are among the major fungal insect pathogens being explored for biocontrol purposes, majorly due to their ease of production, relative safety and ubiquity. They make up a very significant share of all commercial mycoinsecticides (de Faria and Wraight 2007; Mascarin and Jaronski 2016). Most *Beauveria*-based biopesticides are wettable powders, while a smaller proportion is in concentrated suspension or emulsifiable suspension formulations. Many successes have also been recorded by applying *B. bassiana* in an integrated approach based on the combination of *Beauveria* and other natural-derived botanical insecticides (Rizwan *et al.,* 2019). Some notable companies involved in the manufacture and distribution of *B. bassiana* based products are LAM International (USA), Koppert (Brazil), and MicosPlag (Colombia).

1.8 *B. bassiana* substrate utilization

The growth and the production of both primary and secondary metabolites by any organism are greatly influenced by the environmental conditions, more specifically, the nutrients available in the growth medium. Hence, for the commercial production of enzymes as well as other important biological metabolites, the utilization of cost-effective substrates or nutrients, especially the carbon and the nitrogen sources, during the fermentation process is critical. It is a well-established fact that most microbes prefer easily metabolizable carbon sources, particularly glucose, over an alternative, less metabolizable sugars. The ability of *B. bassiana* to effectively utilize glucose and other simple sugars for biomass growth, production of enzymes, spores and other biomolecules have been reported (Fernandes *et al.,* 2012; Santi *et al.,* 2019). However, simple sugars which include glucose and dextrose have been shown to repress the production of some *B. bassiana* enzymes such as chitinase and amylase (Dhar and Kaur 2010; Fernandes *et al.,* 2012). This is in agreement with studies which showed that glucose, lactose etc., repress the expression of genes and synthesis of enzymes related to catabolism of alternative carbon sources (Bruder *et al.,* 2015). In addition, purified simple sugars come at a relatively high cost, making it not feasible for industrial bioproduction; for instance, the cost of glucose accounted for 80% of the total medium cost in a fermentation set up (Sibi 2015).

Generally, cheaper fermentation substrates drastically decrease production costs in industrial fermentation. In this regard, different *B. bassiana* strains have been shown to possess the ability to utilize complex substrates as their energy source (Zhang *et al.,* 2019a; Alves *et al.,* 2020). Furthermore, the use of agro-industrial residues as an alternative carbon source for industrial fermentation is a highly significant means of combating environmental waste accumulation. These economic substrates have been used for the production of *B. bassiana* enzymes and other products during both SmF and SSF (Santa *et al.,* 2005; Nuñez-Gaona *et al.,* 2010; Alves *et al.,* 2020). *B. bassiana* chitinase production was carried out using wheat bran, cornmeal and other complex carbon sources (Zhang *et al.,* 2004). In addition to the agro-industrial residues, other readily available natural polymers such as chitin have also served as important substrates in chitinase production by *B. bassiana* (Elawati, Pujiyanto and Kusdiyantini 2018). The effects of nitrogen, being a critical element in industrial fermentation media, has also been investigated on the growth, blastospore production, and extracellular enzyme production of *B. bassiana*. Due to its complex eukaryotic metabolism, *B. bassiana*, like most other fungi have the preference for organic nitrogen sources for their growth and during industrial fermentation for various bioproducts (Dhar and Kaur 2010; Dhawan and Joshi 2017). Thus, of the few studies carried out to reveal the effects of nitrogen sources on its enzyme production, yeast extract and peptone have been the most frequently used (Zhang *et al.,* 2004; Elawati, Pujiyanto and Kusdiyantini 2018). However, readily available natural complex substrates have not been sufficiently explored for *B. bassiana* growth and industrial fermentation.

1.9 Safety of *B. bassiana* for human use

The industrial use of fungal enzymes, like every other product, demands that they must be harmless to humans, animals as well as the environment. It is also important that they comply with applicable regulatory standards, hence, the safety of the production strain, especially their *toxigenic potential*, continues to be the key factor in evaluating the safety of microbial enzymes. Many commercial products have been developed from *B. bassiana*, and numerous investigations on the different biological, environmental and toxicological safety aspects of the fungus have been carried out in recent times (Vestergaard *et al.,* 2003; Zimmermann 2007; Chauhan, Ranjan and Jindal 2018; Pande and Mishra 2018). *B. bassiana* is generally regarded as safe for humans, animals and other non-target organisms (Zimmermann 2007; Keswani, Singh and Singh 2013) and

recently, the human exposure risk assessment of some of its metabolites have also confirmed its safety for human use (Wu, Patocka and Kuca 2019). *Beauveria* species are rarely known as agents of human infections, however, they have been isolated from clinical material in a few cases. The fungus was reported as the causative agent of mycotic keratitis (Tu and Park 2007; Pariseau *et al.,* 2010) and in two cases of disseminated infection in immunosuppressed patients (Henke *et al.,* 2002; Tucker *et al.,* 2004). Other reports concerning this fungus include that of Sigler (2002), however, it has been shown many times that some of the pathogenic isolates in these cases may have been erroneously identified as *B. bassiana*. For instance, *B. bassiana* was listed as a synonym to *Isaria shiotae,* a fungus implicated in a case of human abscess, however, ITS sequencing has since shown that the two fungi are entirely different (Hoog 1972). In another case, the pulmonary mycotic infection was attributed to *B. bassiana*, but the isolate was found to have been a misidentified *Acrodontium crateriforme* strain (Freour, Lahourcade and Chomy 1966). It is also worth noting that most of these reported cases involve debilitated patients, immune-compromised patients or people who have earlier suffered some sort of trauma (Henke *et al.,* 2002; Zimmermann 2007). Thus, the few clinically isolated *B. bassiana* strains are most probably secondary opportunistic colonizers in those cases. Furthermore, the fungus has also been found to cause allergies in some workers engaged in the industrial production of *B. bassiana* -based formulations because they were regularly exposed to high concentrations of its spores (Keswani, Singh and Singh 2013). The potential allergenicity of *B. bassiana* by the characterization of its specific allergens has been highlighted and precautions were recommended, especially while using *B. bassiana* for biological control applications (Westwood, Huang and Keyhani 2006). Similar observations have also been made in other industrially important fungi from which allergens have been isolated such as *Penicillium chrysogenum* (Jami *et al.,* 2010), *Saccharomyces cerevisiae* (Levetin *et al.,* 2016), etc. Hence, it is pertinent not to overestimate the potential risks and the overall safety concerns of *B. bassiana* allergenicity.

Although *B. bassiana* produces many secondary metabolites including well-characterized mycotoxins, none of these metabolites has been found to be detrimental to human health or carcinogenic in nature. BEA, one of the best-known *B. bassiana* metabolites, is a natural contaminant of cereals and has been shown *in vitro* to possess different biological properties (Manyes *et al.,* 2018). However, it has been shown that

several antioxidant mechanisms protect animal cells against oxidative stress produced by BEA, thus rendering them insignificant (Mallebrera *et al.,* 2018). Oosporein is another *B. bassiana* metabolite found to cause erythrocyte morphology disruptions; meanwhile, it also possesses a broad spectrum of bioactivities. However, being a rather strong organic acid, it was posited that oosporein could hardly be assimilated into animals, hence it is less likely to find its way into the food chains and affect human health (Seger *et al.,* 2005; Hu, Li and Zhang 2016). Bassianin, beauveriolides, tennelin, etc., are some other metabolites from *B. bassiana*, however, no toxicity has been linked to any of them. Thus, judging from available literature, *B. bassiana* has never been identified as the basic cause of any human disease as there are no reports of its invasive growth or systemic infection in healthy humans. Therefore, the fungus has low pathogenic potential in humans and thus, it may be well argued that *B. bassiana* is a safe organism for industrial bioproduction.

1.10 Research problem and justification

Though an industrially important organism, *B. bassiana* has been mostly studied for its ecological role as an entomopathogen and as an endophyte, as well as its wide use as a biocontrol agent with little or no focus on its other industrial potentials. It has also been shown to possess the inherent ability to switch its metabolism and phenotype in order to adapt to the different conditions required for the endophytic and entomopathogenic states, producing different levels of metabolites and enzymes in the process (Luo *et al.,* 2015). Different studies have however, revealed that enzyme production is a core factor in the entomopathogenicity and endophytism of *B. bassiana*, as well as its less-studied saprophytic role, however, there has been no focus on harnessing the potentials of the fungus for industrial enzyme production (Cito *et al.,* 2016; Elawati, Pujiyanto and Kusdiyantini 2018; Mancillas-Paredes *et al.,* 2019). In particular, there are currently no comprehensive scientific reports on the industrial potential of carbohydrate-active enzymes from *B. bassiana*. This is in spite of the fact that the safety of the fungus for human and animal use has been established in many studies that showed that *B. bassiana* strains are non-pathogenic to mammals, birds and plants (Vestergaard *et al.,* 2003; Zimmermann 2007). Furthermore, unlike in many other fungi where readily available plant biomasses have been used for carbohydrate-active enzymes production (Kubicek, and Kubicek, 2016, Saldarriaga-Hernández *et al.,* 2020), these substrates have not been used for the production of such enzymes in *B. bassiana*. Preliminary studies in our lab

have shown the potentials of an isolated *B. bassiana* strain to utilize various plant biomasses for its growth and secrete some industrially important enzymes, specifically, carbohydrate-active enzymes (amylase, cellulase, pectinase and xylanase) while growing on these substrates. However, the mechanism behind the utilization of plant lignocellulosic biomass by *B. bassiana* as its energy and carbon sources has not been elucidated in any study. Furthermore, the physicochemical and kinetic properties of these CAZy enzymes from *B. bassiana* have either been uncharacterized or not fully characterized as previous research have focused mainly on the chitinases (Fang *et al.,* 2005; Al Khoury *et al.,* 2019), lipases (Vici *et al.,* 2015; Doolotkeldieva *et al.,* 2019) and proteases (Borgi *et al.,* 2016; Cito *et al.,* 2016) from the fungus. Therefore, in this study the atypical ability of a *B. bassiana* strain to secrete different carbohydrases while utilizing lignocellulosic biomass was investigated. In this regard, the genetic basis of this metabolic versatility, as well as the conditions necessary for the production of these carbohydrases were studied. Attempts were also made to evaluate the physicochemical properties of the enzymes as well as their potentials in the saccharification of biomass and other industrial applications.

1.11 Aim and objectives

1.11.1 Aim

To investigate the production, biochemical properties and applications of biomass-degrading carbohydrases from *Beauveria bassiana*.

1.11.2 Objectives

- Enzymatic profiling of *B. bassiana* carbohydrases during fermentation on lignocellulosic biomass.
- Comparative analysis of *B. bassiana* transcriptome under endophytic and submerged fermentation conditions.
- Optimization of different process parameters for enhanced production of *B. bassiana* carbohydrases using response surface methodology.
- Purification and characterization of selected *B. bassiana* carbohydrases.
- Evaluation of the efficacy of *B. bassiana* carbohydrase in the saccharification of plant biomass, juice clarification and wastepaper deinking.

CHAPTER TWO

Carbon utilization profile and transcriptomic analysis of *Beauveria bassiana* SAN01 under different trophic conditions

Abstract

The environmental role of *Beauveria bassiana* as a saprophyte has become a focus of various scientific enquiries in recent times. Recently, an endophytic fungus with significant biomass-degrading activity was isolated from onion leaves in our laboratory and identified as *B. bassiana* by rDNA-ITS sequencing. This *Beauveria* strain designated as *B. bassiana* SAN01was observed to proliferate remarkably on different lignocellulosic biomass while simultaneously secreting various glycoside hydrolases. Hence, further studies were focused on the characterization of this novel strain and investigation of the metabolic and physiological changes occurring during the transition from its well-known role as an endophyte to a biomass-degrader. In this regard, the quantitative enzyme screening of *B. bassiana* SAN01 confirmed its ability to secrete biomass-degrading enzymes such as amylase, cellulase, laccase, pectinase and xylanase at significant levels. Furthermore, the metabolic profiling of *B. bassiana* SAN01 using the Biolog phenotypic microarray revealed the preference of polyols, pentoses, N-acetyl-D-glucosamine and a few other carbon sources. More importantly, the phenotypic plasticity of the fungus to basal media (control), plant extract (endophytic) and lignocellulosic biomass (fermentation/saprophytic) were elucidated by comparative genome-wide transcriptome analyses. The transcriptomic results demonstrated that a clear molecular distinction exists between the fungus under the different trophic states/conditions. In total, 4.42, 4.79 and 5.03% of the 10,365 predicted genes in *B. bassiana* SAN01 were differentially expressed between the endophytic vs fermentation states, endophytic vs control and the fermentation vs control states, respectively. It was further observed that the differentially expressed genes were involved in major biological processes associated with lignocellulose fermentation. These identified biological processes include but are not limited to carbohydrate metabolism, protein metabolism, cellular transport, oxidative stress and cell adhesion. CAZy annotation of *B. bassiana* SAN01 transcriptome corroborated the significant upregulation of glycoside hydrolases such as amylases, cellulases, chitinases, glucanases, lignases, pectinases and xylanases under fermentation condition. The results of this study highlight the endophytic to the saprophytic adaptation of *B. bassiana* SAN01 for the deconstruction of plant biomass. It is expected that these remarkable results will enhance future research targeted at the alternative industrial applications of the fungus, especially in the production of different carbohydrases.

2.1 Introduction

Beauveria bassiana is a filamentous fungus, referred to as an entomopathogenic fungal endophyte, having shown the ability to infect different insects, arachnids as well as nematodes; and also found to exist asymptotically in plants (Jensen *et al.,* 2020; Nishi *et al.,* 2020). Its renowned inherent entomopathogenic properties have made it the fungi of choice in the biological control of insects (Kim *et al.,* 2019; Bara and Laing 2020) and other pests including arachnids (Canassa *et al.,* 2020) and nematodes (Zhang *et al.,* 2020). In the same vein, its endophytic traits are being currently explored for their application as a growth promoter in different crop plants (Barra-Bucarei *et al.,* 2020b; Kuzhuppillymyal-Prabhakarankutty *et al.,* 2020). Besides its aforementioned entomopathogenic and endophytic lifestyles, *B. bassiana* has a less studied and less described environmental lifestyle which revolves around its saprophytic role in different ecosystems. This lifestyle may be viewed from one perspective as facultative, resulting from the subsequent adaptative shift from its two well-known entomopathogenic and endophytic lifestyles after the mortality or senescence of its insect and plant host, respectively (Chen *et al.,* 2017; McKinnon *et al.,* 2017; Ibrahim *et al.,* 2019). On the other hand, the fungus has been shown *ab initio* to grow and proliferate on different plant dry matter without any influence or linkage from its other biological states (Afifah and Saputro 2020; Permadi *et al.,* 2020). For instance, *B. bassiana* is typically cultivated for its blastospores using different agro-residues (Dhar, Jindal and Gupta 2016; Belay and Tenkegna 2017). Hence, this signifies that the fungus possesses an inherent ability to switch its metabolism and phenotype between different ecological roles in response to varying environmental circumstances.

Recently, experiments in our laboratory have revealed that a *B. bassiana* culture isolated in its endophytic state from onion leaves has the ability to utilize different biomass such as wheat bran, oatmeal and corn cob for its growth. It was remarkable that the growth of the fungus on these lignocellulosic substrates was accompanied by the extracellular production of various carbohydrate-active enzymes. The carbohydrase profiling of the fungal strain showed different production levels of biomass-degrading enzymes including amylase, cellulase (endoglucanase), laccase, pectinase (polygalacturonase) and xylanase. It is generally observed that these characters are unusual of endophytes and more likely of saprophytic fungi.

Although the ability of different endophytic fungi to switch to the saprophytic mode with a simultaneous change in metabolism and physiology has been observed in nature, the underlying mechanism of this change has not been well investigated, and particularly not in *B. bassiana.* Similarly, a deep understanding of the processes of gene regulation as well as the processes of protein secretion in a microbe is considered valuable. This is because the cell's ability to regulate these activities is important in its metabolism of different substrates and its continued survival in the environment. In the long run, it has been noted that an understanding of the "protein secretion mechanism" will allow the application of different microorganisms as "cellular factories" for the mass-production of industrially important proteins (Tjalsma *et al.,* 2000; Du and van Wezel 2018). In this regard, the "omics" tools, which include secretomics, proteomics, transcriptomics etc., have been widely used to identify and elucidate the enzyme repertoire in different industrially important organisms (Xie *et al.,* 2010; Alfaro *et al.,* 2016; Grosse-Holz *et al.,* 2018). Hence, insights into the adaptation response by *B. bassiana* under endophytic and fermentative/saprophytic conditions utilizing a joint transcriptomic and phenotypic microarray approach is presented in this chapter.

RNA sequencing (RNA-Seq), a high-throughput sequencing technology, has found immense applications in transcriptomics study because of its relatively higher resolution, low sampling bias, and broader expression range coverage (Stark, Grzelak and Hadfield 2019). This technology has been used to investigate different eukaryotic transcriptomes, especially fungi, under different growth, metabolic and environmental conditions with high sensitivity and low false-positive rates (Pawlik *et al.,* 2019; Jeon *et al.,* 2020; Srivastava *et al.,* 2020). Available literature has shown that the transcriptome of *B. bassiana* under different entomopathogenic conditions has been a subject of many investigations (Yang *et al.,* 2016; Lai *et al.,* 2017; Chen *et al.,* 2018a). However, there are no studies elucidating the transcriptome of the fungus under endophytic conditions. Previously, Luo *et al.,* (2015) gained some insights into the metabolic changes in *B. bassiana* under simulated entomopathogenic and endophytic conditions by analysing the secretome. However, despite various studies showing the ability of different strains of *B. bassiana* to metabolize and grow significantly on different lignocellulosic biomass, the gene expression pattern of the fungus under the fermentation/saprophytic condition has not been investigated. Thus, to explore the metabolic profile and physiological phenotype associated with the fermentation state and carbohydrase production, the transcriptomes

of *B. bassiana* SAN01 under fermentation and endophytic state were compared and analysed in this study. The fungus was grown on different substrates and under conditions that mimic the three different trophic states (mentioned previously) to evaluate its primary and secondary gene expression. The metabolic mechanisms of biomass degradation and endophytism were annotated by analysing the transcriptomes of *B. bassiana* with wheat bran (saprophytic/fermentation) or banana corm extract (endophytic) as the sole carbon sources and potato dextrose broth (*in vitro*) as the laboratory control.

By integrating the transcriptomic results of the fungus with its previously established genome (Xiao *et al.,* 2012), some molecular markers related to its biomass fermentation as well as its more studied endophytic role were identified and elucidated. In addition, the carbon utilization of cultures from *B. bassiana* SAN01 conidia was profiled using the Biolog Phenotypic MicroArray (PM) system. The Biolog PM technology has been previously used to accurately determine microbial nutritional requirements and global phenotypic characterization of co-inoculated *Beauveria* species (Canfora *et al.,* 2017) and other microbes (Reverberi *et al.,* 2013; Chaturvedi, DeFiglio and Chaturvedi 2018). The system has also been noted to complement genomic and proteomic studies in both eukaryotic and prokaryotic organisms (Borglin *et al.,* 2012; Reverberi *et al.,* 2013). Hence using these aforementioned methods, notable evidence to describe the changes during the transition from the endophytic to saprobic/fermentative modes were shown. Results from this study revealed novel and remarkable insights into the mechanisms of trophic adaptation in *B. bassiana* at the molecular level. Importantly, several novel candidate genes and biochemical pathways that should be examined in future experiments focused on the *B. bassiana* were presented. The valuable information obtained in this research will also be useful in understanding the cellular events occurring in other environmentally versatile organisms, especially the entomopathogenic, endophytic and saprophytic fungi.

2.2 Methodology

2.2.1 *Fungal isolation and maintenance*

The fungus was isolated in its endophytic state from onion leaves according to Caicedo *et al.,* (2019) method. Briefly, healthy onion leaves were collected in sterile polythene bags for the isolation of different endophytic fungi. After four days of incubation at 30°C, individual colonies were picked up and re-cultured on potato dextrose agar (PDA). The colonies were then sub-cultured thrice after which the purity of each colony was examined under an optical microscope. Subsequently, the isolate was selected based on the production of different carbohydrate-active enzymes as determined qualitatively (data not shown). Subsequently, the isolate was grown on oatmeal dodine agar (ODA) for 10 days at 30°C, after which fungal conidial suspensions were prepared as described previously (Beer *et al.,* 2020). The conidial suspension was stored at −80°C in a cryoprotective solution (10% v/v glycerol, 0.85% w/v NaCl) until further use.

2.2.2 Molecular identification

2.2.2.1 *DNA extraction*

Mycelia harvested from single spore cultures of the *Beauveria* isolate grown on oatmeal dodine broth for 10 days were subjected to DNA isolation using the ZR fungal DNA isolation kit (QIAGEN, Germany). The quality and concentration of DNA were evaluated by 1% agarose gel electrophoresis and the nanodrop spectrophotometer, respectively (Nsa *et al.,* 2020).

2.2.2.2 *ITS amplification*

The ITS region of the rDNA was amplified using primers ITS1 and ITS4 (White *et al.,* 1990). The primer details are as follows; ITS1 (TCCGTAGGTGAACCTGCCC) & ITS4 (TCCTCCGCTTATTGATATGC). Amplification reactions were carried out with 25 µL reaction mixtures containing 12.5 µL of 2X PCR mix (ThermoFisher Scientific, USA); 25 pmolmL^{-1} primers and 100 ng genomic DNA. The amplification cycle consisted of an initial denaturation at 95°C (5 min) followed by 35 cycles at 95°C (1 min), 55°C (1 min), and 72°C (3 min) and a final extension at 72°C (10 min). Amplified ITS rDNA region of the *Beauveria* isolate was purified using QIAquick PCR purification kit (QIAGEN, Germany), according to the manufacturer's instructions and sequenced according to Mehmood *et al.,* (2019). The sequences were compared to those in GenBank

(http://www.ncbi.nlm.nih.gov/) using Mega BLAST. The sequences with the highest homology and total score with the query were then noted for further analysis. All the DNA sequences were aligned with the program ClustalW and the resulting multiple-alignment file was used for phylogenetic analyses. The evolutionary relationship tree was inferred by the Neighbour-joining method using the Phlogeny.fr web server with default parameters. Bootstrap values of more than 70% are listed at the nodes (Dereeper *et al.,* 2008).

2.2.3 Enzyme profiling of *Beauveria bassiana* SAN01 during fermentation on lignocellulosic biomass

B. bassiana SAN01 was cultivated at 30°C for 12 days in shake flasks (120 rpm) containing 100 mL mineral medium (1 gL^{-1} KH_2PO_4, 0.5 gL^{-1} $MgSO_4$, 0.5 gL^{-1} $MgSO_4$, 0.25 gL^{-1} NaCl, 0.2 gL^{-1} $CaCl_2$, gL^{-1} $FeSO_4$) and wheat bran (4% w/v) as the sole carbon source. The culture fluid was harvested, centrifuged and the resulting supernatant was used as crude enzyme for the quantitative enzyme screening. Assays for amylase (Saad *et al.,* 2021), cellulase (Khan *et al.,* 2021), laccase (Ezike *et al.,* 2021), pectinase (Aggarwal, Dutta and Sheikh 2020) and xylanase (Bailey *et al.,* 1992) were carried out. One unit (U) of enzyme activity is defined as the amount of enzyme required to liberate 1 µmol of respective reaction product per min at 30°C.

2.2.4 Carbon utilization profile of *B. bassiana* SAN01 using phenotypic microarray

B. bassiana SAN01 was further characterized using the Omnilog™ system (Biolog, Inc., Hayward, CA) according to the manufacturer's instructions. The carbon assimilation profiles of *B. bassiana* under standard conditions were evaluated using Biolog FF plates (Biolog, Inc., Hayward, CA). The FF MicroPlate test panels contained 95 wells, each with a different carbon-containing compound, respectively, and one blank well, as a control. The prefilled, dried 96 well microplates contained a redox dye, Iodonitrotetrazolium violet (INT), which colourimetrically measure mitochondrial activity resulting from oxidation of metabolizable carbon sources. The inoculum for the plates was prepared by scrapping the *Beauveria* conidia from the agar surface, suspending it in 16 mL of FF inoculum media tubes (Biolog, Inc., Hayward, CA) and thoroughly mixing for uniformity. The turbidity of the spore suspension was measured at 590 nm using the Biolog Tubidometer to meet the required value (~75% transmittance) (Mchunu *et al.,* 2013). Into each well, 100 µl of the spore suspension was added and the

plates, in triplicates, were incubated in the dark at 30°C for 3 days. Subsequently, the assimilation rate (respiration rate) and biomass growth were measured using the Biolog Microstation. The Microstation computed the colour developed by fungal respiration at 490 nm and the turbidity, reflecting biomass production at 750 nm (Mao *et al.,* 2020).

2.2.5 Simulation of endophytic and fermentation conditions for *B. bassiana* SAN01 growth

Banana corm extract (BCB), prepared according to Niere *et al.,* (2006) method (with some modifications), was used to simulate the endophytic growth conditions for *B. bassiana* SAN01. Briefly, corms from approximately 50 cm high suckers of the Cavendish banana types collected from Port Shepstone, South Africa, were pared to remove roots and the adhering soil. The corms were then diced into pieces of approximately 1 cm^3 using a stainless-steel knife; 1 kg of the corm tissue was homogenized using a blender and boiled in 1 L distilled water for 20 min. Subsequently, the mixture was passed through muslin cloth to remove suspended particles. The resultant solution was kept in a biofreezer overnight and lyophilized. In contrast, commercial wheat bran (WB) was used as the growth media for fermentation conditions. The WB was dried at 40°C in a drier until constant weight, pulverised to 1.0 mm mesh size and stored for further use. While for the laboratory conditions, potato dextrose broth (PDB) was used as the basal media. For fungal growth, 4 g of BCB, WB and PDB were measured into 100 mL mineral solution (1 gL^{-1} KH_2PO_4, 0.5 gL^{-1} $MgSO_4$, 0.5 gL^{-1} $MgSO_4$, 0.25 gL^{-1} NaCl, 0.2 gL^{-1} $CaCl_2$, gL^{-1} $FeSO_4$) in 250 mL flasks and sterilized at 121°C for 15 min. The sterilized media were inoculated with 1 mL of the *B. bassiana* SAN01 spore suspension (1 x 10^7 spores mL^{-1}) and incubated for 12 days under darkness in static conditions at 30°C. Subsequently, the mycelial mat from each condition was harvested for biomass estimation and RNA isolation.

2.2.6 Transcriptomic analysis of *B. bassiana* SAN01 under different trophic states

2.2.6.1 *Preparation of B. bassiana SAN01 total RNA*

B. bassiana SAN01 mycelia from the simulated endophytic, fermentation and basal media (control) conditions were collected by centrifugation from the 12-day old culture and washed with sterile phosphate-buffered saline to remove any media components. Subsequently, the mycelia were ground into a fine powder using a pestle and a mortar under liquid nitrogen and the RNA was isolated using the RNeasy Mini Kit (QIAGEN,

Germany) according to the manufacturer's protocol. All RNA samples were treated with RNase-free DNase I (ThermoFisher Scientific, USA) to eliminate DNA contaminants. The concentration and integrity of the pooled total RNA were checked using a nano-spectrophotometer and 1% agarose gel.

2.2.6.2 *cDNA libraries preparation and RNA sequencing*

The total RNA quantity and integrity were assessed using a Qubit RNA assay kit (Invitrogen, USA) and a 4200 TapeStation instrument (Agilent Technologies, Germany). Approximately 1 μg of RNA was used for double-stranded cDNA synthesis using Maxima H minus double-stranded cDNA synthesis kit (Thermo Fisher Scientific, USA) primed with random hexamers. Illumina sequencing libraries were then prepared using Nextera DNA Flex Library Prep Kit and IDT for Illumina Nextera DNA UD Indexes (Illumina, USA) according to the manufacturer's instructions. Paired-end 150 bp sequencing was performed on a Nextseq 550 instrument with the 300-cycle mid-output reagent kit (Illumina, USA). The sequencing was carried out at the Sequencing Core Facility at the National Institute for Communicable Diseases (NICD), Johannesburg, South Africa.

2.2.6.3 *RNA-seq data analysis*

Generated raw reads were quality controlled and filtered (Q>5 and length > 50 bp) using FastQC (v0.11.8) and trim Galore (v0.6.2; https://github.com/FelixKrueger/TrimGalore), respectively. Subsequently, transcript quantification was performed by quasi-mapping the clean reads onto the transcriptome of *B. bassiana* strain ARSEF 2860 as the reference, using Salmon (Ibrahim *et al.,* 2021).

2.2.6.4 *Identification of differentially expressed genes*

Differentially expressed genes (DEGs) between the endophytic, fermentation (saprophytic) and control conditions (basal media) were identified using DESeq2 (version 1.18.1) in conjunction with the Salmon read abundance quantification tool (Sparks *et al.,* 2020). A *p*-value was determined to demonstrate the differences in expression between samples, while False discovery rates (FDRs) were used to calculate the *p-value* threshold. $FDR \leq 0.05$ and $\log^2 Ratio \geq 1$ were considered statistically significant (Tang *et al.,* 2018). The count data and transcript abundance were expressed in Transcripts per million (TPM) while further analyses were carried out using R (R Core Team, 2015) and Perl. The codes for constructing the heatmap, PCA scatter plot and the

volcano plot are available at GitHub (https://github.com/richysix/zfs-devstages) (White *et al.,* 2017).

2.2.6.5 *CAZymes identification and analysis*

For functional predictions of CAZymes, HotPep tool (Busk *et al.,* 2017) was used. The conserved motifs in Peptide Pattern Recognition (PPR) library were identified (Ravichandran *et al.,* 2020). In addition, the substrate specificities of the identified CAZymes were inferred by manual inspection of CAZy (www.cazy.org) and the BRENDA databases (www.brenda-enzymes.org) (Pilgaard *et al.,* 2019).

2.2.6.6 *Gene ontology analysis*

Gene ontology (GO) analyses were performed in OmicsBox. The functional analysis evaluated GO IDs from all GO categories (Biological Process, BP; Cellular Component, CC; Molecular Function, MF). Assignment of enzyme codes was also conducted within OmicsBox (Oppert *et al.,* 2020).

2.3 Results and discussion

2.3.1 ITS amplification of *B. bassiana* SAN01 genome

The rDNA-ITS gene sequences from the fungal isolate showed ~100% identity values when compared with the top hit BLAST results, which were all found to be *B. bassiana* strains, with 100% query cover. The endophytic *B. bassiana* isolate was subsequently referred to as *B. bassiana* SAN01. It was further observed from the phylogenetic tree that interspecific sequence divergence in the ITS region between *B. bassiana* SAN01 and other strains of the fungus such as *B. bassiana* SBI Bb01, *B. bassiana* SBI Bb02, *B. bassiana* SF 661, *B. bassiana* SF 676, *B. bassiana* SF 684, and *B. bassiana* SF 807 is zero (Figure 2.1). The phylogenetic tree was separated into 5 different clades, with *B. bassiana* SAN01 and other *B. bassiana* strains occupying one of the clades. Other *Beauveria* species including *B. brongniartii, B. autralis, B. sungii*, etc., were also identified, sharing 90-97% identity with the query. The close phylogenetic relationship and probably, the evolutionary relationship of the strain with other entomopathogenic fungi including *Akanthomyces*, *Cordyceps*, and *Lecanicillium* species was also highlighted on the tree. It is interesting to note that most of these fore-mentioned entomopathogenic fungi share the dual entomopathogenic and endophytic lifestyle with *B. bassiana* as many of them have also been shown to be endophytic (Nicoletti and

Becchimanzi 2020). The sequence of the amplified ITS region has been deposited at the National Centre for Biotechnology Information (NCBI) databank with accession no: CMN 544593.

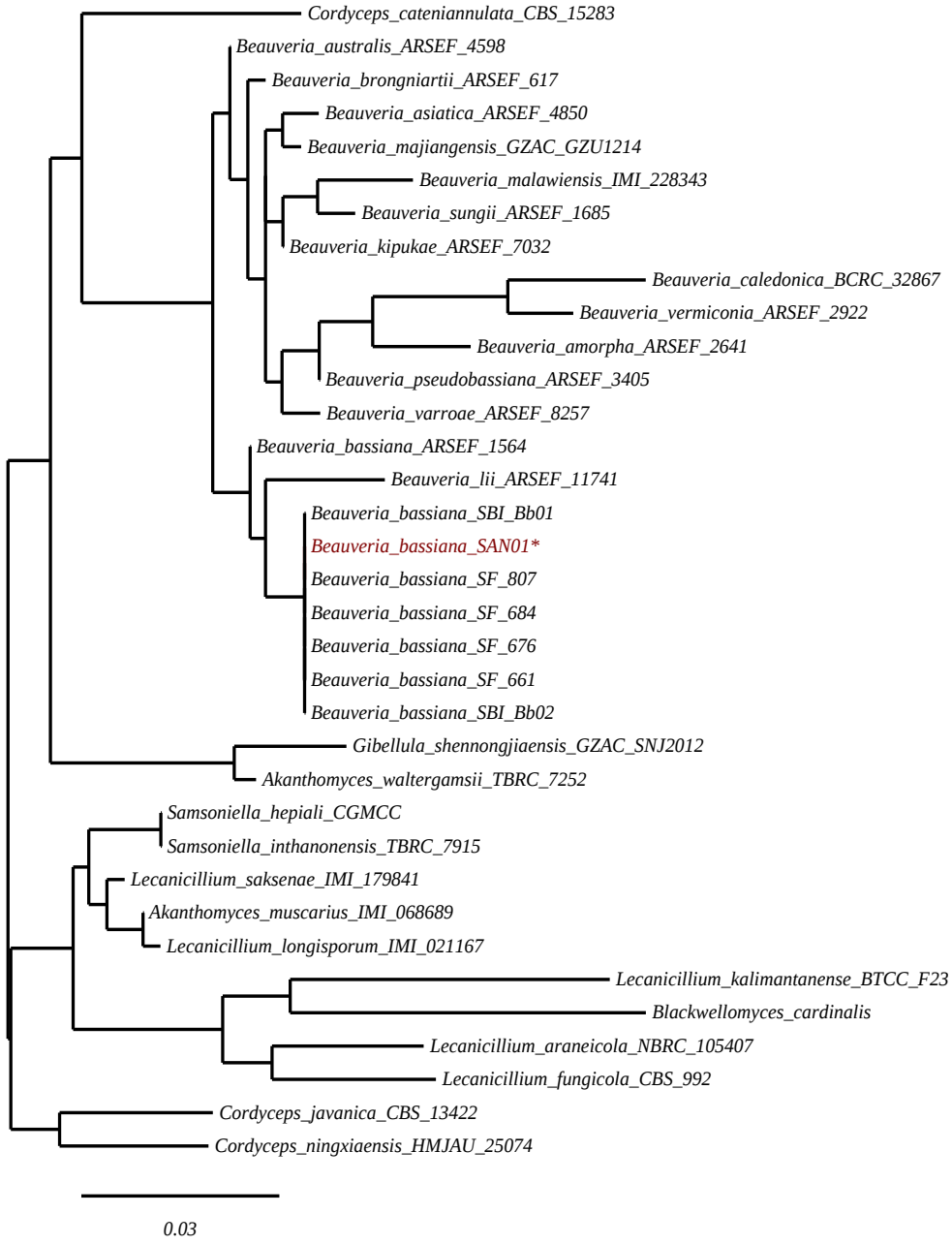

Figure 2.1: Phylogenetic tree showing the relationship between *B. bassiana* SAN01 ITS sequence and other closely related fungi. The evolutionary relationship tree was inferred by the Neighbour-joining method using the Phlogeny.fr web server with default parameters. Bootstrap values of more than 70% are listed at the nodes (Dereeper *et al.,* 2008). The GenBank accession numbers for the ITS gene sequence of the strains examined in this study are shown in Appendix 1. The asterisk indicates the query strain.

2.3.2 Carbohydrase profile of *B. bassiana* SAN01 during fermentation on lignocellulosic biomass

Results of the enzyme profile of *B. bassiana* SAN01, with a special focus on some of its biomass-degrading enzymes, are shown in Table 2.1. The quantitative screening showed significant extracellular secretion of amylase, cellulase (endoglucanase), laccase, pectinase (polygalacturonase) and xylanase. The production level of amylase from *B. bassiana* SAN01 while utilizing wheat bran as the sole carbon source under unoptimized conditions was 18.62 ±0.41 UmL^{-1}. Recently, Ryali *et al.,* (2020) demonstrated amylase production in a *Beauveria* strain, though at a lower level (~6.5 UmL^{-1}). However, while the study by Ryali *et al.,* (2020) made use of glucose as the main carbon source in addition to yeast extract and peptone, *B. bassiana* SAN01 amylase production was achieved with wheat bran as the sole carbon source.

The production of endoglucanase was demonstrated previously in *B. bassiana* both qualitatively (Petlamul *et al.,* 2017) and quantitatively (Petlamul and Boukaew 2019). However, endoglucanase production by *B. bassiana* SAN01 is significantly higher than the production level of 3.59 UmL^{-1} recorded previously (Petlamul and Boukaew 2019). The production level of endoglucanase observed in this study was 15.73 ±0.81 UmL^{-1}. Furthermore, unlike the wheat bran used in this study, carboxymethylcellulose, a pure synthetic compound was used to support endoglucanase production in the previous study (Petlamul and Boukaew 2019).

Laccase, a multi-copper oxidase involved in biomass deconstruction was also shown to be produced by *B. bassiana* SAN01 at a production level of 1.41±0.06 UmL^{-1}. Furthermore, it is significant that laccase production was achieved using wheat bran as the sole energy source and without any laccase inducer, such as copper. Recently, a *B. bassiana* strain was shown qualitatively to secrete laccase during its pathogenicity on insects to evade the host's immune defences (Lu *et al.,* 2021). Hence, this is the first study to determine the laccase from *B. bassiana* quantitatively. The production of polygalacturonase (pectinase) by *B. bassiana* SAN01 was also assessed. According to the available literature, the polygalacturonase activity observed in the study, 25.68 ± 1.16 UmL^{-1}, is the highest achieved so far. However, the production of polygalacturonase from *B. bassiana* was shown qualitatively in a previous study by Fernandes *et al.,* (2012). Notably, a high production level of xylanase was recorded with *B. bassiana* SAN01 in this study. The production level of 292.56 ± 13.37 UmL^{-1} observed in *B. bassiana* SAN01

is the highest recorded so far for any *Beauveria* species being approximately 8-fold higher than the production level observed earlier in *B. bassiana* B14532 (39 UmL^{-1}) (Petlamul and Boukaew 2019). Furthermore, unlike the readily available agro-residue utilized by *B. bassiana* SAN01 for xylanase production in this study, Petlamul and Boukaew (2019) made use of pure xylan for *B. bassiana* B14532 xylanase production. According to available literature, this is also the highest xylanase production level observed in any entomopathogenic fungi.

Table 2.1: Quantitative screening of some biomass-degrading enzymes from *B. bassiana* SAN01

Enzyme	Production level (UmL^{-1})
Amylase	18.62 ±0.41
Cellulase (Endoglucanase)	15.73 ±0.81
Laccase	1.41 ± 0.06
Pectinase (Polygalacturonase)	25.68 ± 1.16
Xylanase	292.56 ± 13.37

2.3.3 Carbon utilization profile of *B. bassiana* SAN01

The carbon utilization pattern of *B. bassiana* SAN01 was evaluated using the FF MicroPlate test plate (Appendix 2). The 95 substrates in the microplate were divided into 15 classes in addition to water, and the average absorbances for all analytes in each category were evaluated. These classes include aliphatic organic acids, biogenic and heterocyclic amines, glucosides, heptoses, hexosamines, hexoses, Kreb's-cycle intermediates, L-amino acids, oligosaccharides, pentoses, peptides, polyols, polysaccharides, sugar acids, water and others (Reverberi *et al.,* 2013). The data obtained from the Biolog microplate reader were subsequently analysed by hierarchical cluster analysis (Figure 2.2 & 2.3). Results showed 4 distinct clusters for carbon assimilation measured at 490 nm (Figure 2.2), while 3 main clusters were computed for biomass growth at 750 nm (Figure 2.3). The general assimilation hierarchical cluster revealed that

the most assimilated carbon sources were in Cluster III while the least assimilated ones were grouped in Cluster IV. The medium assimilated carbon sources were in Clusters I and II. The top thirteen highly assimilated carbon sources by the fungus were xylitol, N-acetyl-D-glucosamine, D-ribose, D-sorbitol, turanose, D-xylose, D-melibiose, β-methyl-D-glucoside, glycyl-L-glutamic acid, sucrose, D-gluconic acid, L-proline and L-phenylalanine in that order.

Polyols such as sorbitol and xylitol have been widely distributed in fungi, serving various metabolic roles. A fungal consortium was shown previously to utilize xylitol at a rate higher than all other carbon sources used (Gryta, Frąc and Oszust 2020); a similar observation was also made in a *Trichoderma* strain (Wang and Zhuang 2020). Likewise, sorbitol has been shown to promote increased growth rate in different fungi (Patriarca *et al.,* 2011). The ability of a *B. bassiana* strain to metabolise N-acetyl-D-glucosamine, D-sorbitol and turanose at a relatively high rate in FF microplates has been reported (Canfora *et al.,* 2017). The highest utilization of N-acetyl-D-glucosamine observed in this study is not unexpected as it is the building block of chitin, the main component of fungal cell walls, as well as a major component of *B. bassiana*'s target hosts such as insects. This sugar has been shown to support the highest respiration and growth in different fungal species including *Benjaminiella poitrasii, Mycotypha microspora* and *Saksenaea oblongispora* (Pawłowska *et al.,* 2019).

Turanose, which was more metabolized than its isomer, sucrose, has been highlighted as a potential indicator of virulence in various studies, as well as a promoter of mycelial growth (Loesch, Hutwimmer and Strasser 2010; Kaur *et al.,* 2015). It was observed that more than 50% of the most metabolized carbon compounds were sugars while the remaining metabolites were amino-acids and dipeptides. Of all the metabolites evaluated in this study, the least metabolizable and least growth supporting carbon sources were glucuronamide, D-galacturonic acid, α-methyl-D-glucoside, N-acetyl-D-mannosamine, sedoheptulosan, β-cyclodextrin, α-cyclodextrin, uridine, D-glucuronic acid, D-psicose, L-lactic acid, D-lactic acid methyl ester, gentiobiose, succinamic acid and β-methyl-D-galactoside. Previous studies have recorded low respiration and slow biomass growth in fungi utilizing cyclodextrin (Zhu *et al.,* 2020), glucuronamide (Fuentes and Quiñones 2016) as well as, N-acetyl-D- mannosamine and sedoheptulosan (Canfora *et al.,* 2017). Furthermore, the inhibitory effects of some of these metabolites on fungal growth across different strains have been highlighted in many studies (Deepthi *et al.,* 2016; Wang *et*

al., 2016a; Mamat *et al.,* 2018; Shehata *et al.,* 2019). Similar patterns of sugar assimilation were also observed in the biomass growth analyses, except that the classification in the biomass growth analyses has been widened. For instance, the most highly assimilated sugars clustered together in cluster III of the assimilation plot have been included in the larger cluster I of the biomass growth plot. Thus, this biomass growth plot cluster I contain the highest growth supporting carbon sources. This notion was confirmed by the very high correlation between the rate of sugar assimilation and the rate of biomass growth shown in the correlation scatter plots (Figure 2.4, respectively). From the scatter plot, the positive correlations between the respiration rate and assimilation rates of the different analytes are highlighted by the simultaneous increase in the values on both the x- and y-axes. The strength of the positive relationship is also demonstrated by the fact that the data points on the plot are clustered closely tending to form a straight line with a slope of ~ +1. The Pearson correlation coefficient between carbon assimilation and biomass growth was also computed to be 0.93, which further reinforces the high correlation between the two variables. Compared to some other fungal strains, *B. bassiana* SAN01 exhibited high substrate utilization efficiency. The high efficiency may be used as an indicator of the ecological role of the strain as such microbes have been noted to be biomass-degrading or endophytic or parasitic as the case may be (Wang and Zhuang 2020). In this regard, *B. bassiana* has been shown in different studies to belong to all of the afore-mentioned ecological classes.

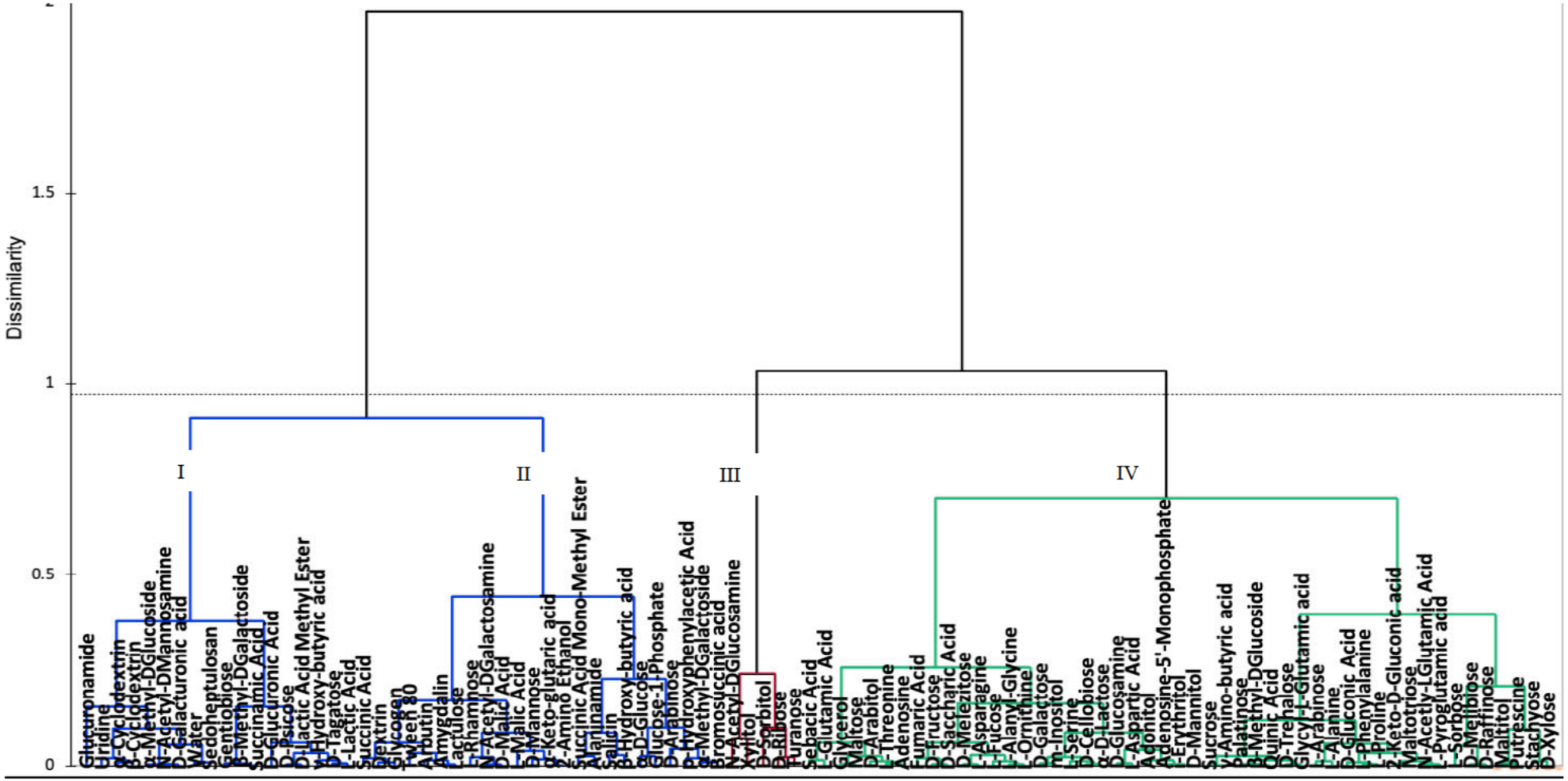

Figure 2.2: Joining cluster analysis applied to 95 carbon sources based on their assimilation and utilization by *B. bassiana* SAN01 measured at 490 nm using the Biolog system.

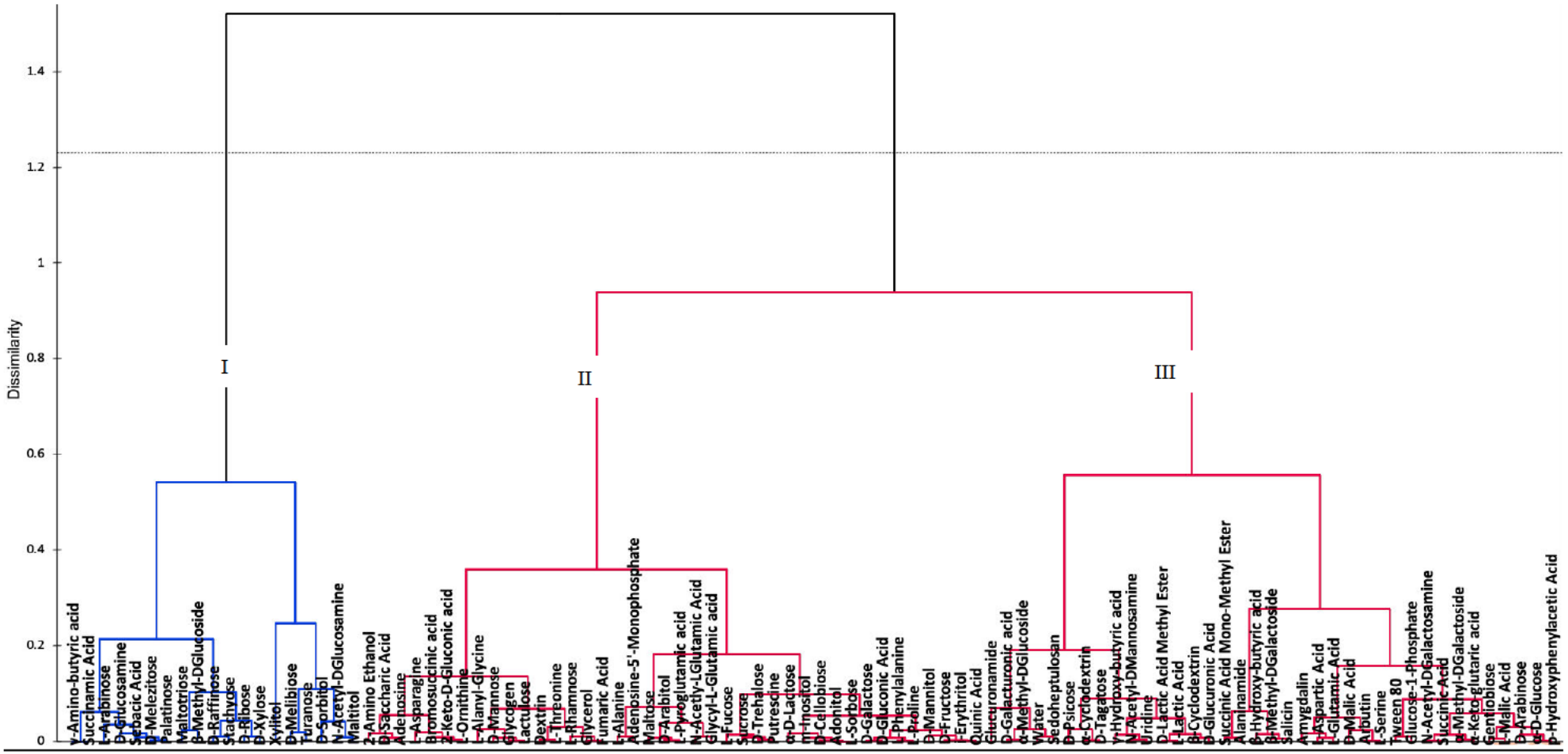

Figure 2.3: Joining cluster analysis applied to 95 carbon sources based on the growth of *B. bassiana* SAN01 measured at 750 nm using the Biolog system.

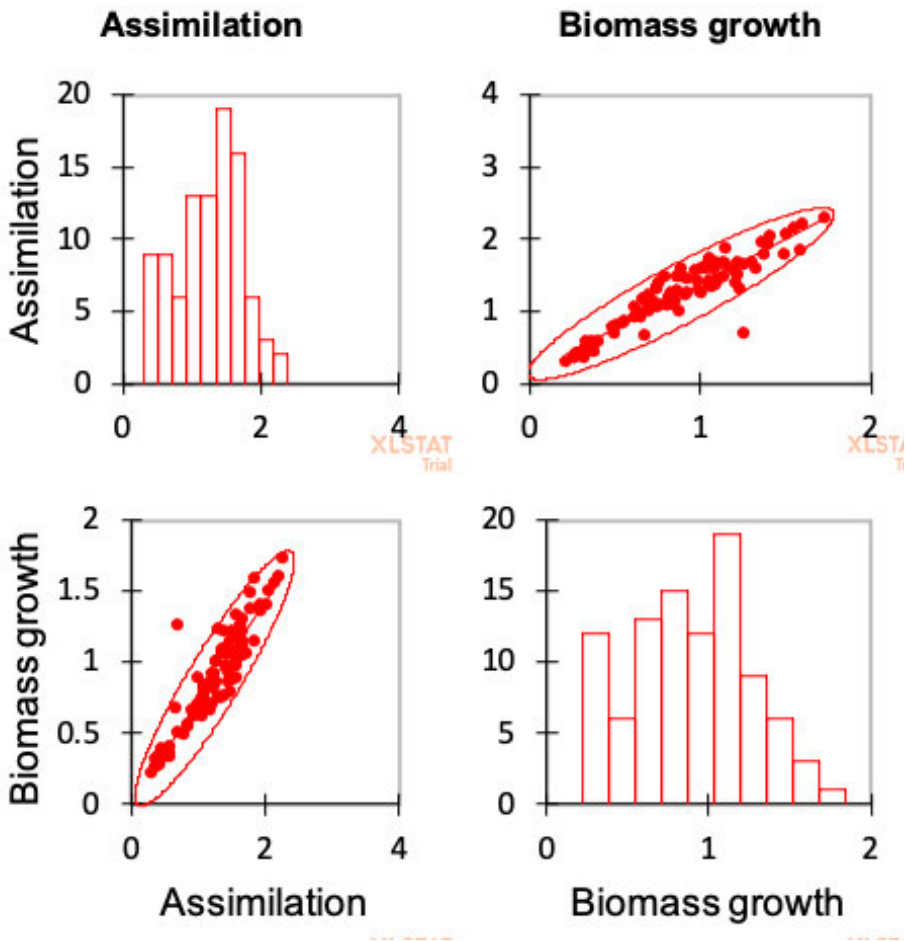

Figure 2.4: Scatter plot showing the correlation between data from assimilation and biomass growth

2.3.4 Transcriptomic analysis

2.3.4.1 *Overview of the sequencing data obtained from B. bassiana* SAN01 *transcriptomic analysis*

To elucidate the dynamic transcriptional reprogramming in *B. bassiana* SAN01 under different trophic states, genome-wide transcriptome analysis was performed using RNA-Seq. In total, paired-end sequencing of cDNA libraries generated a total of 347,059,856 raw reads, and approximately 31,710,101, 36,809,435 and 33,093,009 clean reads were obtained from the endophytic, fermentation and laboratory control groups, respectively. The genome of the reference strain, *B. bassiana* ARSEF 2860, comprises 10,366 protein-coding genes (Xiao *et al.,* 2012). After mapping to the gene models of the *B. bassiana* reference genome, 10,365 putative genes were quantified from the three different trophic

states, indicating that approximately 100% of the *B. bassiana* genes predicted in the reference genome were represented under the three experimental conditions.

2.3.3.2 *Dynamics of differentially expressed genes (DEGs) in B. bassiana* SAN01 *under the different trophic states*

Although *B. bassiana* has been shown to exist under different environmental conditions, utilizing different nutritional sources in the process, the underlying mechanism behind such transition remain largely unknown. Hence, identifying the DEGs within the different groups would help understand this plasticity at the molecular level. In the present study, a differentially expressed gene was considered significant if it had a Log_2fold change of 1.0 over the other trophic state and a false-discovery rate (q-value) of < 0.05 (Ortiz *et al.,* 2019). Pairs of samples were then analysed to obtain information about expression differences among the trophic states. Based on these criteria, a total of 458, 497 and 521 and genes were differently expressed between the endophytic vs fermentation, endophytic vs control and the fermentation vs control groups, respectively (Table 2.2). These data imply that each trophic state has specific characteristics which interfere with specific biological processes in *B. bassiana* SAN01. Between the endophytic and fermentation groups, 185 genes were upregulated in the endophytic state while 273 genes were upregulated in the fermentation state. In addition, compared to the control group, the endophytic state had 182 upregulated genes while the fermentation group had 340 upregulated genes.

Table 2.2: Number of *B. bassiana* SAN01 DEGs under endophytic, fermentation and control trophic states

	Number of differentially expressed genes (log2 fold change > 1, at p < 0.05)	
Growth conditions assessed	**Upregulated**	**Downregulated**
Endophytic vs Control	182	315
Fermentation vs Control	340	181
Endophytic vs Fermentation	185	273

Furthermore, Pearson correlation analysis was carried out to evaluate the reproducibility of DEG library sequencing and reveal the correlation between the biological replicates of each group. A corrected p-value of <0.05 was used as the threshold to judge the significant differences in gene expression. The results showed a strong correlation between replicates of a single condition and a distinct separation between independent conditions (Table 2.3). The square of the Pearson correlation coefficient (R^2) varied between 0.99–1.0 in the endophytic group, 0.948–1.0 in the fermentation group, and 0.99–1.0 in the control group, indicating good operational stability and reliability of DEG library sequencing. In addition, a strong correlation was observed between the endophytic samples and the control samples (0.76-0.8), thus signifying a high similarity between the DEGs within these 2 groups. On the other hand, the fermentation group was weakly correlated with the 2 other groups, having an R^2 value of 0.346-0.354 and 0.32-0.34 relative to the endophytic and control groups.

Table 2.3: Pearson correlation matrix of *B. bassiana* SAN01 transcriptomes under endophytic, fermentation and control trophic states

Variable	Endophyte 1*	Endophyte 2*	Fermentation 1*	Fermentation 2*	Laboratory 1*	Laboratory 2*
Endophyte 1	1					
Endophyte 2	0.99022796	1				
Fermentation 1	0.33104134	0.32459457	1			
Fermentation 2	0.35427626	0.3461916	0.94773373	1		
Laboratory 1	0.80085131	0.7643803	0.32196436	0.34293781	1	
Laboratory 2	0.81997908	0.78605326	0.33205503	0.35256833	0.99086902	1

*1 and 2 represent biological replicates of each sample

Due to the high-dimensional nature of the transcriptome data, multivariate analysis by Principal Component Analysis (PCA) was applied to reduce the dimensions, followed by the visualization of the reduced components on the scatterplot and heatmap. The 2-dimensional PCA scatter plot based on read counts confirmed the distinction of expression profiles of the endophytic, fermentation and control trophic states (Figure

2.5). In addition, it also illustrated the proximity of biological replicates as was earlier observed in the correlation analysis. The PCA plot shows a distinct separation of the fungal strain growing under different trophic states based on their gene expression profiles. PC1 and PC2 accounted for more than 90% of the total variance observed in the dataset. It was observed from the PCA that the largest variance of 96.5% was along PC1 while the variance between the samples along PC2 was 0.1.

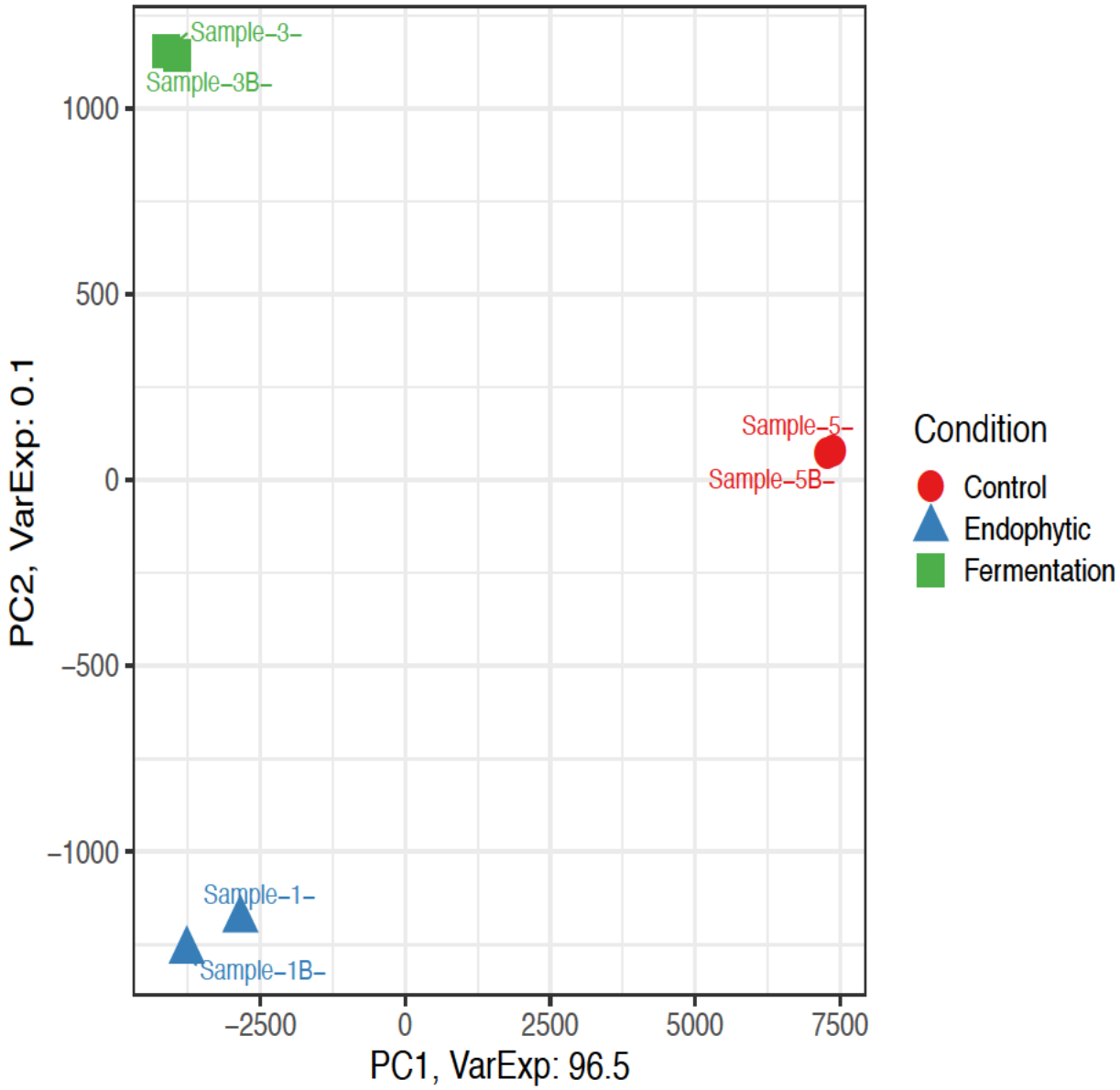

Figure 2.5: Principal component analysis of *B. bassiana* SAN01 DEGs under endophytic vs fermentation vs control conditions. The gene expression data were mean centred prior to PCA. Samples were plotted according to the first and second principal component scores.

A considerable modulation of gene expression in *B. bassiana* SAN01 following growth under the three different growth conditions is elucidated in the global heatmap representation of its gene expression profile (Figure 2.6). The gene expression clustering analysis of DEGs across the trophic conditions effectively established the commonalities in the DEGs. Also, it estimated the similarity of gene functions based on the similarity in expression. Hierarchical clustering analysis of the differentially expressed genes across the three groups indicated that the samples could be divided into two clusters. Cluster I contains the two biological replicates of the fermentation conditions and cluster II encompasses both replicates of the endophytic and control conditions. The results showed that the expression pattern of DEGs under endophytic conditions was closely related to that under control conditions, as was earlier shown in the correlation analysis and the scatter plot. The heatmap also showed that the DEGs could be divided into two main clusters of expression patterns, which consist of the highly expressed genes, BBA 05586 (heat shock protein 70-2), BBA 06516 (heat shock protein Hsp90), BBA 02388 (translation elongation factor 1 alpha) and BBA 08907 (plasma membrane ATPase (Proton pump). The other main cluster group subdivided into 7 smaller clusters consists of the other DEGs, which are moderately and lowly transcribed compared to the first main cluster.

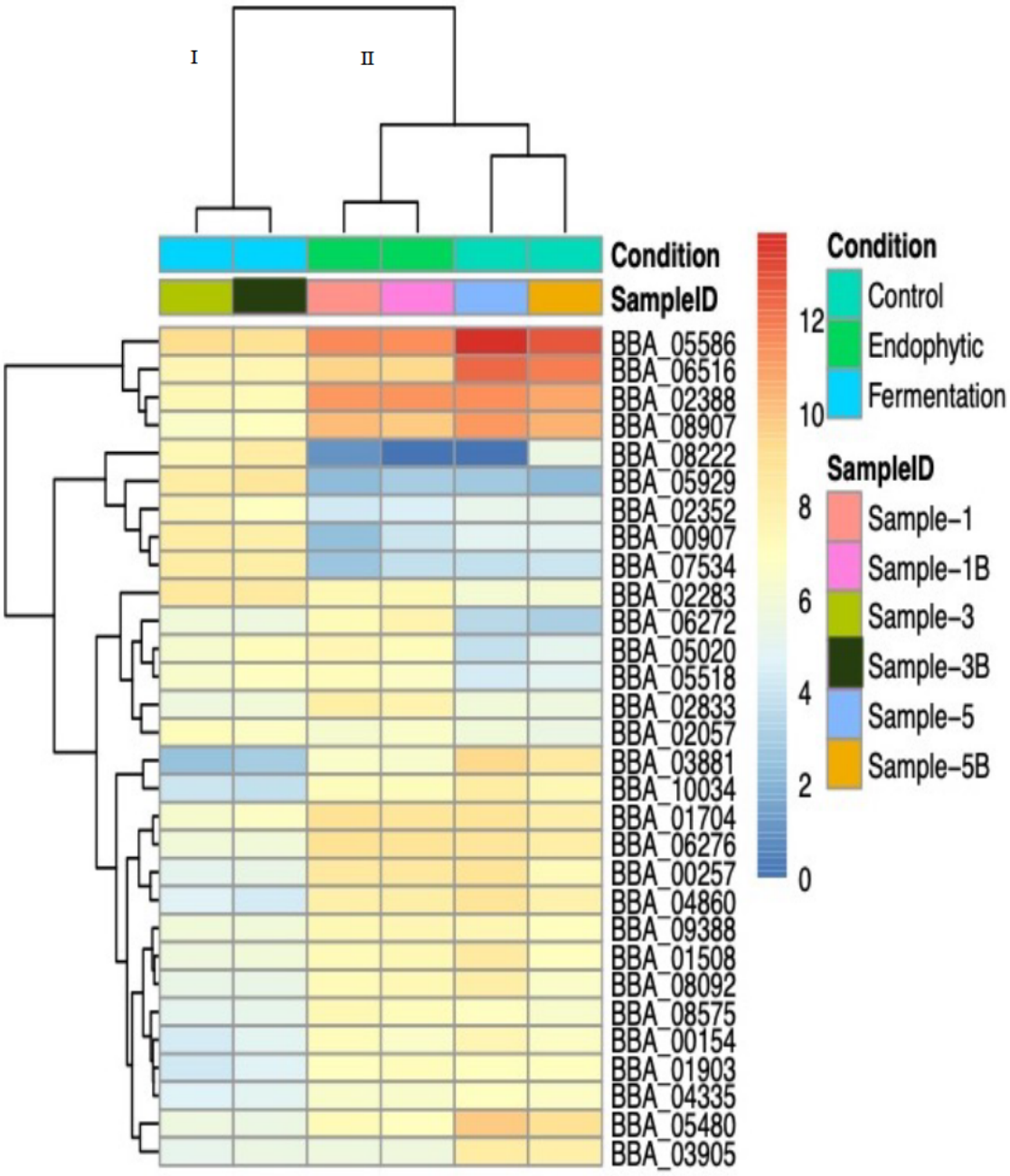

Figure 2.6: Heat map depicting the top differentially expressed genes in *B. bassiana* SAN01 across the endophytic, fermentation and laboratory states. Gene expression in red shows upregulated, while blue represents downregulated genes. Genes were clustered by their expression pattern. The transcription level is depicted in logFC values.

Furthermore, a pairwise comparison was made between the 3 experimental conditions using the volcano plot. The plots show that the number of DEGs is significantly higher between the endophytic and fermentation groups (Fig 2.7 b) compared to the other paired groups (Fig 2.7a & c). Similarly, there are also more highly upregulated genes in the endophytic vs fermentation group (Fig 2.7 b).

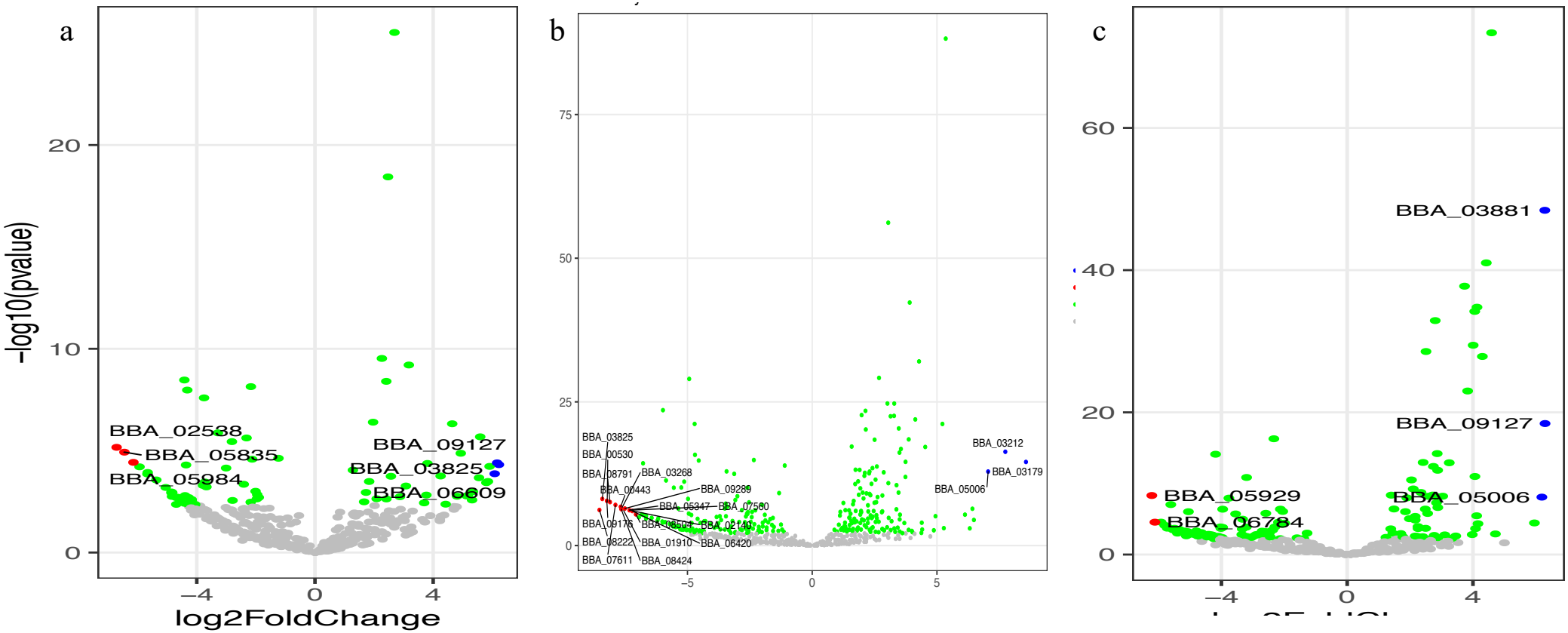

Figure 2.7: Volcano plots of differentially expressed genes (DEGs) in the interaction transcriptome of *B. bassiana* SAN01. The abscissa denotes the fold change in gene expression in different samples while the ordinate represents the statistical significance of the difference in gene expression. (a) control vs endophytic; red and blue dots represent upregulated genes in control and endophytic state respectively (b) endophytic vs fermentation; red and blue dots represent upregulated genes in endophytic and fermentation state respectively (c) control vs fermentation; red and blue dots represent upregulated genes in control and fermentation state respectively. In all of the charts, green dots represent lowly up/regulated genes while grey dots represent non-significant genes.

2.3.4.3 *DEGs between endophytic vs fermentation trophic states of B. bassiana* **SAN01**

The analysis of the DEGs in the endophytic vs fermentation group showed that most of the regulated genes were the genes involved in the metabolism and transportation of amino acids, nucleotides, simple sugars, fatty acids, metal ions, low molecular weight organic substances as well as pH balance. In addition, the genes responsible for the metabolism of carbohydrate polymers were also differentially transcribed. Specifically, the twenty most upregulated genes in the endophytic state relative to the fermentation state are represented in Table 2.4. It ranged from the gene for calcium-transporting ATPase to that of GATA transcription factor which was ~380 and 20 folds higher in the endophytic state. Different ATPases including the calcium-transporting ATPase (Log_2FoldChange; LFC=8.57) and the potassium/sodium efflux P-type ATPase (LFC=5.35), were mostly upregulated in the endophytic state.

The roles of endophytic microbes in plants uptake of metal ions have been highlighted in previous studies (Ren, Li and Gao 2011; Ortiz *et al.,* 2019), and the ATPases have been shown to contribute significantly to these uptakes (Benito *et al.,* 2004). Many of the major facilitator superfamily transporters were also observed to be highly transcribed in the endophytic state. These transporters are actively involved in the trafficking of simple substances across bio-membranes including amino acids, simple sugars, inositols, drugs, nucleosides, organophosphate esters, etc. (Wang *et al.,* 2020a). Hence, the fungus needs these transporters to assimilate the simple compounds prevalent in the endophytic media. Furthermore, these transporters have also been observed to significantly modulate metal ion homeostasis in organisms, reinforcing the heightened increase in ATPases (Lee *et al*., 2021). It was also observed that the transportation mechanism of the fungal strain was supported by different ABC transporters as well as the general substrate transporters as a result of their significant upregulation. Members of the ABC transporters have been identified previously as important factors in plant growth-promoting endophytes (Taghavi *et al.,* 2010; Ali *et al.,* 2014).

A variety of kinases were also observed to be significantly more expressed under the simulated endophytic condition. A notable example is the acetate kinase (LFC=4.94), while others are glycerol kinase (LFC=2.34), hexokinase (3.38), and phosphoenolpyruvate carboxykinase (LFC=2.15). The acetic acid kinase is responsible

for converting acetic acids to acetyl-CoA; in this regard, the high organic acid content of root exudates and plant may be responsible for its observed upregulation. The upregulation of different kinase has also been shown in the fungus *Phomopsis liquidambari*, while in its endophytic state (Zhou *et al.,* 2018). In response to the content of the endophytic growth medium, the genes responsible for the metabolism of amino acids, simple sugars, organic acids and even aromatic compounds were significantly upregulated. For amino acid and peptide metabolism, some of the upregulated genes include indoleamine c3-dioxygenase, general amino acid permease, amino acid/polyamine transporter I, argininosuccinate lyase while for simple sugar malate dehydrogenase.

Table 2.4: Top 20 upregulated genes in *B. bassiana* SAN01 under the endophytic state relative to the fermentation state.

GeneID	Gene Product	log_2-FoldChange	p-value
BBA_03179	Calcium-transporting ATPase	8.567336	2.92E-15
BBA_03212	Phthalate transporter	7.739423	4.9E-17
BBA_05006	Nucleotide sugar dehydrogenase	7.052259	1.31E-13
BBA_10175	Major facilitator superfamily transporter	6.481653	3.48E-05
BBA_10134	Fatty acid hydroxylase superfamily protein	6.422207	3.91E-07
BBA_03270	Hypothetical protein	6.315182	0.001035
BBA_06196	Monooxygenase 2C FAD-binding protein	6.124484	4.21E-06
BBA_04957	Potassium/sodium efflux P-type ATPase	5.352568	6.05E-89
BBA_05116	HCO3- transporter family protein	5.275751	0.000936
BBA_08160	ABC transporter	5.219571	7.03E-22
BBA_09255	Acetate kinase	4.941589	7.83E-06
BBA_04033	General substrate transporter	4.875363	0.002206
BBA_03178	Hypothetical protein	4.733628	0.026165
BBA_07968	Ankyrin repeat protein	4.531228	7.04E-18
BBA_05117	SET domain-containing protein	4.409406	0.001619
BBA_04785	Phosphatidylinositol transfer protein CSR1	4.397571	0.000207
BBA_06033	Lamb/ycsf family protein	4.39139	0.000107
BBA_01102	Fungal specific transcription factor	4.37674	0.006224
BBA_05835	Putative peptide transporter	4.283366	9.14E-33
BBA_02538	GATA transcription factor	4.132582	1.13E-22

The 20 most upregulated genes in the fermentation state relative to the endophytic state are shown in Table 2.5. It was observed that the genes for the hydrolysis of complex polymers including proteins, carbohydrates and lipids form a major part of the genes upregulated in the fermentation state. Non-ribosomal peptide synthetases (NRPS) catalyze the synthesis of highly diverse products in fungi. Although the biological functions of NRPS are largely unknown, they have been shown in some studies to be involved in cell surface properties, morphological and reproductive development, nutrient acquisition, virulence as well as protection against oxidative stress (Iqbal *et al.,* 2019). However, in *B. bassiana*, some products of these genes, such as beauvericin and bassianolide, are involved in host pathogenesis and stress response (Harith-Fadzilah Iqbal *et al.,* 2020). Hence, the significant upregulation of these genes (LFC= 8.53, 7.89 & 7.66) in the fermentation state is not unexpected as it is believed that there is a thin line between host pathogenicity and saphrophytism in *B. bassiana*. This fact was recently described in another group of entomopathogenic fungi belonging to the *Metarhizium* genus (St. Leger and Wang 2020). Further buttressing this point is the upregulation of the gene for cytochrome P450 CYP6001C8 (LFC=8.41). This cytochrome which was also found upregulated in a *B. bassiana* while under stress, was directly involved in cell rescue, cell defence and antioxidative response, which are all key components of its entomopathogenicity (Chu, Feng and Ying 2015).

A large repertoire of proteases was also found to be significantly upregulated in the fermentation/saprophytic state. From Table 2.5, four different proteases were highlighted among the top 20 upregulated genes, signifying their importance under this environmental state. It was also posited that fungal proteases are essential for the activation of hydrolytic enzymes such as β-1,4-endoglucanase (Miao *et al.,* 2019). In addition, the metabolism of the protein component of the plant biomass necessitates the action of different proteases. Furthermore, *B. bassiana* has been known to be a major producer of different proteolytic enzymes, as these enzymes are one of the principal factors in its entomopathogenicity (Gu *et al.,* 2020; Shahriari *et al.,* 2021).

Adhesin and hydrophobins are 2 groups of cell wall proteins that are important for fungal adherence to substrate or host by creating hydrophobic surfaces (Litwin, Nowak and Różalska 2020; Nene and Joshi 2020). In this study, adhesin proteins and hydrophobins were among the highly expressed genes in the fermentation group relative to the endophytic condition with LFC of 6.94 and 8.22, respectively. The function of these

proteins in the adaptation of different fungi to lignocellulosic biomass before subsequent hydrolysis has been shown in previous studies (Nene and Joshi 2020). The genes of these proteins have also been shown to be highly upregulated during the adherence and degradation of biomass (Brown *et al.,* 2016).

The degradation and utilization of plant biomass require an array of enzymes that act synergistically on the various polysaccharides such as cellulose, hemicelluloses, pectin and starch. The potential of *B. bassiana* SAN01 in the deconstruction of biomass is evident from the diversity of enzymes belonging to glycosyl hydrolase which were upregulated. Prominent among the upregulated carbohydrate depolymerases are different isoforms of α-glucosidases, β- glucosidases, polygalacturonase, endoglucanases, pectin lyase and α-xylosidase. Other biomass-degrading enzymes that were observed to be upregulated in the fermentation group are α-glucosidases, cellulases and different hemicellulolytic enzymes. In addition to these glycosyl hydrolases, several other ancillary proteins involved in biomass hydrolysis were also upregulated in the fungal strain. These include laccases, multicopper oxidase, catalase/peroxidase and several glycosyl transporters. This suggests that a significant number of transcripts have differential expression of carbohydrate acting enzymes at the transcript level. An earlier report on the *B. bassiana* genome has revealed 417 genes for the carbohydrate-active enzymes making this fungus a rich repository of biomass-degrading enzymes (Xiao *et al.,* 2012). The transcriptome of the fungus has shown that it encodes potential genes for the digestion of the three major classes of plant cell wall polysaccharides, i.e., cellulose, hemicelluloses, and pectin, as well as the main plant storage polysaccharide, starch.

Table 2.5: Top 20 upregulated genes in *B. bassiana* SAN01 under the fermentation state relative to the endophytic state

GeneID	Gene Product	log_2-FoldChange	p-value
BBA_08222	Nonribosomal peptide synthase 2C	8.52808	6.41E-07
BBA_03825	Cytochrome P450 CYP6001C8	8.41319	7.66E-09
BBA_09176	Alkaline serine protease AoRo	8.23239	1.65E-08
BBA_00530	Hydrophobin 2	8.21658	2.27E-08
BBA_08791	Alkaline serine protease AoRo	8.1059	2.73E-08
BBA_07611	Non-ribosomal peptide synthetase	7.88696	8.45E-08
BBA_00443	Cuticle-degrading protease bassiasin I precursor	7.67838	1.79E-07
BBA_08424	Nonribosomal peptide synthase 2C	7.65505	4.55E-07
BBA_03268	Hypothetical protein	7.61801	2.29E-07
BBA_01910	Hypothetical protein	7.55884	8.37E-07
BBA_09289	Pectin lyase fold	7.51033	3.65E-07
BBA_07560	Hypothetical protein	7.32668	7.16E-07
BBA_05347	Ncp1-like protein	7.31775	6.26E-07
BBA_02140	Hypothetical protein	7.22372	8.89E-07
BBA_06420	Oligopeptide transporter	7.21121	9.64E-07
BBA_08504	Hypothetical protein	7.07051	3.69E-06
BBA_02155	Cytochrome P450 CYP6003A1	6.94775	2.54E-06
BBA_02379	Adhesin protein Mad2	6.94355	1.15E-05
BBA_07294	Protease S8 tripeptidyl peptidase I (cln2)	6.91503	2.94E-06
BBA_03883	Phytase 2C putative	6.83749	3.6E-06

2.3.4.4 *DEGs between endophytic vs control trophic states of B. bassiana* SAN01

The top 20 upregulated genes in the endophytic state relative to the control are highlighted in Table 2.6. The gene for GATA transcription factor (LFC=6.71) was observed to be the most upregulated gene in the endophytic state. This transcription factor has been linked to the utilization of nitrogen sources and is upregulated during nitrogen starvation (Scazzocchio 2000). Wang, Hu and Leger (2005) showed that nitrogen-starvation-responded protein was upregulated 3.07-fold in root exudates by *M. anisopliae* due to nitrogen starvation. Generally, it was observed that most upregulated genes were the ones involved in the inward and outward transportation of extracellular substances. These include a putative peptide transporter, the calcium-transporting ATPase, the TBC domain-containing protein, SOM1 protein, major facilitator superfamily transporter, polyamine transporter TPO5, calcium-transporting ATPase, and the potassium/sodium efflux P-type ATPase. The expression of various pH regulatory proteins was also upregulated in the endophytic state; however, there are no specific metabolic roles for these proteins according to available literature.

Table 2.6: Top 20 upregulated genes in *B. bassiana* SAN01 under the endophytic state relative to the control state

GeneID	Gene Product	log_2-FoldChange	p-value
BBA_02538	GATA transcription factor	6.710258	6.88E-06
BBA_05835	Putative peptide transporter	6.447709	1.19E-05
BBA_05984	pH regulatory protein	6.143352	3.75E-05
BBA_03179	Calcium-transporting ATPase	5.934412	6.24E-05
JBBA_03212	Phthalate transporter	5.66784	0.00014
BBA_06418	Hypothetical protein	5.659826	0.000117
BBA_00125	pH domain-containing protein	5.368382	0.000274
BBA_05774	TBC domain-containing protein	5.049884	0.000638
BBA_06130	Calcium-related spray protein	4.856109	0.001169
BBA_08910	Acetate-CoA ligase	4.854684	0.001065
BBA_04487	SOM1 protein	4.838327	0.001753
BBA_08083	Helix-loop-helix DNA-binding domain-containing protein	4.827529	0.001152
BBA_05052	Glycerol kinase	4.6925	0.00431
BBA_02516	Malate synthase%2C glyoxysomal	4.68327	0.002029
BBA_05604	Hypothetical protein	4.658371	0.001915
BBA_09135	Polyamine transporter TPO5	4.61832	0.00203
BBA_09151	Acetyl-CoA carboxylase	4.563134	0.002808
BBA_00896	Major facilitator superfamily transporter	4.476008	0.002031
BBA_00384	Hypothetical protein	4.473455	0.002657
BBA_04957	Potassium/sodium efflux P-type ATPase	4.418282	3.41E-09

Table 2.7 depicts the 20 most upregulated genes in the control state relative to the endophytic state. The P450 CYP6001C8 (LFC=6.23) gene was highly expressed in the control state in relation to the endophyte state. Previously, the same gene was also significantly downregulated in the endophytic state (Table 2.5). Some of the other upregulated genes in this state have been involved in synthesizing different secondary metabolites and other natural products by microorganisms. Examples of these genes include the thioester reductase domain-containing protein (LFC=6.17) and nonribosomal peptide synthase putative (LFC =5.32) (Mullowney *et al.,* 2018; Iqbal *et al.,* 2019). Different transporters involved in the transportation of sugars and sugar metabolites were found to be upregulated in the control media group. It is believed that the high content of both simple and complex sugars (such as starch) in potato dextrose broth which served as the control growth medium warrants these. These genes include the glycosyltransferase family 22 (LFC=5.56) glucanosyltransferase-like protein (LFC =5.55) and a transferase family protein (LFC=5.8).

Table 2.7: Top 20 upregulated genes in *B. bassiana* SAN01 under the control state relative to the endophytic state

GeneID	Gene Product	log_2-FoldChange	p-value
BBA_03825	Cytochrome P450 CYP6001C8	6.22771	4.87E-05
BBA_09127	Thioester reductase domain-containing protein	6.16508	3.97E-05
BBA_06609	Myosin-cross-reactive antigen	6.0831	0.000136
BBA_06951	Pre-mRNA-splicing factor srp1	5.9578	0.00026
BBA_05769	Fatty acid desaturase	5.90993	5.91E-05
BBA_02834	Allantoate permease	5.85677	0.000326
BBA_07379	Transferase family protein	5.80358	0.000373
BBA_02923	Glycosyltransferase family 22	5.75091	0.000672
BBA_05748	Hypothetical protein	5.67466	0.001063
BBA_04903	Rasp f 7 allergen	5.59331	2.09E-06
BBA_04640	Glucanosyltransferase-like protein	5.55204	0.000214
BBA_03875	Cytochrome oxidase assembly protein	5.52103	0.001826
BBA_04827	Peptide synthetase	5.51585	0.014206
BBA_02714	Phod-like phosphatase	5.37425	0.002131
BBA_03236	Class 2 chitin synthase	5.36851	0.001976
BBA_09850	Putative pyruvate decarboxylase	5.34848	0.001029
BBA_10249	Kynurenine 3-monooxygenase	5.34737	0.016388
BBA_08222	Nonribosomal peptide synthase putative	5.31868	0.002633
BBA_07103	Phospholipid-translocating P-type ATPase	5.29568	0.00905
BBA_02938	Prolyl-tRNA synthetase	5.25588	0.002806

2.3.4.5 *DEGs between fermentation vs control trophic states of B. bassiana* SAN01

A summary of the top 20 upregulated genes in the fermentation (lignocellulose biomass degradation) relative to the control state is given in Table 2.8. Many of the upregulated genes under this trophic condition are involved in depolymerization reactions (biomass degradation), cell wall synthesis, morphogenesis and transport of hydrolytic intermediates and products. A WSC domain-containing protein (LFC= 6.21) was identified as the gene with the highest transcription under this state. This is probably due to the upregulation of exoglucanases essential for the degradation of the cellulose component of the biomass as the WSC domain is present in fungal exoglucanases (Oide *et al.,* 2019). A mediator of RNA polymerase II transcription was highly upregulated during plant biomass metabolism relative to the control media (LFC=6.11). Mediator complexes link transcriptional regulators to RNA polymerase II, and they have been shown to have different biological roles. However, some transcriptional regulators are involved in carbohydrate metabolism, biofilm formation, and morphogenesis (Moran *et al.,* 2019). The increased transcription of the gene for beta-1-3 exoglucanase precursor (LFC=5.61) is also notable. The beta-1-3 exoglucanases have important nutritional roles in both saprobic and parasitic fungi, where they represent primary biochemical offensive weapons for cell wall degradation (Martin *et al.,* 2007). As observed earlier in endophytic vs fermentation, the upregulation of various proteases including the family S53 protease, vacuolar protease A and protease S8 tripeptidyl peptidase I with LFC of 5.8, 5.12 and 5.08, respectively, was also recorded. These proteases are believed to be involved in the deconstruction of plant biomass, as shown recently (Wang, Hart and An 2019). The other notable upregulated genes under this condition include β-glucosidase, pectin lyase, oxoglutarate dehydrogenase, and various transporters.

Table 2.8: Top 20 upregulated genes in *B. bassiana* SAN01 under the fermentation relative to the control state

GeneID	Gene Product	log_2-FoldChange	p-value
BBA_05929	WSC domain-containing protein	6.209587	4.93E-09
BBA_06784	Mediator of RNA polymerase II transcription	6.114193	2.79E-05
BBA_05808	Cell wall protein	5.915537	2.76E-05
BBA_07631	Family S53 protease	5.800693	7.89E-05
BBA_03268	Hypothetical protein	5.782982	8.57E-05
BBA_01910	Hypothetical protein	5.723816	0.000191
BBA_09151	Acetyl-coa carboxylase	5.697121	0.000154
BBA_00792	Beta-1 3 exoglucanase precursor	5.611441	9.28E-08
BBA_07594	Hypothetical protein	5.530993	0.000335
BBA_07560	Hypothetical protein	5.491656	0.000203
BBA_05347	Ncp1-like protein	5.482724	0.000189
BBA_05704	Vegetative cell wall protein gp1	5.395412	0.000953
BBA_06420	Oligopeptide transporter	5.37618	0.00026
BBA_08742	Hypothetical protein	5.339445	0.000293
BBA_08088	Oxoglutarate dehydrogenase	5.238486	0.00081
BBA_08504	Hypothetical protein	5.23548	0.00061
BBA_08372	Hypothetical protein	5.200692	0.000472
BBA_04888	Vacuolar protease A	5.117601	0.002274
BBA_02532	S-layer protein	5.096794	0.000559
BBA_07294	Protease S8 tripeptidyl peptidase I (cln2)	5.080009	0.000594

The 20 most upregulated genes in the control state relative to the fermentation state are displayed in Table 2.9. As shown previously in the endophytic vs control group, a significant portion of the upregulated genes, including thioester reductase domain-containing protein (LFC=6.29), are involved in the microbial synthesis of different secondary metabolites and other natural products (Mullowney *et al.,* 2018). They are also noted to be involved in nitrogen metabolism and protein folding. Ubiquitin proteins were also upregulated with a LFC of 6.29 relative to the fermentation group. Although ubiquitins have been recognized as a diverse group of proteins with largely unknown function, in fungi, they are highly active during nitrogen deprivation (Staszczak 2008). The presence of these transcripts might be due to the low nitrogen content of the PDB medium (Mustafa and Kaur 2009), which served as the growth media under control conditions. This could also give an insight into the upregulation of heat-shock proteins, such as Hsp 70 and Hsp 90, under these conditions. Heat-shock proteins are highly expressed during conditions of stress to fungi, thus, the nitrogen-deprived basal media might be considered as a form of abiotic stress to the *Beauveria* strain (Chen *et al.,* 2018b). Other notable upregulated genes under the control condition relative to the fermentation condition include actin-like proteins, amidohydrolases, beta-tubulins, protein-disulphide isomerase and multi-copper oxidase. It is also remarkable that many hypothetical proteins were found to be upregulated in the control group.

Table 2.9: Top 20 upregulated genes in *B. bassiana* SAN01 in control relative to the fermentation state

GeneID	Gene-Product	log_2-FoldChange	p-value
BBA_09127	Thioester reductase domain-containing protein	6.29198	3.68E-19
BBA_03881	Ubiquitin subgroup	6.2854	3.77E-49
BBA_05006	Nucleotide sugar dehydrogenase	6.1908	8.24E-09
BBA_07277	Hypothetical protein	5.95346	3.59E-05
BBA_10072	Basic proline-rich protein	5.02052	0.112069
BBA_01806	Hypothetical protein	4.99862	0.021991
BBA_04348	Wd-repeat protein	4.98178	0.001204
BBA_05117	SET domain-containing protein	4.91639	0.001598
BBA_07474	Hypothetical protein	4.71271	0.001254
BBA_10068	Hypothetical protein	4.62415	0.001238
BBA_06516	Heat shock protein Hsp90	4.59373	4.1E-74
BBA_09846	Hypothetical protein	4.47684	0.003793
BBA_05415	60S ribosomal protein L10-A-like protein	4.42602	9.42E-42
BBA_10249	Kynurenine 3-monooxygenase	4.334	0.0162
BBA_05586	Heat shock protein 70-2	4.30186	1.36E-28
BBA_04576	Multicopper oxidase	4.15937	4.49E-05
BBA_06118	TPR domain-containing protein	4.13242	0.218853
BBA_08907	Plasma membrane ATPase (Proton pump)	4.12821	1.6E-35
BBA_06951	Pre-mRNA-splicing factor srp1	4.11862	3.51E-06
BBA_05153	Eukaryotic translation initiation factor 3 subunit G	4.08051	0.00022

2.3.5 Gene ontology

The whole transcriptome of the fungus under biomass degradation (fermentation) condition was functionally classified according to Gene Ontology (GO) consortium, an international standard gene functional classification system. In this regard, a total of 5,746 non-redundant unigenes were grouped into the major functional ontologies. Three independent ontologies, which are 'biological process (BP)', 'cellular component (CC)' and 'molecular function (MF)', are used as GO terms to describe gene products according to their functional annotations (Wang *et al.,* 2017a). Thus, based on the InterPro functional annotation, the GO functional categories of the *B. bassiana* SAN01 under fermentation condition is represented in Figure 2.8a-c. The biological process category (Figure 2.8a) occupied the largest proportion (50 terms), followed by the Molecular Function (Figure 2.8b) category (38 terms) and Cellular Component (34 terms) category (Figure 2.8c). For biological process (BP), it was observed that the dominant subcategories were biosynthetic process (1,441), response to stress (1,205) and cellular nitrogen compound metabolic (826), demonstrating the dominated biological activities taking place in *B. bassiana* SAN01 transcriptome. In addition, catabolic process (533), lipid metabolism (448), carbohydrate metabolism (278), amino acid metabolism (253) as well as transport (174) were also highlighted under BP. The afore-mentioned activities are believed to be directly involved in the fungal degradation of lignocellulosic biomass in this study. Under the molecular function category, ion binding (955), molecular function (613), enzyme binding (413) and transmembrane activity (410) were the top 4 most represented. Furthermore, hydrolase activity on glycosyl bond (85), hydrolase activity on non-peptide carbon-nitrogen bonds (54), enzyme regulator activity (196), as well as transferase activity (109) were also observed under the MF category which is also directly involved in biomass degradation.

For the cellular component category, however, the dominant subcategories were protein-complex (1290), cytosol (895), plasma membrane (821), and cytoplasm (789). The extracellular region (247), the extracellular space (39) as well as the extracellular matrix (27) were also annotated under this category. The enzyme code distribution (EC) for *B. bassiana* SAN01 under fermentation condition was also analysed. Mapping contigs from the *B. bassiana* transcriptome to enzyme codes identified sequences from EC classes for hydrolases (862), transferases (757), translocases (456), oxidoreductases (389), ligases (120), lyases (108) and isomerases (84) as shown in Figure 2.9a. The EC subclass for

hydrolases was made up of hydrolytic enzymes acting on acid anhydrides, ester bonds, glycosyl bonds, peptide bonds and carbon-carbon bonds in that order (Figure 2.9b). It was also observed that for the transferases group, enzymes transferring phosphorus-containing groups were the dominant, followed by acyltransferases, glycosyltransferases, enzymes transferring one carbon, alkyl/aryl groups and those transferring sulphur containing groups, in descending order (Figure 2.9c). In addition, a few enzymes transferring molybdenum/tungsten containing groups were also recorded.

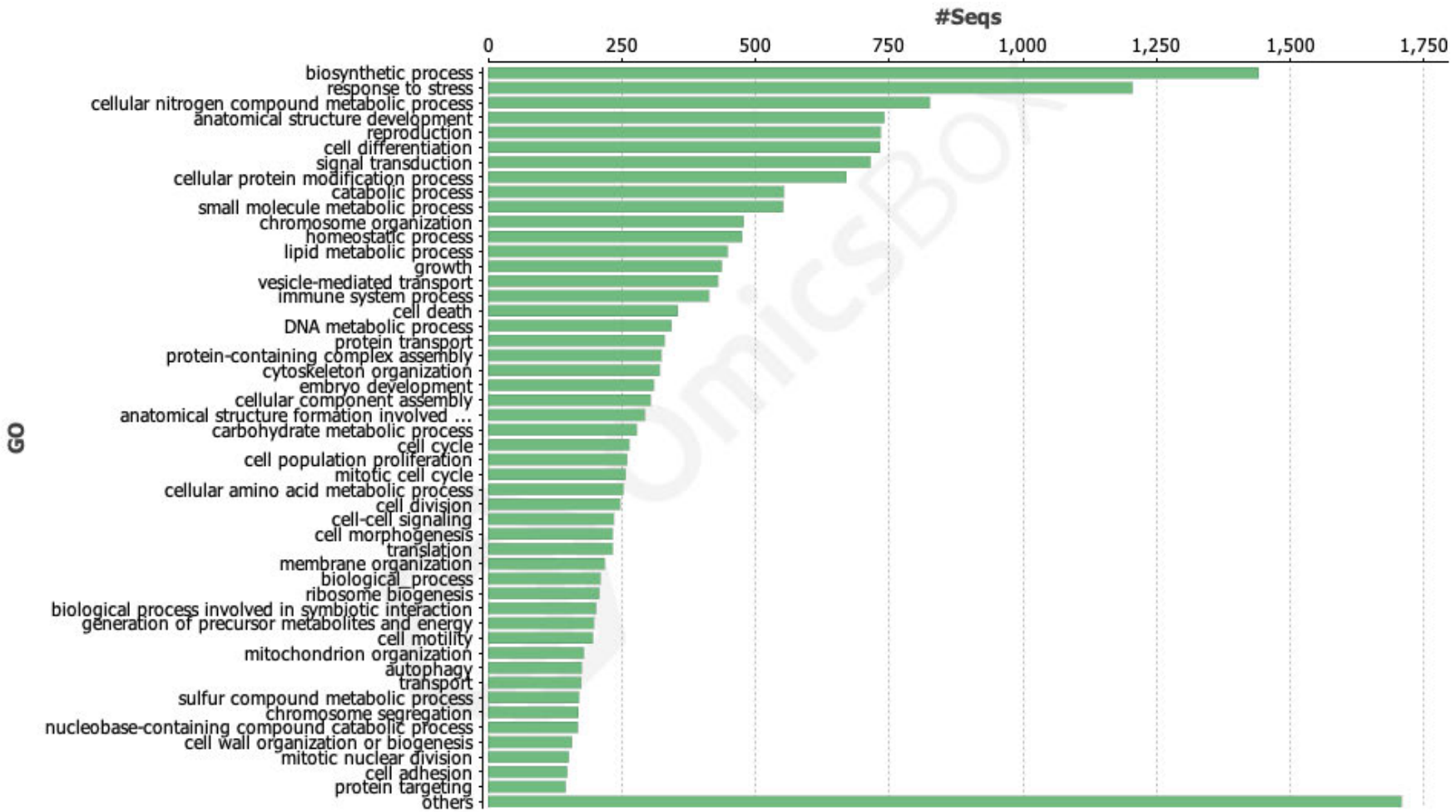

Figure 2.8a: Gene ontology (Biological processes) of *B. bassiana* SAN01 transcriptome under the biomass-degrading condition

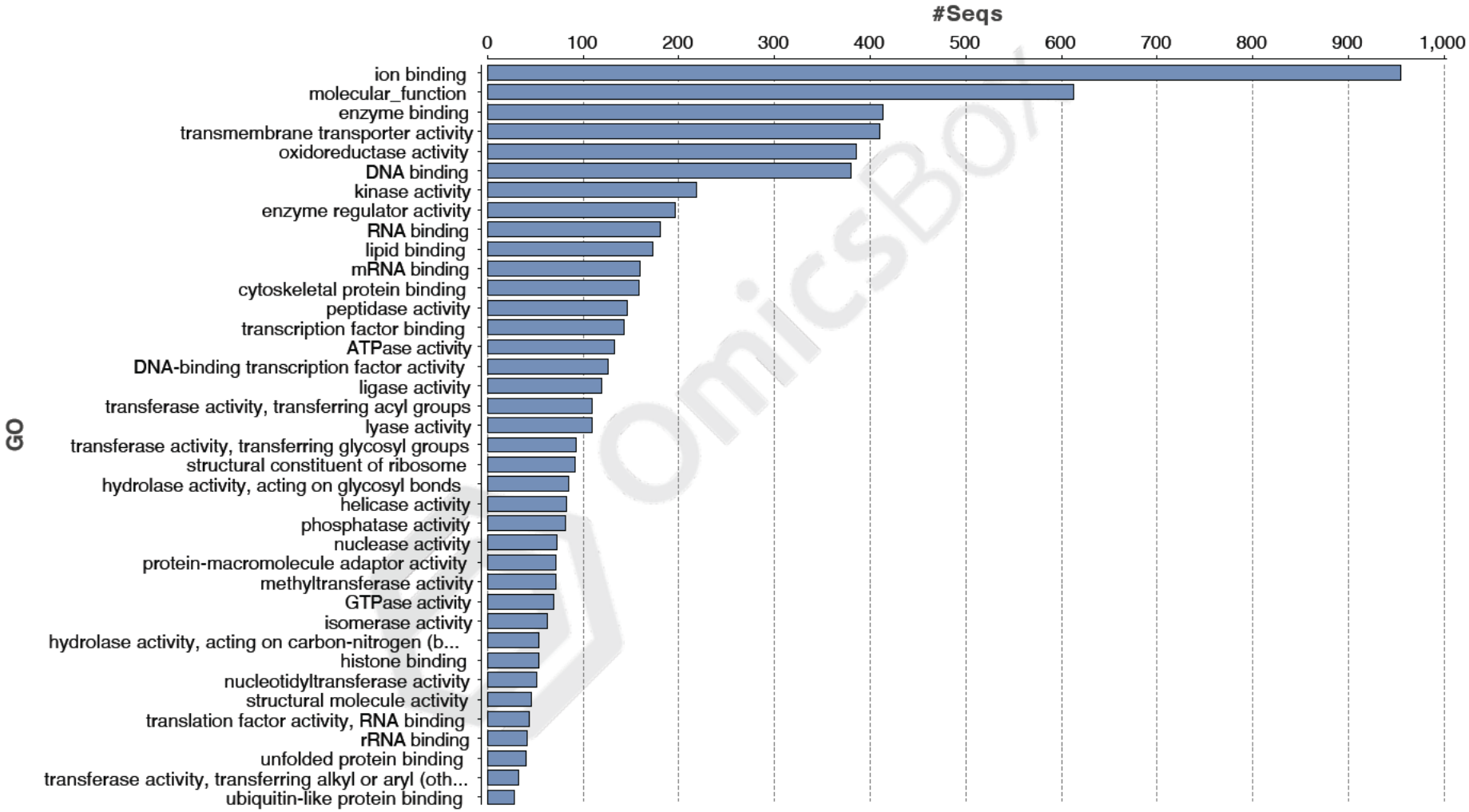

Figure 2.8b: Gene ontology (Molecular function) of *B. bassiana* SAN01 transcriptome under the biomass-degrading condition

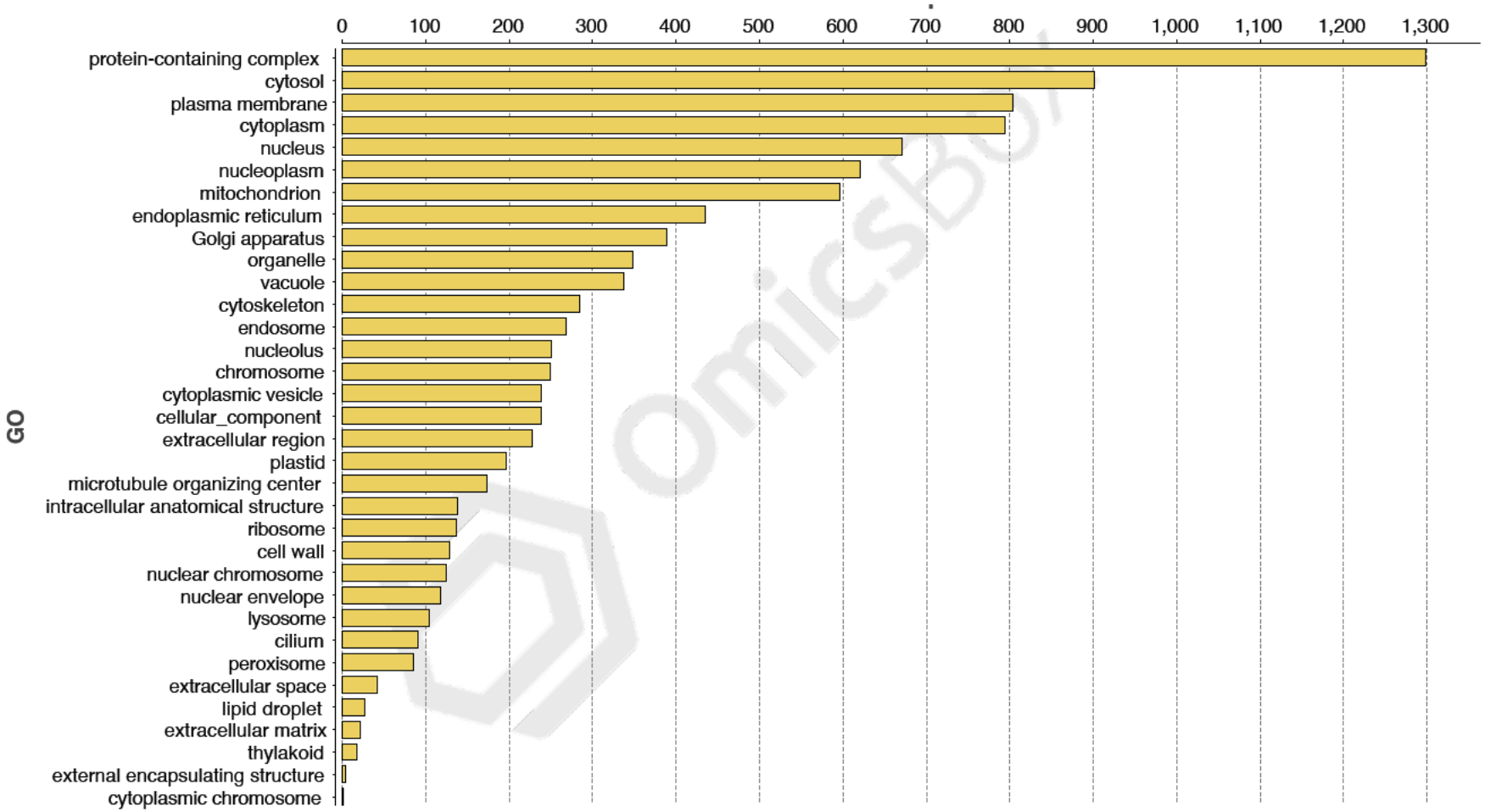

Figure 2.8c: Gene ontology (Cellular component) of *B. bassiana* SAN01 transcriptome under the biomass-degrading condition

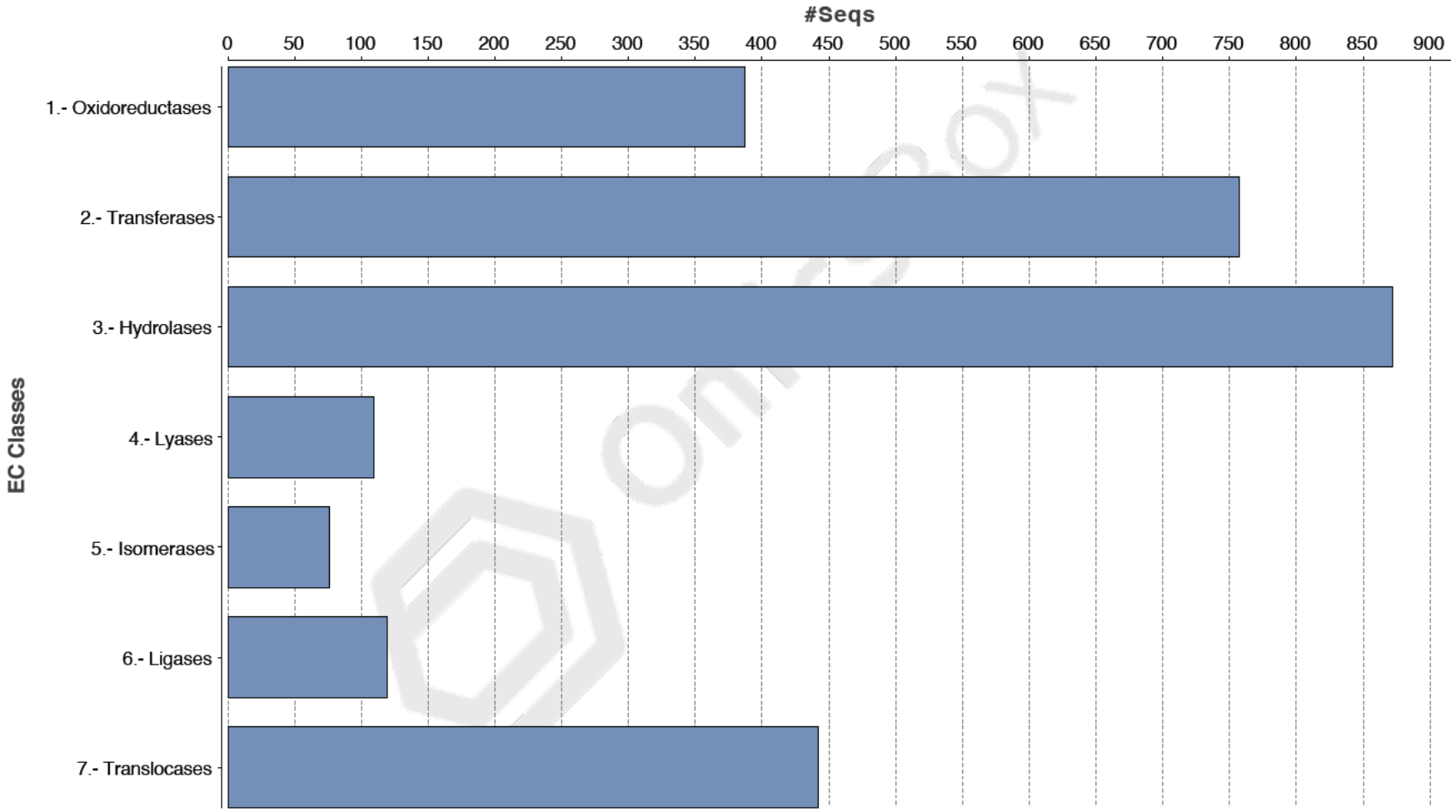

Figure 2.9a: EC code distribution (General EC classes) of *B. bassiana* SAN01 transcriptome under the biomass-degrading condition

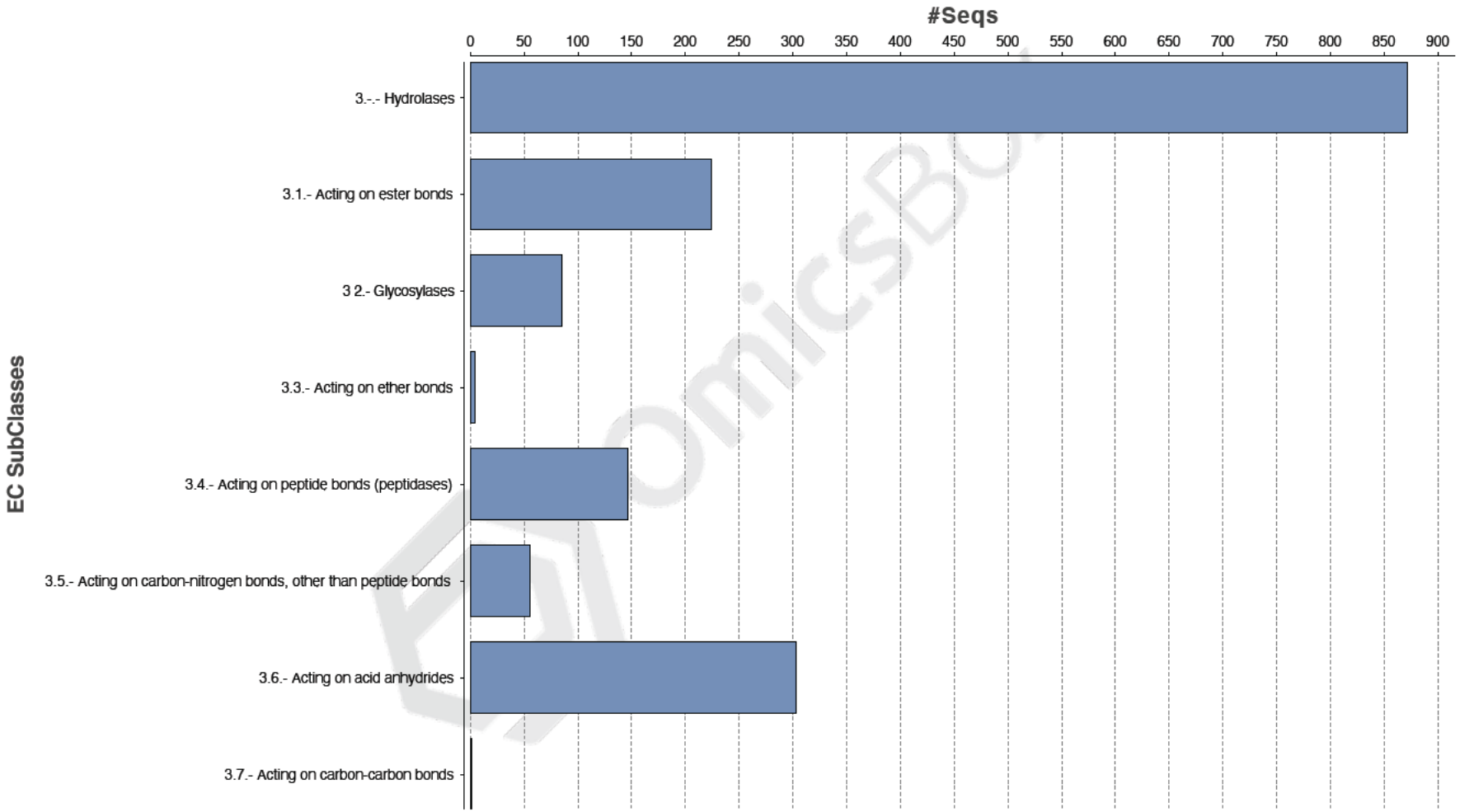

Figure 2.9b: EC code distribution (Hydrolases subgroup) of *B. bassiana* SAN01 transcriptome under the biomass-degrading conditions

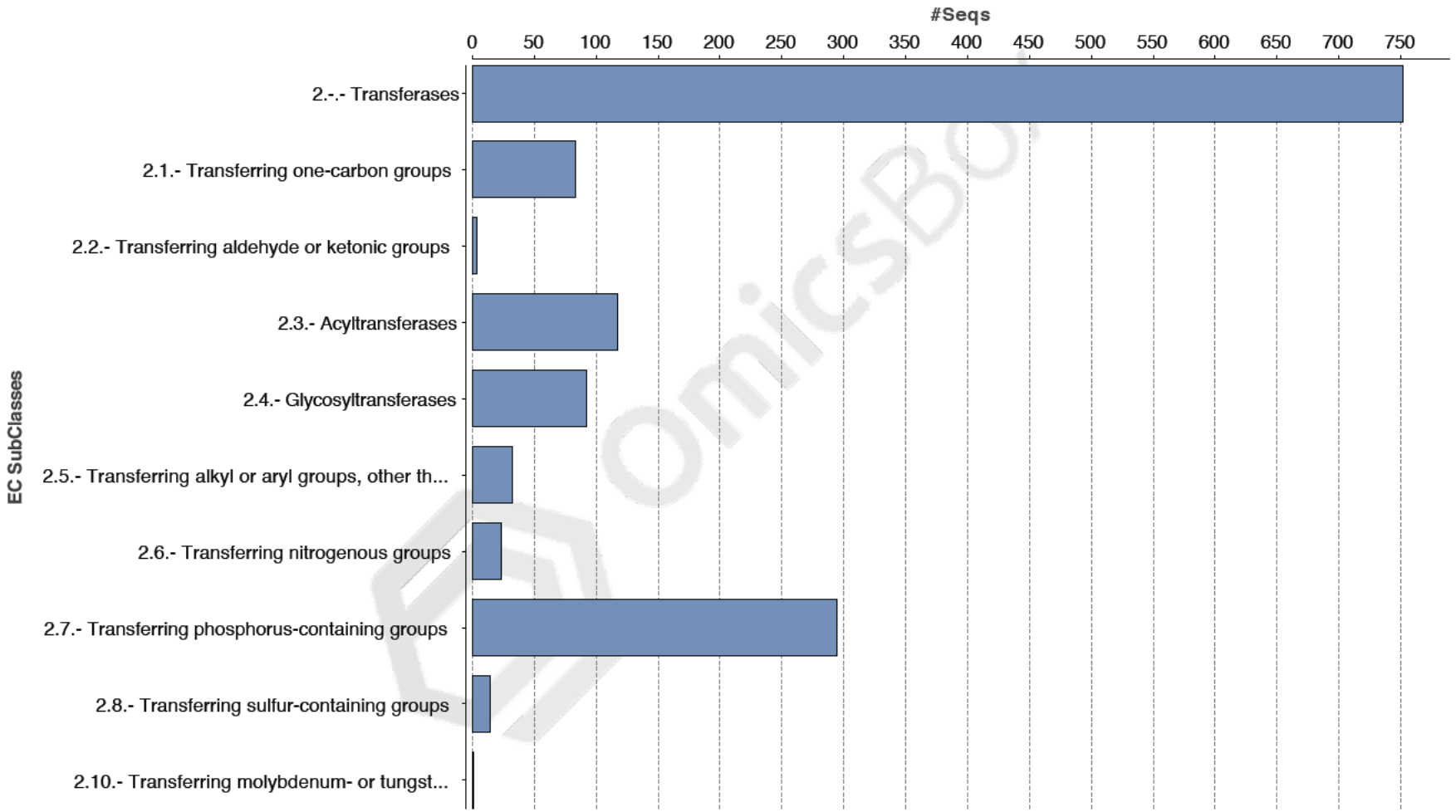

Figure 2.9c: EC code distribution (Transferases subgroup) of *B. bassiana* SAN01 transcriptome under the biomass-degrading condition

2.3.6 CAZy annotation of *B. bassiana* SAN01 biomass-degrading enzymes

As the main aim of this study was the biochemical elucidation of the carbohydrases from *B. bassiana* SAN01, selected CAZymes in the fungal transcriptome with significant contribution to the lignocellulose degradation were examined in depth. The total number of CAZyme-encoding genes identified in *B. bassiana* SAN01 during its growth on plant lignocellulosic biomass was found to be 367. This is higher than the 350 and 251 CAZyme-encoding genes observed previously in *A. niger* and *Trichoderma reesei,* respectively, which are both well-recognized fungi of industrial importance with significant biomass-degrading abilities (Borin *et al.,* 2017). The biomass-degrading enzymes encoded by these *B. bassiana* SAN01 genes were found to belong to different families including the auxiliary activities, carbohydrate-binding module, glycoside hydrolase, glycosyl transferase and carbohydrate esterases. This wide array of carbohydrases results from the need of the fungus to metabolize the different components of the complex growth substrate, wheat bran. Wheat bran has been shown to contain different polysaccharides including celluloses, hemicelluloses, starch, pectin, lignin and others in varying proportion (Onipe, Jideani and Beswa 2015). Hence, the most notable of the *B. bassiana* SAN01 carbohydrase genes involved in the depolymerization and metabolism of polysaccharides are summarised in Table 2.10.

Cellulose has been estimated to make up to 10% of wheat bran (Rahman *et al.,* 2017). In this study, five enzymes were observed to be responsible for cellulose metabolism which includes β-glucosidase, Cel3 proteins, cellobiose dehydrogenase, endoglucanases and exoglucanase. While the β-glucosidases, endoglucanases and exoglucanases have been well characterized for their collaborative ability to degrade cellulose, the Cel3 proteins and cellobiose dehydrogenases are not as well known. The Cel3 proteins have been shown in *Penicillium piceum* to possess the ability to hydrolyze cellobiose to glucose (Gao *et al.,* 2013). While in *Phanerochaete chrysosporium*, cellobiose dehydrogenase has been revealed to hasten cellulose degradation by attenuating cellulase inhibition via oxidation of cellobiose to cellobionic acid (Kracher and Ludwig 2016). The CAZy annotation also revealed the production of some starch metabolising enzymes under the fermentation condition. The starch-degradation machinery of *B. bassiana* SAN01 was made up of glucoamylase which breaks down the starch component of the biomass to maltose, and α-glucosidase which converts the maltose to glucose. Hemicellulases

consist of various types of hydrolytic enzymes that breakdown the more complex hemicellulolytic polysaccharides. Hence, this consortium of enzymes is typically involved in the breakdown of hemicellulolytic polymers, including xylans, arabinoxylans, glucuronoxylan, glucomannans, and xyloglucans (Houfani *et al.,* 2020). In *B. bassiana* SAN01, hemicellulases such as acetyl esterase, alpha-mannosidase, acetylxylan esterases, arabinofuranosidase, beta-galactosidase, and carbohydrate esterases were identified in the degradation of hemicellulolytic component of wheat bran. However, it was noticed that the gene encoding for xylosidase, which is responsible for the degradation of xylooligosaccharides to xylose, was absent in the CAZy annotation. However, the xylosidase gene was elucidated in the list of DEGs (XM_008597041.1), with a log2-fold change of 1.05 relative to the endophytic trophic state (data not shown). The absence of xylosidase may be due to the higher arabinoxylan content of the growth substance (wheat bran) relative to xylan, which also explains the expression of arabinofuranosidase, the debranching enzyme, which removes arabinose substituents from arabinoxylan and arabinoxylooligomers.

Lignin has been identified as one of the most abundant polymers in nature, forming the major components of the plant cell walls along with cellulose and xylan. Previous studies have estimated the lignin content of wheat bran to be 10% (Theander *et al.,* 1995; Merali *et al.,* 2015). Hence, many genes responsible for the degradation of lignin were upregulated in the *B. bassiana* under study. These lignin metabolizing CAZymes were annotated to be aryl-alcohol oxidase, catalase/peroxidase, glucose–methanol–choline oxidoreductase, laccases and multicopper oxidase. Laccases have always been a recurring decimal in the microbial degradation of lignin, representing the most abundant protein expressed during the degradation of high lignin-containing biomass (Rytioja *et al.,* 2017). The important roles of aryl-alcohol oxidase, catalase/peroxidase, glucose–methanol–choline oxidoreductase and multicopper oxidase in biomass degradation by fungi have also been shown previously (Brenelli *et al.,* 2019; Sützl *et al.,* 2019; Serrano, Carro and Martínez 2020).

Pectinases including pectin lyase, polygalacturonase and rhamnogalacturonase were also shown to be induced in this study. Even though pectinases have been annotated in the *B. bassiana* genome (Xiao *et al.,* 2012), there has been no other study to show the upregulation or production of pectin-degrading enzymes in *B. bassiana*. However, it is believed that these genes were upregulated due to the moderate level of pectin in the

media, as shown previously (Bailoni *et al.,* 2005). As annotated in this study, previous studies have also shown the constitutive expression of chitinase in various microbes and entomopathogens in particular (Goughenour *et al.,* 2020). Being an entomopathogen, the genes for the metabolism of chitin were noticeably present in *B. bassiana* SAN01. These include 18 chitinases and a family 9 carbohydrate esterase as well as a hexosaminidase. In comparison to *B. bassiana* SAN01, seven chitinase genes were shown to be induced in another *B. bassiana* strain during its infections of anopheles mosquitoes (Lai *et al.,* 2017). Hence, the higher number of chitinase observed in this study may indicate that *B. bassiana* SAN01 is probably a highly virulent strain. However, this assertion might need to be validated in future studies, as the virulence of the fungus on its insect host is outside the scope of this study. Other glycoside hydrolases highlighted in the *B. bassiana* SAN01 transcriptome are chitosan, cutinase and glucan-degrading enzymes. The presence of these genes or their products have been shown in other *B. bassiana* strains (Zhang *et al.,* 2012; Liu *et al.,* 2020a; Schmaltz *et al.,* 2021) and may be responsible for their insect pathogenesis or their symbiotic association with plants.

Table 2.10: Biomass-degrading enzymes from *B. bassiana* SAN01 and their corresponding CAZy families

Substrate	Enzyme	EC number	CAZy family	Copy number	Reference
Cellulose	β-Glucosidase	3.2.1.21	GH 1	3	(Sun *et al.,* 2020)
	Cel3 proteins	3.2.1.21	GH 3	3	(Gao *et al.,* 2013)
	Endoglucanase	3.2.1.4	GH 5	2	(Yin *et al.,* 2020)
	Cellobiose dehydrogenase	1.1.99.18	AA 3	1	(Gangwar, Rasool and Mishra 2020)
	Endoglucanase B	1.14.99.45	AA9	1	(Sharma, Salwan and Shanmugam 2018)
	Exoglucanase	3.2.1.74	GH 45	1	(Bharadwaj *et al.,* 2020)
Chitin	Chitinase	3.2.1.14	GH 18	18	(Alsina *et al.,* 2020)
	Carbohydrate esterase family 9	3.5.1.25	CE 9	2	(Yamada-Okabe *et al.,* 2001)
	Hexosaminidase	3.2.1.52	GH 20	2	(Konada *et al.,* 2020)
Chitosan	Chitosanase	3.2.1.132	GH 75	2	(Zhou *et al.,* 2020)

Cutin	Cutinase	3.1.1.74	CE 5	3	(Gui *et al.,* 2018)
Lignin	Laccase	1.10.3.2	AA 1	1	(Brenelli *et al.,* 2019)
	Multicopper oxidase	1.10.3.1	AA1	8	(Liu *et al.,* 2020b)
	Catalase/peroxidase	1.11.1.6	AA 2	2	(Kumar *et al.,* 2018a)
	Glucose–methanol–choline oxidoreductase	1.1.3.13	AA 3	5	(Sützl *et al.,* 2019)
	Aryl-alcohol oxidase	1.1.3.38	AA4	1	(Serrano, Carro and Martínez 2020)
Pectin	Pectin lyase/ Polygalacturonase	3.2.1.15	GH 28	3	(Bonnin and Pelloux 2020)
	Rhamnogalacturonases	3.2.1.71	GH 28	1	(Bonnin and Pelloux 2020)
Starch	Alpha-glucosidase	3.2.1.20	GH 31	1	(Kawano *et al.,* 2019)
	Glucoamylase	3.2.1.3	GH 15	1	(Tanaka *et al.,* 2020)
Trehalase	Neutral trehalase	3.2.1.28	GH 37	2	(Sakaguchi 2020)
Xylan	Arabinofuranosidase	3.2.1.55	GH 54	1	(Terrone *et al.,* 2020a)
	Beta-galactosidase	3.2.1.23	GH 35	2	(Herlet *et al.,* 2018)
	Acetylxylan esterases	3.1.1.72	CE 3	1	(Alalouf *et al.,* 2011)
	Carbohydrate esterases 1 & 4	3.1.1.72	CE 1 & 4	3	(Sista Kameshwar and Qin 2018)
	Alpha mannosidase	3.2.1.24	GH 47	2	(Jiménez, Maruthamuthu and van Elsas 2015)
	Acetyl esterase	3.1.1.6	CE 16	1	(Poutanen and Sundberg 1988)
	Polysaccharide deacetylase	3.1.1.72	CE4	1	(Razeq *et al.,* 2018)
	Beta-mannosidase	3.2.1.25	GH 2	2	(Jović *et al.,* 2020)
Laminarin	Beta-1,3-glucanase	3.2.1.58	GH 55	1	(Rodríguez-Mendoza *et al.,* 2019)
	Glucan endo-1,3-beta-glucosidase	3.2.1.39	GH 17	3	(Gelain *et al.,* 2020)
Glucans	Mixed-linked glucanase	3.2.1.6	GH 16	1	(Li *et al.,* 2017)

2.4 Conclusion

The phylogenetic relationship between *B. bassiana* SAN01 and other closely related filamentous fungi was established in this study. These closely related fungi are generally entomopathogenic fungi, including different *B. bassiana* strains and other species belonging to the *Beauveria* genus. Different fungi have been shown previously to possess significant ecological plasticity and the ability to derive their energy from various sources such as their insect prey as entomopathogens, recalcitrant lignocellulosic substrates as saprotrophs, and within living plants as non-clavicipitaceous endophytes. In this regard, *B. bassiana* SAN01's ability and pattern of utilization of a standardized array of sugars were investigated. The phenotypic microarray revealed that *B. bassiana* SAN01 had a very high respiration rate and concomitant biomass growth while utilizing xylitol, N-acetyl-D-glucosamine, D-ribose, D-sorbitol and turanose, in descending order. These results further enriched the knowledge of the metabolic characterization of *B. bassiana* SAN01, particularly its ability to utilize nutritional substrates and its adaptability in different environments.

Furthermore, the genetic bases of the metabolic versatility of the fungus with a special focus on its switch between its observed endophytic and saprophytic (fermentation) trophic modes were studied. The gene expression profile of the fungus revealed the systematic and dynamic phenomena happening at the molecular level during the interaction of organisms with their simulated environments. Hence, this study presents for the first time the transcriptome of *B. bassiana* while utilizing lignocellulosic biomass as its sole nutrients, as well as its transcriptomics under simulated endophytic conditions and while growing on basal media (potato dextrose broth). The data show that despite the more popular entomopathogenic and endophytic roles of *B. bassiana*, the fungus can also secrete a wide array of hydrolytic enzymes which can deconstruct different carbohydrate polymers. These enzymes include amylases, cellulases, glucosidases, pectinases, xylanases and lignin-degrading enzymes. Furthermore, a closer relationship was also established between the fungus in its endophytic state and its cultured state using PDB. It is anticipated that the full value of this dataset will be revealed in the nearest future as the genes identified in this study will provide the foundation for prospective targeted investigations such as microarray studies, RT-qPCR, fermentation studies and genetic manipulation, all aimed at a better understanding of the highly versatile endophytic fungal entomopathogen.

CHAPTER THREE

Optimization of the production of selected carbohydrases from *Beauveria bassiana* SAN01

Part of this chapter has been published: Amobonye, A., Bhagwat, P., Singh, S. and Pillai, S. 2021. Enhanced xylanase and endoglucanase production from *Beauveria bassiana* SAN01, an entomopathogenic fungal endophyte. *Fungal Biology* 125: 39-48.

Fungal Biology 125 (2021) 39–48

Contents lists available at ScienceDirect

Fungal Biology

journal homepage: www.elsevier.com/locate/funbio

Enhanced xylanase and endoglucanase production from *Beauveria bassiana* SAN01, an entomopathogenic fungal endophyte

Ayodeji Amobonye, Prashant Bhagwat, Suren Singh, Santhosh Pillai*

Department of Biotechnology and Food Technology, Faculty of Applied Sciences, Durban University of Technology, P O Box 1334, Durban, 4000, South Africa

ARTICLE INFO

Article history:
Received 6 June 2020
Received in revised form
4 October 2020
Accepted 6 October 2020
Available online 9 October 2020

Keywords:
Beauveria bassiana
Endoglucanase
Xylanase
Optimisation
Saccharification
Sugarcane bagasse

ABSTRACT

This study was undertaken to explore alternative applications of the widely known entomopathogenic/endophytic fungus, *Beauveria bassiana*, besides its sole use as a biocontrol agent. *B. bassiana* SAN01, was investigated for the production of two glycoside hydrolases, xylanase and endoglucanase under submerged conditions. Among the different biomass tested, wheat bran provided the best results for both xylanase and endoglucanase, and their production levels were further enhanced using response surface methodology. Under optimised conditions, heightened yields of 1061 U/ml and 23.03 U/ml were observed for xylanase and endoglucanase, respectively, which were 3.44 and 1.35 folds higher than their initial yields. These are the highest ever production levels reported for xylanase and endoglucanase from any *B. bassiana* strain or any known entomopathogenic fungi. Furthermore, the efficacy of xylanase/endoglucanase cocktail in the saccharification of sugarcane bagasse was evaluated. The highest amount of reducing sugar released from the pretreated biomass by the action of the crude *Beauveria* enzyme cocktail was recorded at 30°C after 8 h incubation. The significant activities of the hydrolytic enzymes recorded with *B. bassiana* in this study thus present promising avenues for the use of the entomopathogen as a new source of industrial enzymes and by extension, other biotechnological applications.

1. Introduction

Entomopathogenic fungi (EPF) are parasitic microbes with the ability to infect and cause significant mortality in arthropodal populations. As a result of their biology, they have been widely and mainly used in the biological control of insects, infecting them by contact and subsequent penetration of their cuticles and eventual multiplication in the hemocoel. However, recent findings have shown the potential of these fungi in different industrial applications. These potentials include the removal of toxic contaminants such as organotin compounds, pesticides, synthetic oestrogens, and as sources of many industrially important secondary metabolites (Litwin et al., 2020). Furthermore, their inherent ability to produce a wide variety of enzymes is now being exploited in the industry to meet the continuous demand for novel biocatalysts (Mondal et al., 2016). The increasing interest in enzymes from entomopathogenic fungi has been mainly attributed to their high specificity of action, and more importantly their harmless effect on non-target organisms (Thakur et al., 2017) In addition, many of these enzymes have also been observed to perform optimally under mild reaction conditions and some under extreme conditions (Mondal et al., 2016). As a result, many researches are now being focused on the potentials of various entomopathogenic fungi for the production of important enzymes (Hasan et al., 2013; Mallebrera et al., 2018).

Many studies have demonstrated that entomopathogenic fungi also play additional roles in nature, most notable of which are endophytism, plant disease antagonism, plant growth promotion, as well as rhizosphere colonisation (Quesada Moraga, 2020). In this regard, different EPF have been isolated from plant sources in their endophytic state and have also been demonstrated to colonise various plant hosts (Nishi et al., 2020). These additional roles are believed to provide multiple opportunities for the alternative uses of entomopathogenic fungi in the industry (Jaber and Ownley, 2018).

Beauveria bassiana is a well-known entomopathogenic filamentous fungus that has been shown to infect different insects (Yasin et al., 2019), other arthropods (Canassa et al., 2019) and nematodes (Kepenekci et al., 2017). The fungus has also been found to exist endophytically in plants, without any deleterious effect on its different plant hosts (Rondot and Reineke, 2018). Thus, like

* Corresponding author.
E-mail address: santhoshk@dut.ac.za (S. Pillai).

https://doi.org/10.1016/j.funbio.2020.10.003
1878-6146/

Abstract

This study was undertaken to explore alternative applications of the widely known entomopathogenic/endophytic fungus, *Beauveria bassiana*, besides its sole use as a biocontrol agent. *B. bassiana* SAN01, isolated locally, was investigated for the production of four glycoside hydrolases, *viz.*, amylase, endoglucanase, polygalacturonase and xylanase, under submerged conditions using readily available agricultural residues. Among the different plant biomass tested, wheat bran was the best carbon source for the production of all the enzymes, and their production levels were further enhanced using response surface methodology. Under optimized conditions, heightened yields of 34.82 UmL^{-1}, 23.03 UmL^{-1}, 51.05 UmL^{-1}, and 1061 UmL^{-1} were observed for amylase, endoglucanase, polygalacturonase and xylanase, respectively, which were approximately 1.79-, 1.35-, 1.87- and 3.44- folds higher than their initial yields. These are the highest ever production levels reported for the four glycosyl hydrolases from any *B. bassiana* strain or any known entomopathogenic fungi. The significant activities of the hydrolytic enzymes recorded with *B. bassiana* thus present other promising avenues for the use of the entomopathogen as a new source of industrial enzymes and by extension, other biotechnological applications.

3.1 Introduction

Beauveria bassiana SAN01 strain was observed to proliferate on different plant biomass and secrete biomass-degrading enzymes, *viz*., amylase, cellulase (endoglucanase), pectinase and xylanase, at significantly high levels. This is quite unusual for a typical entomopathogen or endophytes like *B. bassiana* which propelled the quest to explore this fungus as a novel source for industrially important enzymes, particularly biomass-degrading enzymes. Amylases (3.2.1.1) are hydrolases that catalyze the hydrolysis of internal α-1, 4-glycosidic linkages in starch to yield low molecular weight products, which include glucose, maltose and maltotriose units. Microbial amylases, in particular, have been used in different industries including the food industry (bakery and juice processing), biofuel, textile, detergents, paper and fine chemicals (Sundarram and Murthy 2014). Endo-(1,4)-*β*-D-glucanase (EC 3.2.1.4) are cellulases that randomly attack the internal *O*-glycosidic bonds of the cellulose chain, releasing glucan chains of different lengths. Besides their use in the production of biofuels, cellulases have found wide applications in the paper/pulp, textile, animal feed, recycling, food processing and agricultural industries, amongst others (Keshk 2016; Wang *et al.,* 2019b).

On the other hand, pectinases (polygalacturonase) (E.3.2.1.15) are a special group of enzymes that catalyze the degradation of pectic polymers found in plant cell walls. This unique group of enzymes are important in juice extraction/processing, paper/pulp industry, breweries, oil extraction, and wastewater treatment, to mention a few (Kavuthodi and Sebastian 2018; Radha *et al.,* 2019). Similarly, xylanases (EC 3.2.1.8) are enzymes that cleave the β-1, 4 backbone of the complex plant cell wall polysaccharide xylan. They are found useful in biopulping, biobleaching, as food additives and in improving the quality of baked products (Chen *et al.,* 2019c). The production of all of these polysaccharide-degrading enzymes have been observed in different microbes, both in submerged and solid-state fermentation conditions (Chadha *et al.,* 2019; Tai *et al.,* 2019). Fungal organisms, in particular, have been a valuable source of these enzymes as a result of their ecological roles as the major recycler of the planet and their adaptation to grow on various biomass and obtain their growth nutrients therein (De Beeck *et al.,* 2020). However, maximal enzyme production is required to reduce their cost as well as enhance their applicability in various industrial processes, thus the need for the optimization of production parameters of these biocatalysts is necessary.

Response surface methodology (RSM) is one of the most common optimization techniques employed in diverse academic, industrial and research fields. The RSM process is a group of statistical and mathematical methods used in developing and optimizing process in which a response of interest is influenced by several variables (Manojkumar, Muthukumaran and Sharmila 2020). Typically, response surface models are based on fitting an experimental model to experimental data obtained in regard to an experimental design. It is a valuable tool with important applications in experimental designs, product design and development, as well as in the optimization of existing products and process designs. The major benefit of RSM is the reduced number of experimental runs required to provide sufficient information for a statistically acceptable model. Thus, it is faster and less resource consuming than the traditional "one factor at a time approach" of optimization (Chollom *et al.,* 2020). Furthermore, unlike conventional methods, RSM also puts into consideration the real-time interactions of the different factors as they affect the involved process (Jasni *et al.,* 2020).

Several different methodologies for the response surface process were first introduced by Box and others in the 1950s (Box 1952; Myers 1999) and they have since found applications in many industrial processes, including biotechnology, biochemistry, food science/technology and engineering, amongst others (Anfar *et al.,* 2020; Botinestean *et al.,* 2020; Wu *et al.,* 2020b). These multivariate optimization techniques usually involve an initial stage to screen factors in order to determine and choose the important independent variables out of a possible many. This stage is required to streamline the optimization process to increase efficiency and reduce the number of runs or tests. A second stage involves the evaluation of the major contributing factors resulting in a value for the response to achieve near-optimum output. Subsequently, mathematical/statistical models of the data generated from the experimental design are developed by fitting linear or quadratic polynomial functions, followed by the identification of the optimum values (stationary points) of the evaluated variables.

RSM has been effectively applied in evaluating multiple production variables to predict the optimal conditions necessary for microbial enzyme production processes (Yolmeh and Jafari 2017; Adetunji and Olaniran 2020; Aziz, Elgammal and Ghitas 2020). Hence, the study was aimed at investigating the optimum conditions for the production of extracellular amylase, endoglucanase, pectinase and xylanase by *B. bassiana* SAN01 under submerged fermentation using readily available agricultural residues. The

carbohydrases were selected based on previous research (Petlamul and Boukaew 2019; Ryali *et al.,* 2020), and results obtained from the transcriptomic study described in Chapter 2. In addition, the choice of these enzymes was based on other pilot experiments in our laboratory as well as their documented industrial importance from literature. Two stepwise optimization strategies were employed which included Plackett-Burman design to identify the significant production parameters and Central Composite Design to optimize the levels of the significant variables. To the best of our knowledge, this is the first study to optimize the production of any glycoside hydrolase in *B. bassiana* using lignocellulosic biomass.

3.2 Methodology

3.2.1 Chemicals and reagents

The lignocellulosic materials used in the study were obtained locally in Durban, South Africa. Beechwood xylan, carboxymethyl cellulose (CMC), citrus pectin and 3, 5-dinitrosalicylic acid (DNS) were purchased from Sigma-Aldrich (South Africa). All other chemicals and reagents used were of analytical grade and were obtained from validated suppliers.

3.2.2 Microorganism

The fungus was isolated locally from onion leaves and identified by the amplification of its rDNA ITS region (Gene Accession Number: MN544934). The strain designated as *Beauveria bassiana* SAN01 was grown on potato dextrose agar (PDA) slants at 30°C for five days and subsequently stored at 4°C. The inoculum was prepared by suspending the spores on sterile 0.1% Tween-20 to give a final count of 1x 10^7 spores mL^{-1}.

3.2.3 Screening of lignocellulosic biomass

Seven different, readily available biomass (bambara haulms, banana peel, corn cob, spent tea leaves, sugarcane bagasse (SB), wheat bran and wheat straw) were evaluated as potential substrates for *B. bassiana* SAN01 amylase, endoglucanase, polygalacturonase, and xylanase production. The substrates were dried at 40°C in a drier until constant weight, pulverized to 1.0 mm mesh size and used for media preparation. Fermentation was carried out in 250 mL Erlenmeyer flasks containing 100 mL mineral salt solution and 50 gL^{-1} of the respective plant biomass at pH 5.0, which had been autoclaved at

121°C for 20 min. The flasks were inoculated with *B. bassiana* spores (1 x 10^7 spores) and incubated at 30°C and 150 rpm for 12 days. Subsequently, the culture broth was filtered and centrifuged at 10,000 x g for 15 min at 4°C. The supernatant thus obtained was used as the crude enzyme for subsequent analyses.

3.2.4 Enzyme assay

Amylase, endoglucanase, polygalacturonase and xylanase activities were measured using soluble starch, carboxymethylcellulose (CMC), orange peel pectin and beechwood xylan, respectively at 1% level. The reducing sugars released in the reactions were determined by the DNS method according to (Bailey, Biely and Poutanen 1992). One unit (U) of amylase, cellulase, polygalacturonase and xylanase activity is defined as the amount of enzyme liberating 1 µmol of the respective monomer from the respective substrate per min under standard assay conditions (40°C, 50 mM acetate buffer, pH 5.5).

3.2.5 Statistical optimization of production parameters

The optimization of production parameters for the four enzymes was carried out using Response Surface Methodology (RSM) at two stages. The first stage involved the screening of production parameters, while the second stage involved the optimization of the selected significant variables (Qadir *et al.,*2018).

3.2.5.1 *Plackett-Burman design (PBD*)

The Design Expert 11.0 (Stat-Ease, Minneapolis, USA) Plackett-Burman design was employed for the screening of important media components and culture parameters. Eleven factors were selected from earlier reports (Feng and Ying, 2002; Petlamul and Boukaew 2019; Ryali *et al.,* 2020) and each factor was tested at two levels, high (+) and low (-), resulting in a set of 12 experimental runs (Table 3.1) (Ghosh and Ghosh 2019). The design was intended to demonstrate the individual effect of these variables rather than their cumulative or interactive effect on responses and can be represented by the first-order polynomial equation:

$$Y \quad \beta_0 + \sum \beta_i X_i$$

Where Y is denoted as the predicted response, while βo and βi are the model intercepts and the linear coefficients, respectively, Xi is defined as the level of the independent variable.

All experiments were carried out in triplicates and the average enzyme activities of xylanase and endoglucanase were recorded as the responses. F and P values and the proportion of variance R^2 determined the model significance at $p = 5\%$ level. Table 3.1 shows the factors under investigation as well as the levels of each factor used in the experimental design. The effect of each variable was analysed and the ones that showed the highest influence on the production of the four enzymes were selected for second level optimization by Central Composite Design of RSM.

Table 3.1: Variables and their levels employed in PBD for the screening of parameters affecting amylase, endoglucanase, polygalacturonase and xylanase production by *B. bassiana* SAN01.

Factor	Code	Unit	Low level (-1)	Zero level (0)	High level (+1)
Incubation temperature	A	ºC	27	30	33
pH	B	-	6.0	6.5	7.0
Incubation period	C	hours (h)	264	288	312
Wheat bran (carbon source)	D	gL^{-1}.	20	40	60
Yeast extract (nitrogen source)	E	gL^{-1}.	5	10	15
KH_2PO_4	F	mgL^{-1}.	800	1000	1200
KCl	G	mgL^{-1}.	400	500	600
$MgSO_4$	H	mgL^{-1}.	400	500	600
NaCl	I	mgL^{-1}.	200	250	300
$CaCl_2$	J	mgL^{-1}.	150	200	250
$FeSO_4$	K	mgL^{-1}.	80	100	120

3.2.5.2 Central composite design (CCD)

The three selected process variables having a significant effect on the concomitant production of amylase/polygalacturonase and endoglucanase/xylanase were further optimized using CCD at 5 levels (−1.68, −1, 0, +1, +1.68) to outline the interaction

between the selected variables for the maximization of enzyme production (Table 3.2 & 3.3). All other variables were maintained at zero points as stated in the 2-level factorial design. A full 2^3 factorial design was constructed, leading to 20 experimental runs which consisted of 14 runs for factorial design and 6 runs for the replication of central points. Quantitative data generated from these experimental runs were subjected to regression analysis through response surface methodology to solve multivariate equations. This methodology allows the modelling of a second-order equation that describes the process.

$$Y \quad \beta_0 + \sum_{i=1}^{K} \beta_i X_i + \sum_{i=1}^{K} \beta_{ii} X_i^2 + \sum i \sum \beta_{ij} X_i X_j$$

Where Y denotes the predicted response, k the number of factor variables, β_0 the model constant, βi the linear coefficient, βii the quadratic coefficient and βij the interaction coefficient.

The three selected parameters having significant effects on the simultaneous production of both amylase/polygalacturonase and endoglucanase/xylanase were further optimized using CCD at 5 levels (−1.68, −1, 0, +1, +1.68) for the maximization of enzyme production (Table 3). All other variables were maintained at zero points as stated in the 2-level factorial design. A full 2^3 factorial design was constructed to give 20 experimental runs which consisted of 14 runs for factorial design and 6 runs for central point replication. Quantitative data generated from these experimental runs were subjected to regression analysis through response surface methodology to solve multivariate equations. This methodology allows the modelling of a second-order equation that describes the process.

$$Y \quad \beta_0 + \sum_{i=1}^{K} \beta_i X_i + \sum_{i=1}^{K} \beta_{ii} X_i^2 + \sum i \sum \beta_{ij} X_i X_j$$

Where Y denotes the predicted response, k the number of factor variables, β_0 the model constant, βi the linear coefficient, βii the quadratic coefficient and βij the interaction coefficient.

Table 3.2: Coded and real values of production parameters used for CCD (amylase and polygalacturonase)

Independent Variables	Units	Levels				
		-1.68	-1	0	+1	+1.68
Temperature (A)	℃	24.96	27	30	33	35.05
pH (B)		4.32	5.0	6.0	7.0	7.68
Wheat bran (C)	gL^{-1}.	6.36	20	40	60	73.64

Table 3.3: Coded and real values of production parameters used for CCD (endoglucanase and xylanase)

Independent Variables	Units	Levels				
		-1.68	-1	0	+1	+1.68
Temperature (A)	*℃*	24.96	27	30	33	35.05
Wheat bran (B)	gL^{-1}.	6.36	20	40	60	73.64
Yeast Extract (C)	gL^{-1}.	3.18	10	20	30	36.82

3.3 Results and discussion

3.3.1 Screening of biomass for enzyme production by *B. bassiana* SAN01

Production levels of the selected carbohydrases by *B. bassiana* SAN01 were found to vary significantly across the various agricultural residues used as sole carbon source (Table 3.4). The highest production levels of the four enzymes (19.48 UmL^{-1} for amylase, 17.16±0.41 UmL^{-1} for endoglucanase, 27.37±0.56 UmL^{-1} for polygalacturonase and 304.48±13.25 UmL^{-1} for xylanase) were observed while using wheat bran as the feedstock. Wheat bran has been recognized as model lignocellulosic biomass for industrial enzyme production and has been used in various studies for the production of different carbohydrate-active enzymes in fungi, as well as bacteria (Muthukrishnan 2017; Biswas *et al.,* 2019). The preference of various microbes for wheat bran is believed to be a result of its well-balanced composition which is sufficient to sustain microbial growth

and other metabolic activities of the cells. Proximate studies have shown the substrate to contain various polymers including starch, cellulose, xylan, arabinoxylans, pectin, and sufficient protein to serve as a much-needed nitrogen source (Beaugrand *et al.,* 2004; Babu *et al.,* 2018). Recently, significant amylase production has been recorded in different fungi while utilizing wheat bran as the sole energy source without any supplementation (Oshoma, Okonkwo and Obasuyi 2019; Fadel *et al.,* 2020). In this regard, amylase activities of 140.28 Ug^{-1} and 238.61± 4.72 UmL^{-1} were recorded with *Aspergillus awamori* (Fadel *et al.,* 2020) and *A. niger* (Oshoma, Okonkwo and Obasuyi 2019), respectively. Cellulase production levels of 10.2 UmL^{-1} and 20 UmL^{-1} were also observed from *A. niger* (Akula and Golla 2018) and *Cotylidia pannosa* (Sharma, Garlapati and Goel 2016), respectively with wheat bran as the sole carbon source.

Wheat bran has also been recorded in some studies as the most productive sole carbon source during pectinase production. Pectinase levels of 1.12 UmL^{-1} in *A. oryzae* (Dange and Harke 2018) and 800.0 ± 16.2 Ug^{-1} in *Bacillus subtilis* (Oumer and Abate 2018) were observed in two of such studies. While xylanase levels of 474 UmL^{-1} and 1500 UmL^{-1} were recorded from *A. terreus* (Bakri *et al.,* 2020) and *Bacillus* sp. TC-DT 13 (Rodrigues *et al.,* 2020), respectively. Furthermore, the high production levels of these enzymes during fermentation with wheat bran might be attributed to the high content of non-starch carbohydrates which have been estimated as 70% arabinoxylans, 4% cellulose and 6% β-(1,3) (1,4)-glucan (Sun *et al.,* 2008).

Interestingly, high production levels of the four enzymes (19.48±1.01 UmL^{-1} for amylase, 13.85±0.41 UmL^{-1} for endoglucanase, 17.85±0.33 UmL^{-1} for polygalacturonase and 206.19±4.1 UmL^{-1} for xylanase) were observed while utilizing bambara biomass, an underutilized plant crop grown extensively throughout sub-Saharan Africa. Though *B. bassiana* has been previously shown in different studies to utilize animal by-products (Svedese *et al.,* 2013) and other complex media (Mascarin *et al.,* 2018) for growth and the industrial production of its spores and other important bioproducts, there are currently no studies on *B. bassiana* amylase, cellulase, pectinase or xylanase production using plant biomass.

B. bassiana SAN01 xylanase production was also observed with corn cob, spent tea leaves and banana peel, which were 40-50% of the production levels observed with wheat bran. However, despite using sugarcane bagasse and wheat straw which are known to support high xylanase production in some other fungi (Sanghvi, Koyani and Rajput 2010;

Pandya and Gupte 2012), *B. bassiana* SAN01 produced a relatively lower amount of xylanase using these substrates. Endoglucanase production was also observed with corn cob, spent tea leaves and banana peel as the sole carbon source, though at relatively lower levels. Furthermore, *B. bassiana* SAN01, unlike some other organisms, was unable to utilize sugarcane bagasse and wheat straw for the production of endoglucanase. Similarly, significant production levels of amylase and polygalacturonase (pectinase) were recorded using the banana peel, corn cob and spent tea leaves, while production of both the enzymes was not detected with sugarcane bagasse and wheat straw. It is posited that the presence of relatively higher amounts of inhibitors present in sugarcane bagasse and wheat straw might be responsible for the inability of the fungus to utilize the agro-residues for significant enzyme production (Nouri, Azin and Mousavi 2018; Yuan, Li and Hegg 2018; Soares *et al.,* 2020). Although very low amounts of xylanase were recorded in this study with sugarcane bagasse and wheat straw, the mechanisms that govern the selective secretion of xylanolytic enzymes using the biomasses is not yet understood. Previous studies have overcome the impediment placed on microbial fermentation due to endogenous inhibitors by pretreating these biomass using different methods (Patel, Divecha and Shah 2017; Maibam and Maiti 2020). However, for a fair comparison, in this study, the potentials of sugarcane bagasse and wheat straw along with other biomass were evaluated for enzyme production in their untreated, natural state. Another factor believed to be responsible for this observation is the low carbon/nitrogen ratio of these biomass, as fungi and other microbes require copious amounts of nitrogen and other limiting nutrients during cultivation, especially for fermentation purposes (Bonturi *et al.,* 2017).

It is also noteworthy that the production levels of xylanase enzymes were significantly higher than that of amylase, endoglucanase and polygalacturonase in all the biomass used. This trend is corroborated by other studies where higher xylanase activities relative to endoglucanase (cellulases in general) have been observed in fungi (Iram, Cekmecelioglu and Demirci 2020; Veloz Villavicencio *et al.,* 2020), and even in bacteria (Iram, Cekmecelioglu and Demirci 2020; Yadav *et al.,* 2020). Although the mechanism behind this relationship is not fully known, however, it has been noted that the structure of xylan is less stable and not as tightly packed as that of cellulose, making it more accessible to enzyme action (Sheng *et al.,* 2019). Similarly, higher xylanase production relative to amylase synthesis during the simultaneous release of both the enzymes have

also been observed in previous studies (Guimarães *et al.,* 2006; Shahryari *et al.,* 2019). The production of xylanases in multiple folds relative to that of pectinase has also been shown in different microbes during the concomitant production of both enzymes (Beg *et al.,* 2000; Li *et al.,* 2018a). It is believed that the high concentration of xylan in the biomasses, relative to starch and pectin, is responsible for the higher xylanase production. It is also remarkable that the endoglucanase and xylanase activities observed from *B. bassiana* SAN01 are 5 to 10 folds higher than the maximum level recorded (endoglucanase 3.59 UmL^{-1} and xylanase 39 UmL^{-1}) from another *B. bassiana* strain (Petlamul and Boukaew 2019). Furthermore, the production level of amylase observed from *B. bassiana* SAN01 was ~3-fold higher than in a previous study on *Beauveria* sp. MTCC 5184 (Ryali *et al.,* 2020).

Table 3.4: Screening of lignocellulosic biomass for concomitant production of *B. bassiana* SAN01 carbohydrases

Biomass	Amylase activity (UmL^{-1}) *	Endoglucanase activity (UmL^{-1}) *	Polygalacturonase activity (UmL^{-1})	Xylanase activity (UmL^{-1}) *
Wheat bran	19.48±1.01	17.16±0.41	27.37±0.56	304.48±13.25
Bambara haulm	15.22±0.67	13.85±0.41	17.85±0.33	206.19±4.1
Corn cob	14.12±0.62	9.28±0.41	6.18±0.18	147.12±2.47
Spent tea leaves	5.62±0.31	8.78±0.42	13.44±0.28	141.56±2.93
Banana peel	10.32±5.34	10.17±0.52	14.74±0.41	121.32±5.34
Sugarcane bagasse	0	0	0	45.64±0.83
Wheat straw	0	0	0	21.65±0.13

* Average ±SD of triplicate determinations

3.3.2 Plackett-Burman design

The results obtained from the above experiments showed wheat bran as the best biomass for the production of the four selected enzymes from *B. bassiana* SAN01. It was selected for further optimization using Response surface methodology. In this study, a 12 run PBD was initially used to screen variables having significant effects on all four enzyme

yields. The selected factors with their high and low levels along with the results of their combinational trials are presented in Table 3.5. It was observed that the production of *B. bassiana* SAN01 amylase and polygalacturonase are affected significantly by the same parameters, such as the incubation temperature, the pH of the fermentation media and the concentrations of wheat bran. Whereas the incubation temperature and concentrations of wheat bran and yeast extract were found to influence endoglucanase and xylanase production.

Table 3.5: Plackett-Burman design for eleven variables with coded values along with observed responses.

Run	Coded variable level											Responses (UmL^{-1}) *			
	A	B	C	D	E	F	G	H	I	J	K	AL	EG	PG	XL
1	+1	+1	-1	-1	-1	+1	-1	+1	+1	-1	+1	8.86	8.67	19.97	57.36
2	+1	+1	+1	-1	-1	-1	+1	-1	+1	+1	-1	7.05	8.57	14.14	61.11
3	-1	+1	+1	-1	+1	+1	+1	-1	-1	-1	+1	13.66	9.07	22.57	50.16
4	-1	+1	-1	+1	+1	-1	+1	+1	+1	-1	-1	22.85	10.75	29.26	122.3
5	+1	+1	-1	+1	+1	+1	-1	-1	-1	+1	-1	13.85	9.72	22.04	67.54
6	+1	-1	+1	+1	+1	-1	-1	-1	+1	-1	+1	16.47	9.22	26.34	54.45
7	+1	-1	-1	-1	+1	-1	+1	+1	-1	+1	+1	16.8	8.4	20.71	46.19
8	-1	-1	-1	+1	-1	+1	+1	-1	+1	+1	+1	25.67	14.81	36.22	243.06
9	-1	+1	+1	+1	-1	-1	-1	+1	-1	+1	+1	26.49	13.74	28.35	242.74
10	-1	-1	-1	-1	-1	-1	-1	-1	-1	-1	-1	25.38	12.25	29.09	205.38
11	-1	-1	+1	-1	+1	+1	-1	+1	+1	+1	-1	19.85	9.11	26.35	60.91
12	+1	-1	+1	+1	-1	+1	+1	+1	-1	-1	-1	16.15	9.69	23.38	103.63

* Average of triplicate determinations
*AL: Amylase * EG: Endoglucanase
* PG: Polygalacturonase *XL: Xylanase

The significance of the observed factors on the production of the four glycosyl hydrolases from *B. bassiana* SAN01 is highlighted in the Pareto charts (Appendix 3 & 4). The respective charts have bars of length proportional to the value of the estimated effects, divided by the standard error (Cao *et al.,* 2012). The bars are presented in order of the magnitude and significance of the effects on the enzyme production levels, with the most significant factors coming first. Furthermore, positive effects are illustrated by orange-coloured bars while negative effects are shown by the blue bars. Hence, inferring from the plot for amylase, the factors arranged in the order of significance are temperature > wheat bran > pH; the same order of significance was observed for polygalacturonase. However, for endoglucanase and xylanase, the order observed were temperature > wheat bran > yeast extract and temperature > yeast extract > wheat bran, respectively.

Regression analyses were performed to fit the response function with the experimental data. The summaries of the student *t*-distribution, the corresponding *P*-values, and the parameters estimated are presented in Appendix 5a & b. The analysis of variance for the PB models derived for amylase and polygalacturonase (Appendix 5a) confirmed the observation from the Pareto plots. It revealed that the incubation temperature, pH of the fermentation media and the concentration of wheat bran had the most significant impacts with p-values of 0.0007, 0.0284, 0.0201, respectively for amylase and 0.0004, 0.0097, 0.0027 for polygalacturonase in the same order. The ANOVA for the PB models derived for xylanase and endoglucanase (Appendix 5b) also showed that the incubation temperature, concentration of wheat bran, and yeast extract were the most significant parameters with p-values of 0.0016, 0.0152 and 0.0021 respectively for xylanase production and 0.0018, 0.0081 and 0.0096 for endoglucanase production in a similar order. These low p-values indicate the significance of the respective factors on the production of the four enzymes (Balaji, Chittoor and Jayaraman 2020). The selection of these factors is also in agreement with the previous optimization studies that have identified wheat bran (Das *et al.,* 2013; Hammami *et al.,* 2020), yeast extract (Das *et al.,* 2013; Satti *et al.,* 2019), pH (Gafar *et al.,* 2020; Yazici *et al.,* 2020) and fermentation temperature (Huang *et al.,* 2018; Deng *et al.,* 2020) as important factors affecting enzyme production at the first level in different organisms.

In addition, the interdependence of amylase/polygalacturonase, as well as endoglucanase/xylanase, can be deduced from the observation that the production of the

concomitantly produced enzymes was affected by the same production parameter. Previous studies have shown the significant effects of temperature, pH and substrate concentration on the simultaneous production of amylase and polygalacturonase in some microorganisms (Dalvi and Anthappan 2007; Juwon and Emmanuel 2012). A similar trend was also observed during the simultaneous production of xylanase and endoglucanase from other fungi, *Coprinopsis cinerea* (Huang *et al.,* 2018) and *Trichoderma viride* (Huang *et al.,* 2013), where temperature, nitrogen source, substrate concentration, and pH were identified as critical factors affecting the enzyme yields (Huang *et al.,* 2018).

Furthermore, the significant positive or negative effects of different parameters on *B. bassiana* enzyme production were also confirmed from the coefficient estimates for the models for each enzyme (Appendix 6a & b). An increase in the incubation temperature and pH of the media had negative coefficients, which amount to negative effects on amylase and polygalacturonase production while increasing wheat bran concentration had a positive coefficient that translates into a positive effect. For endoglucanase/xylanase production, increasing temperature and yeast extract affected production negatively as deduced from their coefficient estimates, while increasing wheat bran concentration impacted the enzyme production in a positive manner.

From the analysis of variance, the observed model *F*-values for the polynomial model of amylase (14.52), endoglucanase (14.85), polygalacturonase (21.63) and xylanase (17.05) implied that the models were significant (Appendix 5a & b); thus, there were very low probabilities that the model *F*-values could have occurred due to noise. The determination coefficient R^2 of the amylase model was found to be 0.8449, endoglucanase was 0.8478, while the polygalacturonase and xylanase models were 0.8902 and 0.8648, respectively. Likewise, the signal to noise ratio of the models were 10.861, 11.451, 13.587 and 12.206 for amylase, endoglucanase, polygalacturonase and xylanase, respectively, which are all within the acceptable ranges (Ghosh and Ghosh, 2019).

Thus, the experimental results for the production of the *B. bassiana* glycosyl hydrolase were fitted into first-order models by the equations given below:

Amylase activity = 17.76 – 4.56A + 2.3B + 2.49D

Polygalacturonase activity = 28.87 – 3.77A – 2.15B – 2.73D

Where A, B and D are coded values for incubation temperature, pH and concentration of wheat bran, respectively.

Xylanase activity = 109.57 – 44.52A + 29.38D – 42.64E

Endoglucanase activity = 10.33 – 1.29A + 0.9883D – 0.955E

Where A, D and E are coded values for the incubation temperature, concentration of wheat bran and concentration of yeast extract, respectively.

Hence, the analysis of variance and all other significant measures established that the models predicted for the production of the four carbohydrases from *B. bassiana* SAN01 were sufficient for elucidating the significance of the three chosen factors.

3.3.3 Central composite design

The significant factors obtained from PB were optimized further using CCD. Experimental results obtained at the end of the runs indicated a close agreement between the observed and predicted enzyme activities for both responses (Tables 3.6a & b). Thus, these results highlight the accuracy of RSM in the optimization of fermentation parameters for enhanced enzyme production in *B. bassiana* SAN01. Experimental values showed that amylase production levels are between 10.21 and 36.02 UmL^{-1} while polygalacturonase levels were between 19.34 and 52.63 UmL^{-1} (Table 6a). Furthermore, xylanase activities ranged from 222.93 to 917.34 UmL^{-1} and endoglucanase between 6.38 to 19.42 UmL^{-1} (Table 6b).

Table 3.6a: CCD design and the response of the dependent variables for amylase and polygalacturonase production

	Level			Amylase (UmL^{-1}) *		Polygalacturonase (UmL^{-1})*	
	Coded (A)	Coded (B)	Coded (C)	Actual	Predicted	Actual	Predicted
1	-1	+1	+1	25.49	25.15	40.84	39.44
2	+1	-1	-1	36.02	34.67	52.63	50.73
3	-1.68	0	0	18.33	18.39	25.26	26.82
4	-1	-1	+1	10.21	9.37	19.34	17.32
5	+1	+1	+1	17.05	16.51	24.92	25.42
6	0	0	0	24.74	23.80	39.12	38.59
7	0	0	0	14.39	13.45	26.55	24.08
8	0	+1.68	0	15.72	16.63	25.27	25.12
9	0	0	0	14.92	15.84	24.25	26.40
10	-1	-1	-1	34.25	34.67	50.29	50.73
11	0	0	-1.68	27.85	27.91	42.16	41.79
12	+1	+1	-1	34.90	34.67	51.17	50.73
13	0	0	0	35.04	34.67	49.13	50.73
14	0	0	0	26.94	27.26	41.36	40.49
15	0	0	0	23.52	23.36	36.16	34.05
16	+1.68	0	0	27.09	27.05	36.17	37.28
17	0	0	+1.68	33.90	34.67	49.07	50.73
18	0	-1.68	0	34.11	34.67	52.28	50.73
19	+1	-1	+1	14.36	15.75	25.67	29.05
20	-1	+1	-1	27.02	27.35	38.18	39.60

* Average of triplicate determinations

Table 3.6b: CCD design and the response of the dependent variables for endoglucanase and xylanase production

	Level			Xylanase (UmL^{-1}) *		Endoglucanase (UmL^{-1}) *	
	Coded (A)	**Coded (B)**	**Coded (C)**	**Actual**	**Predicted**	**Actual**	**Predicted**
1	-1	+1	+1	447.41	452.16	11.21	11.42
2	+1	-1	-1	480.26	458.62	13.08	12.90
3	-1.68	0	0	541.53	545.90	12.38	12.09
4	-1	-1	+1	270.60	273.35	6.16	6.42
5	+1	+1	+1	333.75	331.92	9.53	9.94
6	0	0	0	851.15	859.56	18.61	19.05
7	0	0	0	876.60	859.56	19.58	19.05
8	0	+1.68	0	389.97	399.79	10.46	9.99
9	0	0	0	847.28	859.56	18.72	19.05
10	-1	-1	-1	630.75	615.69	15.21	14.82
11	0	0	-1.68	833.18	866.56	20.06	20.29
12	+1	+1	-1	493.04	473.40	11.90	11.66
13	0	0	0	845.42	859.56	19.27	19.05
14	0	0	0	823.65	859.56	18.68	19.05
15	0	0	0	917.34	859.56	19.42	19.05
16	+1.68	0	0	293.20	312.71	8.96	9.22
17	0	0	+1.68	469.21	459.71	12.04	11.77
18	0	-1.68	0	222.93	236.99	6.38	6.82
19	+1	-1	+1	248.80	245.41	7.51	7.10
20	-1	+1	-1	736.27	722.78	15.32	15.75

* Average of triplicate determination

The results presented in Tables 3.6a & b were also confirmed by the Predicted versus Actual value plots. The predicted versus actual value plots of outputs for the CCD plots of amylase, polygalacturonase, endoglucanase, and xylanase are presented in Appendix 7 & 8. These diagnostic plots also indicate close agreements between actual data and the data predicted by the models. Hence the observed tendencies in the linear regression fit of these plots were considered adequate enough to validate the model within the experimental range studied (Ghafari *et al.,* 2009; Elkelawy *et al.,* 2020).

The magnitude, as well as the respective positive and negative effects of the parameters on the production of the individual enzymes were deduced from the Coefficient estimate analysis (Appendix 9a-d). Positive linear effects were observed for all the three optimized parameters with regards to amylase and polygalacturonase production. However, while pH with a coefficient estimate of 3.40 had the highest effect on amylase production, wheat bran concentration with an estimate of 4.30 was shown to be the most effective on polygalacturonase production. In addition, the positive linear effect of wheat bran and a negative linear effect of temperature and yeast extract on the production levels of both endoglucanase and xylanase were recorded. Moreover, the concentration of yeast extract showed the highest effect in both cases (coefficient = -120.96 (xylanase), -2.53 (endoglucanase).

The models generated for the responses were quadratic, and the selected *P*-levels of linear and interactive variables were then fitted into the quadratic polynomial equations shown below:

Amylase activity = $34.63 + 2.26A + 3.40B + 3.18C - 3.14AB + 1.83AC - 0.684BC - 5.34A^2 - 4.64^2 - 4.48C^2$

Polygalacturonase activity = $50.73 + 1.49A + 4.19B + 4.30C - 4.96AB + 2.40AC - 1.48BC - 6.78A^2 - 6.11B^2 - 6.49C^2$

Where A = Incubation temperature; B = pH and C= Wheat bran concentration

Likewise, the quadratic models generated for endoglucanase and xylanase activities are given below:

Xylanase activity = $859.56 - 69.33A + 48.4B - 120.96C - 23.08AB + 32.38AC + 17.93BC - 152.12A^2 - 191.33B^2 - 69.44C^2$

Endoglucanase activity = $19.05 - 0.8517A + 0.9418B - 2.53C - 0.5400AB + 0.6525AC + 1.02BC - 2.97A^2 - 3.76B^2 - 1.07C^2$

Where A = Incubation temperature; B = Wheat bran concentration and C= Yeast extract concentration

The characteristics of the four generated models were evaluated to determine their reliability, which showed that both the models were adequate. The *F*- and p-values as deduced from the ANOVA (Table 3.7a & b) also highlighted the reliability of the models. The model *F*-values, 146.68 (amylase), 49.47 (polygalacturonase), 192.68 (endoglucanase) and 145.58 (xylanase) and their respective low p-values confirmed the significance of the models, thereby overcoming the probabilities that the model *F*-values could occur due to noise (Tarrsini *et al.,* 2020). The models, as well as their terms (A, B, C, AB, AC, BC, A^2, B^2, C^2), were found to all have p- values less than 0.1, thus are all considered significant and reliable (de Castro *et al.,* 2015). However, the BC in the xylanase model (p-value = 0.1134) was the only term found to be insignificant. The goodness of fit of the model was confirmed by the R^2 values, which are the determination coefficient (Table 7). The closer the values of R^2 to 1, the more the models can explain the variability between the experimental and predicted values (Long *et al.*, 2019).

In the present study, the models showed a high R^2 value for the production of the enzymes. R^2 values of 0.9926, 0.9943, 0.978 and 0.9924 were recorded for the quadratic models of amylase, endoglucanase, polygalacturonase and xylanase production, respectively. These indicate that three models (amylase, endoglucanase and xylanase) can explain more than 99% of the total variation, while the polygalacturonase model can explain above 97% of the variation, thus presenting significant relationships among the evaluated variables. Furthermore, the differences between the adjusted R^2 and the predicted R^2 values in all of the models were less than 0.2, while the signal to noise ratios was above 4.0, thus showing the aptness of the models and their applicability to the design space (Tai *et al.,* 2019). The adequate precision ratio, which is another parameter for model adequacy, is defined as a measure of signal to noise ratio and values greater than 4 are desirable for adequate signals (Long *et al.,* 2019). Thus, the computed Adeq Precision of 36.084 (amylase), 39.462 (endoglucanase), 20.815 (polygalacturonase) and 30.456 (xylanase) observed in this study indicate adequate signals for the production optimization of the four glycosyl hydrolases from *B. bassiana* SAN01.

Table 3.7a: ANOVA of quadratic models for *B. bassiana* SAN01 amylase and polygalacturonase production

Amylase						Polygalacturonase					
Source	**Sum of Squares**	**df**	**Mean Square**	**F-value**	**p-value**	**Source**	**Sum of Squares**	**df**	**Mean Square**	**F-value**	**p-value**
Model	1320.10	9	146.68	149.21	< 0.0001	**Model**	2292.71	9	254.75	49.47	< 0.0001
A	69.89	1	69.89	71.10	< 0.0001	A	30.18	1	30.18	5.86	0.0360
B	157.41	1	157.41	160.13	< 0.0001	B	239.54	1	239.54	46.51	< 0.0001
C	138.52	1	138.52	140.91	< 0.0001	C	253.10	1	253.10	49.15	< 0.0001
AB	78.81	1	78.81	80.17	< 0.0001	AB	197.21	1	197.21	38.29	0.0001
AC	26.75	1	26.75	27.22	0.0004	AC	46.18	1	46.18	8.97	0.0135
BC	3.74	1	3.74	3.80	0.0797	BC	17.46	1	17.46	3.39	0.0954
A^2	411.20	1	411.20	418.29	< 0.0001	A^2	66.,18	1	662.18	128.58	< 0.0001
B^2	310.01	1	310.01	315.36	< 0.0001	B^2	538.06	1	538.06	104.48	< 0.0001
C^2	289.56	1	289.56	294.56	< 0.0001	C^2	607.41	1	607.41	117.94	< 0.0001

Amylase: R^2 = 0.9926, Adjusted R^2 = 0.9860, Predicted R^2 = 0.9580, Adequate precision AP= 36.084

Polygalacturonase: R^2 = 0.9780, Adjusted R^2 = 0.9583, Predicted R^2= 0.8639, Adequate precision AP= 20.815

df; degree of freedom. *Significant p- values at $P \leq 0.1$

Table 3.7b: ANOVA of quadratic models for *B. bassiana* SAN01 xylanase and endoglucanase production

Xylanase						Endoglucanase					
Source	**Sum of Squares**	**df**	**Mean Square**	**F-value**	**p-value**	**Source**	**Sum of Squares**	**df**	**Mean Square**	**F-value**	**p-value**
Model	1.120E+06	9	1.244E+05	145.58	< 0.0001*	**Model**	428.72	9	47.64	192.68	< 0.0001
A	65642.30	1	65642.30	76.81	< 0.0001*	A	9.91	1	9.91	40.07	< 0.0001
B	31991.51	1	31991.51	37.43	0.0001*	B	12.11	1	12.11	48.99	< 0.0001
C	1.998E+05	1	1.998E+05	233.79	< 0.0001*	C	87.60	1	87.60	354.32	< 0.0001
AB	4259.65	1	4259.65	4.98	0.0496*	AB	2.33	1	2.33	9.44	0.0118
AC	8337.28	1	8337.28	9.76	0.0108*	AC	3.41	1	3.41	13.78	0.0040
BC	2572.60	1	2572.60	3.01	0.1134	BC	8.28	1	8.28	33.50	0.0002
A^2	3.335E+05	1	3.335E+05	390.19	< 0.0001*	A^2	126.92	1	126.92	513.34	< 0.0001
B^2	5.276E+05	1	5.276E+05	617.30	< 0.0001*	B^2	204.08	1	204.08	825.44	< 0.0001
C^2	69499.62	1	69499.62	81.32	< 0.0001*	C^2	16.36	1	16.36	66.18	< 0.0001

Xylanase: R^2 = 0.9924, Adjusted R^2 = 0.9856, Predicted R^2 = 0.9716, Adequate precision AP= 30.456

Endoglucanase: R^2 = 0.9943, Adjusted R^2 = 0.9891, Predicted R^2= 0.9860, Adequate precision AP= 39.462

df; degree of freedom. *Significant p- values at $P \leq 0.1$

Furthermore, contour plot and response surface plots were generated based on the quadratic equations derived from the four CCD models to understand the interactions among the independent variables and to determine their values for attaining maximum enzyme production. These plots represent the interactions of two variables while keeping the third variable at its zero levels. For amylase and polygalacturonase production, the interaction between the independent variables i.e., the concentration of wheat bran & pH, the concentration of wheat bran & incubation temperature as well as pH & incubation, all showed significant effects on both responses (Figure 3.1 & 3.2). Similarly, the concentration of wheat bran & yeast extract, the concentration of wheat bran & incubation temperature as well as yeast concentration & incubation all showed significant effects on endoglucanase and xylanase production (Figure 3.3 and 3.4). Distinct peaks were observed for all of the responses which indicated that the models encompassed the optimum region for the production of the enzymes.

An increase in amylase and polygalacturonase production was observed with elevating pH and incubation temperature until the maximum levels of ~34 UmL^{-1} and 50 UmL^{-1} (Figure 3.6 and 3.7) were reached. The peak of the enzyme production was observed at approximately pH 6.0 and 30°C which has been shown previously to be the optimum physiological condition for *B. bassiana* growth and metabolism (Padmavathi, Devi and Rao 2003; Mishra, Kumar and Malik 2015). The effects of these factors on the production of both enzymes were noticed to diminish beyond these optimum values, which is probably due to the decreased metabolic rate of the fungus at higher pH and temperature as well as the denaturing effects of these conditions on the enzymes. A steep increase in the production of both enzymes was also observed with an increase in substrate concentration until the optimum concentration of ~40 gL^{-1}. Increasing the amount of wheat bran beyond the optimum level had less significant effects on the production level. Furthermore, the interaction between the pH of the media and the incubation temperature (Figure 3.1a and 3.2a) had the maximum influence on amylase and polygalacturonase production while wheat bran- pH interaction (Figure 3.1e and 3.2e) had the least effect. This is because the more elliptical the contour plots, the more significant the interactions between corresponding variables, whereas the more circular the less the interactions (Bhagwat *et al.,* 2018).

In the same vein, an initial increase in xylanase and endoglucanase production was observed with increasing wheat bran and temperature until peak levels of ~850 UmL^{-1} and ~20 $UmL^{-1,}$ respectively, after which steep declines were observed (Figure 3.3 and 3.4). Thus, it can be assumed that the production of both enzymes is mainly dependent on wheat bran as the carbon source. Furthermore, a wheat bran concentration of approximately 44 gL^{-1} and incubation temperature of around 29°C was considered optimum for the simultaneous production of both enzymes in shake flask cultures. These results are corroborated by many other studies, where critical components such as the carbon source and nitrogen, at lower levels, failed to produce sufficient enzyme yield, while further increase up to optimal concentrations showed heightened enzyme production, which subsequently diminished at higher concentrations (Bagewadi, Mulla and Ninnekar 2018; Thite, Nerurkar and Baxi 2020). It was also observed from plots showing the interactions of yeast extract and incubation temperature that higher levels of these factors had negative impacts on the production of the two enzymes. Hence, the plots showed that a significant increase in yeast extract had a negative effect on the accumulation of both enzymes. The negative effects of the high concentration of nitrogen sources on carbohydrase production have been suggested in earlier studies (Abdella, Segato and Wilkins 2019). In addition, from the graphs, it can be deduced that the interaction between wheat bran and yeast extract concentration (Figure 3.3e and 3.4e) is shown to be the most significant in both models while that between wheat bran and incubation temperature is the least (Figure 3.3a and 3.4a).

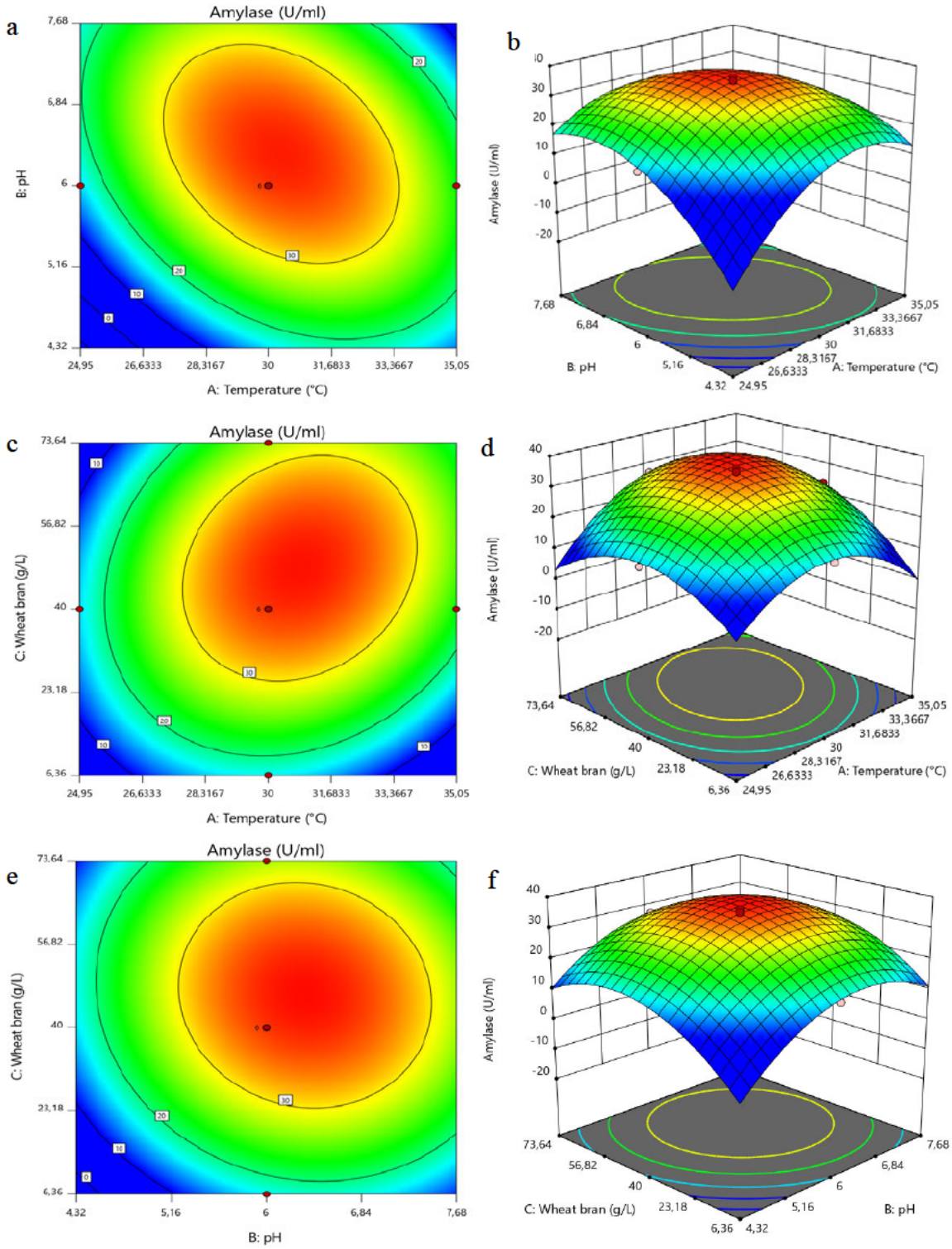

Figure 3.1: Response surface plots showing the interactions between the variables for amylase production from *B. bassiana* SAN01: contour (a) & 3D plots (b) of pH-temperature interaction; contour (c) and 3D plots (d) of wheat bran- temperature interaction; contour (e) and 3D plots (f) of wheat bran-pH interaction.

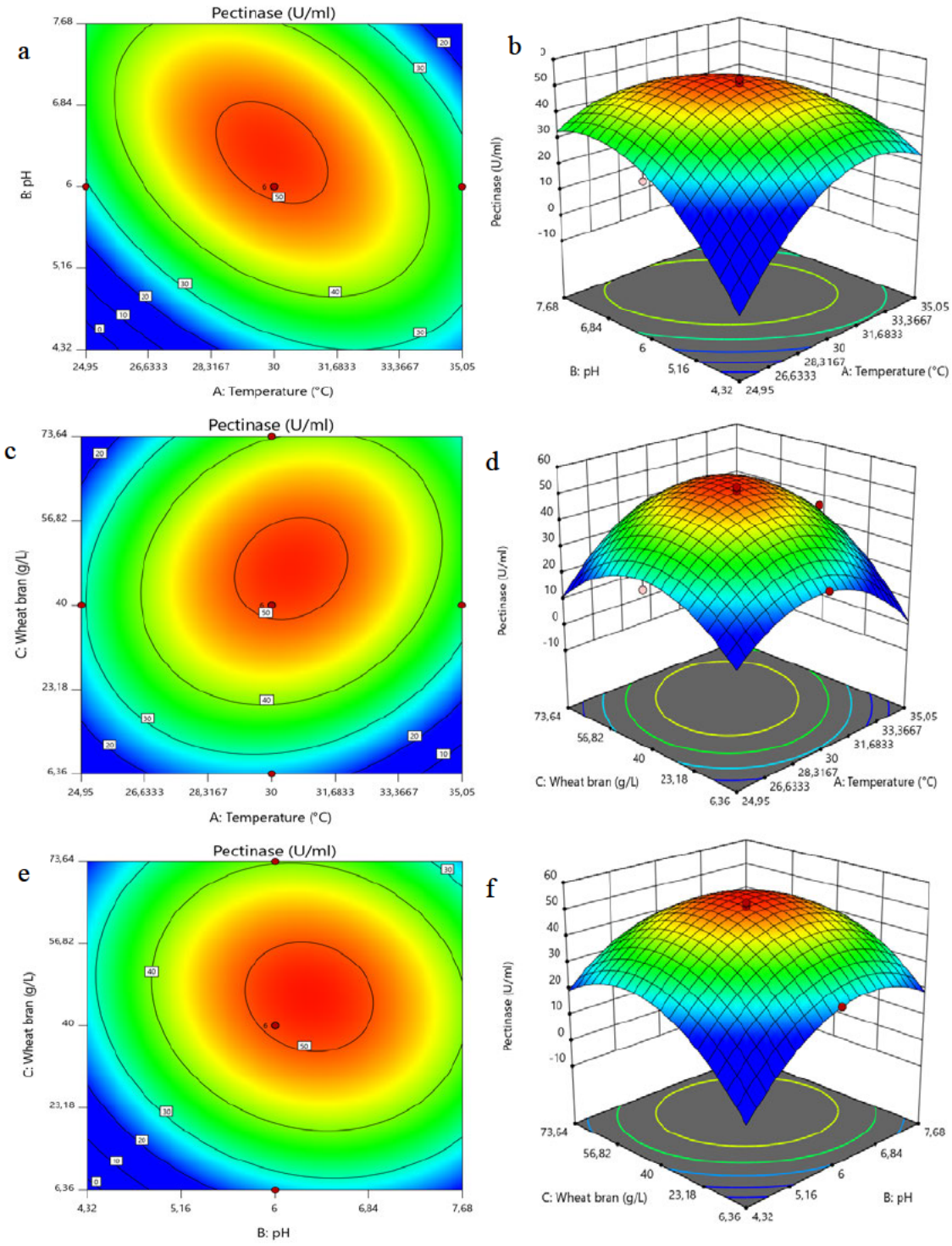

Figure 3.2: Response surface plots showing the interactions between the variables for polygalacturonase production from *B. bassiana* SAN01: contour (a) & 3D plots (b) of pH-temperature interaction; contour (c) and 3D plots (d) of wheat bran- temperature interaction; contour (e) and 3D plots (f) of wheat bran-pH interaction.

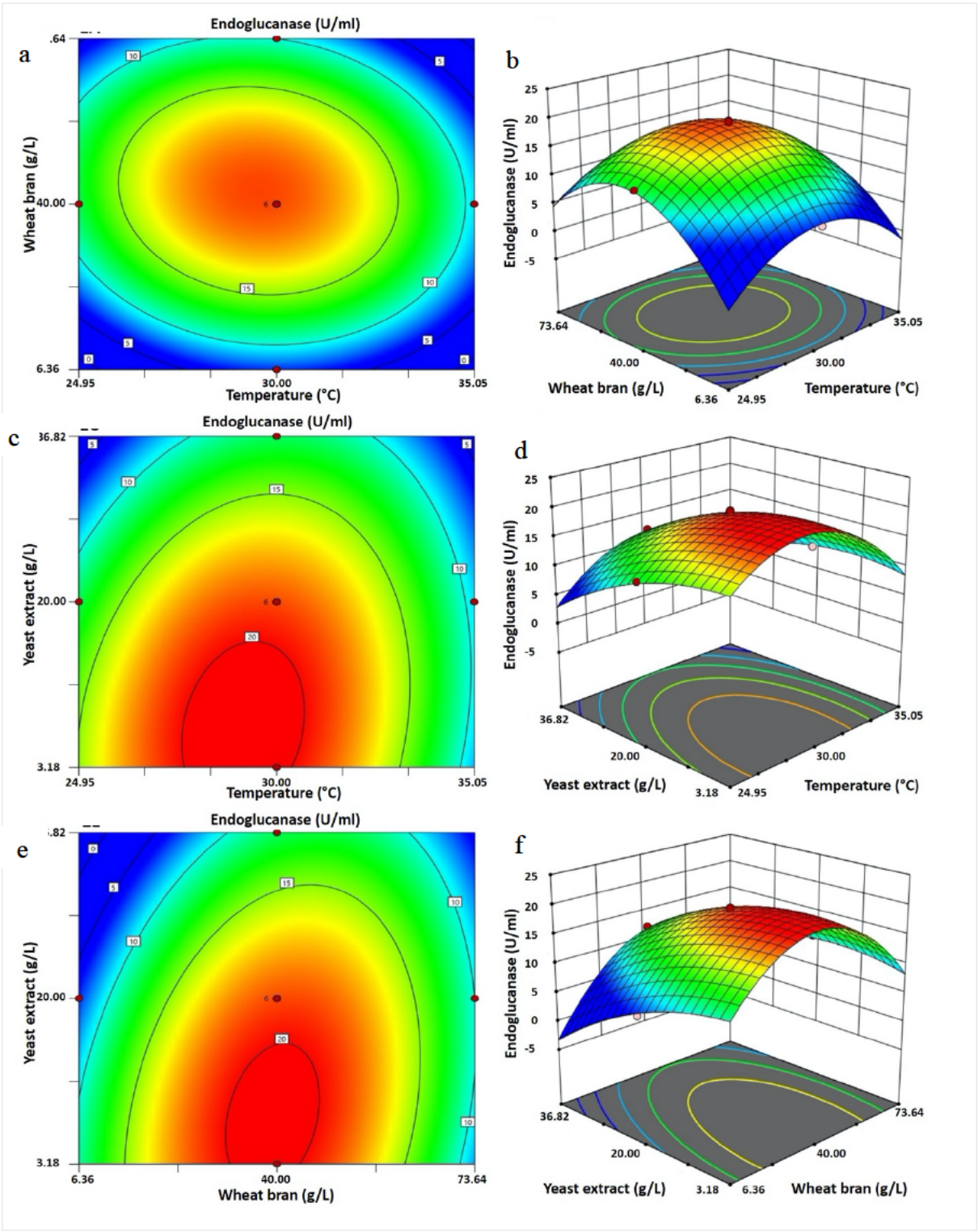

Figure 3.3: Response surface plots showing the interactions between the variables for endoglucanase production from *B. bassiana* SAN01: contour (a) & 3D plots (b) of wheat bran-temperature interaction; contour (c) and 3D plots (d) of yeast extract- temperature interaction; contour (e) and 3D plots (f) of yeast extract-wheat bran interaction.

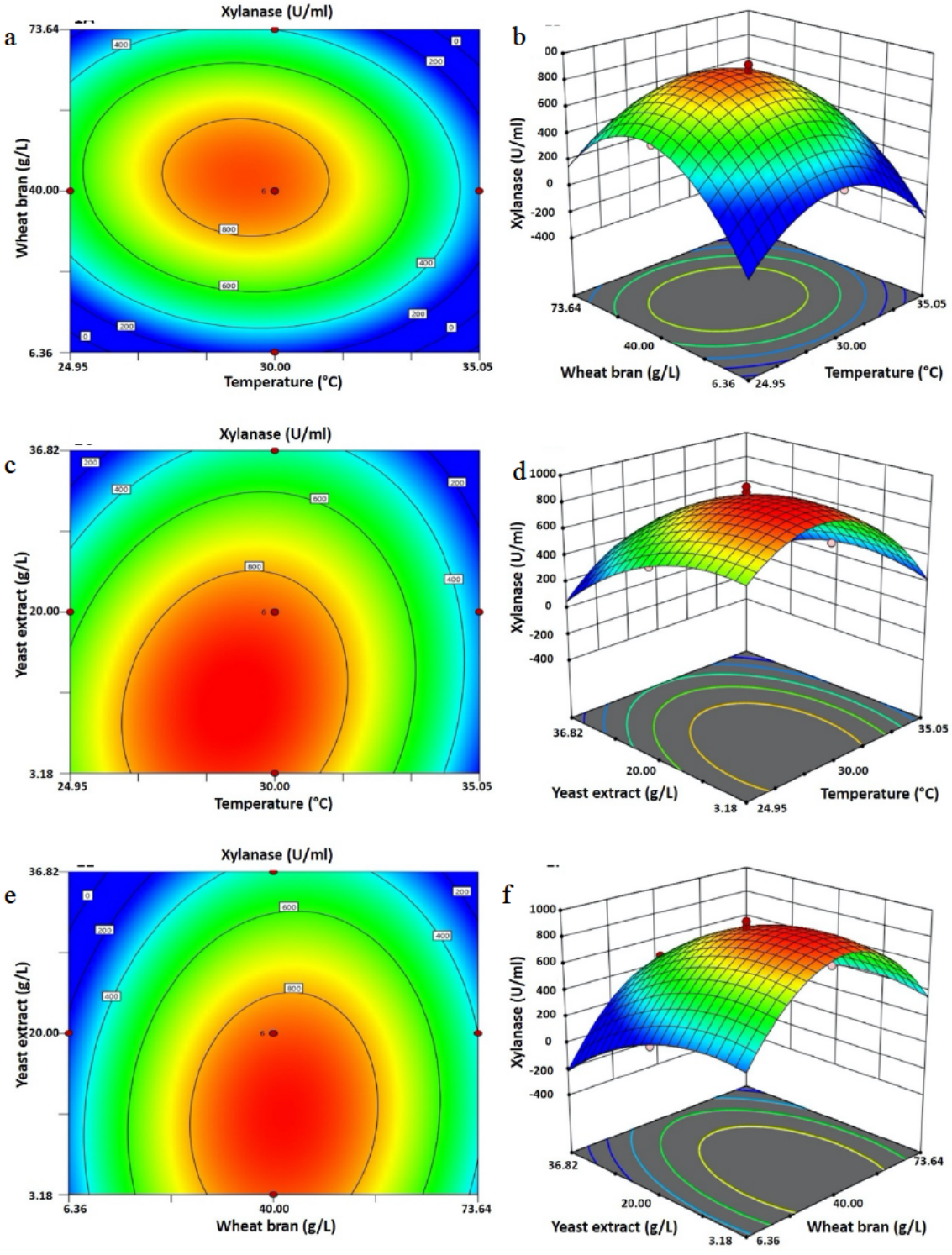

Figure 3.4: Response surface plots showing the interactions between the variables for xylanase production from *B. bassiana* SAN01: contour (a) & 3D plots (b) of wheat bran-temperature interaction; contour (c) and 3D plots (d) of yeast extract- temperature interaction; contour (e) and 3D plots (f) of yeast extract-wheat bran interaction.

3.3.4 Validation of the experimental model

The adequacy of the models was further confirmed and validated by the four enzymes, amylase, endoglucanase, polygalacturonase and xylanase using the derived optimal conditions. The optimum conditions predicted for amylase and polygalacturonase production were pH 6.28, incubation temperature of 30.42°C and wheat bran concentration of 47.2 gL^{-1}. The predicted production level of amylase, 35.87 UmL^{-1} was in close agreement with the experimental value of 34.82 ±1.44 UmL^{-1}. A close agreement was also observed between the predicted polygalacturonase production 51.98 $UmL^{-1}$and the actual level 51.05 ±1.92 UmL^{-1}. Furthermore, the conditions predicted for xylanase production were wheat bran (46.39 gL^{-1}), yeast extract (12.41 gL^{-1}) and incubation temperature (29.12°C); while the optimal conditions predicted for endoglucanase production were wheat bran (42.0 gL^{-1}), yeast extract (11 gL^{-1}) and incubation temperature (29°C). The predicted value of 1061 UmL^{-1} for maximum xylanase production, suggested by the model was in close agreement with the experimental value of 1047±42 UmL^{-1}. Similarly, 23.08 UmL^{-1} predicted for maximum endoglucanase production was found to be close to the actual value of 23.21±1.07 UmL^{-1}. Hence, the observed proximity between the predicted and experimental values indicate that the generated models gave an adequate prediction of both responses. Thus, by applying the factorial designs to the fermentation process, there were a 1.79- and 1.87-fold increase in amylase and polygalacturonase activity compared to unoptimized production levels of 19.48 UmL^{-1} and 27.37 UmL^{-1}, respectively. Similarly, a 3.44- and 1.35-fold increase in xylanase and endoglucanase activity compared to unoptimized production levels of 304.48 UmL^{-1} and 17.16 UmL^{-1}, respectively, were also recorded. These results are remarkable as the enzyme production levels achieved in this study are the highest recorded for any *Beauveria* species or any entomopathogenic fungi, for that matter, based on available literature.

3.4 Conclusion

This study has shown the potential of a novel strain of an entomopathogenic fungus, *B. bassiana* SAN01, to utilize various agricultural residues as substrates for its growth as well as for the production of hydrolytic enzymes, specifically cellulolytic and hemicellulolytic enzymes. Based on the available literature, it can be said that this is the first report giving detailed medium optimization of xylanase and endoglucanase from *B.*

bassiana. After optimizing the production medium, the yield of amylase, endoglucanase, polygalacturonase and xylanase were enhanced up to 1.79, 1.35, 1.87 and 3.44 folds, respectively, as compared with the unoptimized production medium. Furthermore, less than 10% differences between the predicted and experimental production levels of the four enzymes are adequate to justify the validity of the response models of the enzymes. The optimum enzyme production parameters in this study may serve as a future reference for multi-enzyme cocktail production from *B. bassiana* in subsequent investigations. In addition, these findings are expected to stimulate the exploration of *B. bassiana* for the production of industrial enzymes and other bio-based products along with its use as a biocontrol agent.

CHAPTER FOUR

Purification and characterization of *Beauveria bassiana* SAN01 carbohydrases

Abstract

The present study describes the purification and characterization of four different extracellular carbohydrases, *viz.*, xylanase, amylase, endoglucanase, and polygalacturonase from a newly isolated entomopathogenic fungal endophyte, *Beauveria bassiana* SAN01. The *B. bassiana* SAN01 xylanase was purified to homogeneity with a specific activity of 324.2 Umg^{-1} and SDS-PAGE analysis revealed the molecular mass of the enzyme to be ~37 kDa. The purified xylanase performed optimally at pH 6.0 and 45ºC. The xylanase was observed to obey Michaelis-Menton kinetics towards beechwood xylan with apparent K_m of 1.98 $mgmL^{-1}$, V_{max} of 6.65 $\mu Mmin^{-1}$ and k_{cat} of 0.62 s^{-1}, showing high substrate specificity for xylan containing polymers. The purified xylanase was strongly inhibited by Ag^{2+} and Fe^{3+} while it was enhanced by $Co^{2+}$and Mg^{2+}. The three other enzymes were partially purified by ammonium sulphate precipitation and ultrafiltration to a specific activity of 2.9 Umg^{-1} (amylase), 2.72 Umg^{-1} (endoglucanase), and 3.1 Umg^{-1} (polygalacturonase). The optimum pH of the partially purified amylase, endoglucanase, and polygalacturonase was found to be 6.0, 6.0 and 7.0, respectively, while they performed optimally at 35, 35 and 45ºC, respectively. This work presents the first report on the purification and characterization of the four selected carbohydrases from *B. bassiana*.

4.1 Introduction

In line with the continuous search for novel enzymes, some focus has since been shifted to entomopathogenic (Mondal *et al.,* 2016; Litwin, Nowak and Różalska 2020) and endophytic fungi (Rodriguez, Gonzalez and Rodríguez Giordano 2016; Mandal and Banerjee 2019) as novel sources of industrially important biocatalysts. *B. bassiana* appears to be a top candidate in this regard, as the fungus has been shown to produce different enzymes in significant quantities and with distinct biochemical properties (Borgi and Gargouri 2016; Ryali *et al.,* 2020). A lot of attention has, however, been given to the major enzymes produced by *B. bassiana,* which are the chitinases, lipases and proteases (Zhang *et al.,* 2004; Zibaee, Sadeghi-Sefidmazgi and Fazeli-Dinan 2011; Zibaee and Ramzi 2018). These principal enzymes have been well elucidated in different studies highlighting their roles in the fungus' entomopathogenicity as well as its endophytism.

Recently, different strains of *B. bassiana* have been isolated and characterized for the production of biomass-degrading enzymes, which is indicative of their less elucidated environmental role as a saprophyte (Ntsobi *et al.,* 2020). In this regard, different production levels of biomass-degrading enzymes including amylase, beta-glucosidase, endoglucanase, and xylanase have been recorded from the fungus in different studies (Borgi and Gargouri 2016; Petlamul *et al.,* 2017; Ryali *et al.,* 2020). Amylases (3.2.1.1) are depolymerases that catalyze the hydrolysis of internal α-1, 4-glycosidic linkages in starch to yield low molecular weight monomeric and oligomeric products such as glucose, maltose and maltotriose. In particular, microbial amylases have been used in different industries, including the food industry (bakery and juice processing), textile, biofuel, detergents, paper, and fine chemicals (Sindhu *et al.,* 2017; Far *et al.,* 2020).

Endo-(1,4)-*β*-D-glucanase (EC 3.2.1.4) are cellulases that randomly attack the internal *O*-glycosidic bonds of the cellulose chain, releasing glucan chains of different lengths. Besides their prominent use in biofuels production, cellulases have found wide applications in the paper/pulp, textile, animal feed, recycling, food processing, and agricultural industries, amongst others (Keshk 2016; Wang *et al.,* 2019b). On the other hand, pectinases (polygalacturonase; E.3.2.1.15) are a special group of enzymes that catalyze the degradation of pectic polymers found in plant cell walls. This unique group of enzymes are important in juice extraction/processing, paper/pulp industry, breweries, oil extraction, and wastewater treatment, to mention a few (John *et al.,* 2020; Thakur and

Mukherjee 2020). Similarly, xylanases (EC 3.2.1.8) are the key enzymes that cleave the β-1, 4 backbone of the complex plant cell wall polysaccharide xylan. They are useful in biopulping, biobleaching, functional food production, and nutritional improvements of lignocellulosic feeds (Chen *et al.,* 2019c; Petry and Patience 2020).

The production of several polysaccharide-degrading enzymes has been observed in different microorganisms, especially bacteria and fungi (Chadha *et al.,* 2019; Tai *et al.,* 2019; Ezeilo, Wahab and Mahat 2020; Far *et al.,* 2020). However, for the carbohydrases to be effectively and efficiently applied in different industrial processes, they need to fulfil a number of desirable requirements. These requirements which revolve around their robustness under industrial operations may include stability at specific pH or over a wide range of pHs, thermostability, high specific activity, strong resistance to different metals, solvents and other chemical additives. Other specifications may also include their cost-effectiveness, eco-friendliness, ease of use and recyclability. Hence, the need arises to evaluate the biochemical characteristics of these biological catalysts in order to optimize their performance to suit various applications.

Many studies have evaluated the properties of various enzymes in their crude form (Atalla and El Gamal 2020; KC *et al*., 2020; Steiner and Margesin 2020); however, purification of enzymes has been noted to be essential for detailed biochemical, biophysical and molecular characterization. Although the ultimate degree of purity of a specific protein or enzyme is a function of its end use, purification to homogeneity is highly desirable, despite being highly expensive, laborious and time-consuming (Bajpai 2014). It also helps in the accurate determination of the enzyme's structure at the primary, secondary, tertiary and quaternary levels. Hence, this study focused on the purification and biochemical characterization of selected glycoside hydrolase, *viz.*, amylase, endoglucanase, polygalacturonase, and xylanase from *B. bassiana* SAN01. Although successful attempts have been made at the purification of chitinases (Havukkala *et al.,* 1993; Fan *et al.,* 2007b), lipases (Zibaee, Sadeghi-Sefidmazgi and Fazeli-Dinan 2011) and proteases (Ryali *et al.,* 2020) from *B. bassiana*, there are currently no reports on the purification of any of the selected carbohydrases from the fungus.

4.2 Methodology

4.2.1 Chemicals and reagents

The wheat bran used in the study was obtained locally in Durban, South Africa. Beechwood xylan, carboxymethyl cellulose (CMC), citrus pectin, yeast extract and 3, 5-dinitrosalicylic acid (DNS) were purchased from Sigma-Aldrich (South Africa). All other chemicals and reagents used were of analytical grade and were obtained from validated suppliers.

4.2.2. Microorganism

The fungus was isolated locally from onion leaves and identified by the amplification of its rDNA ITS region (Gene Accession Number: MN544934). The strain designated as *Beauveria bassiana* SAN01 was grown on potato dextrose agar (PDA) slants at 30°C for five days and subsequently stored at 4°C. The inoculum was prepared from 5-day old cultures by suspending the spores in sterile 0.1% Tween 20 to give a final count of 1 x 10^7 spores mL^{-1}.

4.2.3 Enzyme production

Fermentation was carried out in 250 mL Erlenmeyer flasks containing 100 mL of optimized media for the production of the respective enzymes, as described in Chapter 3. Briefly, optimum conditions for both amylase and polygalacturonase production were wheat bran (47.2 gL^{-1}), pH 6.28 and incubation temperature, 30.4°C. While for endoglucanase, the conditions were wheat bran (42.0 gL^{-1}), yeast extract (11 gL^{-1}) and incubation temperature (29°C). Furthermore, the conditions used for xylanase production were wheat bran (46.39 gL^{-1}), yeast extract (12.41 gL^{-1}) and incubation temperature (29.1°C). All media were autoclaved at 121°C for 20 min and subsequently inoculated with 1 mL of the spore suspension (1 x 10^7 spores mL^{-1}). The flasks were then incubated at their respective optimum temperatures and 150 rpm for 12 days. Subsequently, the culture broths were filtered and centrifuged at 10,000 x g for 15 min at 4°C. The supernatants thus obtained were used as the crude enzyme for subsequent analyses.

4.2.4 Enzyme assay

Amylase, endoglucanase, polygalacturonase and xylanase activities were measured using soluble starch, carboxymethylcellulose (CMC), orange peel pectin and beechwood xylan, respectively at 1% (w/v). The reducing sugars released during the reactions were determined by the DNS method, according to Bailey, Biely and Poutanen (1992). One unit (U) of amylase, cellulase, polygalacturonase and xylanase activity is defined as the amount of enzyme liberating 1 µmol of the respective monomer from the respective substrate per min under standard assay conditions (40°C, 50 mM acetate buffer, pH 5.5).

4.2.5 Protein estimation

Protein concentration in the culture filtrates was estimated according to a modified Lowry method using Bovine serum albumin (BSA) as the standard (Hartree 1972).

4.2.6 Enzyme purification

4.2.6.1 *Ammonium sulphate precipitation*

The crude enzymes were purified by precipitation, according to Guillaume *et al.,* (2019). Solid ammonium sulphate was added slowly to the crude enzyme filtrate with gentle stirring to bring to 30% saturation (fraction I), 60% saturation (fraction II), and 90% saturation (fraction III) in a sequential manner. The precipitates obtained from each saturation were dissolved in a minimal volume of 0.01 M sodium acetate buffer (pH 5.5) and dialyzed against the same buffer for 48 h at 4°C.

4.2.6.2 *Ion-exchange chromatography*

Ion-exchange chromatography was performed according to Kohli, Joshi and Varma (2020) using an AKTA protein purifier system (GE Healthcare Life Sciences). The precipitated and dialyzed enzyme was loaded to Q Sepharose Fast Flow column (5 mL) previously equilibrated with 20 mM sodium acetate buffer (pH 5.5). A continuous NaCl gradient (0-1 M) was used for elution and 1.5 mL fractions were collected. Fractions showing significant xylanase activity were pooled, subsequently concentrated and desalted using Amicon Ultra-0.5 Centrifugal Filters, with 3 kDa molecular weight cut-off.

4.2.6.3 *Size exclusion chromatography*

Concentrated fractions obtained after ion-exchange chromatography were filtered under vacuum through 0.45 µm pore size filters (Millipore) to remove any suspended particle. Size exclusion chromatography was carried out on a Superdex® 200 10/300 GL (GE Healthcare Life Sciences) column, using the AKTA purifier. A sample volume of 0.5 mL was injected into the system, while NaCl (0.15 M) in sodium acetate buffer (20 mM, pH 5.5) served as the elution buffer (Melnichuk *et al.,* 2020). Fractions (0.2 mL) were collected and the ones with significant xylanase activity were pooled and used for further analysis.

4.2.7 Characterization of enzymes

4.2.7.1 *pH optima and pH stability*

To determine the optimum pH of the *B. bassiana* carbohydrases, the enzyme activities were evaluated at different pHs using the following buffer systems: acetate (pH 3.0–6.0), phosphate (pH 7.0), Tris–HCl (pH 8.0–9.0) and Glycine–NaOH (pH 10.0). For the pH stability evaluation, the enzymes were pre-incubated at the above-mentioned pHs for 30 to 240 min at 30 min intervals, followed by measuring the residual enzyme activities (Gu *et al.,* 2021).

4.2.7.2 *Temperature optima and thermostability*

The enzyme activities of the completely purified xylanase and the partially purified amylase, endoglucanase and polygalacturonase were investigated by incubating the reaction mixtures at different temperatures. For temperature optima, the enzyme activities were determined between 25 and 70°C at 5°C intervals. The thermostability of enzymes was evaluated by pre-incubating the enzymes between 25 and 60°C for 30 to 180 min at 30 min intervals and measuring their residual activities (Ozdemir *et al.,* 2018).

4.2.7.3 *Effect of metal ions and salt concentration on enzyme activity*

The effects of various metal ions including Ag^{2+} ($AgNO_3$), Ba^{2+} ($BaCl_2$), Co^{2+} ($CoCl_2$), Cu^{2+} ($CuSO_4$), Fe^{2+} ($FeSO_4$), Fe^{3+} ($FeCl_3$), Hg^{2+} ($HgCl_2$), Mg^{2+} ($MgSO_4$), Na^{+} (NaCl), and Zn^{2+} ($ZnSO_4$) were determined at 1 mM and 10 mM concentration by adding them to the enzyme reaction mixture and incubating under standard assay conditions (Mhiri *et al.,* 2020).

4.2.7.4 *Effect of various additives on enzyme activity*

The effects of various additives including β-mercaptoethanol (BME), dithiothreitol (DTT), ethylenediamine tetra-acetic acid (EDTA), phenylmethylsulphonyl fluoride (PMSF), sodium dodecyl sulphate (SDS), Tween 20 and Triton X-100 were determined at 1 mM and 10 mM concentration by adding them to the enzyme reaction mixture and incubating under standard assay conditions.

4.2.7.5 *Effects of different solvents on enzyme activity*

The effects of different organic solvents, including acetone, benzene, butanol, chloroform, ethanol, hexane, isopropanol, methanol and toluene, were evaluated. Enzymes were incubated in solutions containing each solvent (10%, v/v) at room temperature with constant agitation at 120 rpm for 1 h. Subsequently, aliquots were withdrawn and the relative activities were determined under standard assay conditions (Zhu *et al.,* 2020).

4.2.8 Kinetic study and substrate specificity

To evaluate the substrate specificity of *B. bassiana* SAN01 xylanase, different reaction mixtures containing the same amount of enzyme and an equimolar amount (10 μM) of specific substrate were incubated under the standard assay conditions. The substrate included arabinoxylan, beechwood xylan, oat spelt xylan, CMC, pectin from citrus peel, and soluble starch. The Michaelis constant (K_m) value of the purified enzyme was estimated using a range of beechwood xylan concentrations between 0.1-20 $mgmL^{-1}$. The apparent K_m value of the purified enzyme was calculated from the Hanes-Woolf plots relating [S]/ v to [S] (Ahmed *et al.,* 2020). Furthermore, the k_{cat} (enzyme turnover number) and the catalytic efficiency were calculated accordingly (Segel 1975; Marangoni 2003).

4.2.9 Analysis of protein pattern by SDS-PAGE

The molecular mass of the completely purified *B. bassiana* carbohydrase, i.e., xylanase, was evaluated by SDS–PAGE. The analysis was carried out on a Mini PROTEAN gel electrophoresis unit (Bio-Rad) using 12% cross-linked polyacrylamide gels and 5% stacking gel (Laemmli 1979). A wide range (6.5-200 kDa) protein ladder (ThermoFisher Scientific) was used as the protein marker (Bhardwaj *et al.,* 2020).

4.2.10 Zymogram analysis of xylanase

The sample was prepared in the standard SDS PAGE treatment buffer without boiling and without a reducing agent. Afterwards, a zymogram was obtained using a 10% polyacrylamide gel containing 0.2% beechwood xylan (Sigma Aldrich). After electrophoresis, the gel was immersed for 30 min in 2.5% (v/v) Triton-X to renature the enzyme and washed in 50 mM sodium acetate buffer (pH 6.0) before final incubation in the same buffer (Tsai *et al.,* 2019). After 2 h incubation at 40°C, the gel was stained with 0.2% Congo red (Sigma-Aldrich) and washed with 1 M NaCl. The gel was finally immersed in 1% acetic acid for better contrast.

4.2.11 Statistical analysis

All experiments were performed in triplicates, and their average values with standard deviation are presented. One-way analysis of variance (ANOVA) and Student's t-test were used for data analysis. The values $p < 0.05$ were considered significant.

4.3 Results and discussion

4.3.1 Purification and characterization of *B. bassiana* SAN01 xylanase

4.3.1.1 *Purification* of *B. bassiana* SAN01 *xylanase*

B. bassiana SAN01 xylanase produced under submerged fermentation was purified to homogeneity using a series of purification steps, including ammonium sulphate precipitation, ion-exchange chromatography, ultrafiltration and size exclusion chromatography. The xylanase was precipitated using ammonium sulphate (30–60% saturation) to yield an active pellet with a specific activity of 111.29 and 1.56 purification fold. The salt-precipitated enzyme preparation was then dialyzed and purified further by ion-exchange and size exclusion chromatography using Q Sepharose Fast Flow and Superdex 200 10/300 GL columns, respectively. The specific activity of the xylanase increased with each purification step to the maximum value of 369.39 Umg^{-1} of protein after size exclusion chromatography. In addition, a 2.8% yield and a purification fold of 4.96 were achieved after the final purification step. The overview of *B. bassiana* SAN01 xylanase purification is summarised in Table 4.1.

Table 4.1: Purification table of *B. bassiana* SAN01 xylanase

Purification Step	Total activity (U)[b]	Total Protein (mg)[c]	Specific activity (Umg^{-1})	Yield (%)	Purification fold
Crude enzyme[a]	106100	1452	73.07	100	1
Ammonium sulphate precipitation[d]	31272	281	111.29	29.47	1.52
Ion exchange chromatography	5047	28.5	177.1	4.75	2.42
Ultrafiltration	4016	14.7	273.2	3.78	3.74
Size exclusion chromatography	2971.6	8.2	362.39	2.8	4.96

a Obtained from 100 mL of cell-free culture extract of *B. bassiana* submerged fermentation
b Enzyme activity measured as described in the methods section.
c Protein concentration determined by Lowry-Hartree assay using BSA as the standard.
d Enzyme was precipitated using ammonium sulphate (30-60% saturation)

SDS-PAGE analysis of the purified xylanase from *B. bassiana* SAN01 yielded a single band (Figure 4.1a), which confirmed the homogeneity of the enzyme. The molecular weight of the purified enzyme was estimated to be 36.7 kDa. Xylanases from fungal organisms have been reported to vary from low molecular to high molecular weight proteins. Recently, a xylanase of the same size was purified from *Aspergillus oryzae* (Bhardwaj *et al.,* 2020), while lower sized xylanases were obtained from other fungi including *A. flavus* (Chen *et al.,* 2019b) and *A. niger* (Podestá *et al.,* 2019). Hence, based on the observed size and its estimated isoelectric point (probably between 4.5 and 6.5), it could be classified as acidic high-molecular mass xylanase. Biely *et al.* (1997) has grouped such xylanases under the glycanase family 10. Furthermore, this molecular weight is in close agreement with the 37 kDa size of a *B. bassiana* xylanase curated on the UniProt database (UniProt ID: A0A0A2WJL0). As presented in Figure 4.1b, the zymogram confirms the xylanase activity and its migration pattern on the gel. The clear zone of the zymogram corresponded to the position on SDS-PAGE and the desired molecular weight of protein, which highlights the xylanase activity of the enzyme.

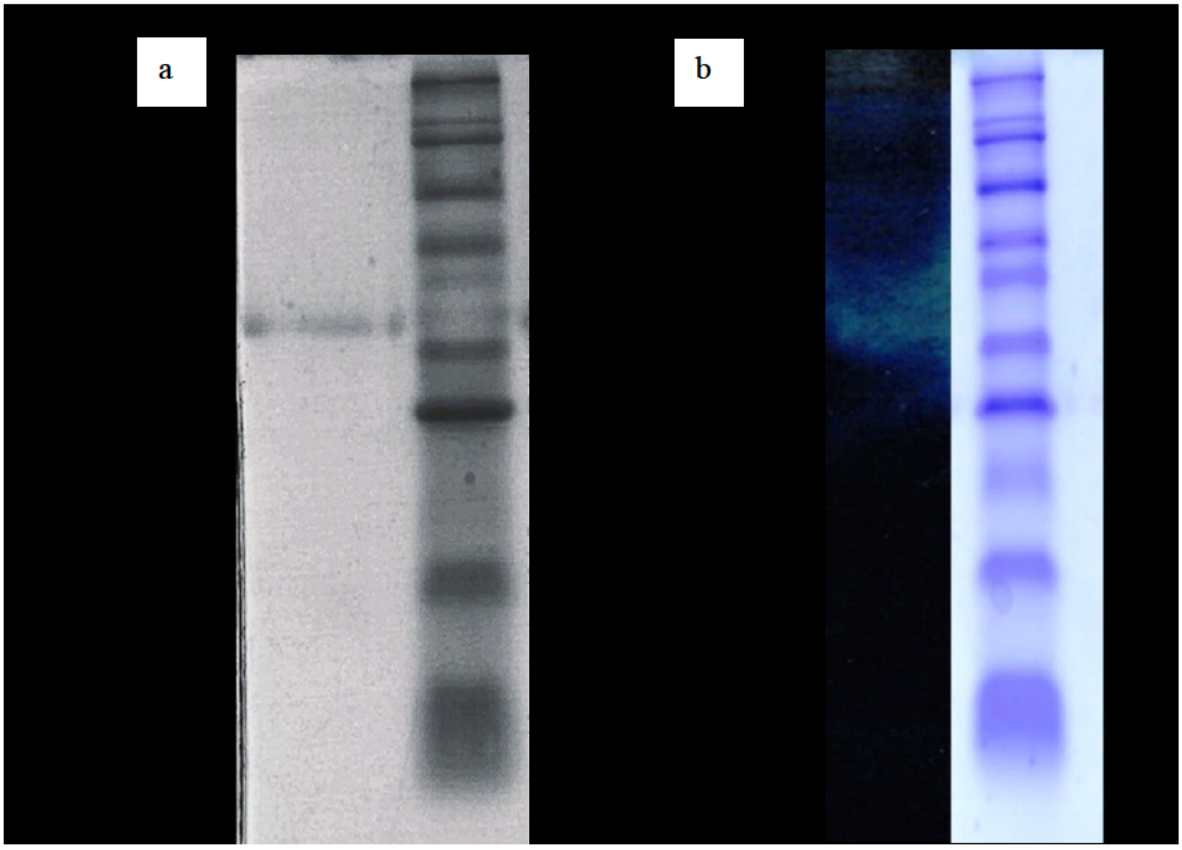

Figure 4.1: (a) *B. bassiana* SAN01 xylanase on 12% SDS-PAGE gel. Lane AF: Active fraction, MWM: Wide range protein marker (ThermoFisher Scientific 6.5-200 kDa) (b) Xylanase activity on Native PAGE gel containing 0.5% beechwood xylan, AF: Active fraction, MWM: Wide range protein marker (ThermoFisher Scientific 6.5-200 kDa).

4.3.1.2 *Biochemical characterization of B. bassiana* SAN01 *xylanase*

Substrate binding and biocatalysis of enzymes are primarily dependent on the charge distribution of the enzyme as well as the substrate molecules, hence enzyme activity is significantly influenced by pH. The optimal pH of the purified *B. bassiana* SAN01 xylanase was observed to be pH 6.0, while it also exhibited significant activities between pH 5 and 8, showing 70 to 100% activity within that pH range (Figure 4.2). Beyond this pH range, the enzyme lost more than 70% of its activity at pH 4.0 and more than 50% of its initial activity at pH 9.0.

Most fungal xylanases, and enzymes in general, have been noted to be acidophilic (Hassan *et al.,* 2019), although some of these enzymes have also been shown to tolerate alkaline conditions (Huang *et al.,* 2020; Somboon *et al.,* 2020). Previous studies have shown the optimal pH of crude xylanases from other *B. bassiana* strains to be pH 6.0

(Ryali *et al.,* 2020) and pH 6.5 (Petlamul and Boukaew 2019). It was also observed that the enzyme showed greater stability at an acidic range than alkaline range, as the enzyme retained more than 60% of its activity at pH 5.0-6.0 after 2 h incubation (Figure 4.3). Furthermore, the enzyme retained 70% of its initial activity at its optimum pH (pH 6.0) after 4 h incubation. The pH stability of xylanolytic enzymes between pH 5.0 and 7.0, 5.0–8.0, 4.5–8.0, and 4.5–7.5 have been reported from *Penicillium sclerotiorum* (Knob and Carmona 2010), *Rhizophlyctis rosea* (Huang *et al.,* 2019) and *Lichtheimia ramose* (Alvarez-Zúñiga *et al.,* 2017), respectively. Thus, the enzyme properties suit their application in the food industry, where most of the production processes are in acidic and/or neutral conditions, as well as in the biofuel industry for the hydrolysis of lignocellulosic materials which is also carried out at acidic pHs.

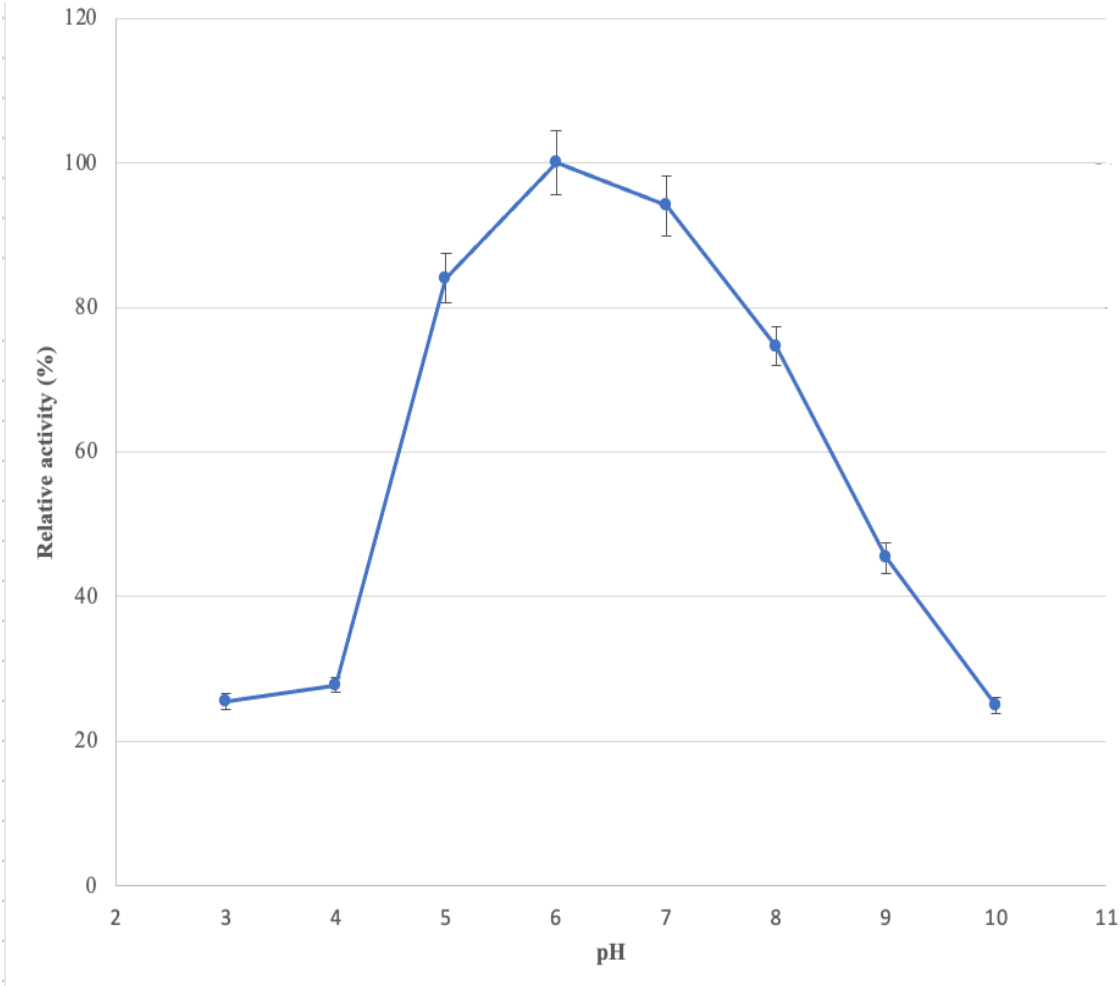

Figure 4.2: Effect of pH on the activity of *B. bassiana* SAN01 xylanase; each point represents the mean (n = 3) ± SD

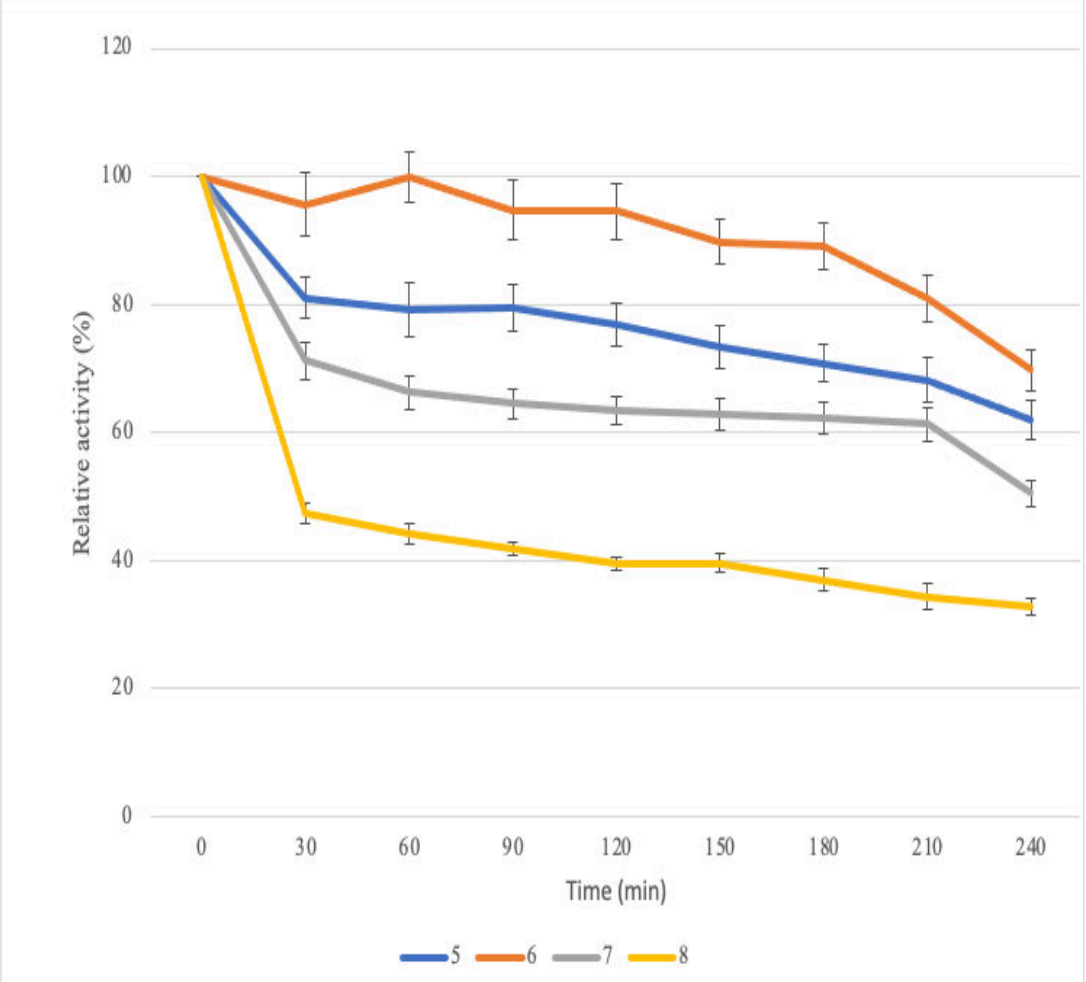

Figure 4.3: Effect on pH on the stability of *B. bassiana* SAN01 xylanase; each point represents the mean (n = 3) ± SD

The optimum temperature of the xylanase was observed to be 45°C; however, it exhibited remarkable activity between 35 and 60°C (Figure 4.4). Beyond the optimum temperature range, the enzyme activity decreased with increasing temperature, and the xylanase was significantly denatured at 70°C, with only 30% of the optimum activity retained. The pH optima of the *B. bassiana* SAN01 xylanase is close to the optimal temperature of 50°C recorded earlier with crude *Beauveria* sp. MTCC 5184 (Ryali *et al.,* 2020). Other microbial xylanases that are active in the mesophilic range as well as in the lower thermophilic range have been described recently. Examples include xylanases from *Penicillium roqueforti* (Marques *et al.,* 2018), *Pediococcus acidilactici* (Adiguzel *et al.,* 2019), *Pleurotus ostreatus* (Zhuo *et al.,* 2018) and *Streptomyces rochei* (Li *et al.,* 2018b) with optimal temperatures of 35, 40, 55 and 60°C, respectively. Thermal inactivation of enzymes has been identified as a major drawback during the utilization of enzymes in different industrial applications, hence there is a need to evaluate the thermal stability

under varying conditions. The purified xylanase was found to be highly stable between 25 and 45°C (Figure 4.5), retaining half of the activity within this range after 120 min. The enzyme was most stable at room temperature, retaining 90% of initial activity after 240 min of incubation; it was observed to retain only 50% of its initial activity after 120 min at its optimum temperature, 45°C. At temperatures over 45°C, the xylanase stability decreased with respect to the incubation time. However, the xylanase from *B. bassiana* SAN01 was more stable than some of the other xylanases reported. For example, from *Penicillium sclerotiorum* (Knob and Carmona 2010), *Streptomyces cyaneus* (Ninawe, Kapoor and Kuhad 2008), and *Penicillium chrysogenum* (Terrone *et al.,* 2018), a larger percentage of their activities were lost within a similar time frame. Hence, *B. bassiana* xylanase is expected to be most suitable for industrial processes carried out between 25 and 45°C.

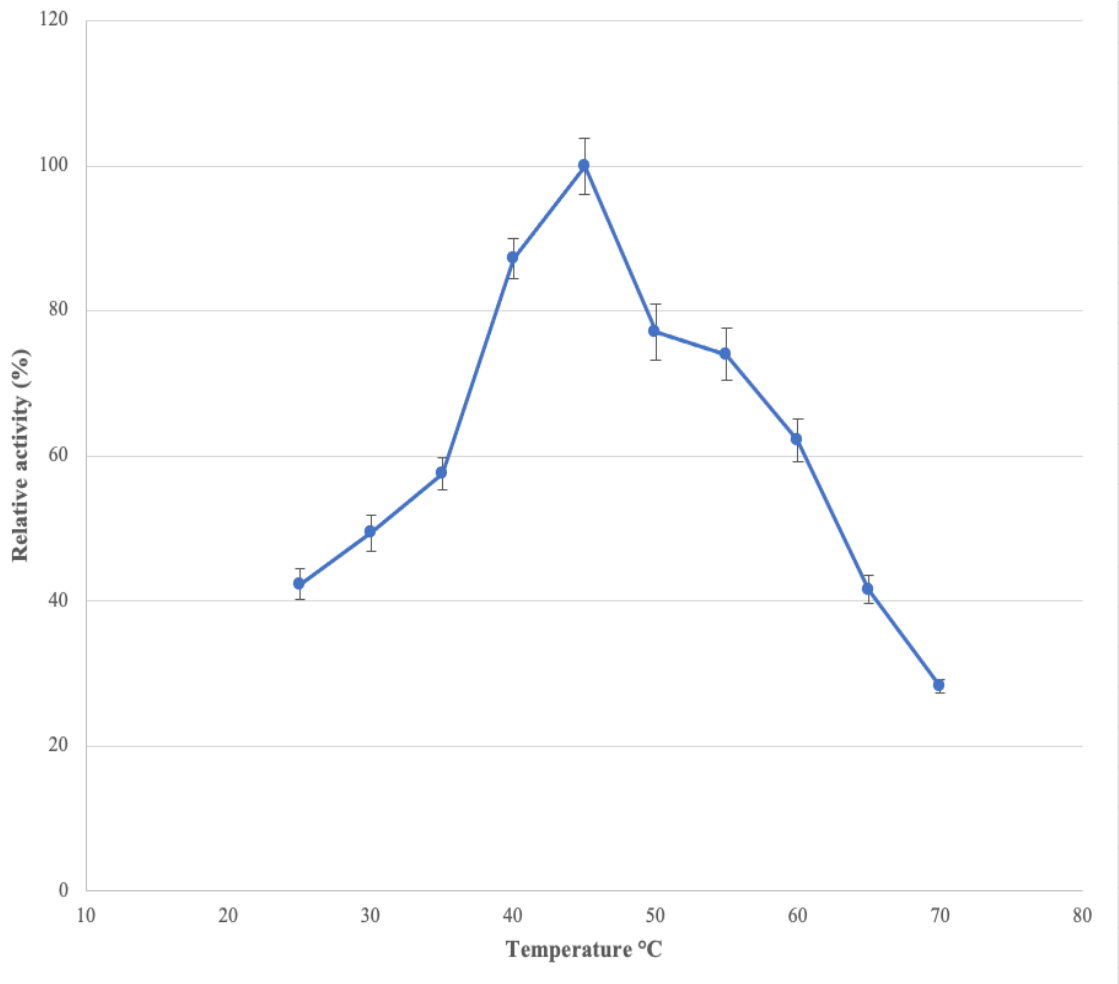

Figure 4.4: Effect of temperature on the activity of *B. bassiana* SAN01 xylanase; each point represents the mean (n = 3) ± SD.

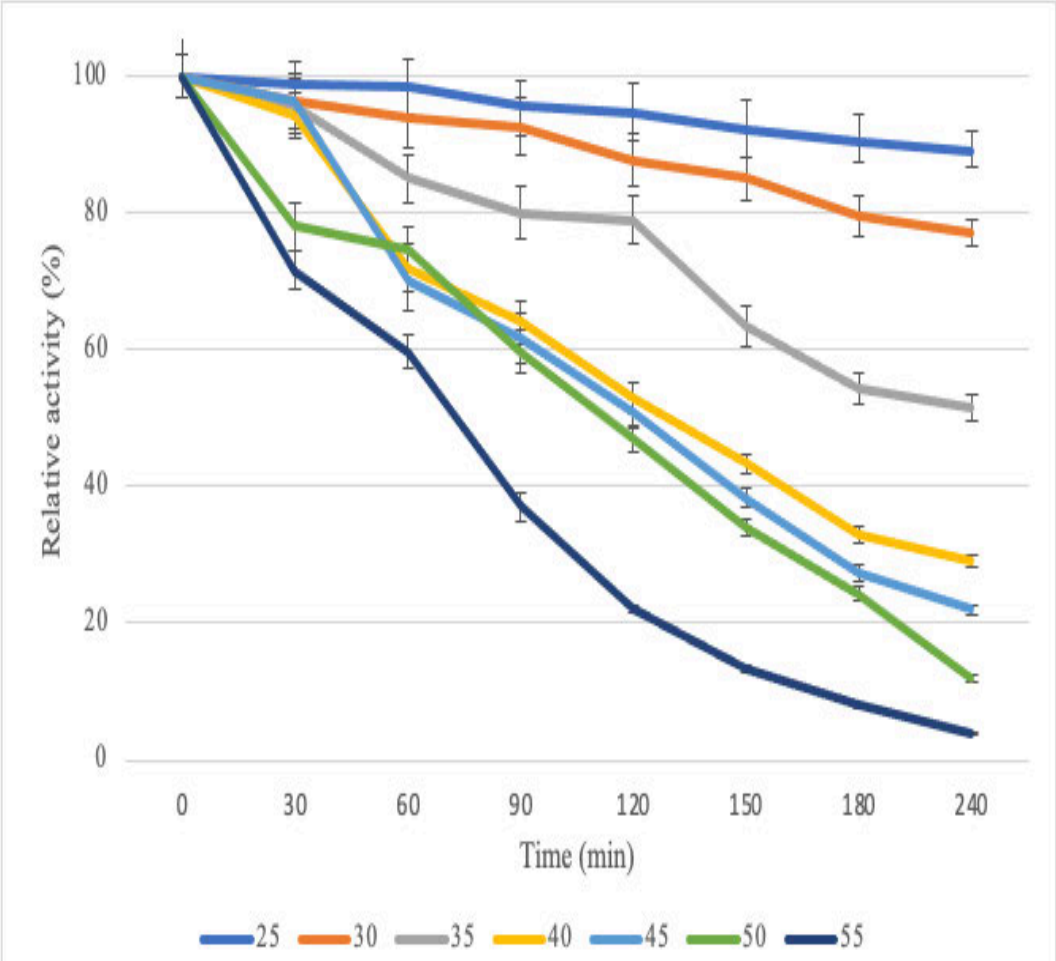

Figure 4.5: Effect on temperature on the stability of *B. bassiana* SAN01 xylanase: each point represents the mean (n = 3) ± SD

The activating and inhibitory effects of different compounds including metal compounds, modulators, as well as organic solvents, on *B. bassiana* SAN01 xylanase were evaluated. The enzyme activity was stimulated by Ba^{2+}, Co^{2+} and Mg^{2+} and inhibited by Ag^{2+}, Fe^{3+}, Hg^{2+}, Na^{+} and Cu^{2+}, while Fe^{2+} and Zn^{2+} did not alter it significantly (Table 4.2). It is noteworthy that the enzyme's activity was increased by Ba^{2+}, Co^{2+} and Mg^{2+} (10 mM) to 107.92, 144.49 and 114.97% of its original value. Generally, it can be said that the xylanase was not affected much by the metal ions, as it retained >70% of its enzymatic activity in the presence of most of the ions investigated in this study, at both 1 mM and 10 mM concentrations. The positive effects of Ba^{2+}, Co^{2+} and Mg^{2+} on the activity of xylanase from *Streptomyces thermocerradoensis* (Gama *et al.,* 2020), *Aspergillus ochraceus* (Michelin *et al.,* 2014) and *Halomonas meridiana* (Palavesam 2015; Lin *et al.,* 2018), respectively, have been reported previously. Similarly, previous research has also highlighted the inhibitory effects of Ag^{2+}, Fe^{3+}, Hg^{2+} and Na^{2+} on xylanases from

Paenibacillus sp. (Zheng *et al.,* 2014; Lin *et al.,* 2018), *Halomonas meridiana* (Palavesam 2015) and *Thermomyces lanuginosus* (Souza *et al.,* 2018), respectively. It is believed that Hg^{2+} inhibition may be as a result of the ion's interaction with sulfhydryl groups within the xylanase, suggesting the presence of cysteine residue in or around the enzyme's active/binding site (Wu *et al.,* 2018a). Metal ions have been known to influence the activity of enzymes through various means. The metallic ions accept or donate electrons, activating electrophiles or nucleophiles in the process. They can also act as electrophiles or mask the influence of nucleophiles, thus preventing unwanted side reactions (de Cassia Pereira *et al.,* 2017). Besides, they may facilitate enzyme-substrate binding through the co-ordinate bond formation and holding the reacting groups in the optimum orientation. They may also stabilize the catalytically active conformation of enzymes (Bajaj and Manhas 2012). Industrial processes are usually run in big metallic reactors, with several production processes involving various metal ions. Hence, it is considered that the relative stability of *B*. *bassiana* SAN01 xylanase in the presence of the metal ions mentioned in the study is a remarkable advantage in its potential industrial applicability.

Table 4.2: Effect of different metal ions on *B. bassiana* SAN01 xylanase activity

Metal ions	Relative activity (%)[a]	
	1 mM	10 mM
Control	100	100
Ag^{2+}	64.31 ± 3.18	30.83 ± 1.44
Ba^{2+}	94.27 ± 3.13	107.92 ± 6.51
Co^{2+}	137.44 ± 7.93	144.49 ± 7.92
Cu^{2+}	99.55 ± 4.71	77.53 ± 3.04
Fe^{2+}	92.95 ± 4.19	89.86 ± 5.84
Fe^{3+}	61.67 ± 3.02	77.09 ± 2.51
Hg^{2+}	92.95 ± 4.49	71.80 ± 3.16
Mg^{2+}	111.013 ± 5.16	114.97 ± 5.97
Na^{+}	85.02 ± 4.02	76.65 ± 3.82
Zn^{2+}	101.76 ± 5.15	95.15 ± 4.18

[a]Data are shown as mean±SD (n=3); control had no chemical addition

Additives such as EDTA, Triton X-100, SDS, among others, have been shown to have varying effects on different hydrolytic enzymes with accompanying effects during enzyme production or industrial application. The effects of some important chemical additives/ reagents on the activity of *B. bassiana* SAN01 xylanase are shown in Table 3. β-mercaptoethanol (BME), dithiothreitol (DTT), and ethylenediaminetetraacetic (EDTA) were observed to significantly enhance the activity of the enzyme. The xylanase activity was increased by 49.33 and 21.14% in the presence of 10 mM BME and DTT, respectively, while the highest increase in activity (~ 90%) was observed in the presence of 1 mM EDTA. Previous studies have shown BME and DTT's stimulatory effects on xylanase activity (Adigüzel and Tunçer 2016; Hamid and Aftab 2019). The stability of xylanase in the presence of BME suggests the absence of any major disulphide bond in the xylanase as BME is a disulphide-bond reducing agent (Saleem *et al.,* 2021). In contrast, the non-inhibitory effect of EDTA on the xylanase indicates the probable

absence of metallic prosthetic groups in the enzyme. The non-inhibitory effect of EDTA has also been observed in some other fungal xylanases (Basit *et al.,* 2018).

The surfactants evaluated in this study, i.e., SDS, Triton X-100 and Tween 20 exhibited varying inhibitory effects on the enzyme (Table 4.3). Different xylanases have been noted to be inhibited by these surfactants in recent investigations (Hamid and Aftab 2019). It was suggested that the negative effects of SDS on xylanase activity are due to the interference of the detergent in the enzymes' hydrophobic regions as well as the tertiary structure, leading to denaturation (Bhardwaj *et al.,* 2020). However, it was noticed that Tween 20 inhibited *B. bassiana* xylanase only at higher concentration (Table 4.3). Phenylmethylsufonyl fluoride (PMSF) at both lower and higher concentrations reduced the enzyme activity by around 50%. PMSF specifically binds to the serine residues in proteins, and it is a well-known inhibitor of serine/cysteine peptidases (Rahimnahal *et al.,* 2020). The PMSF inhibition observed in this study may indicate the presence of active site serine residues in the xylanase. Recent studies have also highlighted the inhibition of fungal xylanases by PMSF (Ullah *et al.,* 2019; Terrone *et al.,* 2020b).

Table 4.3: Effect of different additives on *B. bassiana* SAN01 xylanase activity

Additives	Relative activity (%)[a]	
	1 mM	10 mM
Control	100	100
BME	123.34 ± 6.02	149.33 ± 6.27
DTT	109.69 ± 5.63	121.14 ± 5.74
EDTA	189.42 ± 7.33	125.55 ± 6.61
PMSF	55.67 ± 2.68	50.47 ± 3.06
SDS	65.19 ± 2.79	56.38 ± 2.52
Tween 20	103.08 ± 4.37	88.15 ± 4.26
Triton X-100	90.30 ± 4.37	89.86 ± 3.84

[a]Data are shown as mean±SD (n=3); Control had no chemical addition

The effect of various alcoholic and non-alcoholic solvents on *B. bassiana* SAN01 xylanase activity is presented in Table 4.4. The activity of the enzyme was enhanced in the presence of isopropanol (120%), ethanol (110%), and hexane (120%). In contrast, it was inhibited in the presence of acetone, butanol, benzene, methanol and toluene. Similar observations for xylanase stimulation in the presence of isopropanol, ethanol (Adhyaru, Bhatt and Modi 2014), and hexane (Gaur *et al.,* 2015) were recorded previously. Similarly, xylanases from various sources have also been recently demonstrated to be susceptible to the inhibition by acetone, butanol, benzene, methanol and toluene (Hamid and Aftab 2019; Saleem *et al.,* 2021). In this study, the solvents that significantly enhanced the activity of the xylanase (ethanol and isopropanol) were more polar than the inhibitory solvents such as benzene and toluene. The relationship between the polarity of solvents and enzyme activity has been highlighted previously (Gupta 1992; Kim, Clark and Dordick 2000; Silva *et al.,* 2018a). The stimulatory effect of polar organic solvent on an enzyme was attributed to the creation of an appropriate biphasic interface between the organic solvent and water, creating more accessibility of the substrate for the enzyme (Khamessan, Kermasha and Marsot 1994). It has also been noted that increased or reduced structural flexibility of enzymes is primarily responsible for the stimulation or inhibition of enzymatic activities, respectively, in organic solvents (Klibanov 2001; Li *et al.,* 2020). Hence, it is posited that the xylanase from *B. bassiana* SAN01 may contain a high proportion of random coils, thus increased structural flexibility, which might be responsible for its relative significant stability in some organic solvents. Biocatalytic reactions in the organic phase offer several advantages such as increased solubility of hydrophobic substrate facilitating effective reactions, lower microbial contamination and recyclability (Adhyaru, Bhatt and Modi 2014). Hence, the results from this study provide essential data for the applicability of *B. bassiana* SAN01 xylanase in industrial reactions involving organic solvents. Particularly, its significant ethanol-tolerance could endear its use in simultaneous saccharification and bioethanol fermentation as well as in the clarification of alcoholic beverages.

Table 4.4: Effect of different organic solvents on *B. bassiana* SAN01 xylanase activity

Organic Solvent	Relative activity (%)[a]
Control*	100
Acetone	82.7 ± 4.06
Benzene	81.39 ± 3.88
Butanol	77.20 ± 3.02
Chloroform	86.97 ± 4.42
Ethanol	110.69 ± 5.74
Hexane	104.65 ± 3.63
Isopropanol	120 ± 6.18
Methanol	67.44 ± 1.86
Toluene	87.44 ± 3.86

[a]Data are shown as mean±SD (n=3).
*Control had no chemical addition

4.3.1.3 *Kinetic analysis of B. bassiana* SAN01 xylanase

The kinetic properties of *B. bassiana* SAN01 xylanase were determined using a Hanes-Woolf plot and the enzyme was observed to obey Michaelis-Menten kinetics (Figure 4.6). The kinetic parameters were computed from the kinetics curve, according to Deyhimi and Nami (2012). The enzyme was found to have a K_m value of 1.98 $mgmL^{-1}$ and V_{max} of 6.65 $\mu Mmin^{-1}$. This observed K_m is lower when compared to some other fungal xylanases such as xylanases from *T. lanuginosus* (Lin *et al.,* 1999), *Aspergillus niveus* (Sudan and Bajaj 2007), *A. niger* (Uday *et al.,* 2017) with K_m values of 3.26, 18.5, and 2.89 $mgmL^{-1}$, respectively. The lower K_m of *B. bassiana* xylanase indicates its higher affinity for its substrate, thus the enzyme activity will not be significantly impaired at low substrate concentrations. Furthermore, the catalytic rate constant (k_{cat}) and the catalytic efficiency (k_{cat}/Km) of the enzyme under study were 0.62 s^{-1} and 0.3131 mL $s^{-1}mg^{-1}$, respectively. The K_{cat} represents the amount of bound substrate molecules converted to the desired product per unit time, while k_{cat}/Km measures the catalytic efficiency of enzymes for a specific product. Thus, *B. bassiana* SAN01 can have a

significant enzyme turnover and perform efficiently under the investigated reaction conditions. However, it is difficult to make a logical comparison between the k_{cat} and k_{cat}/Km of *B. bassiana* SAN01 xylanase and other xylanases due to the various computation and units employed in other studies. The various limitations in comparing the two constants have also been highlighted previously (Eisenthal, Danson and Hough 2007; Carrillo, Ceccarelli and Roveri 2010). For instance, the k_{cat} of fungal xylanases from *Pichia stipitis* (Ding et al., 2018), *Scytalidium candidum* (Eneyskaya et al., 2020) were estimated as 1354 s^{-1}, 12.6 ± 0.63 s^{-1} while their k_{cat}/Km were estimated as 301 $mLs^{-1}mg^{-1}$ and 57.27 ± 2.86 $s \cdot mM^{-1}$ respectively. However, ignoring the limitation mentioned earlier, the xylanase in this study has lower catalytic efficiency compared to the ones from *P. stipitis* (Ding et al., 2018), *S. candidum* (Eneyskaya et al., 2020) . The efficiency of *B. bassiana* SAN01 xylanase can be improved upon by protein engineering especially through directed evolution.

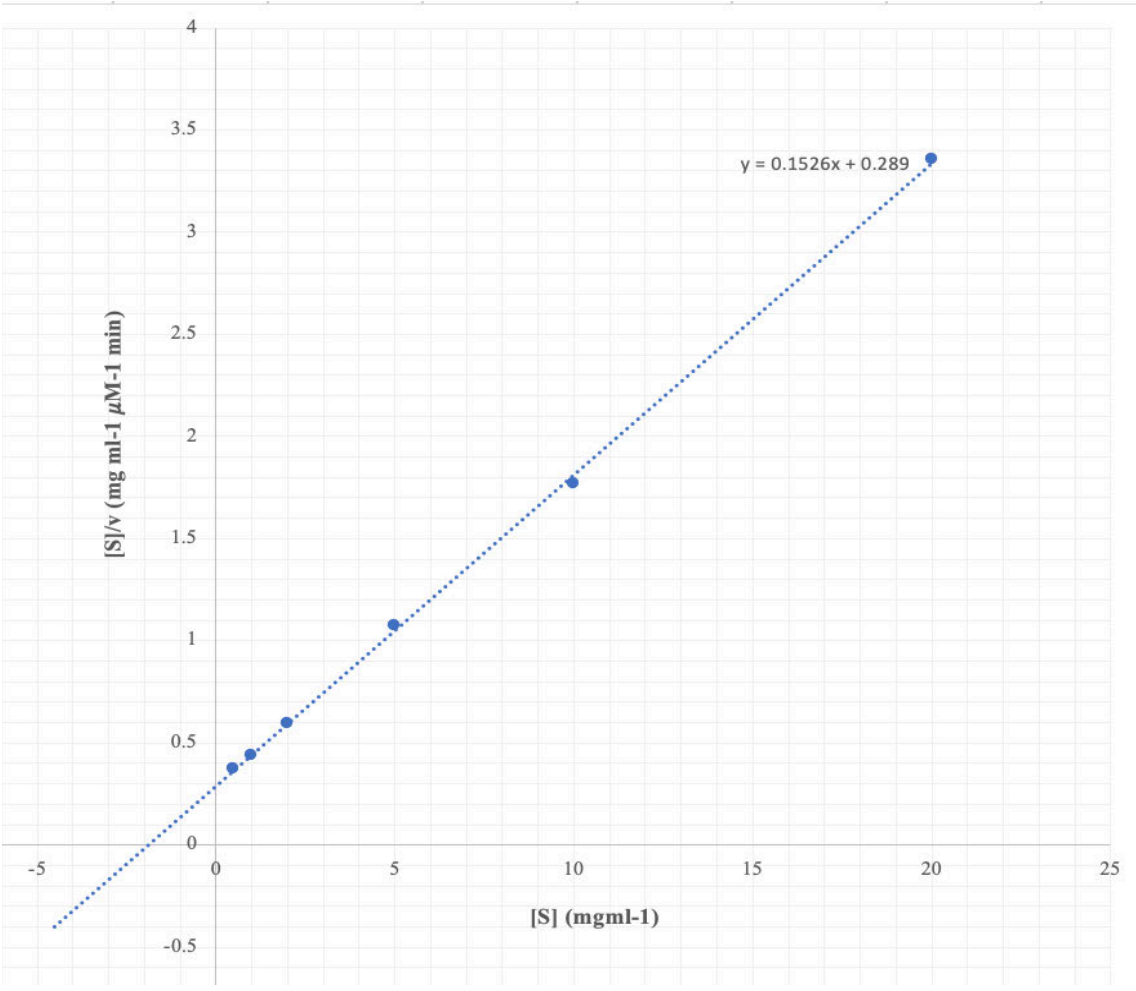

Figure 4.6: Hanes-Woolf plot ([S]/v vs [S]) for *B. bassiana* SAN01 xylanase activity

The substrate specificity of purified xylanase from *B. bassiana* SAN01 was evaluated against various polymeric substrates. It was observed that the xylanase had high specificity towards xylan-containing substrates (Table 4.5). *B. bassiana* xylanase exhibited substrate specificity in the order beechwood xylan> oatspelt xylan> arabinoxylan> carboxymethylcellulose (CMC). The purified enzyme showed no detectable activity towards avicel, pectin and starch, under the same reaction conditions. These results indicated that the purified xylanase is highly specific for the hydrolysis of hemicellulosic substrates. Similar results were observed in xylanase from *Paenibacillus barengoltzii* (Liu *et al.,* 2018) and *Trichoderma* sp. (Fu *et al.,* 2019). Furthermore, it was demonstrated that the enzyme could also act partially on cellulose. Based on the nature of the substrate used for the cellulase activity (CMC), it could also be inferred that the enzyme is more likely to be involved in "endo" attacks. Different xylanases with varying cellulase activities have been characterized in previous studies (Fredriksen *et al.,* 2019; Wang *et al.,* 2019a). These enzymes are considered desirable in catalytic reactions with mixed substrates, for example, plant lignocellulosic biomass which is made up of cellulose and hemicelluloses.

Table 4.5: Substrate specificity of *B. bassiana* SAN01 xylanase

Substrate	Relative activity
Arabinoxylan	76.28 ± 3.36
Avicel	0
Beechwood xylan	100
CMC	17.12 ± 0.56
Oatspelt xylan	87.7 ± 4.16
Pectin	0
Soluble starch	0

4.3.2 Partial purification and characterization of *B. bassiana* SAN01 amylase

A specific activity of 2.9 Umg^{-1}, purification fold of 1.6 and an enzyme yield of 36.7% was achieved after the partial purification of *B. bassiana* SAN01 amylase using ammonium sulphate precipitation and ultrafiltration. While the optimum pH of the enzyme was observed to be 6.0, it also showed significant activities between pH 4.0 and

pH 8.0. *B. bassiana* SAN01 amylase was observed to be active, between 60 and 100%, within this pH range (Figure 4.7). Beyond this range, the enzyme lost close to 60% of its activity at a low pH of 3.0 and high pH of 9.0. At pH 10.0, the enzyme lost more than 80% of its initial activity. An amylase from another strain, *Beauveria* sp. MTCC 5184 (Ryali *et al.,* 2020) was shown to have a similar optimal pH as *B. bassiana* SAN01 amylase. The optimal pH range observed for the amylase in this study also falls within the physiological pH range of the fungus. In this regard, *B. bassiana* strains have been shown in various studies to display robust growth within pH 4.0 and 10.0 (Karthikeyan, Shanthi and Nagasathya 2008; Luo *et al.,* 2018). In addition, recent studies have shown amylases from various fungal sources with an optimum pH of 6.0. For example, amylases from *Rhizomucor miehei* (Wang *et al.,* 2020b) and *Fomitopsis palustris* (Tanaka *et al.,* 2020). It was also observed that *B. bassiana* SAN01 amylase showed greater stability at pH 4.0-8.0 as the enzyme retained more than half of its initial activity within this pH range after 2 h (Figure 4.8). The amylase also showed significant stability at its optimal pH as it was observed to retain approximately 90% of its initial activity at this pH, after 240 min. The stability profile of *B. bassiana* amylase is consistent with recent data obtained on amylases from *Aspergillus niger* (Wang, Li and Lu 2018), *Bacillus amyloliquefaciens* (Du *et al.,* 2018) and *Streptomyces fragilis* (Nithya *et al.,* 2017). Enzyme activity and stability at low pH values have been noted to be desirable for amylases, especially for their industrial saccharification of starch which has a natural pH of 5.0 (Wu *et al.,* 2018b). This shows that the use of acid-stable enzyme such as *B. bassiana* SAN01 amylase might eliminate the need for additional pH adjustment during saccharification processes as well as reduce by-products formation.

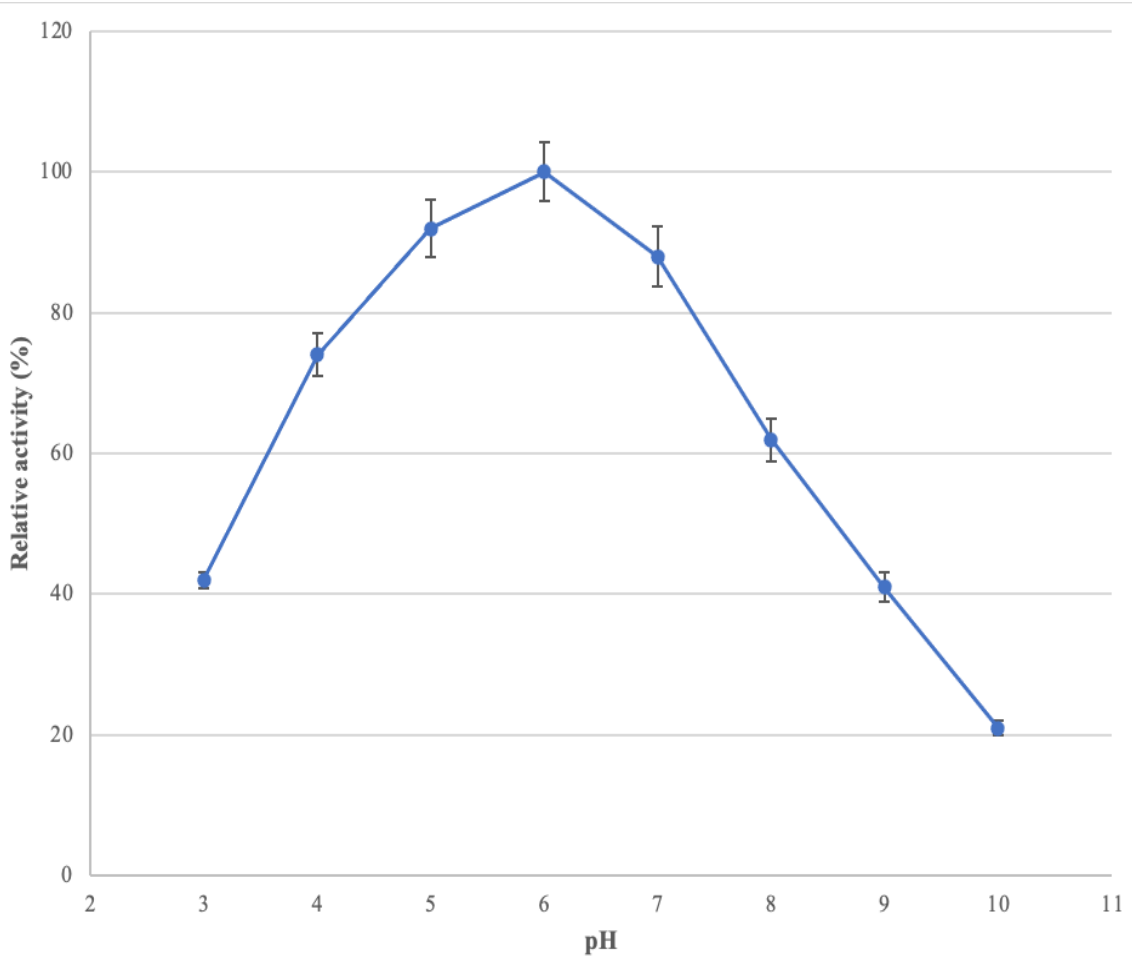

Figure 4.7: Effect of pH on the activity of *B. bassiana* SAN01 amylase; each point represents the mean (n = 3) ± SD

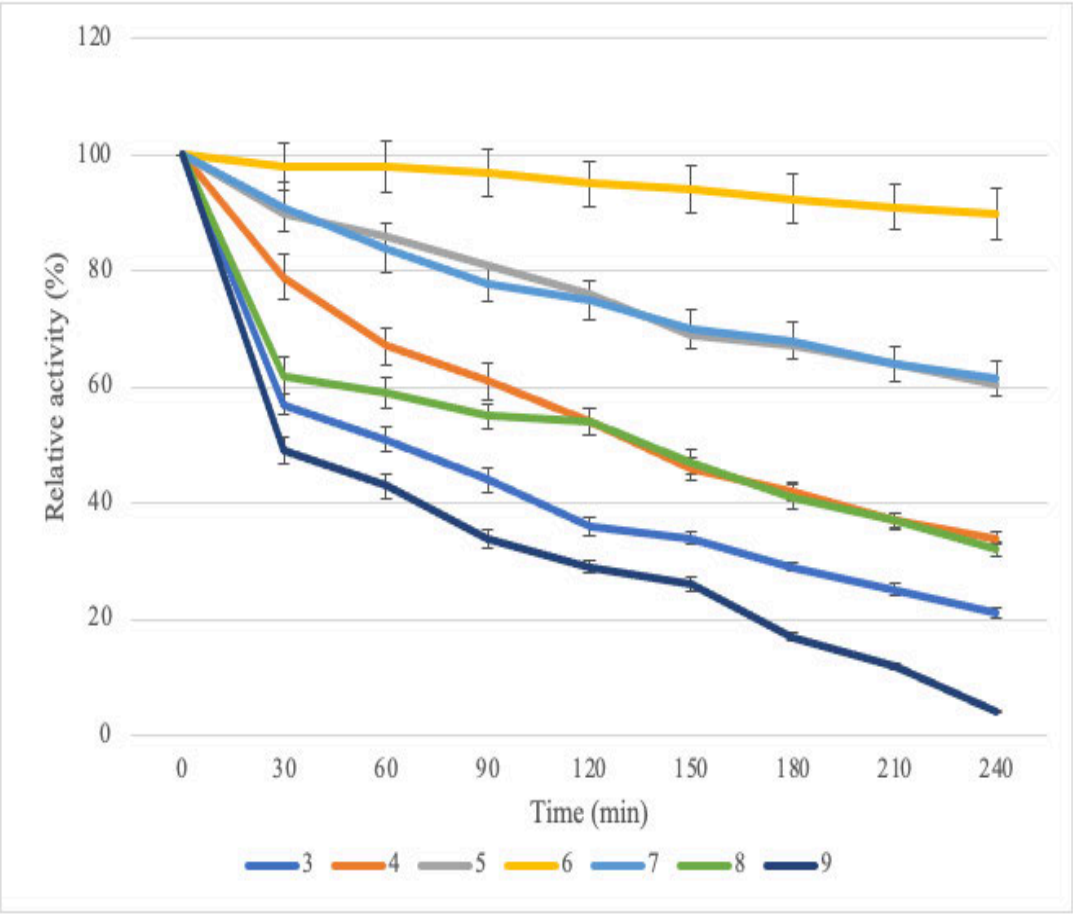

Figure 4.8: Effect of pH on the stability of *B. bassiana* SAN01 amylase; each point represents the mean (n = 3) ± SD

The optimum temperature of *B. bassiana* SAN01 amylase was observed to be at 35°C and it exhibited significant activity in the mesophilic range of 35 to 45°C (Figure 4.9). Compared to its maximum activity at 35°C, the enzyme exhibited 74, 78 and 60% activity at 30, 40 and 45°C, respectively. Beyond the optimum temperature range, the enzyme activity was observed to decrease with increasing temperature, and it was almost completely inactivated at 70°C. It is observed that the optimal temperature of the *B. bassiana* SAN01 amylase is within the physiological temperature of the fungus which varies geographically between 28 and 35°C (Fargues *et al.,* 1997; Seid *et al.,* 2019). Furthermore, the observed optimum temperature is also close to that recorded earlier for an amylase from another *B. bassiana* strain which performed optimally at 40°C (Feng and Ying, 2002). Recent investigations have also shown different fungal amylases with optimal activity at the mesophilic range, such as amylases from *A. niger* (Wang *et al.,*

2016b) and *Cordyceps farinose* (Roth *et al.,* 2019). The partially purified amylase from *B. bassiana* SAN01 was also found to be stable between 25 and 45°C (Figure 4.10), retaining approximately half of its initial activity within this range after 120 min. However, the enzyme activity decreased sharply beyond 50°C and it lost almost all of its activity after 240 min when incubated at 55°C.

The thermostability of the amylase recorded in this study is consistent with previous data obtained from other fungal amylases, including *Aspergillus niger* (Wang, Li and Lu 2018), *A. oryzae* (Sahnoun *et al.,* 2012) and *Penicillium camemberti* (Nouadri *et al.,* 2010).

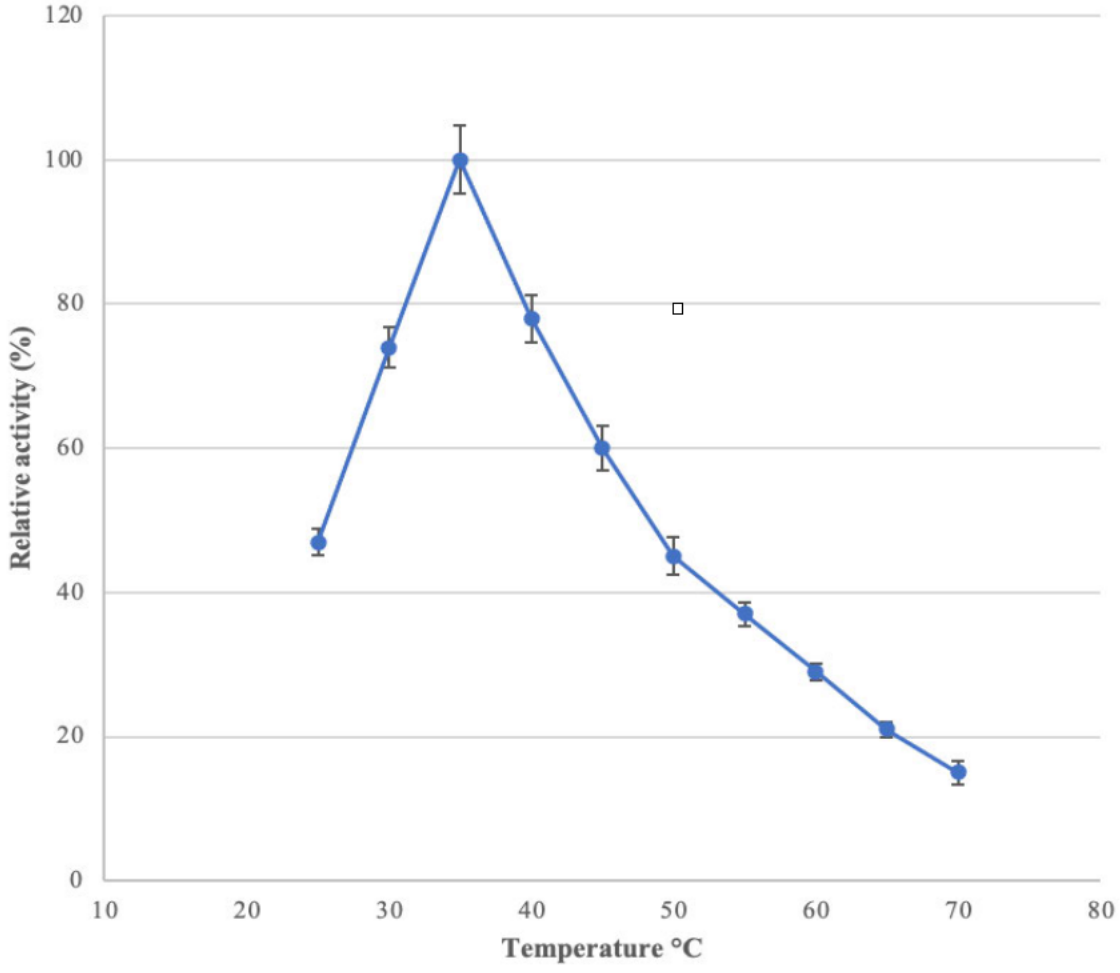

Figure 4.9: Effect of temperature on the activity of *B. bassiana* SAN01 amylase; each point represents the mean (n = 3) ± SD

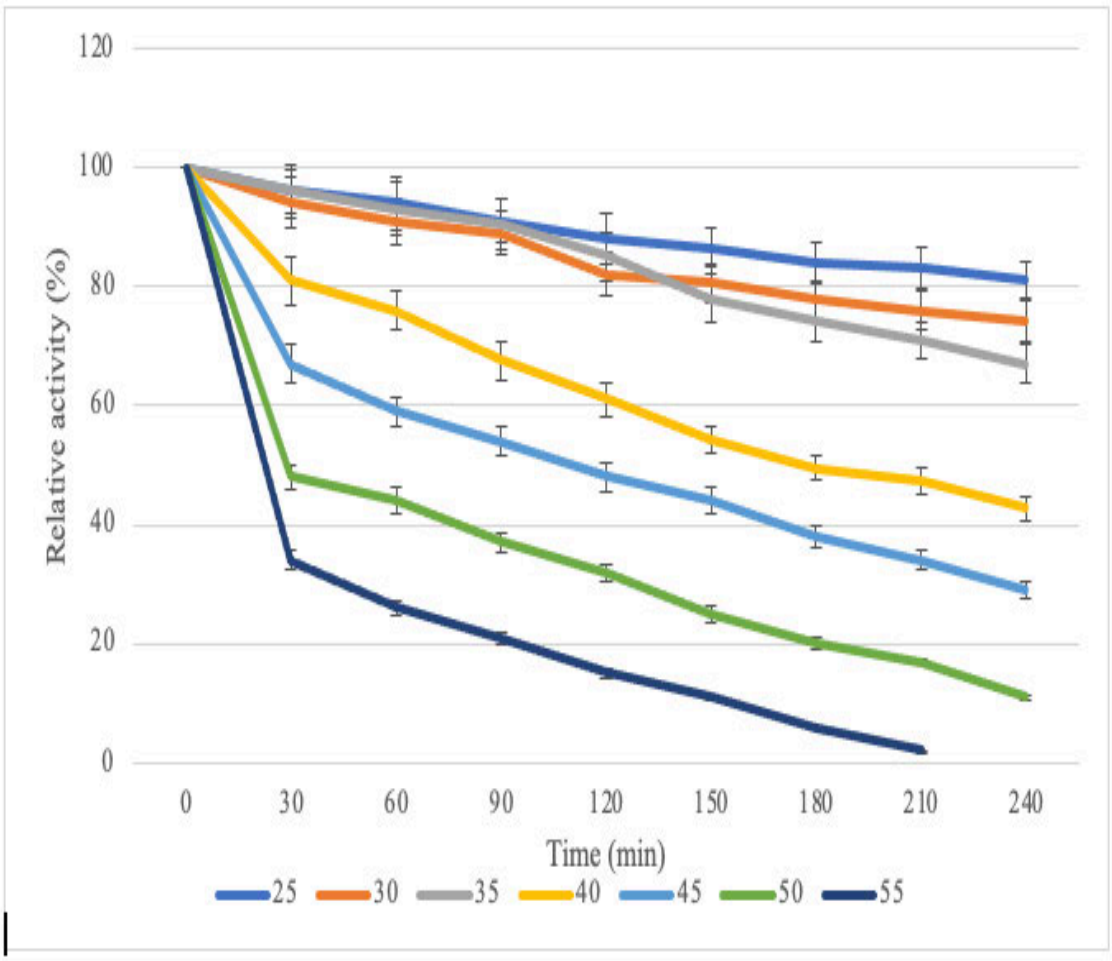

Figure 4.10: Effect of temperature on the stability of *B. bassiana* SAN01 amylase; each point represents the mean (n = 3) ± SD

4.3.3 Purification and characterization of *B. bassiana* SAN01 endoglucanase (cellulase)

B. bassiana SAN01 endoglucanase was purified by a two-step strategy which includes ammonium sulphate precipitation and ultrafiltration. Subsequent to the partial purification of the endoglucanase, a specific activity of 2.72 Umg^{-1}, purification fold of 1.7 and a yield of 30.7% was attained. The endoglucanase from *B. bassiana* SAN01 showed optimal activity at pH 6.0 and was significantly active between pH 3.0 and pH 8.0. The endoglucanase can be regarded as acidophilic as it exhibited above 50% of its total activity at the acidic pH range (Figure 4.11). In addition, *B. bassiana* SAN01 showed 93 and 68% of its optimum activity at pH 7.0 and 8.0, respectively. In accordance with results from this study, a *B. bassiana* endoglucanase with optimal pH of 6.0 was reported recently by Petlamul and Boukaew (2019). Other fungal endoglucanases such

as *Fusarium* spp. (deb Dutta *et al.,* 2018) and *Trichoderma longibrachiatum* (Pachauri *et al.,* 2020) endoglucanases were also shown recently to be optimally active at pH 6.0.

The pH stability of the endoglucanase was also evaluated by preincubating the enzyme for 4 h at various pHs and measuring the remaining activity (Figure 4.12). The residual activity was observed to be 92, 82, 75 and 54% of the control at pH 6.0, 7.0, 5.0 and 8.0, respectively, after 240 min. However, the enzyme was rapidly inactivated after 150 min at lower pHs of 3.0 and 4.0 and higher pH of 9.0. Recent research has shown the endoglucanase from *Botrytis ricini* to be stable within a similar pH range as *B. bassiana* SAN01 endoglucanase (Silva *et al.,* 2018b).

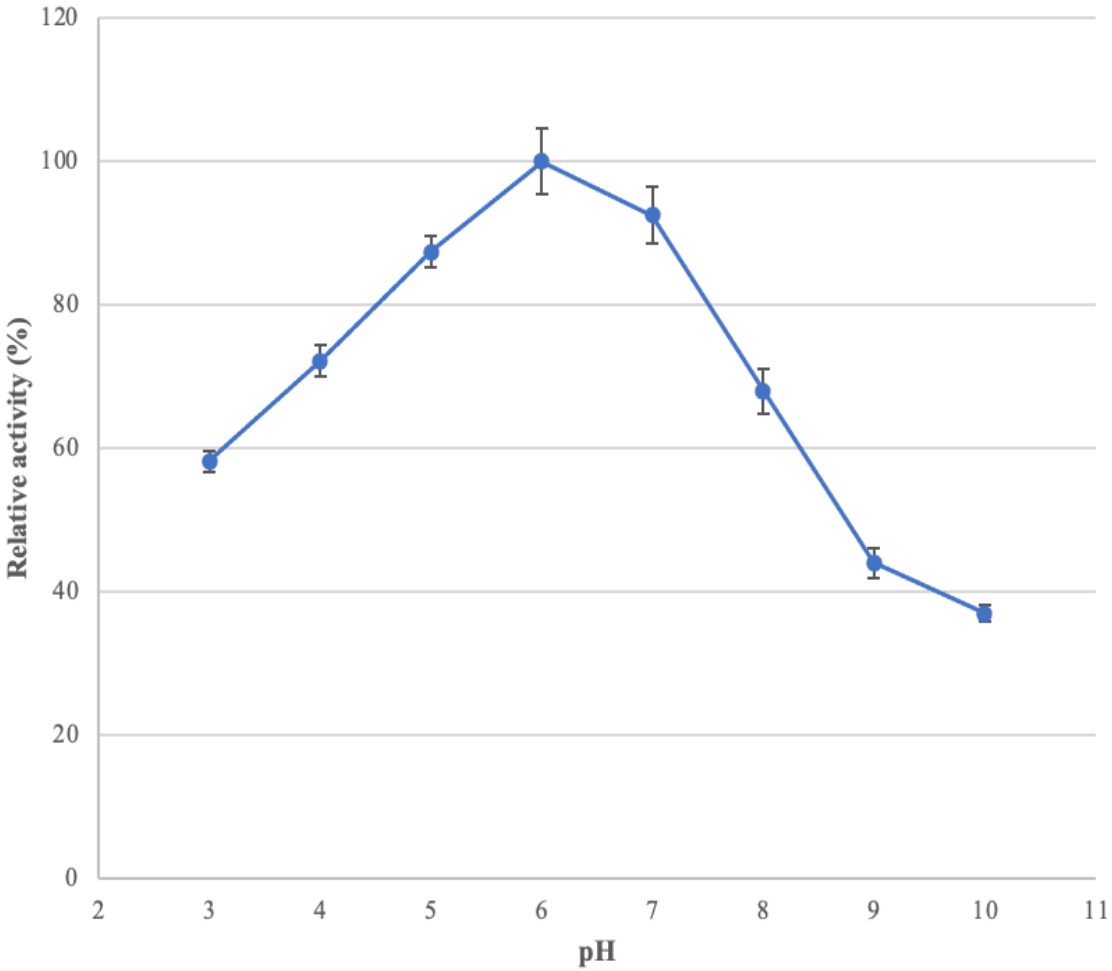

Figure 4.11: Effect of pH on the activity of *B. bassiana* SAN01 endoglucanase; each point represents the mean (n = 3) ± SD

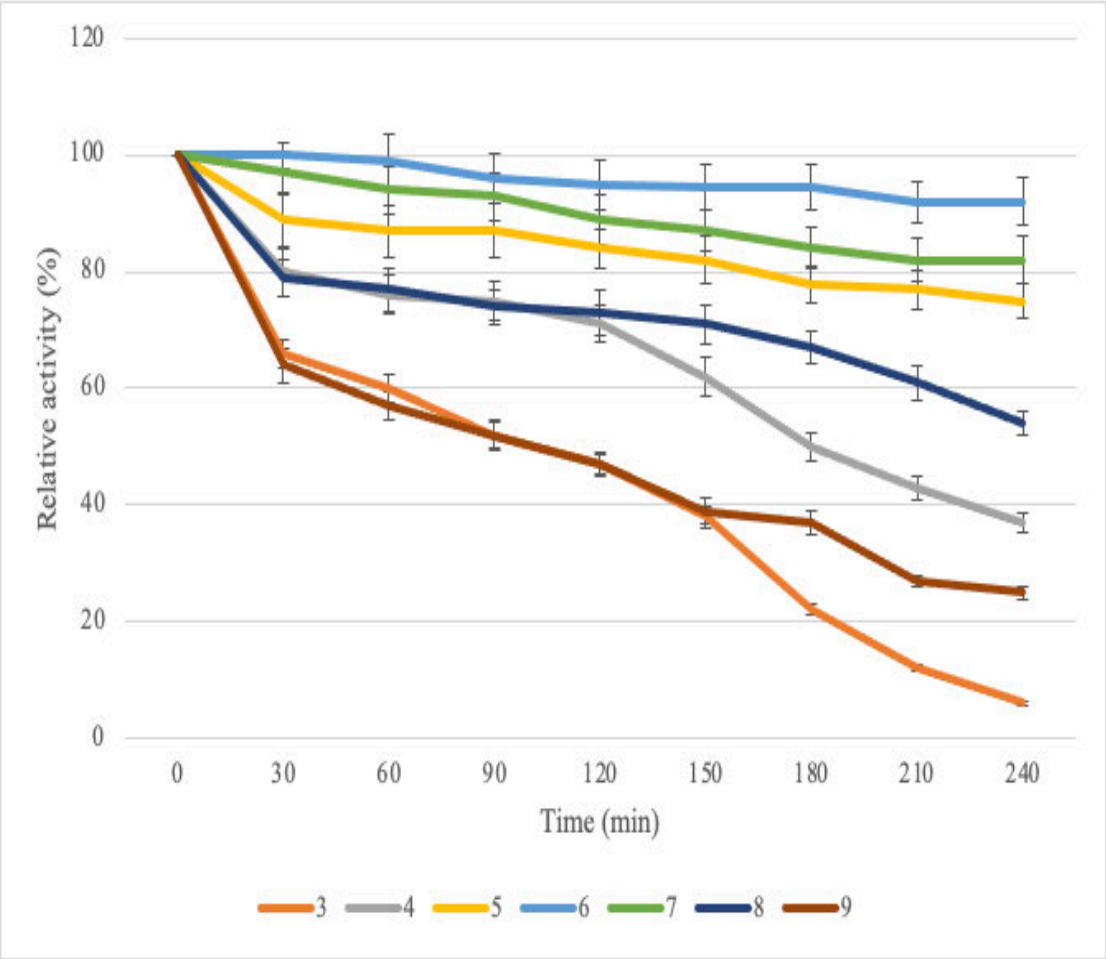

Figure 4.12: Effect of pH on the stability of *B. bassiana* SAN01 endoglucanase; each point represents the mean (n = 3) ± SD

The optimum temperature of *B. bassiana* SAN01 endoglucanase was observed to be 35°C while also exhibiting significant activity between 30 and 60°C (Figure 4.13). It was noticed that the enzyme activity increased with increasing incubation temperature until the maximum value was attained at 35°C. A further increase in temperature led to a reduction in the activity of the enzyme. In this regard, 70% of the enzyme activity was lost at 70°C. It could be inferred that the pH optima of *B. bassiana* SAN01 endoglucanase recorded in this study is close to the physiological temperature of the fungus (Seid *et al.,* 2019). According to available literature, very few fungal endoglucanases perform optimally at 35°C, as most of them have an optimal temperature between 40 and 50°C. However, endoglucanases from other microbes that have been shown to perform optimally at 35°C include endoglucanase from *Ganoderma lucidum* (Manavalan *et al.,* 2015) and *Salinivibrio* sp. (Wang *et al.,* 2009).

The partially purified endoglucanase exhibited significant stability at 25-55°C (Figure 4.14), retaining at least 50% of its initial activity within this range after 240 min incubation. The stability of the enzyme rapidly decreased after 150 min, at temperatures of 50°C and above. The endoglucanase from *Ganoderma lucidum* also exhibited a similar thermostability profile (Manavalan *et al.,* 2015). It could be noted that the remarkable activity and stability of *B. bassiana* SAN01 amylase at a mesophilic range could promote the application of the enzyme in industrial processes that require mild temperature conditions with less energy demand.

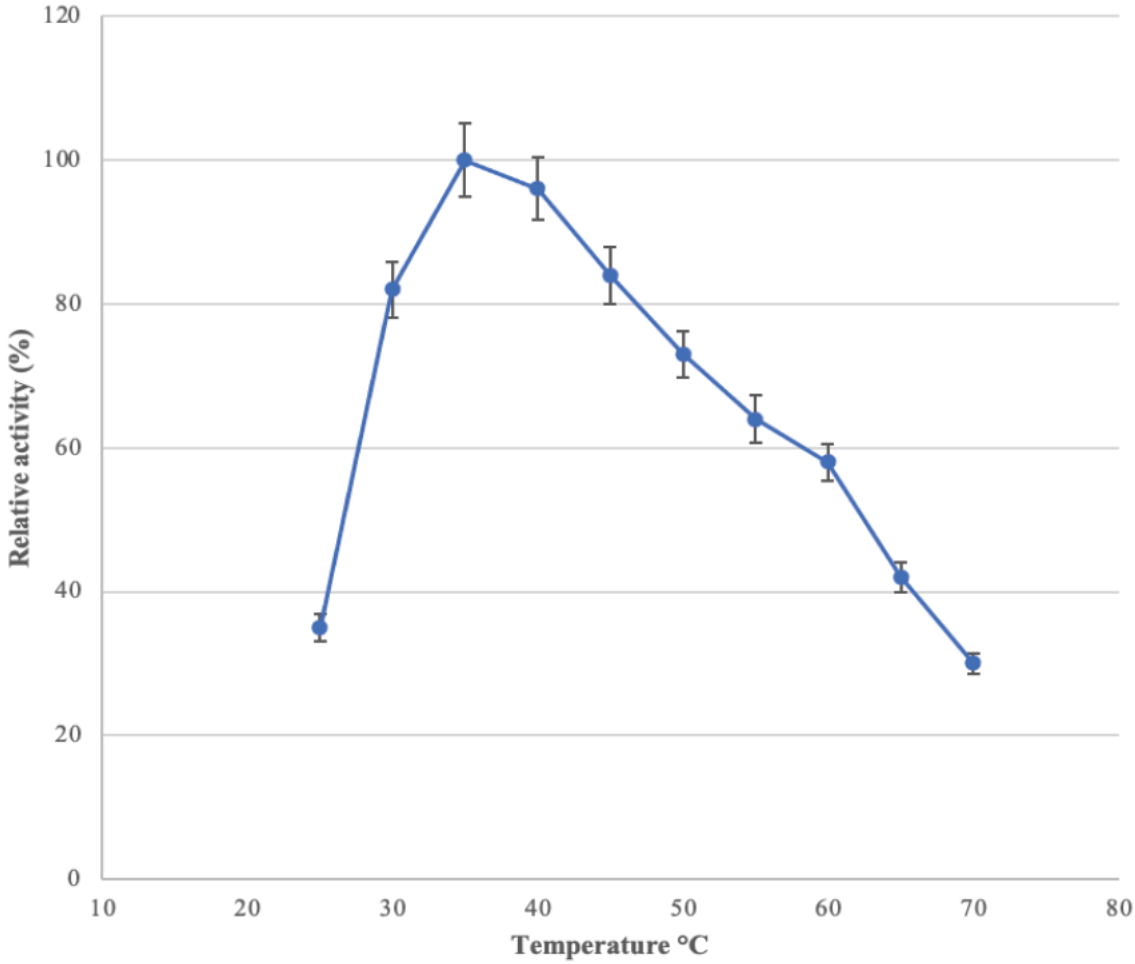

Figure 4.13: Effect of temperature on the activity of *B. bassiana* SAN01 endoglucanase; each point represents the mean (n = 3) ± SD

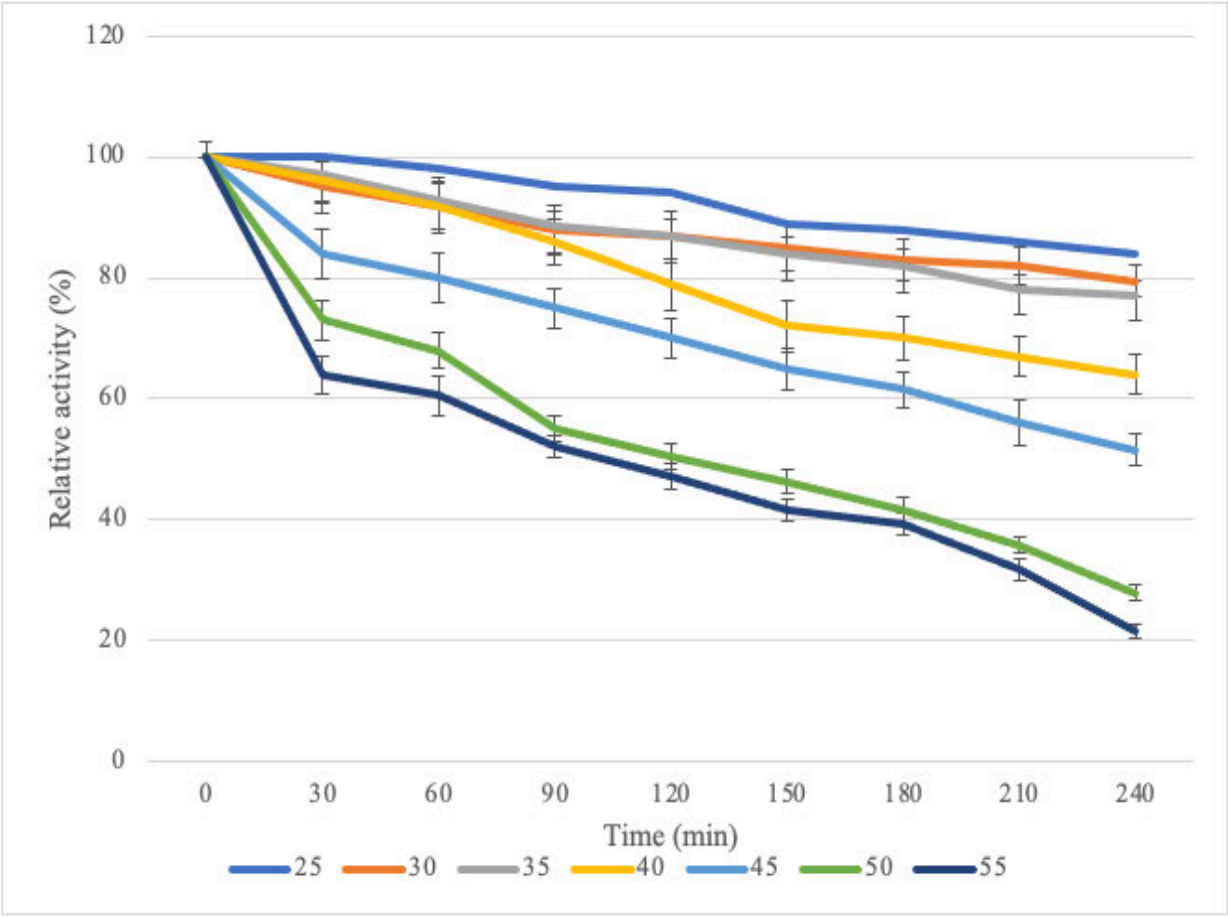

Figure 4.14: Effect of temperature on the stability of *B. bassiana* SAN01 endoglucanase; each point represents the mean (n = 3) ± SD

4.3.4 Purification and characterization of *B. bassiana* polygalacturonase SAN01 (pectinase)

The polygalacturonase enzyme produced by the submerged fermentation of *B. bassiana* SAN01 cultures was partially purified by a combination of ammonium sulphate precipitation and ultrafiltration. The partial purification led to a specific activity of 3.1 Umg^{-1}, purification fold of 1.4 and a yield of 37.5%. Results demonstrated that the maximum activity of the pectinase enzyme produced from *B. bassiana* SAN01 was observed at pH 7.0 (Figure 4.15). Furthermore, the enzyme showed significant activity between pH 5.0 and pH 9.0. Compared to the maximal activity at pH 7.0, the relative activities at pH 5.0, 6.0, 8.0 and 9.0 were 60, 95, 78 and 52%, respectively. At pH 10, the enzyme lost approximately two-thirds of its optimum activity.

The pH optimum of *B. bassiana* SAN01 is similar to the value reported for polygalacturonase from *Aspergillus niger* (Ahmed *et al.,* 2016) and *Penicillium occitanis* (Sassi *et al.,* 2016). The stability of the enzyme was also assessed at pH 3.0-9.0. It was also observed that *B. bassiana* SAN01 polygalacturonase showed greater stability between pH 5.0 and 8.0. The enzyme retained more than half of its initial activity within this pH range after 2 h (Figure 4.16). Furthermore, the enzyme retained close to 90% of its initial activity at its optimum pH after 240 min. The higher stability of fungal pectinases in acidic and neutral media has been highlighted previously by some authors (Pedrolli and Carmona 2010; Sassi *et al.,* 2016). Polygalacturonases from *Aspergillus niger* MTCC 478 (Anand, Yadav and Yadav 2017a) and *A. flavus* MTCC 7589 (Anand, Yadav and Yadav 2017b) were shown recently to exhibit significant stability within pH 5.0 and 9.0, similar to *B. bassiana* SAN01 polygalacturonase, although the enzymes were more stable at pH 3.0 and 4.0.

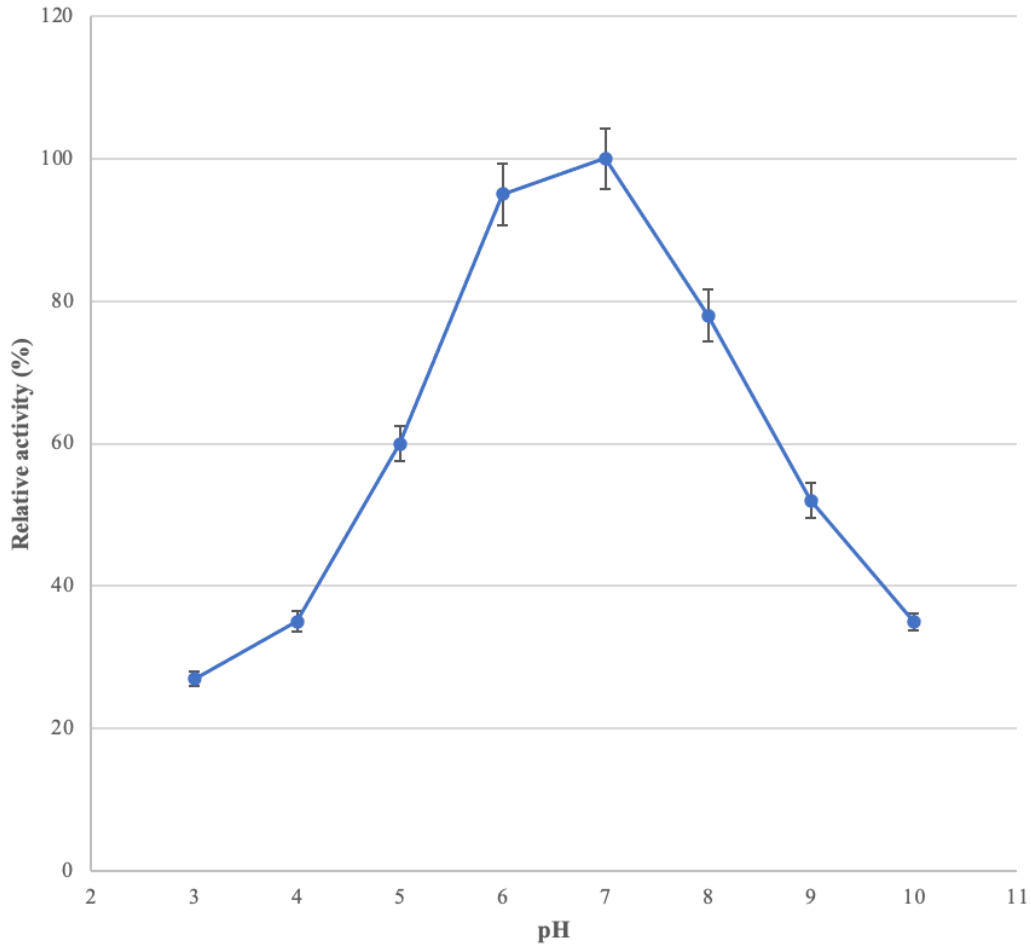

Figure 4.15: Effect of pH on the activity of *B. bassiana* SAN01 polygalacturonase; each point represents the mean (n = 3) ± SD

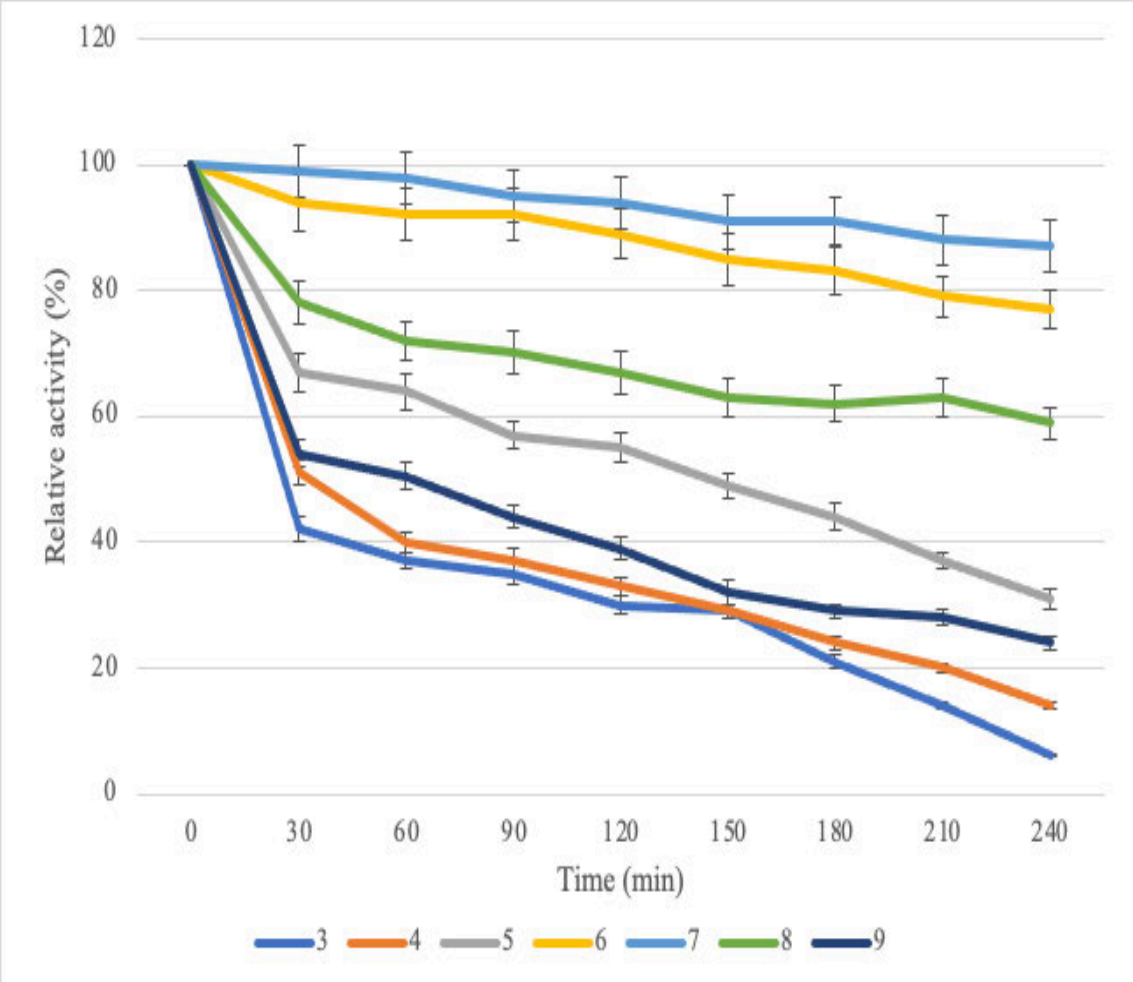

Figure 4.16: Effect of pH on the stability of *B. bassiana* SAN01 polygalacturonase; each point represents the mean (n = 3) ± SD

The optimum temperature of *B. bassiana* SAN01 polygalacturonase was recorded at 45°C and it exhibited significant activity between 25 and 65°C (Figure 4.17). The enzyme activity increased from 62% at 25°C till it reached the maximal activity at 45°C. Beyond the optimum temperature, the enzyme activity decreased with increasing temperature. Polygalacturonase from *Sckrotinia sclerotiorum* (Riou, Freyssinet and Fevre 1992) and *Penicillium janczewskii* (Amin *et al.,* 2020) were shown previously to possess maximum activity at 45°C. Other fungal polygalacturonase with varying optimal temperatures ranging from psychrophilic to thermophilic range have also been shown recently. *Tetracladium* sp. (Carrasco *et al.,* 2019), *Aspergillus tamarii* (Munir et al., 2020) and *Calonectria pteridis* (Ladeira Ázar *et al.,* 2020) were described to produce polygalacturonase with optimal activities at 15°C, 35°C and 60°C, respectively. The

partially purified polygalacturonase from *B. bassiana* SAN01 was also found to be relatively stable between 25°C and 50°C (Figure 4.18), retaining at least 50% of its initial activity within this range after 120 min. The enzyme showed remarkable stability at both 25 and 30°C, retaining ~ 90% of its initial activity after 240 min under both conditions. The thermostability exhibited by the polygalacturonase in this study is consistent with some earlier reports (Beg *et al.,* 2000; Silva *et al.,* 2007; Anand, Yadav and Yadav 2017b).

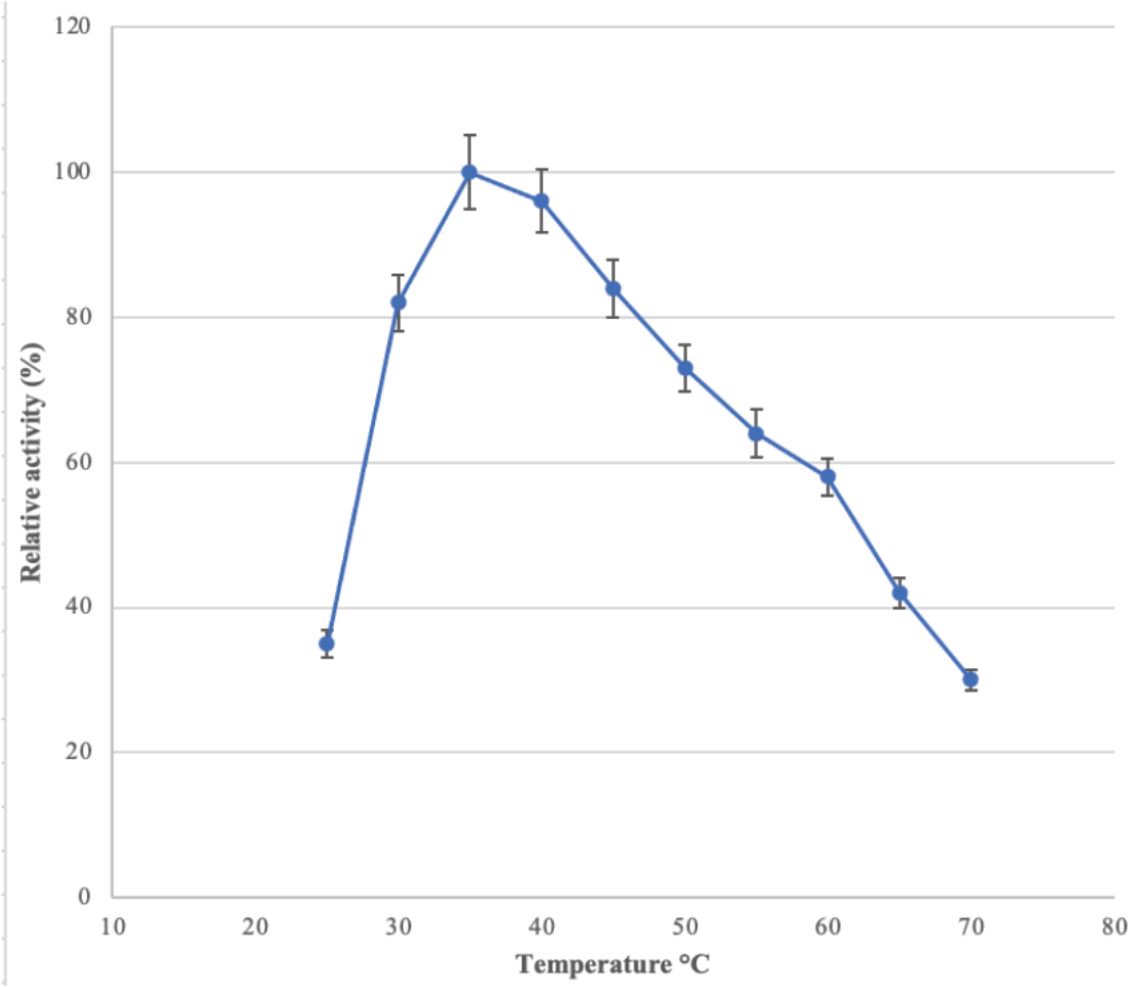

Figure 4.17: Effect of temperature on the activity of *B. bassiana* SAN01 polygalacturonase; each point represents the mean (n = 3) ± SD

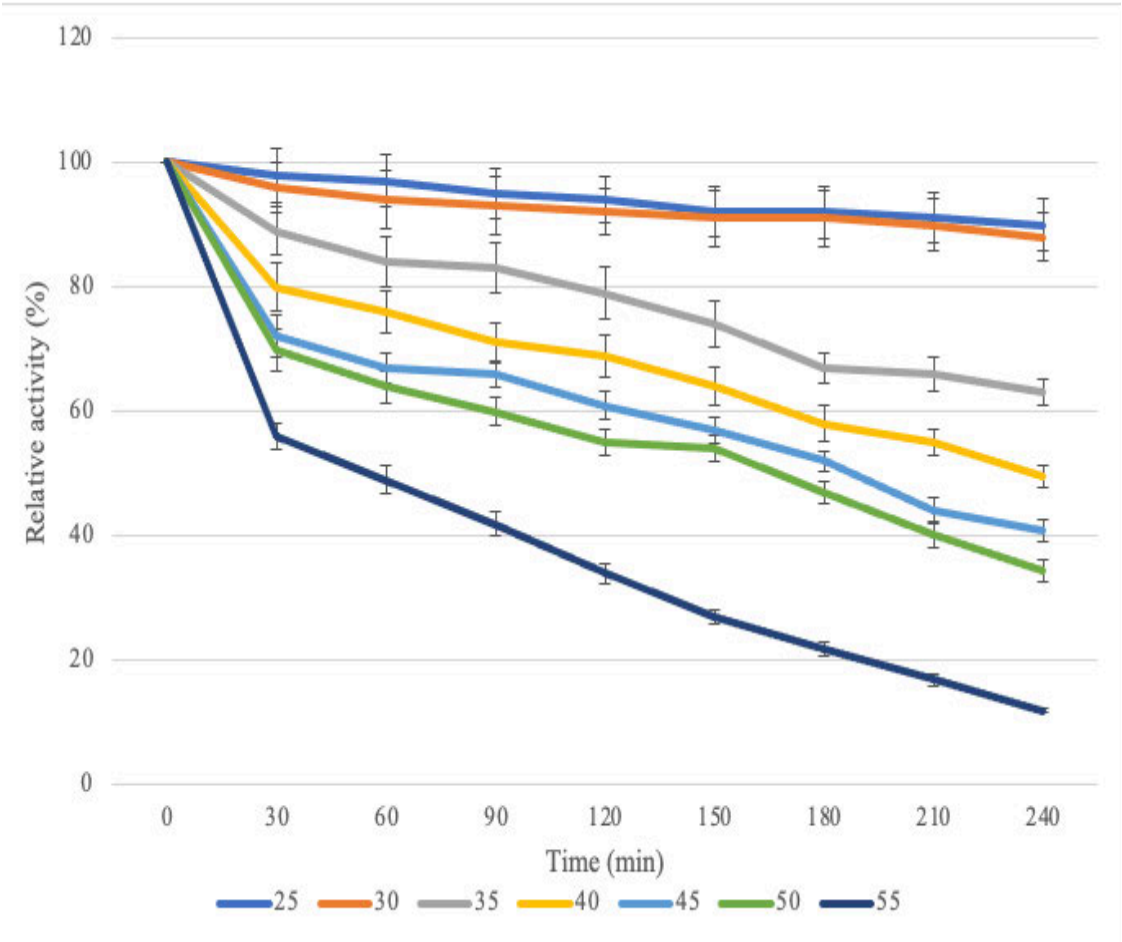

Figure 4.18: Effect of temperature on the stability of *B. bassiana* SAN01 polygalacturonase; each point represents the mean (n = 3) ± SD

4.4 Conclusion

In this chapter, the biochemical characteristics of four carbohydrases, i.e., amylase, endoglucanase, polygalacturonase and xylanase from *B. bassiana* SAN01 were evaluated. All of the glycoside hydrolases were observed to be active and stable over a wide range of pH, from acidic to slightly alkaline. Furthermore, the enzymes were also shown to be generally mesophilic in nature. The xylanase, which was purified to homogeneity, was found to be stable in the presence of various metal compounds, organic solvents and other additives. However, further studies are required to optimize the purification processes for amylase, endoglucanase, and polygalacturonase and their physicochemical characterization. The biochemical characteristics of the enzymes highlighted in this study form a strong basis for enhancing future biotechnological applications of *B. bassiana* SAN01 carbohydrases as well as their structural characterization.

CHAPTER FIVE

Application of *Beauveria bassiana* SAN01 carbohydrases

Abstract

This chapter focuses on the applications of four selected carbohydrases, *viz*., amylase, endoglucanase, polygalacturonase and xylanase, from the fungus *Beauveria bassiana* SAN01. The efficacy of partially purified *B. bassiana* SAN01 endoglucanase-xylanase cocktail and its amylase-polygalacturonase cocktail in the saccharification of sugarcane bagasse and in the clarification of pear juice, respectively, were evaluated. In addition, the potential of purified *B. bassiana* SAN01 xylanase in the deinking of wastepaper was also assessed. Results showed that the crude endoglucanase-xylanase cocktail released the highest amount of reducing sugar from the biomass at 30°C after 8 h incubation. In the same vein, the partially purified amylase-polygalacturonase cocktail was demonstrated to effectively clarify pear juice with a 1.37-fold improvement in clarity recorded under optimal conditions. The enzyme-assisted pear juice treatment significantly lowered browning index (-14.34%), turbidity (-19.72%) and viscosity (-33.08%), while it elevated reducing sugars release (9.55%). Furthermore, the enzymatic clarification of the pear juice did not show any detrimental effect on the antioxidant potential of the juice, unlike in some other methods employed for juice clarification. For the deinking study, the purified *B. bassiana* SAN01 xylanase was effective in deinking wastepaper through its enzymatic disassociation of the fibre-ink bonds as demonstrated by scanning electron microscopy and infrared spectroscopy. Under optimal reaction conditions of 40.17°C incubation temperature, 17.7 h incubation time and an enzyme load of 983.6 UmL^{-1}, the rate of deinking was recorded to be 106.72% when compared to the control. The significant potential of the *B. bassiana* SAN01 glycoside hydrolases recorded in this study presents other promising avenues for using the entomopathogen as a new source of important biocatalysts and by extension, other biotechnological applications.

5.1 Introduction

B. bassiana is a widely known entomopathogen globally used as a biopesticide to control insects, nematodes, and arachnids (Youssef, El-Nagdi and Lotfy 2020; Sayed *et al.,* 2021). For example, blastopores from the fungus are used commercially for biocontrol applications in agriculture. Various strains of the fungus have also been isolated as endophytes from plants, existing symbiotically with different plant hosts (Mattoo and Nonzom 2021; Mwamburi 2021). Furthermore, endophytic *B. bassiana* has also been shown to confer protection on its host plants against pathogens and pest (Barra-Bucarei *et al.,* 2020a; Qin *et al.,* 2020), as well as additional benefits such as growth promotion (Barra-Bucarei *et al.,* 2020b) and drought tolerance (Kuzhuppillymyal-Prabhakarankutty *et al.,* 2020). However, research has shown that the fungus, like many other entomopathogens and endophytes, possesses many other potentials that could be explored for industrial purposes. Specifically, *B. bassiana* has been noted to be a source of many secondary metabolites such as beauvericin, oosperin, tricyclic diterpenoid, bassianolide A-C, etc., with diverse industrial potentials (Ávila-Hernández *et al.,* 2020; Du *et al.,* 2020). Furthermore, the entomopathogen has also been shown in different studies to secrete a wide array of hydrolytic enzymes (Petlamul and Boukaew 2019; Alves *et al.,* 2020; Ryali *et al.,* 2020). However, among the enzymes reported from *B. bassiana,* most attention has been placed on chitinases, lipases and proteases, which have all been well characterized and evaluated for industrial applications (Mancillas-Paredes *et al.,* 2019; Gonçalves *et al.,* 2020; Schmaltz *et al.,* 2021). Similar to the whole fungus, the insecticidal effects of the three enzymes have also been highlighted in various studies (Gu *et al.,* 2020, Kim and Je 2010). In addition, the potential of *B. bassiana* lipase in biodiesel catalysis (Gonçalves *et al.,* 2020), as well as that of the proteases in tissue culture experiments (Shankar, Rao and Laxman 2011) and as a broad range detergent have been demonstrated (Pal and Ghosh 2017).

Recently, researchers have highlighted the ability of different *B. bassiana* strains to produce other enzymes besides the above- mentioned three enzymes. Of particular interest is the ability of the fungus to secrete copious amounts of different carbohydrases such as amylases, cellulases, glucosidase, and xylanase (Petlamul and Boukaew 2019; Ryali *et al.,* 2020). These are all industrially important biocatalysts with diverse applications in the food, bioenergy, paper, and animal feed industries, to mention a few. Although these enzymes have been sourced from various bacteria and fungi, the relative

safety of *B. bassiana* for human and animal use justifies its use as a notable source of the enzymes (Zimmermann 2007). Preliminary investigations have revealed that a novel strain of the fungus, *B. bassiana* SAN01 isolated in our laboratory, can secrete some glycosyl hydrolases, including amylase, cellulase (endoglucanase), pectinase (polygalacturonase) and xylanase. Despite the significant potentials of these enzymes from a non-toxic microbe, the industrial applicability of these *B. bassiana* glycosyl hydrolases has not been assessed in any study. Hence, this study was focused on evaluating the applicability of the *B. bassiana* SAN01 carbohydrases in three different applications i.e., biomass saccharification, deinking of wastepaper and juice clarification. The study investigated the potential of crude endoglucanase-xylanase enzyme cocktail from *B. bassiana* SAN01 in the hydrolysis of alkaline-pretreated sugarcane bagasse under different conditions. Similarly, the efficacy of the partially purified *B. bassiana* SAN01 amylase-polygalacturonase cocktail in the clarification of pear juice was also evaluated. Finally, the potential of the purified xylanase from the same fungus in the deinking of wastepaper was also assessed.

5.2 Methodology

5.2.1 Preparation and purification of the enzymes

Different enzyme preparations were used for the three different applications investigated in this study. Protein purification is a highly expensive and onerous task, hence, the scope of the study was restricted to the complete purification of one of the enzymes, xylanase, as shown in Chapter 4, Section 4.3.1.1, while the other three enzymes were partially purified. In this regard, enzyme cocktails of amylase-polygalacturonase and xylanase-endoglucanase were prepared because of their concomitant production by *B. bassiana* SAN01 as shown in Chapter 3 of this study. While crude xylanase-endoglucanase cocktail was used for biomass saccharification, the amylase-polygalacturonase enzyme cocktail used for fruit juice clarification was partially purified shown previously in Chapter 4, Section 4.3.2. In addition, the amylase-polygalacturonase enzyme cocktail was further subjected to decolourization and filter sterilization. Briefly, 1% activated charcoal was added to the amylase-polygalacturonase enzyme solution and incubated at 4°C for 30 min with continuous stirring (Kareem *et al.,* 2011). The mixture was then centrifuged at 5000 xg for 10 min to recover the clear supernatant. Finally, it was passed through sterile syringe filters (0.2 μm) to remove microbial contaminants and other

suspended solids. *B. bassiana* SAN01 xylanase which was earlier purified to homogeneity in this study (Chapter 4, Section 4.3.1.1), was used for the deinking of wastepaper.

5.2.2 Enzymatic hydrolysis of lignocellulosic biomass using *B. bassiana* SAN01 xylanase-endoglucanase cocktail

Enzymatic saccharification of sugarcane bagasse was carried out using the *B. bassiana* SAN01 xylanase-endoglucanase cocktail. The biomass was chopped into small pieces, oven-dried at 70°C for 24 h, ground in a hammer mill and sieved to get a particle size of 2–5 mm. The powdered biomass was subjected to alkali pretreatment in 4% NaOH solution and neutralized using 1 M HCl (Shahabazuddin *et al.,* 2018). For enzymatic hydrolysis, 1% (w/v) of biomass residues was incubated with a crude enzyme cocktail (~500 U xylanase and 10 U endoglucanase) in 20 mL of sodium acetate buffer (0.1 M, pH 5.0) for 12 h and incubated at different temperatures (30, 40 and 50°C) with continuous agitation at 120 rpm in a shaking water bath (Dutra *et al.,* 2017). The enzyme dosage was selected based on a previous study (Thomas, Parameswaran and Pandey 2016) and preliminary experiments conducted in our laboratory. Sodium azide (0.005%) was added to the reaction mixture to prevent microbial contamination. Samples were withdrawn every two hours and analysed for the reducing sugars released, using the DNS method (Bailey, Biely and Poutanen 1992).

5.2.3 Juice clarification with *B. bassiana* SAN01 amylase-polygalacturonase cocktail

5.2.3.1 *Juice processing*

Pears (Forelle varieties) weighing ~170 g on average were purchased from a local store in Durban, South Africa. The fruits were washed thoroughly to remove surface dirt and deseeded manually. The fruits were subsequently chopped, and the juice was extracted using a juicer. The extract was strained through a stainless-steel sieve with a pore diameter of 3 mm to accomplish the separation of most of the suspended matter. Subsequently, the extract was subjected to vacuum filtration for further removal of any suspended pulp. The final juice was pasteurized at 95°C for 1 min (Petruzzi *et al.,* 2017).

5.2.3.2 *Enzyme-assisted pear juice clarification*

For each treatment, 50 mL of pear juice was subjected to different enzyme treatment conditions (Table 5.1) using the amylase-polygalacturonase cocktail. The three process

parameters selected for the optimization of enzyme treatments by central composite design (CCD) and their ranges were identified from previous studies (Saxena *et al.,* 2014; Uzuner 2018) and also based on preliminary experiments conducted in our laboratory. They include the enzyme load (expressed in amylase activity), incubation time and incubation temperature. Incubation was performed in a shaking water bath with continuous agitation at 50 rpm while the pH of the juice was kept at its natural pH value (pH = 3.9). The partially purified enzymes (~40 U amylase and 60 U polygalacturonase) was used in the optimization process and the enzyme dose was chosen based on preliminary lab experiments. The enzyme treatment was terminated by inactivating the proteins by heating the suspension at 90°C for 1 min. Afterwards, the juice samples were filtered through a muslin cloth, and the filtrates were retained for further analyses. The experimental design and the selected process variables used in the optimization of juice clarification are summarized in Table 5.1. In each experiment, juice clarity was determined as the response. The optimization design was made of 15 combinations including 5 replicates of the centre point.

Table 5.1: Experimental range and levels of independent process variables affecting clarification of pear juice

Independent variables	**Units**	**Levels**				
		-1.68	-1	0	+1	+1.68
Enzyme load (AL/PG) * (A)	UmL^{-1}	20/26.6	24.22/32.21	30/40	35.77/45.57	40/60
Temperature (B)	°C	30	34.23	40	45.78	50
Time (C)	h	1	1.42	2	2.58	3

* Enzyme activity expressed in terms of amylase/ polygalacturonase activities
AL: Amylase; PG: Polygalacturonase

5.2.3.3 *Evaluation of fruit juice characteristics*

5.2.3.3.1 Juice clarity, browning index and turbidity determination

The percent transmittance (% T) is considered a measure of juice clarity and was measured at 660 nm using distilled water as the blank. To determine the browning index,

5 mL of juice sample was mixed with 5 mL of 95% ethanol and centrifuged at 4000 x g for 10 min. The supernatant obtained was passed through a 0.45 µm membrane filter, and the absorbance was measured at 420 nm (Uçan, Ağçam and Akyildiz 2016). While the turbidity of the juice was determined using a Turbidometer (Turbiquant 1100, Germany) and the results were reported in nephelometric turbidity units (NTU) using hexamethylenetetramine solution as a standard (Pradhan, Abdullah and Pradhan 2020).

5.2.3.3.2 Reducing sugars, total dissolved solids and titratable acidity

Reducing sugars released after the enzymatic treatment of pear juice was determined using the DNS method (Bailey *et al*., 1992). Total soluble solids were measured using a digital refractometer with automatic temperature compensation (Atago, USA) and expressed as °Brix (%). The pH of the juice was measured using a benchtop pH-meter (Hanna Instruments, Inc. USA), while the titratable acidity was estimated by titrating 10 mL of the diluted juice (1:10; juice: distilled water) with 0.1 N NaOH solution, using phenolphthalein as an indicator. The acidity value was calculated as citric acid (0.0064 acid factor) equivalents (Santana *et al.,* 2020).

5.2.3.3.3 Viscosity and colour measurement

The viscosity of the samples was measured using a Brookfield LVDV-III digital rheometer (USA) at 25°C fitted with a steel cone-plate (C40/4) under a constant shear rate of 100/s (Domingues *et al.,* 2011). The colour parameters (CIE L* a* b*) of the raw and treated pear juice samples were measured using a ColourFlex EZ Spectrophotometer (Hunter Associates Laboratory Inc., USA), where L value indicates lightness while a* denotes the red/green value ((+): red; (−): green) and b* the yellow/blue value ((+): yellow; (−): blue). Furthermore, the chroma (C*) of the samples were calculated according to the formula $C* = \sqrt{(a*)^2 + (b*)^2}$ (Uçan *et al*., 2016).

5.2.3.3.4 Antioxidant activities of enzyme-clarified juice

5.2.3.3.4 1 Total antioxidant capacity

Reaction mixtures containing pear juice sample (100 µL) and DPPH (3.9 mL, 50 µM) in methanol were incubated in a water bath at 37°C for 30 min. The change in absorbance was measured at 517 nm using a spectrophotometer, and the radical scavenging activity was analysed by the equation:

$$DPPH\ (\%\ inhibition) = [(Abs0 - Abs1)/Abs0] \times 100$$

where Abs_0 and Abs_1 are the absorbance values of blank and test samples, respectively (Wang, Vanga, & Raghavan, 2019).

5.2.3.3.4.2 Total phenolic content

The total phenolic content of juice samples was analysed using a modified Folin-Ciocalteu method. Each sample (0.1 mL) was mixed with 0.75 mL of diluted Folin-Ciocalteu reagent (10% v/v) and incubated for 5 min at room temperature and 0.75 mL of 2% sodium carbonate solution was added. After incubation for 15 min at room temperature, the absorbance of the solution was read at 750 nm. Gallic acid was used as the standard, and the total polyphenol was expressed as gallic acid equivalents (mg GAE L^{-1}) (Romero-González *et al.,* 2020).

5.2.3.3.4 3 Total flavonoid content

The total flavonoid content (TFC) of juice samples was estimated spectrophotometrically based on the aluminium chloride colourimetric method (Cheng *et al.,* 2016). A 0.5 mL of the juice sample was added to 4.5 mL of aluminium chloride reagent consisting of 10% aluminium chloride (0.1 mL), 1 M potassium acetate (0.1 mL), 95% ethanol (1.5 mL) and distilled water (2.8 mL). The absorbance of the reaction mixture was measured at 415 nm after incubation at room temperature for 30 min. The TFC in each solvent was calculated based on a standard calibration curve of quercetin while the TFC was expressed in quercetin equivalent (mg QE L^{-1}). The aluminium chloride reagent mixture alone, without the addition of the sample was used as a blank.

5.2.3.3.4.4 FRAP (Ferric reducing ability of plasma) assay

The FRAP assay was performed using a modified Wang *et al*. (2019) method. Briefly, FRAP reagent was prepared from a combination of 300 mM acetate-glacial acetic acid buffer (pH 3.6), 20 mM ferric chloride and 10 mM 4,6-tripryridyl-s-triazine (prepared in 40 mM HCl) in ratio 10:1:1 respectively. The FRAP assay was performed by incubating 1 mL of dH_2O, 25 µL sample and 1 mL of the FRAP reagent at 37°C. The absorbance at time zero and after 40 min was recorded at 593 nm (Kumar *et al.,* 2020). Ferrous sulphate was used as the standard while the FRAP activity was expressed as µmol Fe (II) mL^{-1}.

5.2.4 Deinking of wastepaper

5.2.4.1 *Optimization of deinking process*

Waste printed paper was collected, shredded and diced further into smaller pieces using scissors. The paper pieces were soaked in warm distilled water for 2 h to remove the adhering surface dust particles and pulverized using a rotary laboratory blender (Eberbach Corp, Michigan, USA). The resulting pulp slurry was drained using cheesecloth and oven-dried at 45°C for 4 h. Subsequently, 400 mg dried pulp was incubated in 5 mL sodium acetate buffer (pH 6.0, 50 mM) and subjected to different experimental conditions as summarized in Table 2. For the CCD optimization of the wastepaper deinking, process parameters were selected and their ranges were determined based on preliminary experiments and previous studies (Saxena *et al.,* 2014; Cerreti *et al.,* 2017). These are the enzyme load, incubation time and incubation temperature (Table 5.2). The design was made of 15 combinations including 5 replicates of the centre point; the release of ink and reducing sugars were the expected output. The incubation was done in a constant temperature water bath (35°C) with continuous agitation at 50 rpm while enzyme treatment was terminated by inactivating the enzymes by heating the reaction mixture at 90°C for 5 min. Heat-denatured xylanase served as the control. After enzymatic treatment, the pulp filtrate was separated by centrifugation at 5000 xg for 5 min and analysed.

Table 5.2: Coded and uncoded variables of the response surface design for xylanase-assisted paper deinking

Independent Variables	**Units**	**Levels**				
		-1.68	-1	0	+1	+1.68
Temperature (A)	ºC	35	36.47	40	43.54	45
Time (B)	h	6	7.76	12	16.25	18
Enzyme load (C)	UmL^{-1}	500	573.23	750	926.78	1000

5.2.4.2 *Release of ink*

The deinking of the printed paper was evaluated by recording the absorbance at 596 nm for the release of colour (diazo reactive black 5) (Thomas, Ushasree and Pandey 2014). All experiments were conducted in triplicate, and their mean values are presented. The reducing sugar released for each sample was also evaluated using the DNS method (Bailey, Biely and Poutanen 1992).

5.2.4.3 *Scanning Electron Microscopy*

Pulp samples were gradually dehydrated with different gradients of acetone, followed by absolute alcohol, according to Chutani and Sharma (2015). Subsequently, samples were air-dried, coated with a thin gold film and viewed under a scanning electron microscope (SEM) (Zeiss; EVO 18, Germany) at 20 kV to observe the surface morphology. Electron micrographs were taken at X500, X1000, X2000 and X5000 magnifications.

5.2.4.4 *FTIR analysis*

The surface functional groups of the enzyme-treated pulp and non-treated control was studied by Fourier transformed infrared (FTIR) spectrometry using the attenuated total reflectance (ATR) measuring cell. The infrared spectrometer (FT-IR CARY 630, Agilent Technologies) with a range of 650 to 4000 cm^{-1} was used for the samples with an average of 32 scans (Borges *et al*., 2020).

5.3 Results and discussion

5.3.1 Biomass saccharification

The deconstruction of different lignocellulosic biomass by *B. bassiana*, especially in the utilization of the biomass for its nutrition and growth, has been described in various studies (Nuñez-Gaona *et al.,* 2010; Alves *et al.,* 2020). In this regard, the enzymatic machinery necessary for this degradation has also been identified (Petlamul and Boukaew 2019; Ryali *et al.,* 2020). However, the potential of these enzymes in the hydrolysis of lignocellulosic biomass and the simultaneous production of reducing sugar has not been demonstrated in any previous studies. Thus, the suitability and efficacy of selected *B. bassiana* SAN01 carbohydrases in the saccharification of sugarcane bagasse (SB) was evaluated in this study.

The sugarcane bagasse was initially subjected to alkaline pretreatment to reduce its lignin component. Alkaline pretreatment has been routinely used to enhance subsequent

enzymatic hydrolysis of biomass as it has been noted to produce fewer inhibitors in comparison to acid pretreatment (Kim, Lee and Kim 2016; Kucharska *et al.,* 2018). This pretreatment method was also selected because of the higher xylanolytic activity of the fungal strain under investigation. Studies have shown that alkali pretreatment significantly increases the availability of hemicelluloses for further hydrolysis (Asgher, Ahmad and Iqbal 2013). Subsequently, the efficiency of *B. bassiana* SAN01 xylanase-endoglucanase enzyme cocktail on SB saccharification was investigated. The enzymatic hydrolysis of the pretreated SB resulted in a significant release of reducing sugars across different time intervals and incubation temperatures (Figure 5.1). The highest amount of reducing sugars (200.64 ± 8.67 mg/g of biomass) was released at 30°C, which is around the growth temperature for the fungus. A significantly high amount of reducing sugars was observed at 40°C; sugars released at this temperature were approximately 80-90% of that released at the optimum temperature. Surprisingly, a significantly lower amount of the desired products was noticed at 25°C (122.47 ± 5.29 mg/g of biomass). The enzymatic saccharification at room temperature is believed to be low, due to the reduced molecular movement and minimized effective collisions between the enzymes and the substrate at low temperatures.

Similarly, a relatively lower amount of the desired products was also formed at 50°C, which suggests the impaired activity of *B. bassiana* SAN01 enzymes at a higher temperature. Furthermore, irrespective of the incubation temperature, reducing sugar release increased with increased reaction time until it peaked at 8 hours. Thus, it was observed that the enzyme cocktail from *B. bassiana* SAN01 could hydrolyze SB optimally at 30ºC after 8 h. In contrast to our results, most enzymatic saccharification of biomass has been shown at a higher temperature of 40ºC and more (Lamounier *et al.,* 2018; Prajapati *et al.,* 2020). It is believed that saccharification at high temperature increases the cost of production of reducing sugars from lignocellulosic biomass due to the higher energy input required to produce heat for increased temperature. In addition, a higher temperature could also enhance the faster denaturation of enzymes which limit enzyme action. Hence, pragmatically the xylanase-endoglucanase enzyme cocktail from *B. bassiana* SAN01 with an optimum hydrolysis temperature of 30ºC substantiates its application potential. For instance, these enzymes cocktail could be very effective in simultaneous saccharification and fermentation for ethanol production from lignocellulose. This process could lead to different advantages including reduced end-

product inhibition of the enzymatic hydrolysis as the production of reducing sugar will be accompanied by an instantaneous bioconversion to ethanol. In addition, the investment costs will be reduced as a result of the coupling of enzymatic biomass saccharification and ethanol production by the fermentative microbes, especially yeasts. Unlike in many other hydrolytic enzymes (Olofsson, Bertilsson and Lidén 2008), the optimum temperature observed for *B. bassiana* SAN01 enzymatic saccharification is similar to that of yeast. In addition, the *B. bassiana* SAN01 crude carbohydrase cocktail also compares favourably with results from studies with other fungi such as *Aspergillus fumigatus* (Lamounier *et al*., 2018), *Penicillium chrysosporium*, *Pycnoporus sanguineus*, *Tramates versicolor* (Cardoso *et al.,* 2018) and *Phanerochaete chrysosporium* (Waghmare *et al.,* 2018).

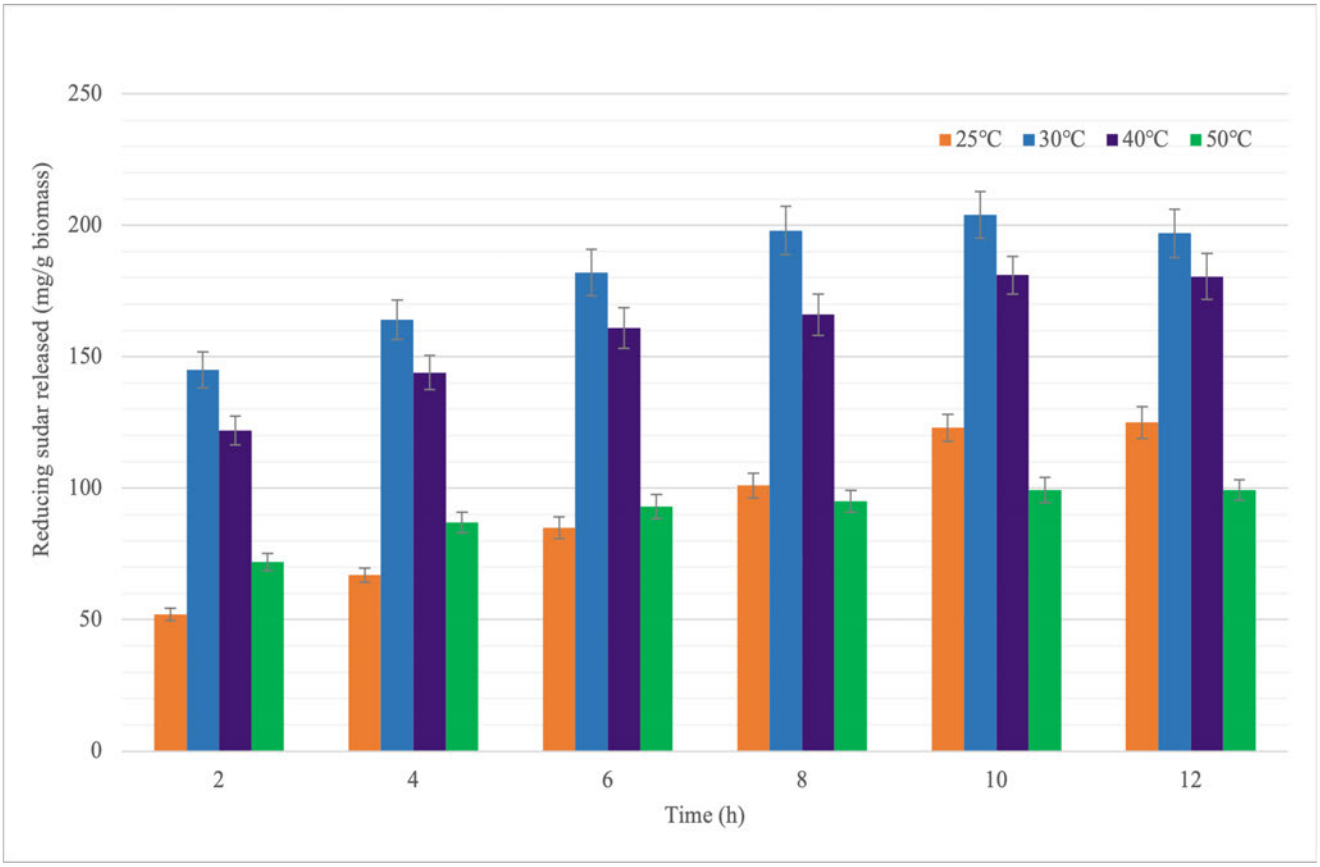

Figure 5.1: Total reducing sugar profile of *B. bassiana* SAN01 xylanase-endoglucanase saccharified sugarcane bagasse

5.3.2 Enzyme-assisted clarification of pear juice

5.3.2.1 *Optimization of pear juice treatment*

The efficacy of the amylase-polygalacturonase cocktail in the clarification of pear juice was evaluated by RSM using a CCD design. The clarity under different conditions was measured as the response (Table 5.3). In the design of 20 experimental runs, pear juice clarity, taken as a response, varied greatly from 25.46% and 100% with varying process conditions (Table 5.3). Compared to the control, the highest clarity at 100% was recorded at ~34ºC, after 2.6 h incubation at an enzyme load of 35.77/47.57 UmL^{-1} (amylase/ polygalacturonase activities). The results showed that juice clarity was significantly affected and improved by the optimization of the enzyme load, incubation temperature and incubation time. It is posited that the amylase-polygalacturonase enzymes hydrolysed the starch and pectin in the juice into different monomers and oligomers, causing protein-sugar complexes which aggregated into larger particles and settled, thus improving the juice clarity. Similar findings from previous studies corroborate the current study results (Sorrivas, Genovese and Lozano 2006; Ahmed and Sohail 2020).

Table 5.3: CCD optimization of pear juice clarification design and the response of the dependent variables

	Level			Clarity (%) *	
	Coded (A)	Coded (B)	Coded (C)	Actual	Predicted
1	+1.68	0	0	74.87	77.72
2	0	-1.68	0	38.48	41.28
3	0	+1.68	0	61.95	64.75
4	0	0	-1.68	32.51	36.41
5	0	0	+1.68	65.72	69.62
6	+1	-1	+1	100.00	99.46
7	0	0	0	56.12	53.02
8	-1.68	0	0	25.46	28.31
9	0	0	0	58.06	53.02
10	-1	-1	-1	39.22	38.68
11	0	0	0	51.19	53.02
12	+1	+1	-1	36.79	36.25
13	0	0	0	59.15	53.02
14	-1	+1	+1	38.22	37.68
15	0	0	0	57.53	53.02

* Average of triplicate determinations
**Significant p- values at $P \leq 0.1$

The reliability of the model was confirmed from the F -value (41.06) and p-values as observed from the ANOVA (Appendix 10). The model, as well as some of the terms (A, B, C, AB, AC, A^2 & B^2), were found to be significant judging from their p- values (de Castro, Castilho and Freire 2015). However, exceptions were noticed in BC and C^2 with p-values greater than 0.1, which suggests that the interactive effect of B and C are not consequential. The model showed a high R^2 value of 0.9685 (Appendix 10), which demonstrates that the model can account for approximately 97% of the total variation and represent significant relationships among the selected variables i.e., the enzyme load, incubation temperature as well as incubation time.

In addition, the interactions between the selected factors, as it affects the optimized clarification of pear juice, were also represented in contour and response surface plots. The interaction between A (enzyme load) and B (incubation temperature) was found to be moderately significant (p-value 0.0726) where, with the increasing dose of enzyme, a simultaneous increase in juice clarification was observed. While with increasing temperature, the clarifications seem moderately increasing (Figure 5.2a). The interaction between A (enzyme load) and C (incubation time) was most significant (p-value < 0.0001), where both incubation time and enzyme load were found to be interacting considerably with each other (Figure 5.2b). A lower dosage of the enzyme (20 UmL^{-1}) and incubation time (1 h) failed to clarify the juice effectively while a sharp increase in clarification was observed with a steady increase in both the factors studied, keeping the temperature at zero levels (40°C). While the interaction among B (incubation temperature) and C (incubation time) was found to be statistically insignificant (p-value 0.8473) suggesting little interactions of the components with each other (Figure 5.2c), where the level of enzyme dosage studied (30 UmL^{-1}) might be responsible for the observable interactions amongst studied components suggesting enzyme dose again as the most critical factor which is corroborated by the lowest p-value.

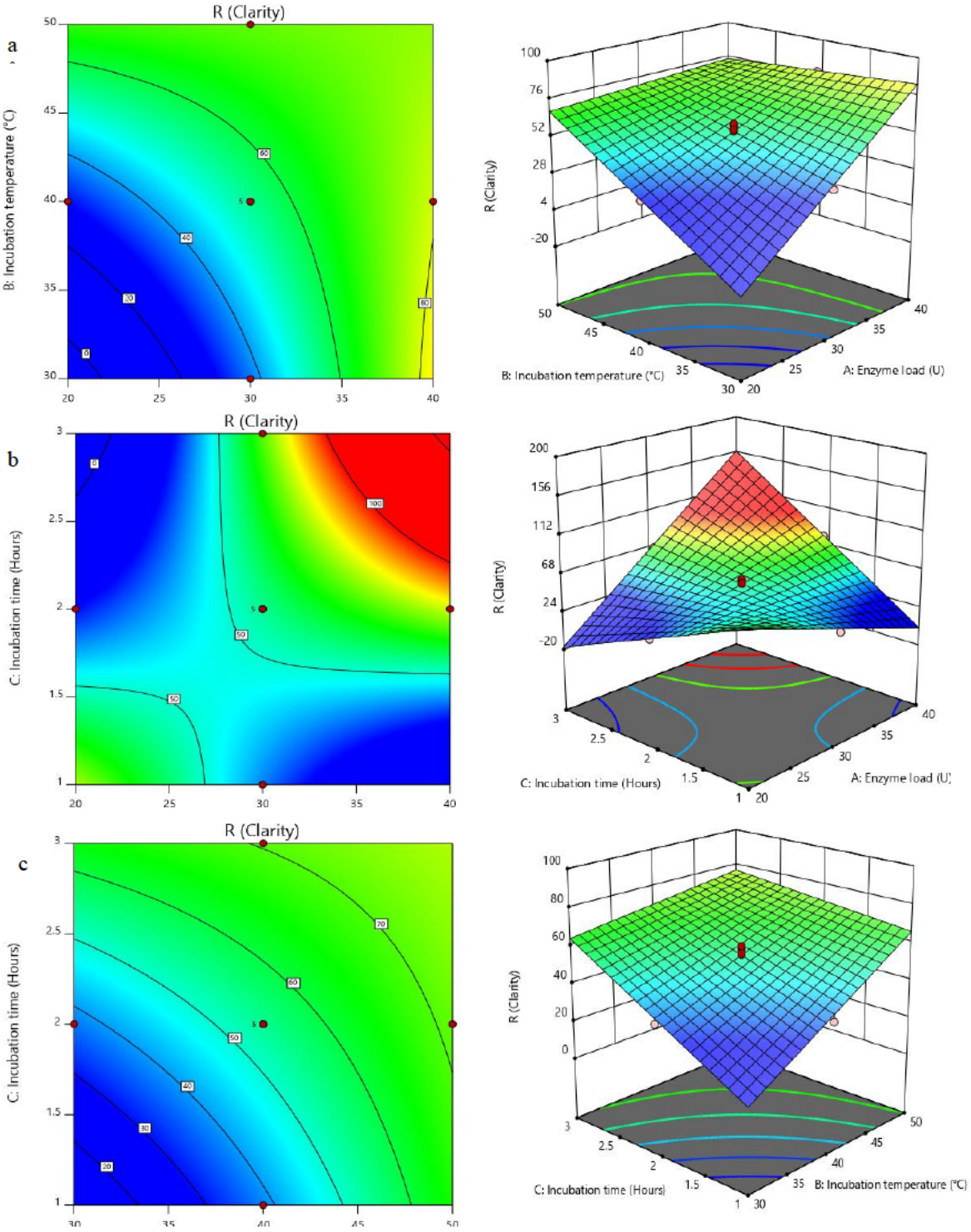

Figure 5.2: Response surface plots showing the interactions between the variables for enzymatic clarification of pear juice: (a) contour & 3D plots of enzyme load - incubation temperature interaction; (b) contour & 3D plots of enzyme load - incubation time interaction; (c) contour & 3D plots of incubation time - incubation temperature interaction.

5.3.2.2 *Validation of the experimental model*

The adequacy of the models was further confirmed and validated by carrying out the enzyme treatment using the derived optimal conditions. The conditions predicted for optimum pear juice clarification were enzyme load (39.37/53.36 UmL^{-1}; amylase/polygalacturonase), incubation temperature (36.87°C) and time (2 h 45 min). As suggested by the model, the predicted value of maximum clarification, 140.65%, was in close agreement with the experimental value of 137±7.1% (Table 5.4). Hence, it can be stated that the close proximity between the predicted and experimental values point to the adequate prediction of the generated model. Thus, by applying the CCD designs to the enzymatic clarification of pear juice, a 1.47-fold increase in clarity was recorded.

Table 5.4: Validation of juice clarification model

Optimized parameters	Enzyme load (AL/PG)* UmL^{-1}	Temperature °C	Time h	Predicted output (% clarity)	Actual output (% clarity)
	39.37/53.36	36.87	2.75	140.65	137

* Enzyme activity expressed in terms of amylase/ polygalacturonase activities
AL: Amylase; PG: Polygalacturonase

5.3.2.3 *Effect of B. bassiana* SAN01 *amylase-polygalacturonase cocktail on pear juice properties*

Various treatment methods are currently used in fruit juice processing in general, and juice clarification in particular, in order to increase their appeal to prospective consumers. These methods include centrifugation (Ghosh, Pradhan and Mishra 2018), membrane-filtration (Abd-Razak *et al.,* 2021), heat (Saad, Mohamed and Ramadan 2020), ultrasound (Yildiz *et al.,* 2021) and enzymatic treatments (Azimi, Hosseini and Khodaiyan 2021; Perreault *et al.,* 2021). However, these methods have been shown to either enhance or reduce the physical properties of the juices, which is an indicator of the juice quality (Bhattacharjee *et al.,* 2017). Hence, in order to evaluate the feasibility of *B. bassiana* SAN01 amylase-polygalacturonase treatment in pear juice processing, the effects of the cocktail on its properties were evaluated.

The colour of food products is a major determining factor in customer preference, especially in fruit juices. The lighter or brighter the juice, the better. Browning, both enzymatic and non-enzymatic, has been noted for its detrimental effects on the nutrition and sensory appeal of fruit products, such as pear juice (Bharate *et al.,* 2014). The dark colour of pear juice has been noted to be responsible for its non-preference by consumers, as dark coloured fruit products are usually associated with deterioration; hence, a reduction of this dark colour is desirable (Beveridge and Wrolstad 1997; Singh, Jawandha and Gill 2020). In this study, the browning index of the untreated pear juice was reduced from 0.258 to 0.221 after the enzymatic clarification. Hence, a ~14% reduction in browning subsequent to enzymatic treatment was recorded which is both significant and desirable (Table 5.5). A similar trend has also been shown in a previous study on carrot juice (Tadakittisarn *et al.,* 2007). Enzymatic browning in fruit juices has been ascribed to the action of polyphenol oxidase and has been identified to be a major concern in the processing of pear for juice production (Jiang *et al.,* 2016).

A significant improvement in the colour (lightness) of the juice was recorded subsequent to enzyme treatment as the L-value has increased from its initial value of 14.23 to 17.53, after treatment (Table 5.5). The increase in L-value was also observed in a recent study on pectinase application in extracting juices from pears (Gani *et al.,* 2020). Furthermore, an increase of 32.52% and 69% in the redness and yellowness, respectively, of the enzyme-treated pear juice was observed in comparison to control (Table 5.5). The positive changes in the a* and b* values of food samples have also been recorded in previous studies (Lachowicz, Oszmiański and Kolniak-Ostek 2018). The increase in the colour intensity and the brightness of the processed juice was also shown by the significant increase in the chroma value from 3.91 to 6.33. This trend was also observed previously by Pathare, Opara and Al-Said (2013).

Viscosity and turbidity have been a quality discriminant in fruit juice processing, as it affects food product stability (Sharma, Patel and Sugandha 2017; Salehi 2020). A reduction in the viscosity of fruit juice is considered important as it prevents problems such as fouling of membrane surfaces encountered during the subsequent filtration process. Besides, consumers have shown a preference for juice products with relatively lower viscosity (Salehi, 2020). With the fungal enzyme treatment, the viscosity of pear juice was reduced by one-third of its initial value of 3.87 mPa.s to 2.59 mPa.s (Table 5.5). A similar reduction has also been highlighted in previous clarification studies of

various juices, including apricot, banana, and sapodilla (Sharma, Patel and Sugandha 2017).

It has been noted that turbidity in fruit juice results from unhydrolyzed complex carbohydrates; hence the hydrolysis of pectin and starch has been identified as a major step in reducing the turbidity (Sorrivas, Genovese and Lozano 2006). The efficacy of the *B*. *bassiana* SAN01 carbohydrase cocktail in the clarification process was highlighted by ~ 20% reduction in the turbidity of the pear juice. The enzyme clarification decreased the turbidity of the juice sample from 1410.72 to 1132 NTU (Table 5.5). A similar reduction in juice turbidity was also observed in apple, grape and peach juices, using fungal polygalacturonase (Amin *et al.,* 2017) and amylase (Sorrivas, Genovese and Lozano 2006).

The pH, titratable acidity and total dissolved solids (Brix %) have been noted to be important in the quality control of fruit juices, especially as it concerns their stability on storage (Adedeji and Ezekiel 2020). However, in this study, only minor fluctuations were observed between the pH, titratable acidity and total dissolved solids of the control and the treated juice (Table 5.5). While the pH of the control juice was 3.93, the treated juice was shown to be 3.79. Similarly, the titratable acidity of the control and treated samples were observed to be 0.28 and 0.29, respectively. Furthermore, the Brix values of the untreated and treated samples were 8.9 and 9.2%, respectively. Similar trends were observed for titratable acidity and total dissolved solids in previous enzymatic treatments of banana and strawberry juices, where the pH, titratable acidity and total dissolved solids were barely affected (Barman *et al.,* 2015; Sandri and Silveira 2018). The observed reduction in the pH and increase in titratable acidity is believed to be due to the release of galacturonic acid which is the hydrolytic product of pectin while the increase in Brix (%) could be due to the enzyme-facilitated degradation of the carbohydrate complex in the cell walls (Kyamuhangire *et al.,* 2002; Bora, Handique and Sit 2017).

The effect of the amylase-polygalacturonase treatment is also demonstrated by the ~10% increase in reducing sugars after processing (Table 5.5). The expected increase in reducing sugar is a result of the hydrolytic action of the glycosyl hydrolase on the carbohydrate polymers (pectin and starch) present in the raw juice. The increase in sugars has also been observed in different studies (Yang *et al.,* 2019; Adedeji and Ezekiel 2020). The increase in reducing sugar complements the reduction in the viscosity and turbidity, as a linear relationship exists between the clearance of complex sugars (substrates) and

the production of reducing sugars (products) (Yang *et al.,* 2019). In addition, the reducing sugar is expected to significantly increase the sweetness and flavour of the juice products, thus, limiting the need for extra sweeteners during further processing.

Table 5.5: Effect of enzyme treatment on pear juice properties

	Raw juice	**Enzyme treated juice**	**Percent change***
Browning index	0.258	0.221	-14.34
Colour L	14.23 ± 0.34	17.53 ± 0.41	23.19
a*	-1.23	-0.83	32.52
b*	3.71	6.27	69
C*	3.91	6.33	61.89
pH	3.93 ± 0.04	3.79 ± 0.03	-3.56
Reducing sugars ($mgmL^{-1}$)	75.48 ± 2.26	82.61 ± 2.74	9.55
Titratable acidity ($g100\ mL^{-1}$)	0.28	0.27	-3.57
Total dissolved solids (Brix %)	8.9±0.1	9.2±0.2	3.37
Viscosity (mPa.s)	3.87 ± 0.17	2.59 ± 0.11	-33.08
Turbidity (NTU)	1410.72 ± 73.5	1132 ± 34.64	-19.72

** Average of triplicate determinations
**Significant p- values at $p \leq 0.1$

5.3.2.4 *Effect of B. bassiana amylase-polygalacturonase cocktail on the antioxidant* properties *of pear juice*

The increase in juice consumption has been ascribed to the reported health benefits of their antioxidants (Ern, Aron and Eng 2016), hence, it is important to determine the effect of the enzymatic treatment on the antioxidant properties of fruit juices. Pectinase treatment has particularly been shown in a few studies to have a negative effect on the total antioxidant capacity of fruit juices (Chen *et al.,* 2012). However, a slight increase in the total antioxidant activity was observed after the enzymatic treatment of the pear juice in this study. The total antioxidant activity increased from 66.04 in the untreated n

juice sample to 68.17 DPPH % in the enzyme-treated fruit juice (Table 5.6). The effects of different food processing methods on the bioaccessibility and bioavailability of antioxidants have been highlighted in previous studies (Castro *et al.,* 2020). Hence, it is hypothesized that the amylase-polygalacturonase enzyme cocktails were involved in the different interactions between pear juice antioxidants and its pectin, as well as the amylose and amylopectin molecules (Ribas-Agustí *et al.,* 2018).

Phenolics, including flavonoids, contribute the most to the antioxidant activities observed in fruits and their products (Shah *et al.,* 2015). In this study, the total phenolics were not significantly affected while there was a significant increase in total flavonoids. A non-significant change from 318.02 mg GAE L^{-1} in the control juice to 312.95 mg GAE L^{-1} in the treated sample was observed in the phenolic content (Table 5.6). However, the total flavonoids increased from their control value of 118.64 to 136.81 mg QE L^{-1} subsequent to enzyme clarification (Table 5.6). Pear juices are very rich in phenolic compounds, including arbutin, chlorogenic acid, epicatechin, quercetin-3-glucoside, quercetin-3-galactoside, and quercetin-3-rutinoside (Schieber, Keller and Carle 2001). It is posited that the hydrolytic action of the enzymes might have broken down these compounds into their aglycone moieties, thus the observed significant increase in total flavonoids. This was highlighted previously in the enzymatic hydrolysis of flavonoids from bergamot orange (Mandalari *et al.,* 2006). Furthermore, it has also been noted that the enhancement of total antioxidative activity may be a result of an increase in released flavonoid aglycones (Gu, Duan and Yu 2019).

The *in vitro* FRAP assay has been noted to be one of the best indices of antioxidant activity in fruit juices and other fruits products (Sethi *et al.,* 2020). The antioxidant activities, as measured using the FRAP method were also shown to be slightly reduced due to *B. bassiana* SAN01 enzyme cocktail treatment. The ferric reducing antioxidant power of the treated juice was found to change slightly from the initial value of 133.12 µmol Fe (II) mL^{-1} to 132.67 µmol Fe (II) mL^{-1} after enzymatic treatment (Table 5.6). Hence, it can be inferred from these results that *B. bassiana* SAN01 amylase-pectinase treatment has no negative impact on the antioxidant indices of treated pear juice samples relative to the untreated control samples.

Table 5.6: Antioxidant properties of untreated and enzyme-treated pear juice

	Untreated juice*	Enzyme treated juice*
Total antioxidant (DPPH %)	66.04 ± 2.19	68.17 ± 3.04
Total phenolics (mg GAE L^{-1})	318.02 ± 12.32	312.95 ± 7.25
Total flavonoids (mg QE L^{-1})	118.64 ± 3.43	136.81 ± 4.71
FRAP (µmol Fe (II) mL^{-1})	133.12 ± 5.01	132.67 ± 6.67

* Average of triplicate determinations
**Significant p- values at $p \leq 0.1$

5.3.3 Deinking of printed paper by *B. bassiana* SAN01 xylanase

5.3.3.1 *Optimization of deinking process*

The deinking potential of *B. bassiana* SAN01 xylanase was evaluated on printed paper and this was optimized using a central composite design of RSM. The three selected conditions that affected enzymatic deinking, *viz.*, incubation temperature, time and enzyme load, were optimized for the enhancement of the process. The rate of deinking was observed to vary markedly with the conditions tested in the ranges of 28.27%-100% as represented in Table 5.7, thus indicating the efficacy of *B. bassiana* SAN01 xylanase in the removal of the ink. The highest clarification efficacy recorded in this study was at 36.47ºC, 573.23 UmL^{-1} enzyme load and 16.25 h incubation. In contrast, the lowest clarification efficacy was observed at the same temperature and enzyme dosage (36.47ºC, 573.23 UmL^{-1}), but at a lower incubation time of 7.76 h. The deinking efficiencies of xylanases have been shown in many studies. Xylanases, alone and in combination with other enzymes such as cellulases and laccases, have been used for wastepaper deinking (Gupta *et al.,* 2015; Kumar *et al.,* 2018b). Furthermore, the enzyme has also been coupled with other treatment methods, such as ozone treatment, for deinking both on a laboratory and industrial scale.

Fungal carbohydrases, such as *B. bassiana* xylanase, have been noted to be more suited for the deinking process as most fungal xylanases exhibit optimal activities in the acidic pH range, which incidentally is the pH of writing and printing papers (Dutt *et al.,* 2012; Desai and Iyer 2016). It is believed that the enzymes dislodge chromophores from the

paper fibres by modifying the ink-fibre surface properties through increased relative hydrophobicity. Furthermore, hemicellulose hydrolysis on the fibre-ink interphase also contributes significantly to the detachment of the chromophores (Pommier *et al*., 1990; Kumar and Satyanarayana 2014). The efficient removal of these ink compounds from wastepaper will facilitate their recyclability, thus preserving our fragile natural resources by reducing the production of virgin papers from trees and tackling waste generation simultaneously. In addition, a significant amount of reducing sugars was released during the deinking process, ranging between 140.28 and 212.56 mgg^{-1} (Table 5.7). Earlier studies have also highlighted the simultaneous release of reducing sugars along with ink chromophores during enzymatic deinking of paper (Chutani and Sharma 2015; Gupta *et al.,* 2015). This can be attributed to the hydrolytic action of the enzyme on the hemicellulosic components of the paper fibre. The release of reducing sugar further emphasizes the valorisation of wastepaper in the recycling process as this sugar can be found useful in other downstream industrial processes. Biofuel production using reducing sugars from wastepaper has been noted to be a promising approach towards sustainable energy; however, this potential is impeded by the hazardous ink present. Earlier studies have demonstrated the enzymatic saccharification of paper pulp subsequent to bioethanol (Saini *et al.,* 2020), biohydrogen (Lakshmidevi and Muthukumar 2010), and phenyllactic acid (Kawaguchi *et al.,* 2014) production.

Table 5.7: CCD optimization of xylanase-assisted printed paper deinking and the response of the dependent variable

	Level			Deinking (%)		Reducing sugar (mg/g)	
	Coded (A)	Coded (B)	Coded (C)	Actual	Predicted	Actual	Predicted
1	+1.68	0	0	59.68	59.84	167.70	166.64
2	-1	-1	-1	28.27	28.11	121.50	122.56
3	0	-1.68	0	45.83	45.99	174.17	173.11
4	0	0	0	66.90	68.00	198.67	194.28
5	+1	+1	-1	52.08	51.92	168.62	169.68
6	0	0	-1.68	43.33	43.49	140.28	139.22
7	0	0	0	71.16	68.00	190.45	194.28
8	0	0	0	68.27	68.00	187.67	194.28
9	-1	+1	-1	100.00	99.84	196.74	197.80
10	0	0	0	69.04	68.00	197.74	194.28
11	0	+1.68	0	73.45	73.61	202.00	200.94
12	0	0	0	64.97	68.00	194.77	194.28
13	0	0	+1.68	94.32	94.48	212.56	211.50
14	-1.68	0	0	51.66	51.82	159.78	158.72
15	+1	-1	+1	53.51	53.35	170.47	171.53

* Average of triplicate determinations
**Significant p- values at $P \leq 0.1$

Statistical analysis of the model was performed with the F-test for analysis of variance (ANOVA) as shown in Appendix 11. The model was confirmed to be valid from the observed F -value (123.02) and p-values. The significant effect of all of the model terms (A, B, C, AB, AC, BC A^2, B^2 & C^2) were also deduced from their respective p- values which were all less than 0.1. The model showed a high R^2 value of 0.9955, which indicates that the model can account for approximately 100% of the total variation and also represent significant relationships among the chosen variables.

The effect of the variable changes on the responses can also be observed on the contour and surface plots (Figure 5.3a-c) which showed the effects of temperature, time, and enzyme dose on ink removal from the printed paper. The incubation time, temperature and enzyme load showed significant effects on the deinking process (Figure 3). An increase in deinking was recorded with increasing temperature and incubation time until the maximum levels of ~100 % were attained at ~40°C and 17 h. The effects of temperature were observed to be negative beyond the optimum temperature, while time had no significant effects after 17 h. The effects of temperature and reaction time on the enzymatic removal of ink from waste paper have been highlighted previously (Chutani and Sharma 2015). The enzyme load and incubation temperature showed that with an increase in enzyme load, a simultaneous increase in the deinking was observed; however, the efficiency of the enzyme-assisted deinking began to reduce above 40°C. For every unit increase in temperature, multiplied the effect of enzyme load on the deinking process. As expected, the plots highlighting the interaction between enzyme load and time showed an almost linear relationship between the two factors. The observed response increased with increasing enzyme load and reaction time, even beyond the optimum values.

5.3.3.2 *Validation of the experimental model*

A validation experiment was carried out to establish the validity of the statistical experimental strategies. The experimental conditions were 40.17°C incubation temperature, 17.7 h incubation time and an enzyme load of 983.6 UmL^{-1}. The observed value of deinking, 106.72%, was found to be close to that estimated by the RSM model, 113.19%. This demonstrates that the RSM with a central composite design analysis is efficient in optimizing xylanase-assisted deinking of printed paper.

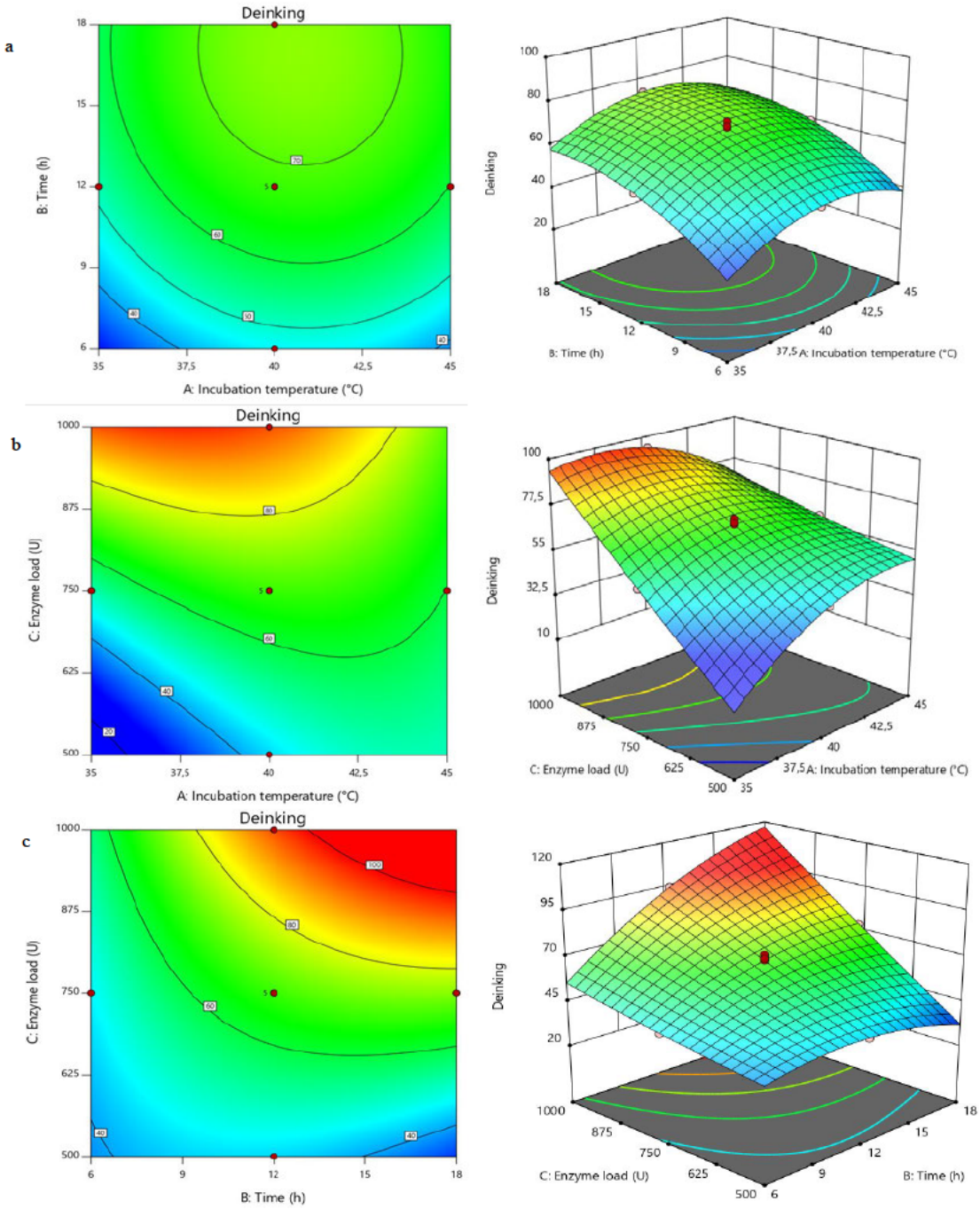

Figure 5.3: Response surface plots showing the interactions between the variables for wastepaper deinking: (a) contour & 3D plots of enzyme load - incubation temperature interaction; (b) contour & 3D plots of enzyme load - incubation time interaction; (c) contour & 3D plots of incubation time - incubation temperature interaction.

5.3.3.3 *Scanning Electron Microscopy*

The morphological modification of the xylanase- treated paper pulp and untreated control were observed under the scanning electron microscope. The images (Figure 5.4) confirmed that the xylanase from *B. bassiana* SAN01 significantly modified the structure of pulp fibres. Compared to the control sample, more rugged surfaces, cavities, cracks and disorganized external fibres were observed in the xylanase treated pulp highlighting the alteration of the pulp fibrils at a molecular level resulting from the enzymatic attack. The observed extensive damage and greater porosity signify that *B. bassiana* SAN01 xylanase can degrade the xylan matrix that holds the pulp cellulose microfibrils, thereby leading to surface ink detachment. Similar morphological changes at the ultrastructure level have been observed in enzyme-treated pulps (Przybysz Buzała *et al*., 2016; Sridevi *et al*., 2016).

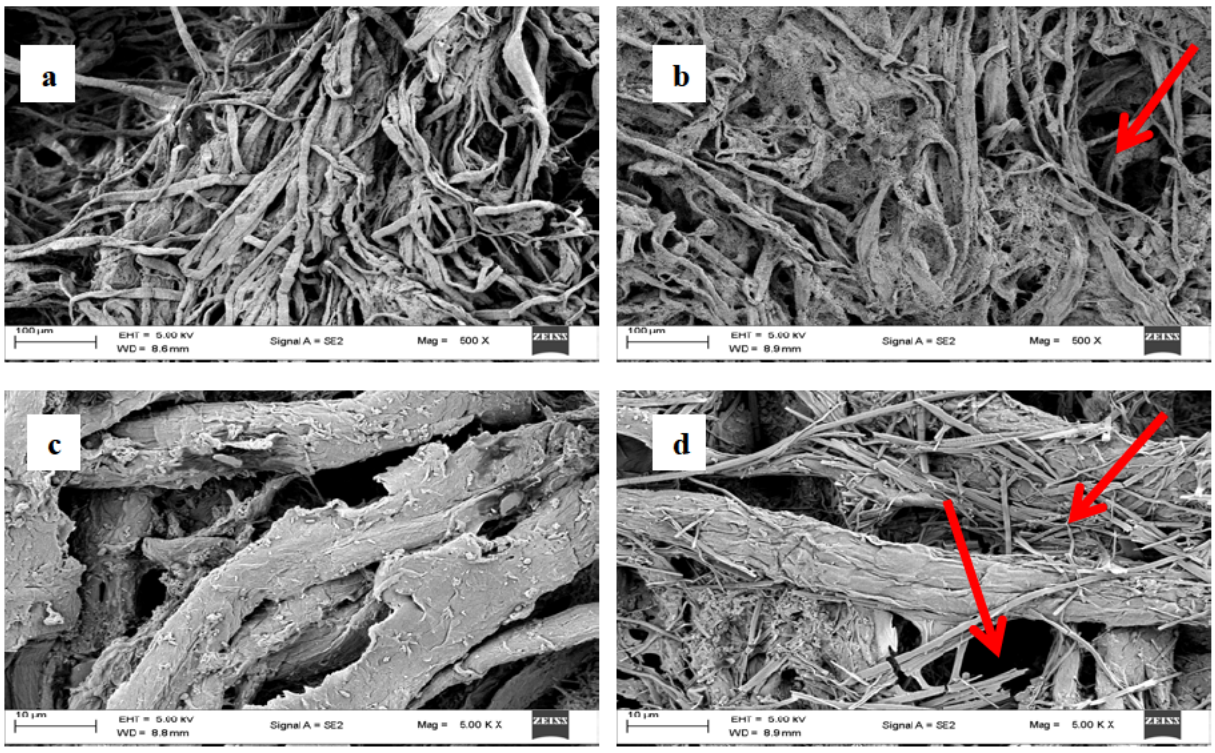

Figure 5.4: Scanning electron micrographs of (a) untreated pulp (500X), (b) xylanase treated (500X), (c) untreated pulp (5000X) and (d) xylanase treated pulp (5000X). Arrows indicate fibrillation and perforation on the fibre surface.

5.3.3.4 *FTIR analysis*

The alteration in the structure of xylanase deinked paper samples was characterized using FTIR and compared with the untreated controls (Figure 5.5). The distinct peak between 3600 and 3200 cm^{-1}, which was present in all the paper samples, is ascribed to the hydroxyl groups of cellulose as well as hemicellulose (at 1058, 1315, 898–895 cm^{-1}) and lignin content (at 1510–1508, 1605 and 1652 cm^{-1}). An earlier study has also shown higher peak intensity at the same wavenumbers in the control pulp in comparison to the treated pulp (Kumar *et al.,* 2018b). The peak at 1434 cm^{-1} is believed to be indicative of the CH_2OH group in ink and is observed to be less intense in the test samples. Furthermore, the peaks at 2851 and 2920 cm^{-1} represent the oil content of the ink and they were also of less intensity in the treated samples (Saini *et al.,* 2020). These spectra confirm the release of chromophores, hydrophobic compounds and phenolics from printed paper fibres, subsequent to the hydrolytic action of the xylanase. FTIR spectra obtained in this enzyme-assisted deinking are similar to other spectra observed in earlier studies (Desai and Iyer 2016; Kumar *et al.,* 2018b).

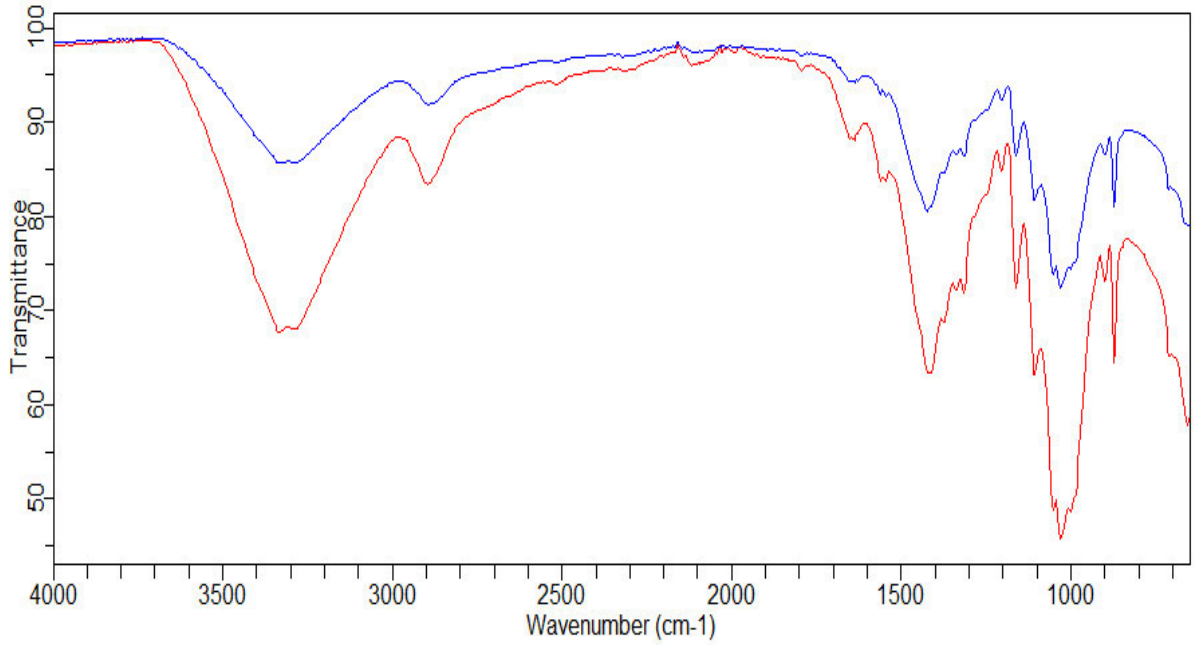

Figure 5.5: FT-IR spectrum showing the changes in the paper pulp during enzymatic treatment in the range of 4000-600 cm^{-1} — Enzyme treated pulp, — Control pulp.

5.4 Conclusion

This study has brought to the fore, for the first time, the applicability of different glycoside hydrolases from the widely known entomopathogen, *B. bassiana*. In this regard, the efficacy of amylase, endoglucanase, polygalacturonase and xylanase from the novel strain *B. bassiana* SAN01 were clearly demonstrated in the saccharification of plant biomass, fruit juice processing, as well as in wastepaper recycling. The saccharification of sugarcane bagasse with significant production of reducing sugars was achieved using *B. bassiana* SAN01 crude xylanase-endoglucanase cocktail. Furthermore, the effectiveness of the amylase-polygalacturonase cocktail in the clarification of pear juice has also demonstrated the potential of the fungus. The analysis of the physical characteristics as well as the biochemical properties of the enzyme-treated juice revealed that the *B. bassiana* SAN01 amylase-polygalacturonase had no detrimental effects on the quality of the pear juice. Finally, efficient deinking of wastepaper with an accompanying release of reducing sugars was also recorded using the purified xylanase from *B. bassiana* SAN01. Hence, in addition to the established safety of the fungus and its products, findings from this study further underscore the applicability of the fungus in many industrial processes. These findings are expected to stimulate the exploration of *B. bassiana* for industrial enzyme production and other bio-based products along with its use as a biocontrol agent.

CHAPTER SIX

In silico structural elucidation of *Beauveria bassiana* chitinases and xylanase

Part of this chapter has been published in *Process Biochemistry* (2021) 100:207-216. *Bhagwat, P., *Amobonye, A., Singh, S. and Pillai, S. A comparative analysis of GH18 chitinases and their isoforms from *Beauveria bassiana*: An *in-silico* approach.
*Bhagwat, P. and Amobonye, A contributed equally to this work as first authors.

Process Biochemistry 100 (2021) 207–216

Contents lists available at ScienceDirect

Process Biochemistry

journal homepage: www.elsevier.com/locate/procbio

A comparative analysis of GH18 chitinases and their isoforms from *Beauveria bassiana*: An *in-silico* approach

Prashant Bhagwat, Ayodeji Amobonye, Suren Singh, Santhosh Pillai *

Department of Biotechnology and Food Technology, Faculty of Applied Sciences, Durban University of Technology, P O Box 1334, Durban, 4000, South Africa

ARTICLE INFO

Keywords:
Beauveria bassiana
Chitinase family 18
Protein-ligand docking
Allosamidin
Chitotriose thiazoline
In-silico analysis

ABSTRACT

Fifteen different chitinases from various *Beauveria bassiana* strains were selected and their physicochemical characteristics, secondary structure evaluation and functional analyses were conducted using multiple bioinformatics tools. The molecular mass of chitinases varied from 34.25 to 49.27 kDa, and theoretical pI from 4.81 to 7.94 respectively. Most of the chitinases were hydrophilic, thermostable and negatively charged with good *in vivo* half-life. Nearly all the chitinases were extracellular with half of them having the standard secretory peptide, and chitinase family 18 active site motif. Phylogeny, multiple sequence alignment and indel analysis confirmed the presence of highly conserved active site residues in seven sequences. Furthermore, a three-dimensional model of chitinase (AIT18869.1) was constructed using the SWISS-MODEL server and validated by ERRAT, Verify 3D and RAMPAGE. The presence of 98.1 % of its residues in the Ramachandran plot's favoured region further established the quality of the model. CASTp and MetaPocket 2.0 analysis followed by protein-ligand docking using allosamidin and chitotriose thiazoline, suggested Asp-208, Gln-242, Gln-265 and Asn-268 as the most conserved active residues for the enzyme. The information gathered through the *in-silico* approach would be beneficial in unravelling the properties of *B. bassiana* chitinases *in vitro*, which could be subsequently exploited for various industrial applications.

1. Introduction

Chitin is the most abundant amino-polysaccharide in nature and trails only behind cellulose. It is a linear polysaccharide made up of (1-4) -linked 2-acetamido-2-deoxy-β-D-glucopyranose monomers which are structurally similar to cellulose; with the only difference being the acetamide group (-$NHCOCH_3$) at the C-2 position. Chitin is ubiquitous and is the primary building block that gives support to the exoskeletons of crustaceans, insects, as well as fungal cell walls [1]. The chitins have tremendous applications in medicine, for tissue engineering and wound care dressing, and in agriculture, to control arthropod pests and fungal pathogens [2].

Chitinases (EC 3.2.1.14) are hydrolytic enzymes responsible for the degradation of chitin into its monomeric and oligomeric units by the cleavage of β-1,4-O-glycosidic bonds [3]. Chitinases have immense potential in a wide range of industrial applications, most specifically in agriculture, food and medical industries, as chitinase-based processes are eco-friendly, economic as well as non-hazardous. Restorative applications of chitinases include their use in the manufacture of single-cell proteins, in the biocontrol of fungal plant pathogens [4], production of functional foods and medicines, *etc.* [2]. Chitinolytic enzymes are classified based on their amino acid sequences into two families, family 18 and 19. These two families have dissimilar amino acid sequences and hence, display different tertiary structures. Family 18 chitinases are made up of a catalytic $(\alpha/\beta)_8$ barrel domain, while the family 19 chitinases possess a bi-lobed structure which is dominated by α-helices. Both families also differ in their mechanism of catalysis; family 18 chitinases have a retaining mechanism, which results in chitooligosaccharides being in the β-anomeric configuration, whereas family 19 chitinases have an inverting mechanism and consequently produces α-anomers [5].

Beauveria bassiana is widely acclaimed for its use as a biopesticide against insect pests [6]. Interestingly, chitinases from B. bassiana and other entomopathogenic fungi have been identified as important virulence factors in their pathogenicity towards arthropods and nematodes [7]. These chitinases act synergistically with other enzymes such as proteases and lipases to degrade the cuticle of insects and other animals. The well-elucidated involvement of B. bassiana chitinases in its

* Corresponding author.
E-mail address: santhoshk@dut.ac.za (S. Pillai).

https://doi.org/10.1016/j.procbio.2020.10.012
Received 20 June 2020; Received in revised form 10 October 2020; Accepted 19 October 2020
Available online 21 October 2020

.

Abstract

Fifteen different chitinases from various *Beauveria bassiana* strains as well as one xylanase were selected to gain an insight into the structural characteristics of *B. bassiana* carbohydrases. Their physicochemical characteristics, secondary structure evaluation and functional analyses were conducted using multiple bioinformatics tools. The molecular mass of chitinases varied from 34.25 to 49.27 kDa, while the xylanase was predicted to be 37 kDa. Most of the enzymes were hydrophilic, thermostable and negatively charged with high *in vivo* half-life. Nearly all the chitinases were extracellular with half of them having the standard secretory peptide; the same was observed for the evaluated xylanase. Furthermore, three-dimensional models of a selected chitinase and the xylanase were constructed using the SWISS-MODEL server and validated by ERRAT, Verify 3D and MolProbity. The presence of approximately 90% of the amino acid residues in the Ramachandran plot's favoured region further established the quality of both models. The binding site predictions followed by protein-ligand docking suggested Asp-208, Gln-242, Gln-265 and Asn-268 as the most probable active site residues for the chitinase and Thr-85, Ser-86 and Asn-220 for the xylanase. The information gathered through the *in silico* approach would be beneficial in unravelling the *in vitro* properties of *B. bassiana* carbohydrases in general and chitinases and xylanases in particular, which could be subsequently exploited for various industrial applications.

6.1 Introduction

Studies have shown the importance of the structure-function relationship of different biological molecules, especially enzymes and structural proteins. Hence, the elucidation of the structure of enzymes at the primary, secondary, tertiary and quaternary level is a worthwhile endeavour with immense benefits. The information from structural elucidation has served as the framework for modifying enzymes from different organisms, primarily through directed evolution and genetic manipulation. However, the structural characteristics of several important microbial enzymes are yet to be elucidated. *B. bassiana*, which is considered as both an entomopathogen and an endophyte, is widely acclaimed for its use as a biopesticide against insect pests (Das *et al.,* 2021; Singh and Tiwari 2021). Interestingly, chitinases from *B. bassiana* and other entomopathogenic fungi have been identified as important virulence factors in their pathogenicity towards many arthropods as well as nematodes (Berini *et al.,* 2018). The well-elucidated involvement of *B. bassiana* chitinases in its pathogenesis has raised the possibility of their applications in agriculture.

Hence, various investigations have been dedicated to the production, cloning, expression, characterization and the mechanisms of action of chitinases from different *B. bassiana* strains while none has been carried out on the structural and functional properties of the chitinases. Furthermore, recent focus has been placed on *B. bassiana* strains as valuable sources of industrial biocatalysts. In this regard, many studies have since highlighted the production, biochemical characterization and molecular manipulation of biomass-degrading enzymes from these fungi. Xylanase, in particular, has been sourced from different strains of *B. bassiana*. However, like the chitinase, there are no reports on the structure of xylanase from the fungus.

As the biological function and the applicability of proteins are dependent on their native three-dimensional structure, the challenge of protein structure prediction is a fundamental problem across different disciplines and industries. Nuclear Magnetic Resonance (NMR) spectroscopy and X-ray crystallography have long been the ideal techniques for determining protein structures due to their exceptional accuracy. However, their high cost and requirement of technical expertise limit their use (Sarkar *et al.,* 2020). Furthermore, the unavoidable technical limitation where proteins uphold their native state after crystallization warrants the necessity for an *in silico* prediction of protein structures (Gupta, Akhtar and Bajpai 2014). Besides complementing the wet lab set up,

computational techniques for structural elucidation have achieved significant prediction accuracy, increasing their uses in drug design, protein engineering, site-directed mutagenesis and virtual screening, amongst other applications. At the molecular level, it has made it possible to establish the sequence to structure relationships, unveil the novel pathway of protein folding, and determine the active and catalytic sites of different proteins (Walker, Yallapragada and Tangney 2020). Thus, in the present study, an array of readily available computational tools was employed to gain insights into the overall physical parameters; primary, secondary and tertiary structures, functional analysis, domains and motifs, and protein model of *B. bassiana* chitinases and xylanase. In addition to setting a foundation for the experimental determination of the enzyme structures, this computational study would help gain insights into their biological functions and serve as a reference for future protein manipulation to improve their industrial applications.

6.2 Methodology

6.2.1 Retrieval of sequence

The amino acid sequences of 15 chitinases from different *B. bassiana* strains were retrieved from the UniProt Protein Database (https://www.uniprot.org) in FASTA format for computational analysis. The amino acid sequence of xylanase from *B. bassiana* D1-5 was also chosen from the UniProt database. The choice of a single xylanase sequence in this study is based on the proximity of its predicted molecular weight with the actual molecular weight of *B. bassiana* SAN01 xylanase, which was determined previously (Chapter 4, Section 4.3.1.1). Hence, the focus was placed on this particular xylanase. The accession numbers of these enzymes are listed in Appendix 12.

6.2.2 Physicochemical characterization of enzymes

The physicochemical parameters of the selected enzymes, such as the total amino acid composition (with negatively and positively charged residues), instability index, aliphatic index, and grand average of hydropathicity (GRAVY), were computed using the ExPasy-ProtParam tool (http://web.expasy.org/protparam/) (Dutta *et al.,* 2021).

6.2.3 Secondary structure analysis

Secondary structure prediction was performed using the SOPMA server which evaluated the number of helices, sheets, turns and coils present in the protein sequence (http://npsa-pbil.ibcp.fr/) (Geourjon and Deleage 1995). To predict all the possible motifs present in *B. bassiana* chitinases and xylanase, SIB MyHits Motif scan was used (myhits.isb-sib.ch). Furthermore, Pfam (http://pfam.xfam.org/) was used to identify the domains and motifs in the sequences (Mistry *et al.,* 2021).

6.2.4 Functional analysis

Transmembrane helices; Hidden Markov Model (TMHMM) tool by Krogh *et al.,* (2001) was applied to understand the membrane protein topology (www.cbs.dtu.dk/services/TMHMM), and SignalP5.0 using cut-off default (http://www.cbs.dtu.dk/services/SignalP/index.php) for the prediction of secreted proteins (Armenteros *et al.,* 2019). Subcellular localization was predicted using CELLO v.2.5 server (http://cello.life.nctu.edu.tw/) (Yu *et al.,* 2006).

6.2.5 Tertiary structure analysis

The tertiary structures of a selected chitinase and the xylanase were predicted using ExPASy SWISS-MODEL (ProMod3 version 1.0.2) workspace (Pramanik *et al.,* 2018) using the amino acid sequence of the chitinase and xylanase, retrieved from NCBI (Accession no: AIT18869.1 and KGQ08014.1, respectively). The 3D crystal structures of *Saccharomyces cerevisiae* endochitinase (PDB ID: 2UY4) and *Caldicellulosiruptor lactoaceticus* ester-xyloside bifunctional hydrolase (PDB ID: 6A60) retrieved from the Protein Data Bank served as the template for chitinase and xylanase, respectively. The quality of the predicted 3D models was evaluated by the SAVES server using ERRAT and Verify 3D tools (https://servicesn.mbi.ucla.edu/SAVES/) while the Ramachandran plot constructed using the MolProbity server was used to evaluate the energetically allowed regions (Williams *et al.,* 2018).

6.2.6 Docking analysis

Automated docking simulation of the enzymes and their respective ligands were performed using the AutoDock Vina program. For chitinase, the structure of the ligand, allosamidin, a pseudotrisaccharide, was extracted from the crystal structure of *Serratia marcescens* chitinase in complex with allosamidin (PDB ID: 1X6N) using the BIOVIA Discovery Studio software. While the structure of xylotriose, which served as xylanase ligand, was retrieved from PubChem (CID 10201852). The ligands and the previously modelled enzyme structures were pre-processed for hydrogen addition, protein optimization and energy minimization using the Dock Prep tool of UCSF Chimera software. Subsequently, AutoDockTools was used to convert the PDB files of the proteins and their ligands to PDBQT format for further analysis. The online servers, CASTp and MetaPocket 2.0, and NCBI's conserved domain search tool were used to identify the binding pocket associated with the possible active site (Bhattacharjee *et al.,* 2017). For chitinase, a grid box with a size of 40 × 40 × 40 points was used in the configuration file of Autodock Vina while the box was centred at the coordinates; X: 43.03, Y: 21.464, Z: 31.161. For xylanase, a grid box with a size of 60 × 36 × 56 points was used in the configuration file of Autodock Vina while the box was centred at the coordinates; X: 16.104, Y: 12.8, Z: 31.161. The receptor atom positions were fixed, and the torsion angle of the ligand glycosidic bonds was rotated until the rigid docking in program AutoDock Vina allowed the favourable docking. Other docking parameters were set to default. The best model was chosen, and the interactions were visualized

using the BIOVIA Discovery Studio software. The interacting proteins of *B. bassiana* chitinase were predicted by the STRING server (http://string-db.org).

6.3 Results and discussion

6.3.1 *In silico* structural elucidation of *B. bassiana* chitinase

6.3.1.1 *Physicochemical properties of B. bassiana chitinase*

The predicted physicochemical properties as computed by the ProtParam tool showed that the chitinases under investigation had a varied number of amino acids (305 - 449) and molecular weights (34.25 kDa - 49.27 kDa) (Table 6.1). The molecular weight of the enzyme is a critical characteristic for the selection of an appropriate purification protocol. The molecular weight range observed in this study suggests the use of gel exclusion chromatography with Sephadex G-75 SF having a fractionation range of 3-70 kDa, best suited for the purification of chitinases under investigation. Analyses of the sequences showed that the number of negatively charged amino acid residues (aspartate and glutamate) was higher than the number of positive residues (arginine and lysine) in all the strains, except in *B. bassiana* ARSEF 2860 (AIT18872.1) and *B. bassiana* D1-5 (KGQ11645.1) (Table 6.1). Recent findings have suggested the effects of nascent peptide charge on protein translation efficiency and protein expression (Requião *et al.,* 2017). Hence it can be predicted that most of the chitinases in this study, being more acidic, will be polysome-translated proteins.

GRAVY values for all the chitinase were predicted to be negative (Table 6.1). This variable is used to predict the hydrophobicity or hydrophilicity of a protein over the entire amino acid sequence. It was observed that the relationship between the GRAVY score and the hydrophilicity of proteins is inverse, hence, a higher GRAVY score signifies lower hydrophilicity and vice versa (Kyte and Doolittle 1982). Thus, from the values obtained, it could be inferred that all the enzymes are hydrophilic to a large extent, which is in line with their globular structures as enzymes (Magdeldin *et al.,* 2012). The aliphatic index of the chitinases in this study ranged between 59.30 to 88.46. An increase in the aliphatic index is commensurable to the thermostability of globular proteins (Artz *et al.,* 2015). The aliphatic index of 40% chitinases was above 80, while another 40% chitinases were between 61-80 and the rest 20% was around 60. Due to the wide variation in the aliphatic index of chitinases from the same source, *B. bassiana*, it is predicted that the enzymes had varying temperature optima and thermostability.

Table 6.1: Physiochemical parameters of selected *B. bassiana* chitinases using ExPASy's ProtParam tool

	Source organisms	Accession number	Number of amino acids	Molecular weight (kDa)	Theoretical pI	Total number of negatively charged residues	Total number of positively charged	Instability index	Aliphatic index	GRAVY
1	*B. bassiana* ARSEF 2860	AIT18869.1	427	45.06	5.04	34	28	37.92	64.52	-0.174
2	*B. bassiana* ARSEF 2860	AIT18872.1	400	42.37	7.94	29	31	37.70	61.30	-0.250
3	*B. bassiana* ARSEF 2860	AIT18873.1	324	36.22	4.82	48	30	31.56	88.46	-0.207
4	*B. bassiana* ARSEF 2860	AIT18879.1	402	44.19	5.11	45	32	35.28	69.18	-0.322
5	*B. bassiana* ARSEF 2860	AIT18882.1	348	36.79	5.94	26	23	30.14	84.17	-0.027
6	*B. bassiana* ARSEF 2860	AIT18883.1	412	43.98	6.14	24	23	42.98	59.30	-0.322
7	*B. bassiana* ARSEF 2860	AIT18885.1	326	34.65	4.99	36	30	26.56	77.98	-0.173
8	*B. bassiana* ARSEF 2860	EJP63137.1	305	34.25	4.81	47	29	29.77	86.59	-0.299
9	*B. bassiana* ARSEF 2860	EJP64367.1	449	49.27	5.35	64	56	27.32	60.73	-0.594
10	*B. bassiana* D1-5	KGQ07286.1	443	48.48	5.04	64	51	27.44	63.54	-0.516
11	*B. bassiana* D1-5	KGQ10005.1	411	43.83	5.74	24	22	44.22	59.44	-0.345
12	*B. bassiana* D1-5	KGQ11645.1	350	37.88	7.67	30	31	52.95	87.03	-0.107
13	*B. bassiana* JEF-007	PMB63785.1	431	46.99	4.97	62	48	28.23	63.97	-0.485
14	*B. bassiana* JEF-007	PMB65373.1	330	34.91	5.94	26	23	28.12	80.76	-0.099
15	*B. bassiana* JEF-007	PMB65707.1	365	40.95	4.96	56	35	31.76	82.52	-0.338

The amino acid composition of chosen chitinases from *B. bassiana* strains was evaluated and profiled as depicted in Figure 6.1. The results substantiated that alanine and glycine were the most widely distributed amino acids in the selected chitinases. These protein sequences were also rich in amino acids such as leucine, serine, threonine, aspartic acid, valine, proline and isoleucine. Secondary structures of proteins are governed by the inclination of amino acids to form either helix or sheet form. Alanine, leucine, aspartic acid and proline have a high propensity to form helix confirmation, while valine, isoleucine, threonine, glycine, and serine favours the formation of sheet confirmation (Idicula-Thomas and Balaji 2005).

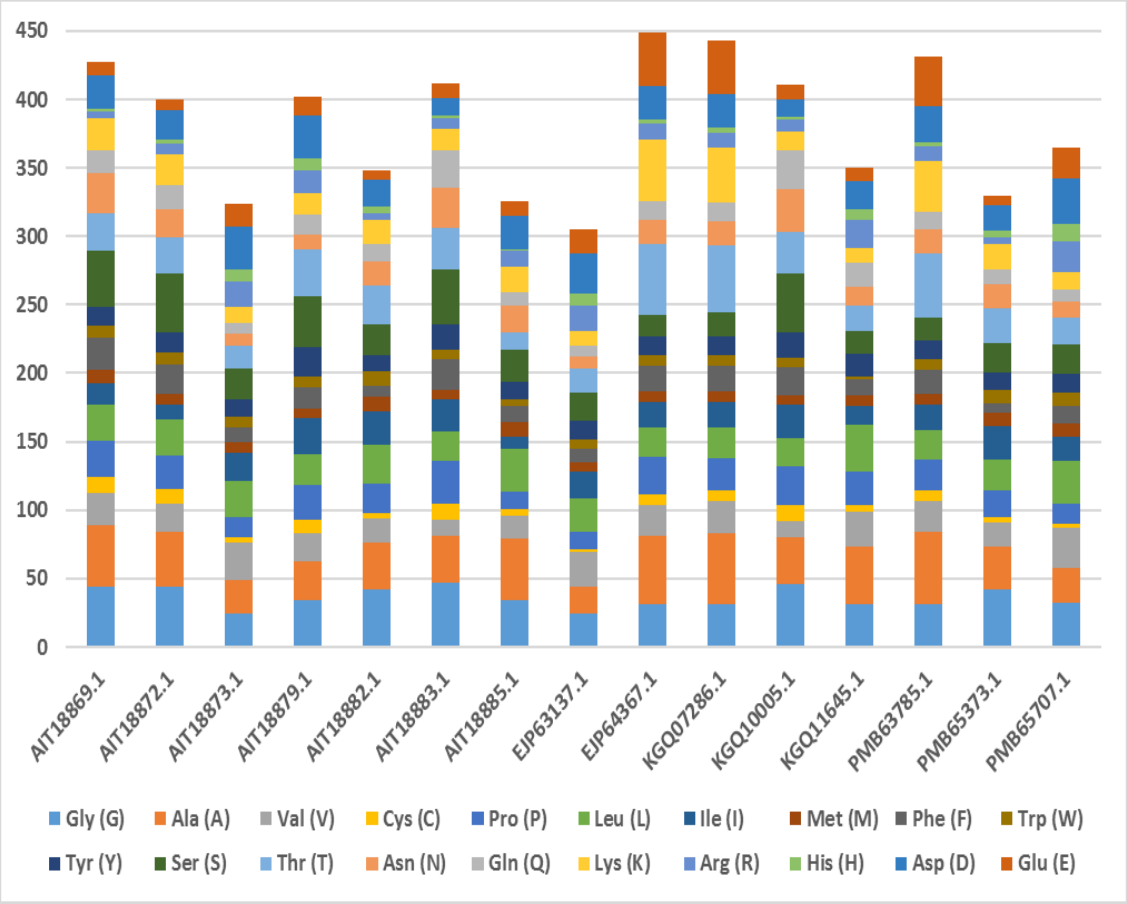

Figure 6.1: Amino acid composition of selected chitinases from *B. bassiana*

6.3.1.2 *Secondary structure analysis of B. bassiana chitinase*

A random coil region dominates the secondary structures of all the analysed chitinases as this conformation has the highest mean value of approximately 46.8% (Figure 6.2). This was followed by the alpha helix region (30.4%), beta-sheet region (15.9%) and beta-turn (6.9%). The dominance of random coils and alpha-helix regions among the

secondary structures indicates the stability of the enzymes and a significant amount of conservation within chitinases from different *B. bassiana* strains (Neelamathi *et al.,* 2009; Gouripur, Kaliwal and Kaliwal 2016).

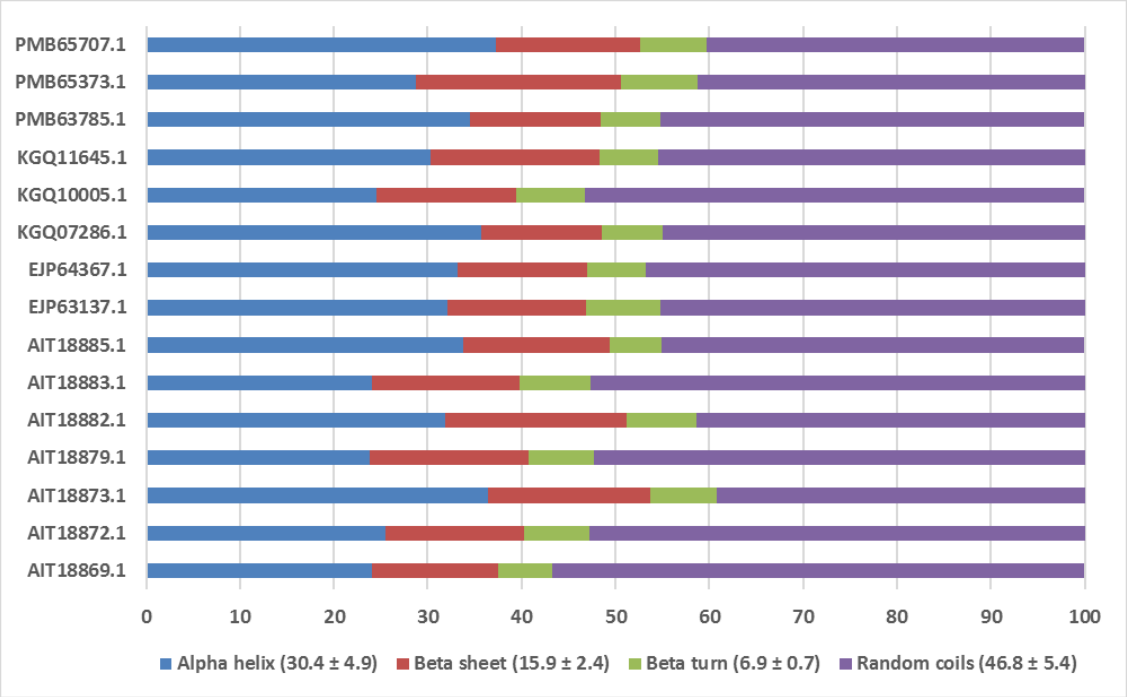

Figure 6.2: Percentage of secondary structure elements in *B. bassiana* chitinases.

The protein signature pattern provides useful biological information associated with the protein family, domain, or functional site (Mishra *et al.,* 2015). The analysis of *B. bassiana* chitinases using the MyHits interactive tool showed the presence of signature pattern sequences belonging to different motifs (Table 6.2) (Finn *et al.,* 2016). The myristoylation sites were the most dominant in all the chitinases under investigation. Myristoylation is a lipid anchor modification found in eukaryotic proteins, which targets proteins to membrane locations. The presence of a significant number of myristoylation sites helps export synthesized chitinases to the extracellular environment as this modification has been shown to be essential in apoptosis, signal transduction, extracellular protein export, etc. (Varland, Osberg and Arnesen 2015). However, some other less occurring motifs, such as the amidation sites, alanine-rich domain, thioredoxin II and the potato type II protease inhibitor were also observed in the chitinases under study. Some of these fewer occurring motifs have been implicated in different cellular

processes, including signal transfer, receptor recognition, and protein maturation (Marino, Eckhard and Overall 2015; Randhawa *et al.,* 2018). Notably, the presence of the potato type II protease inhibitor motif in the chitinases may indicate their propensity to resist proteolytic degradation, which has been observed in some other glycoside hydrolases (Hagspiel, Haab and Kubicek 1989).

Protein phosphorylation is a vital cellular regulatory mechanism as many enzymes and other proteins are either activated or deactivated by phosphorylation and dephosphorylation events, respectively. Phosphorylation plays a significant role in the protein cycle and functions, which is crucial in determining the half-life, subcellular location, and interaction of proteins with other cellular molecules (Ardito *et al.,* 2017). The occurrence of many phosphorylation sites, including cAMP- and cGMP-dependent protein kinase phosphorylation site, casein kinase II phosphorylation site, protein kinase C phosphorylation site and tyrosine kinase phosphorylation site, in *B. bassiana* chitinases indicate that they are tightly controlled enzymes. Similarly, glycosylation is a post-translational modification found in approximately half of all the proteins, particularly in secreted and transmembrane proteins of eukaryotes and some prokaryotes (Taylor and Drickamer 2011).

The Asparagine-N glycosylation site was frequently observed in most of the *B. bassiana* chitinases under study. This site has been found to have a consensus AsnXxxSer/Thr/Cys sequence, where Xxx can be any amino acid besides proline and it is essential in proper folding, oligomerization, solubility and protein stability, as have been shown in some other enzymes (Yang *et al.,* 2015; Goettig 2016; Podzimek *et al.,* 2018). Being a carbohydrate-active enzyme, it is expected that the motifs for the carbohydrate-binding module of glycosyl hydrolases were also found to be present in all the *B. bassiana* chitinases. These modules of different classes with various substrate specificity have been noted to promote catalysis by bringing the substrates into intimate and prolonged association with the carbohydrate degrading enzymes (Shoseyov, Shani and Levy 2006; Zeng *et al.,* 2019). Specifically, the presence of chitinase family 18 active sites was found in 46.66% of the enzymes in this study. The GH18 family chitinase is built of a multidomain architecture, which includes various combinations of the signal peptide, catalytic domains, chitin-binding domains and serine/threonine (S/T)-rich linkers (Huang *et al.,* 2011).

A protein domain is a conserved, tertiary structural unit of a protein with the ability to evolve, function, fold and exist independently of the rest of the protein chain. Thus, most proteins are built of one or several domains that serve as the key mediators for their functions. The analysis of the domains of *B. bassiana* chitinases under evaluation predicted the presence of glycosyl hydrolases 18 domains (Accession no:PF00704.28) in all the fifteen chitinases. This domain is known to include the chitinase class II group which encompasses chitinase, chitodextrinase, the killer toxin of *Kluyveromyces lactis* and various mammalian glycoproteins such as cartilage glycoprotein and the oviduct-specific glycoproteins (Sharma *et al.,* 2016). Besides, some of the chitinases are multidomain proteins as they were predicted to possess the fungal cellulose-binding domain (Accession no: PF 00734.18). These multidomain chitinases include *B. bassiana* ARSEF 2860 (AIT18872.1, AIT18883.1, AIT18869.1) and *B. bassiana* D1-5 (KGQ10005.1). The predicted cellulose-binding domain in the listed chitinases might indicate the ability of these enzymes to also catalyze cellulose as have been shown experimentally in some organisms (Chen *et al.,* 2019a). Furthermore, this could also be due to the fact that cellulose and chitin have closely related polymeric structures and cellulose has been shown to bind directly to chitinases (Li and Wilson 2008)

Table 6.2: Illustration of different motifs of *B. bassiana* chitinases

Accession number	Asn N-glycosylation site	N-myristoylation site	cAMP- and cGMP-dependent protein kinase phosphorylation site	Casein kinase II phosphorylation site	Carbohydrate/ Fungal cellulose-binding domain	Chitinase family 18 active site	Glycosyl hydrolase family 18 active site	Protein kinase C phosphorylation site	Tyrosine kinase phosphorylation	Others
AIT18869.1	4	10	0	5	3	1	2	3	0	3
AIT18872.1	3	10	0	5	3	1	2	3	0	2
AIT18873.1	0	2	0	5	0	0	2	3	2	0
AIT18879.1	1	6	0	9	0	0	2	4	0	3
AIT18882.1	1	11	0	2	0	1	3	1	0	0
AIT18883.1	3	10	1	2	3	1	2	2	0	4
AIT18885.1	3	6	0	4	0	1	2	3	0	1
EJP63137.1	0	2	0	5	0	0	2	2	2	0
EJP64367.1	4	6	1	3	0	0	2	7	3	2
KGQ07286.1	4	6	0	3	0	0	2	4	3	2
KGQ10005.1	3	10	1	2	3	1	1	2	0	5
KGQ11645.1	0	8	2	2	0	0	2	2	0	3
PMB63785.1	3	6	0	3	0	0	2	4	3	2
PMB65373.1	1	11	0	2	0	1	3	1	0	0
PMB65707.1	3	0	0	6	0	0	3	2	2	1

6.3.1.3 *Functional analysis of B. bassiana chitinase*

The compartmentation and localization of different proteins including enzymes have been well linked to their general biological functions and the reactions they catalyze specifically (Kim *et al.,* 2017; Shikano *et al.,* 2018). Furthermore, it is believed that information on the subcellular localization may provide useful insights into the specific enzymatic pathways of proteins and serve as a guide in subsequent wet-lab experiments. A large proportion of the chitinases evaluated in this study were predicted to be extracellular by the subcellular localization predictor, Cello v.2.5. The server utilizes amino acid compositions in discriminating protein sub-cellular localization sites. In agreement with this prediction, chitinases from different strains of *B. bassiana* have been found to be extracellularly secreted as they were detected in culture filtrates (Senthilraja *et al.,* 2018), although a few *B. bassiana* chitinases were predicted to be located in the cytoplasm. However, cytoplasmic chitinases have only been observed in bacteria that possess transporters to traffic the chitin polymers into their intracellular space for degradation (Beier and Bertilsson 2013). It could be possible that the *B. bassiana* strains may possess chitinase that function both in the cells and outside, as a form of enzyme multiplicity which has been noted to be a common feature in the degradation processes of polymers caused by the structural complexity of the substrate. As a result of the high proportion of α-helix structures in *B. bassiana* chitinases, the likelihood that these enzymes are integral membrane proteins was investigated using the TMHMM algorithm.

TMHMM 2.0 is a tool that estimates the probability of a protein portion embedded in the cellular membrane. It also predicts the path that the amino acid chain may follow if the protein is membrane-associated (Yan *et al.,* 2017). The algorithm predicted that a large proportion of the chitinase protein chains were not membrane-associated. It was noticed that approximately the first 30 amino acids of only three of the chitinase sequences had a probability of being transmembrane peptides. The remaining residues which constitute a very large majority, were predicted to have zero or close to zero probabilities of being located in the membrane region. The graphical representation of the two chitinases, one with some probability of being transmembrane and the other with zero probability, is presented in Figures 6.3 a & b. Fungi, in general, are known to mainly depend on their extracellular enzymes for nutrient acquisition from their environment, and even for the immune response (Naranjo-Ortiz and Gabaldón 2019) hence, as suggested by the TMHMM analysis, it is less likely that *B. bassiana* chitinase exists as peripheral

membrane proteins. Besides, the earlier GRAVY score prediction has indicated that the enzymes have a lower probability of being membrane proteins due to their low hydrophobicity.

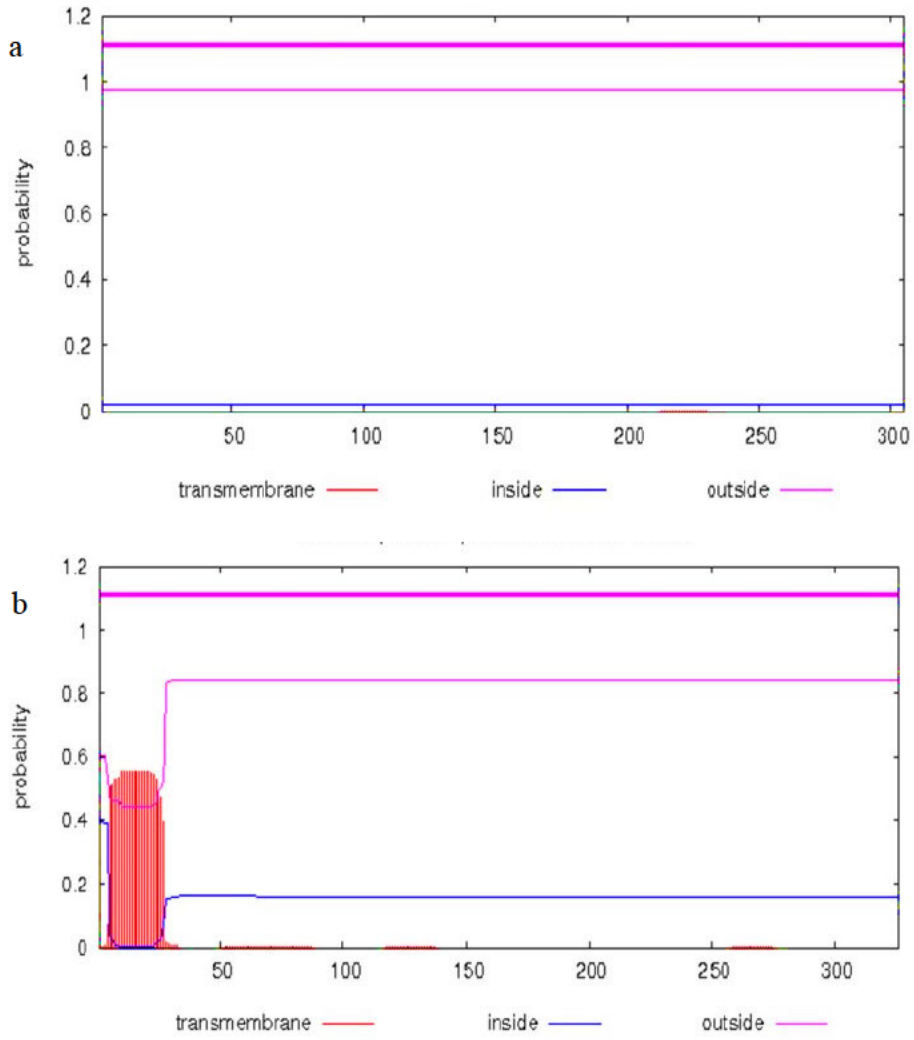

Figure 6.3: Transmembrane helices prediction by TMHMM server ver. 2.0. (a) *B. bassiana* ARSEF 2860 (EJP63137.1) (b) *B. bassiana* ARSEF 2860 (AIT18885.1) chitinases.

Signal peptides or sequences comprising 16–30 amino acid residues are usually found at the N-terminus of proteins. They are involved in the transportation of proteins across different compartments within the cell and outside the cell. In the course of protein transport, these peptides are removed from the mature specific peptidase. The presence of signal peptides in *B. bassiana* chitinases were predicted using the SignalP 5.0-HMM, an online tool based on a hidden Markov model, which relies on protein annotations from publicly available databases such as the SWISS-PROT database (Armenteros *et al.,*

2019). This analysis predicted that the signal peptides of 9 out of the 15 chitinase sequences were found to be of the standard secretory peptide, Sec/SPI, while the others had no N- terminal signal peptide. Besides, the peptidase cleavage site of these enzymes was predicted to be within the 18th and 23rd positions of their sequence with a majority being between the 18-19th position. The Signal P charts for *B. bassiana* D1-5 chitinase (Accession no: KGQ11645.1) with no predicted signal peptide and *B. bassiana* ARSEF 2860 chitinase (Accession no AIT18883.1) with a signal are shown in Figure 6.4 a &b.

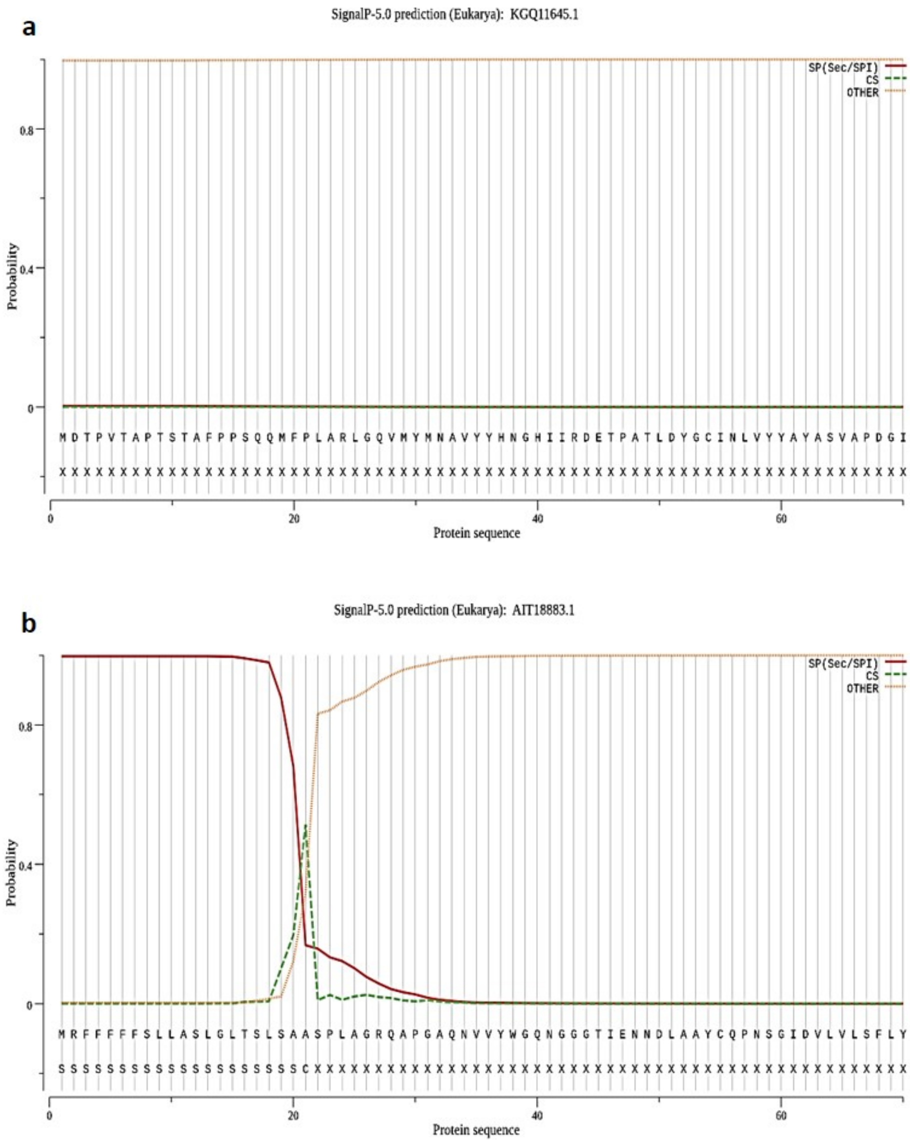

Figure 6.4: SignalP plot for (a) *B. bassiana* D1-5 (Accession no: KGQ11645.1) (b) *B. bassiana* ARSEF 2860 (Accession no: AIT18883.1) chitinases.

6.3.1.4 *Tertiary structure analysis of B. bassiana chitinase*

The tertiary structure of proteins is critical in distinguishing the function of proteins, their interactions with other compounds such as ligands, other proteins, and nucleotides and understanding the phenotypical effects of mutations. The Swiss-Model server was used to predict the three-dimensional structure of *B. bassiana* chitinases based on the known crystal structures of homologous proteins. For the 3D structure prediction, *B. bassiana* ARSEF 2860 (Accession no: AIT18869.1) chitinase was selected as it is the only one with acceptable sequence homology of 40% with any known protein with 3D structure. The 3D structure of *Saccharomyces cerevisiae* Chitinase 1 complexed with acetazolamide (PDB ID: 2UY4) was used as the template for 3D structure prediction of *B. bassiana* chitinase, with 45.36% sequence identity. The predicted chitinase model was viewed and analysed using the PyMOL molecular visualization tool (Figure 6.5).

The analysis revealed that the model (*B. bassiana* chit) is based on the (β/α)8 TIM barrel architecture conserved in the GH18 family. This architecture is formed by the repetition of the basic βαβ building block with the β-strands being followed by α-helices eight times alternating in sequence. αβ and βα loops connecting α-helices to the β-strands and vice versa, contribute significantly to the function as well as the stability of the protein. The predicted model was further evaluated using the SAVES server. The overall quality factor score predicted by ERRAT was 78.29 while Verify 3D showed that 93.71% of the residues had averaged a 3D-1D score of ≥ 0.2 indicating the reliability of model prediction. Furthermore, the stereo-chemical quality of the predicted model was evaluated using the Ramachandran plot which showed a chitinase model with ~ 90% of residues in the most favoured regions and ~ 9% residues in the additional allowed region (Figure 6.6). The total distribution of these residues in the favoured region is evaluated as 98.1% which reflects acceptable model adequacy. A very low percentage of the residues were found in the outlier region (2.5%).

Figure 6.5: 3D structure of *B. bassiana* ARSEF 2860 chitinase showing the (β/α)8 TIM barrel architecture

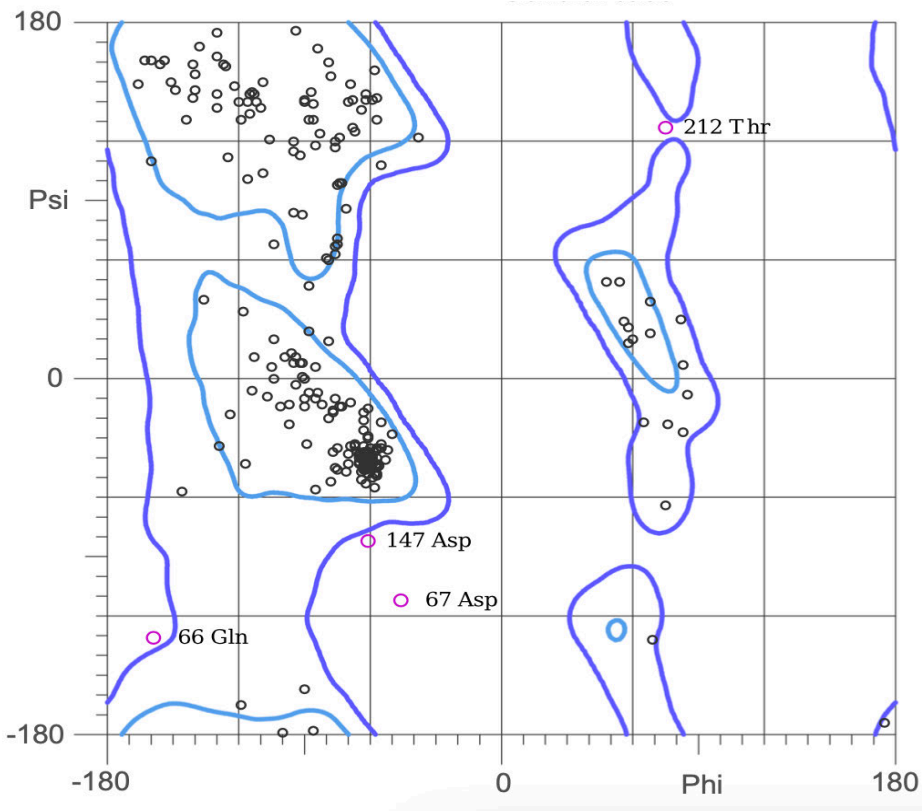

Figure 6.6: Ramachandran plot for *B. bassiana* ARSEF 2860 chitinase showing the number of residues in favoured, allowed and outlier region

6.3.1.5 *Docking analysis of B. bassiana chitinase*

Based on the outputs obtained from the CASTp, MetaPocket 2.0 servers and NCBI's conserved domain search tool, the active pocket of the *B. bassiana* chitinase may contain Tyr-53, Phe-105, Asp-208, Phe-209, Gln-242, Gln-265, Tyr-267, and Trp-344. Previous studies have shown that charged (Arg, His, Asp, Glu) and aromatic residues (Tyr, Trp, Phe) occur more frequently within chitinolytic active sites than elsewhere in the enzyme structure, indicating significant roles related to enzyme function. In contrast, with increasing diversity, some chitinases were shown to have Asn, Gln, Ser, and Thr in their active sites (Liu *et al.,* 2015). Allosamidin is a potent family 18 chitinase inhibitor that is active against insects, fungi, and even protista chitinase (Rao *et al.,* 2003). The structural interactions of allosamidin with several family 18 chitinases have been determined by X-ray crystallography (Bortone *et al.,* 2002; Eide and Sørlie 2018).

The molecular docking of *B. bassiana* chitinase with allosamidin was carried out to elucidate the interacting amino acids from the binding site (Figure 6.7). The docked complexes of *B. bassiana* chitinase with allosamidin showed an affinity score between -7.2 and -6.6, recorded for the nine models generated from the docking analysis. The best-suited ligand with a score of -7.2 was chosen for further analysis which revealed that the ligand interacted with the active site forming 7 hydrogen bonds between its electronegative oxygen atoms and Asp-69, Gln-72, Asp-208, Gln-242, Gln-265 and Asn-268 (Figure 6.8). These results confirm the presence of highly conserved motif DXXDXDXE of the family of GH18 chitinase, where each of the active sites, aspartic acid and glutamic acid, were observed in their amide forms i.e., asparagine and glutamine, respectively. Asparagine and glutamine residues in chitinase active sites were previously shown in a thermostable chitinase from *Thermomyces lanuginosus* (Khan *et al.,* 2015). Asparagine and glutamine residues are well known for their high propensity to hydrogen bonds as their amide group can accept two and donate two hydrogen bonds. In contrast, aspartic acid can accept hydrogen bonds using its carboxyl group (Scheiner, Kar and Pattanayak 2002).

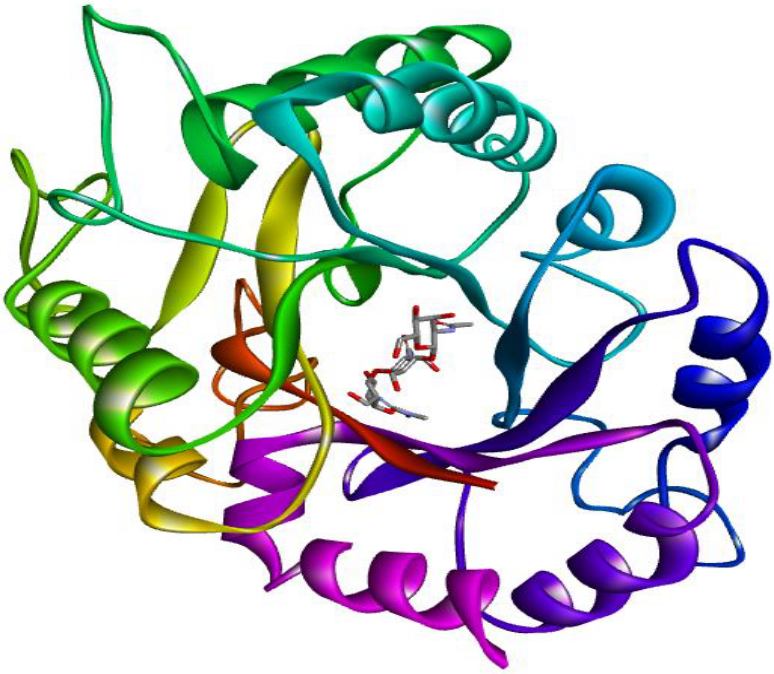

Figure 6.7: *B. bassiana* ARSEF 2860 chitinase-allosamidin complex

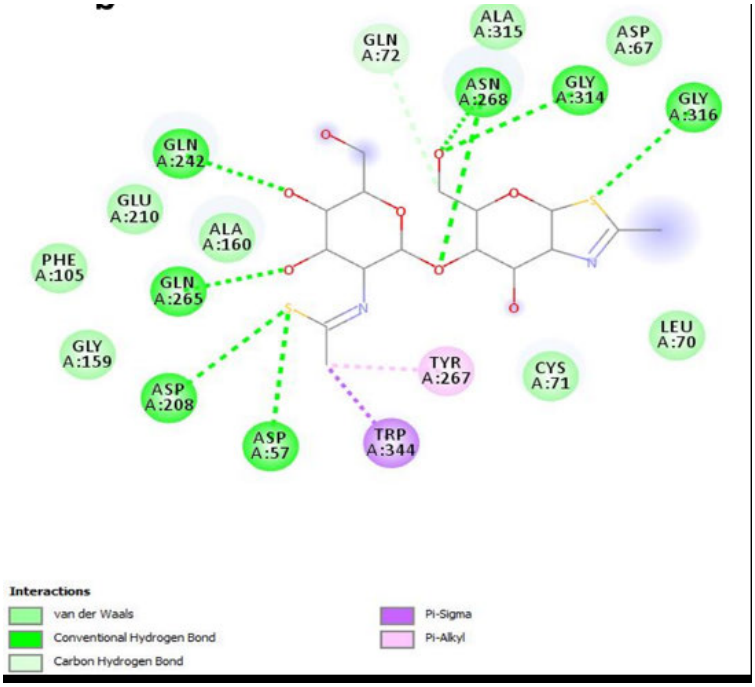

Figure 6.8: Interaction between allosamidin and the ligand sites of *B. bassiana* ARSEF 2860 chitinase.

Protein-protein interactions linked to the *B. bassiana* chitinase (XP_008599616.1) were confidently predicted by the STRING server (Figure 6.9). The STRING database is a powerful tool that uses text mining, coexpression, cooccurrence, and other analyses with data compiled from a large number of organisms. The query protein was confirmed by STRING to be an endochitinase belonging to the glycosyl hydrolase 18 family. Proteins predicted to have the closest interaction with *B. bassiana* chitinase include β-hexosaminidase, a putative protein ybbD, an acidic chitinase, β-glucosidase, β-glucanase, metallothionein expression activator, glycerophosphodiester phosphodiesterase GDE1 and a covalently linked cell wall protein. The β-hexosaminidase has the most pronounced interaction with *B. bassiana* chitinase. Besides having the shortest node with the query, the enzyme also occupies two distinct nodes out of the total ten nodes. This is explained by the fact that β-hexosaminidases are involved with chitinase in the binary chitinolytic system responsible for the degradation of chitobiose and chitooligomers in fungal cell wall regeneration and hyphae formation (Oikawa *et al.,* 2003).

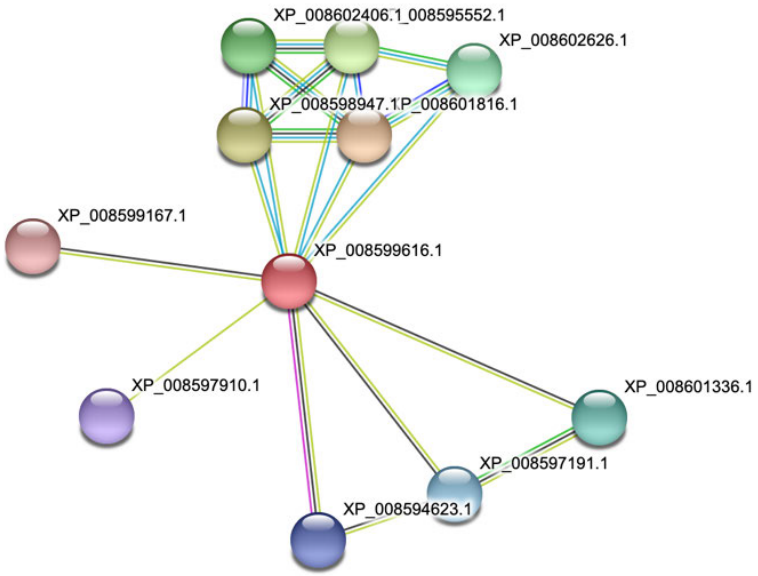

Figure 6.9: Protein-protein functional analysis of *B. bassiana* ARSEF 2860 chitinase

6.3.2 *In silico* structural elucidation of *B. bassiana* xylanase

6.3.2.1 *Physicochemical properties of B. bassiana xylanase*

The physicochemical properties of the selected xylanase as computed by the ProtParam is presented in Table 6.3. The xylanase was predicted to have 330 amino acids and a molecular weight of 37 kDa which coincidences with the actual molecular size obtained from SDS PAGE analysis of *B. bassiana* SAN01 xylanase (Chapter 4, Section 4.3.1.1). The molecular weight range observed in this study suggests that gel exclusion chromatography with Sephadex G-75 SF having a fractionation range of 3-70 kDa is most appropriate for the purification of the enzyme. Further analyses of the xylanase primary sequences revealed that the enzyme had equal numbers of negatively charged amino acid residues (aspartate and glutamate) and positive residues (arginine and lysine).

GRAVY value is an indication of the degree of hydrophobicity/ hydrophilicity of a protein over the entire amino acid sequence. Hence, the GRAVY value for the xylanase was predicted to be -0.387. The relationship between the GRAVY score and the hydrophilicity of proteins has been observed to be inverse, hence, a higher GRAVY score signifies lower hydrophilicity and vice versa (Kyte and Doolittle 1982). Thus, from the values obtained it could be inferred that the xylanase is hydrophilic. The aliphatic index of the xylanase was found to be 75.07. The aliphatic index of a protein is defined as the relative volume occupied by aliphatic side chains, including alanine, isoleucine, leucine and valine. An increase in the aliphatic index has been noted to be indicative of the thermostability of globular proteins (Artz *et al.,* 2015). Hence, the high aliphatic index of the xylanase suggests its relatively high thermostability, which was also shown earlier in the biochemical characterization of the enzyme (Chapter 4, Section 3.1.2).

Table 6.3: Physiochemical parameters of selected *B. bassiana* D1-5 xylanase using ExPASy's ProtParam tool

Physiochemical property	Predicted value
Number of amino acids	330
Molecular weight (kDa)	37
Total numbers of negatively charged residues (Asp + Gln)	32
Total numbers of positively charged residues (Arg + Lysn)	35
Aliphatic Index	75.07
GRAVY	-0.387

The amino acid composition of *B. bassiana* xylanase was evaluated as represented in Figure 6.10. The protein sequence has a larger proportion of aliphatic amino acids including alanine (8%), leucine (8%), glycine (6%), valine (6%) and isoleucine (5%). Alanine and leucine have been noted to have high probabilities of forming helix conformation, while valine and glycine promote beta-sheet conformation (Idicula-Thomas and Balaji 2005). Furthermore, the fundamental role of aliphatic amino acids, particularly valine and isoleucine Ile, in stabilizing the folded protein structure has been previously highlighted. Their contribution is believed to be due to their hydrophobic core formation, as they cluster together to avoid any contact with the water (Hou *et al.,* 2018).

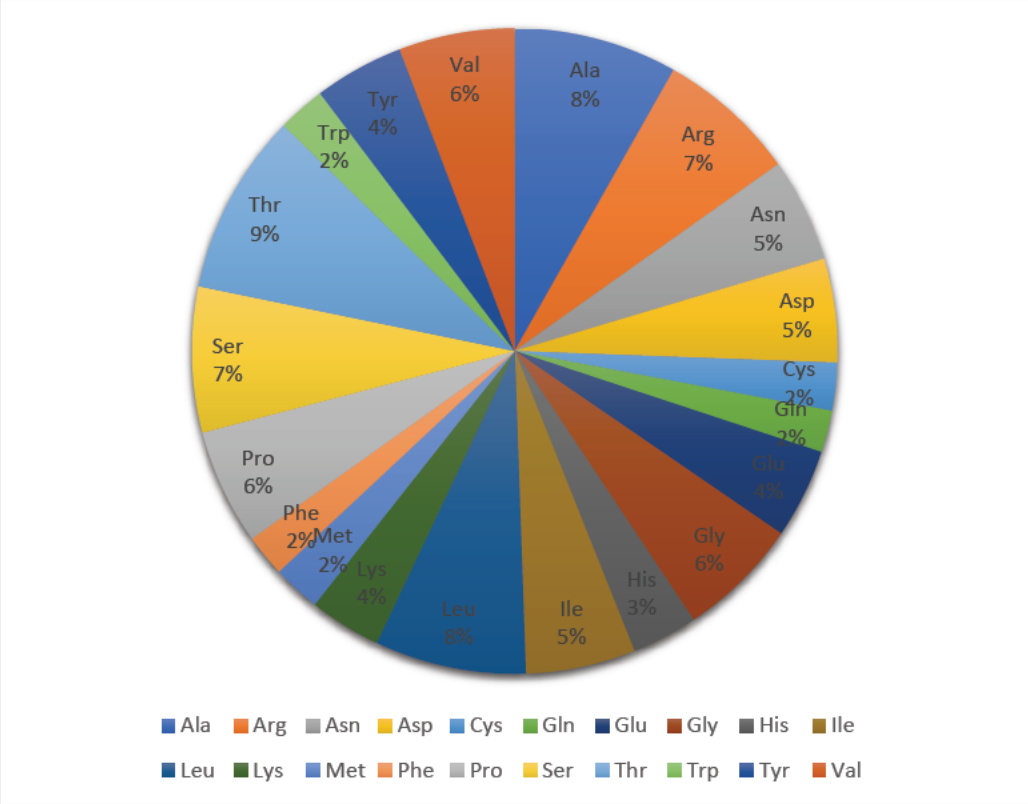

Figure 6.10: Amino acid composition of the selected *B. bassiana* D1-5 xylanase

6.3.2.2 *Secondary structure analysis of B. bassiana xylanase*

The secondary structures of the selected *B. bassiana* xylanase revealed that it is dominated by random coil conformations having the highest computed percentage of approximately 45.76% (Figure 6.11). This was followed by the alpha-helix (37.27%), extended sheet region (12.73%) and beta-turn (4.24%). The positive effects of random coils and alpha-helix regions among the secondary structures on enzyme stability have been shown previously (Neelamathi *et al.,* 2009; Gouripur, Kaliwal and Kaliwal 2016).

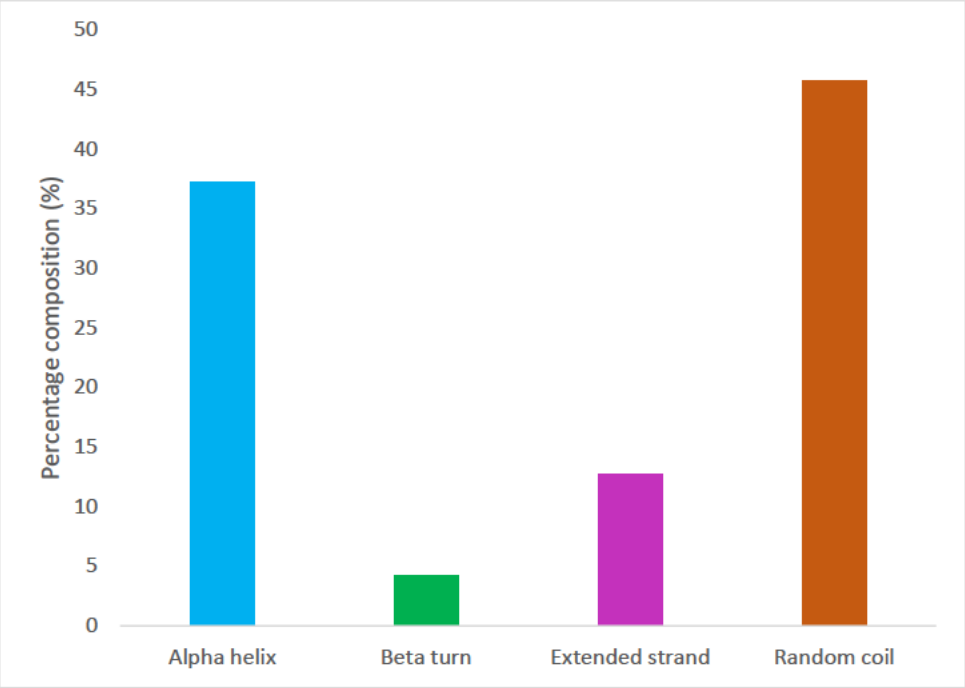

Figure 6.11: Percentage of secondary structure elements in *B. bassiana* D1-5 xylanase

The analysis of *B. bassiana* xylanase motifs using the MyHits interactive tool highlighted few signature pattern sequences belonging to different motifs (Table 6.4). Similar to the chitinases, the myristylation sites were the most dominant in the xylanase enzyme. Furthermore, eight phosphorylation sites, including Casein kinase II and protein kinase C phosphorylation sites were also observed. Besides, two Asparagine-N glycosylation sites were observed in the *B. bassiana* xylanase under study. The significance of these motifs has been discussed earlier in this chapter (Section 3.1.2).

Table 6.4: Illustration of different motifs of *B. bassiana* D1-5 xylanase

Accession number	Asn N-glycosylation site	N-myristoylation site	Casein kinase II phosphorylation site	Protein kinase C phosphorylation site
A0A0A2WJL0	2	3	4	4

The analysis of the *B. bassiana* xylanase domain predicted the presence of alpha/beta hydrolase superfamily and YjeF N-terminal domains in the protein. The alpha/beta hydrolase domain is found in the superfamily of hydrolytic enzymes of different phylogenetic origin and catalytic function but with a common fold. The common fold is an alpha/beta-sheet containing 8 beta strands linked together by 6 alpha-helices. Members of this superfamily possess a catalytic triad, which is usually borne on loops, which are also the most conserved structural features of the fold (Carr and Ollis 2009). The YjeF N-terminal domains have been noted to either exist as single proteins or fusions with other domains and are typically found in hydrolytic enzymes. This domain is made up of a three-layer alpha-beta-alpha topology with alpha helices surrounding a central beta-sheet. The active sites of the YjeF N-terminal domains are highly conserved with a large proportion of acidic residues, this is also typical of the active sites of many hydrolytic enzymes (Carr and Ollis 2009).

6.3.2.3 *Functional analysis of B. bassiana xylanase*

B. bassiana xylanase was predicted with a high probability to be extracellular by Cello v.2.5, the subcellular localization predictor. Previous studies have shown the extracellular secretion of xylanase from *B. bassiana* (Petlamul and Boukaew 2019; Ryali *et al.,* 2020). It has been noted that most microbial xylanases are secreted into the extracellular environment mainly because of the large and complex structure of xylan, the substrate, which hinders its assimilation into the cell (Collins, Gerday and Feller 2005). Furthermore, results obtained earlier in this study confirms this prediction, as *B. bassiana* SAN01 xylanase was amassed from the extracellular secretion in the culture broth (Chapter 3, Section 2.3). The likelihood of the xylanase existing as an integral membrane protein was also evaluated using the TMHMM algorithm (Figure 6.12). The algorithm predicted that no portion of the protein was membrane-associated as all of the amino acid residues were predicted with a probability of ~0 to be transmembrane. This result further validates earlier experimental data observed in this study as well as earlier predictions.

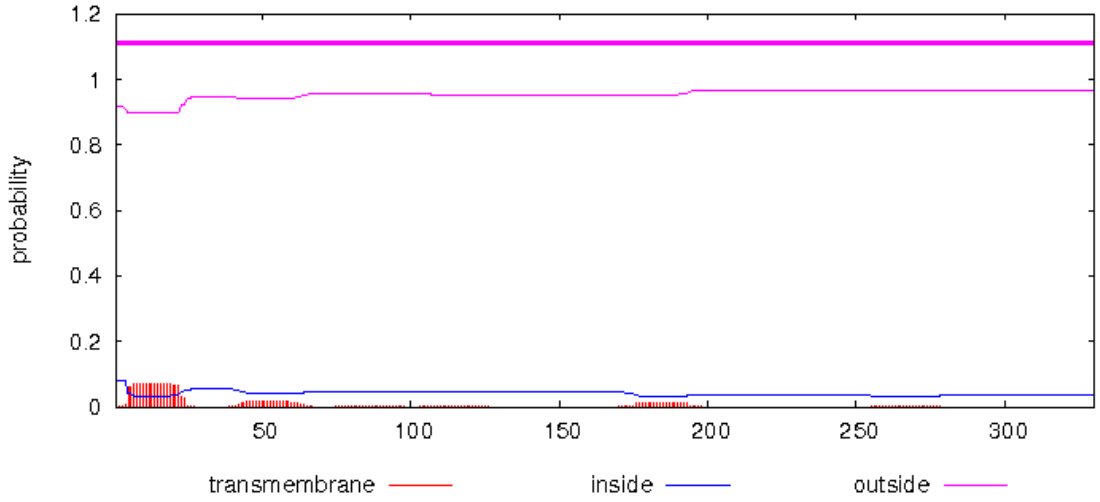

Figure 6.12: TMHMM plot statistics representing the likelihood of *B. bassiana* D1-5 xylanase embedded in the cellular membrane

SignalP 5.0-HMM was also used to predict the presence of signal peptides in *B. bassiana* xylanase (Armenteros *et al.,* 2019). The SignalP prediction showed the presence of signal peptides in the first 22 amino acid residues of the xylanase N-terminal (Figure 14). The standard secretory peptide, Sec/SPI, was the only signal peptide present with a probability of 0.9947. Furthermore, a cleavage site between residues 20 and 22 was also predicted.

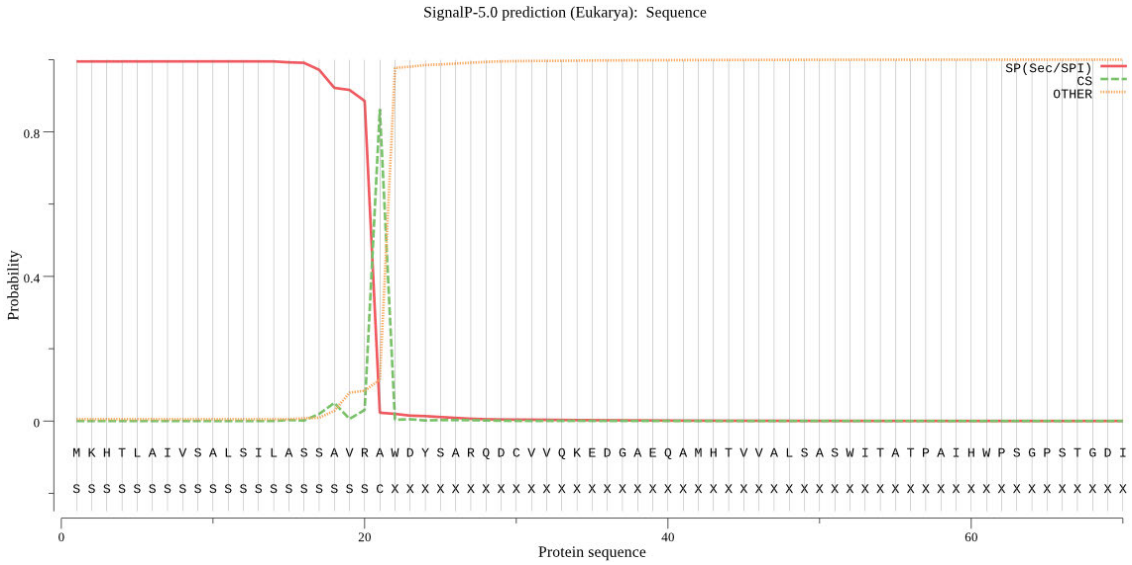

Figure 6.13: SignalP plot for *B. bassiana* D1-5 xylanase

6.3.2.4 *Tertiary structure analysis of B. bassiana xylanase*

The three-dimensional structure of the selected *B. bassiana* xylanase was modelled using the Swiss-Model server based on the known crystal structure of a homologous protein. The crystal structure of acetyl ester-xyloside bifunctional hydrolase from *Caldicellulosiruptor lactoaceticus* (PDB ID: 6A60), which had the highest sequence identity (37%), was used as the template for 3D structure prediction of *B. bassiana* xylanase. Although the commonly accepted sequence identity is ≥40%, there is no size fit all for all protein modelling. Recent investigations have recorded validated results from templates with above 25% with the target sequence (Shahaf *et al.,* 2016; Haddad, Adam and Heger 2020). The analysis of the modelled xylanase (Figure 6.14) showed that it is made of α/β barrel structural domain, in which α-helices and parallel β-strands alternate along the protein backbone. This domain was found common in the NodB-like polysaccharide deacetylase family and it is also closely related to the family 10 xylanases (Collins, Gerday and Feller 2005). The overall quality factor score predicted by ERRAT for the xylanase was 93.84 while Verify 3D showed that 80.37% of the residues had averaged a 3D-1D score ≥ 0.2, indicating the reliability of the predicted model. The stereo-chemical quality of the model as evaluated using the Ramachandran plot showed the xylanase model had 92.6% of residues in the most favoured regions and 6% residues in the additional allowed region (Figure 6.15). The total distribution of these residues in the favoured region is evaluated as 98.6%, reflecting acceptable model adequacy. A very low percentage of the residues were found in the outlier region (1.4%).

Figure 6.14: 3D structure of *B. bassiana* D1-5 xylanase

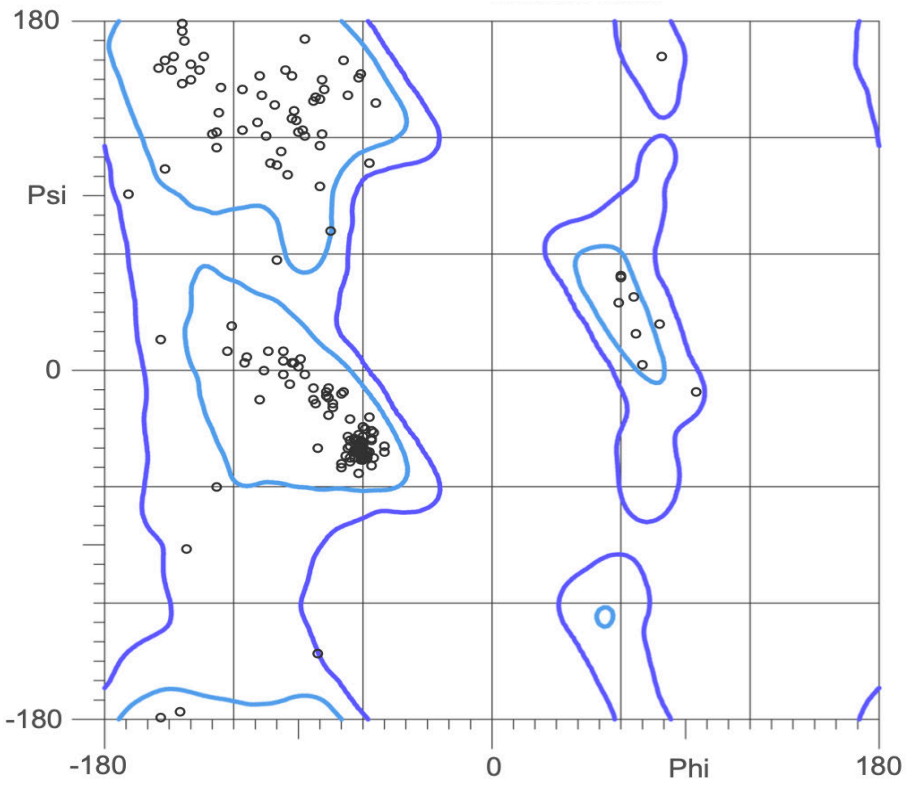

Figure 6.15: Ramachandran plot for *B. bassiana* xylanase D1-5 showing the number of residues in favoured, allowed and outlier region

6.3.2.5 *Docking analysis of B. bassiana xylanase*

The probable active/binding sites of the *B. bassiana* xylanase model were predicted to be Thr-85, Ser-86, Asn-120, Ile-218, Asn-220 and Leu-298. Previous studies have shown the involvement of some of these amino acids in the catalytic and binding sites of fungal xylanases (Sansen *et al.,* 2004; Cheng *et al.,* 2015). Xylotriose is an oligosaccharide, which is produced from the hydrolysis of xylan by xylanase, hence it is the model ligand used to study xylanase-ligand interaction (Conejo-Saucedo *et al.,* 2017; Aronsson *et al.,* 2018; Zheng *et al.,* 2020). The docking of the xylanase from *B. bassiana* D1-5 with xylotriose revealed the energy-favoured conformations of the enzyme (Figure 6.16) and further highlighted by the interacting amino acids from the binding site (Figure 6.17). The xylanase-xylotriose complex showed an affinity score ranging from -6.6 to -6.1 for the nine different conformations. The highest-ranked ligand with a score of -6.6 was selected. It was observed that the ligand interacted with the active site forming both conventional hydrogen, carbon-hydrogen bonds as well as van der Waals interaction with Thr-85, Ser-86, Cys-87, Lys-88, Arg-208, etc. (Figure 6.17). These predicted active residues are also in agreement with the previous prediction recorded from the CASTp analysis.

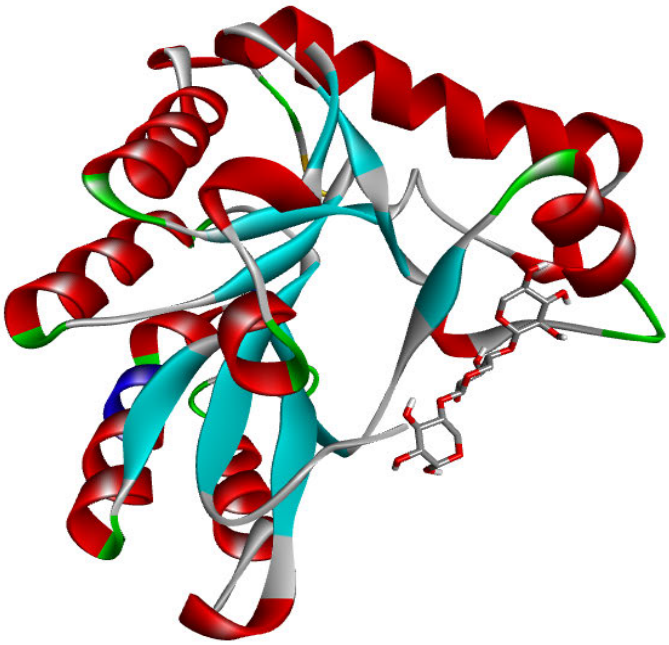

Figure 6.16: *B. bassiana* D1-5 xylanase-xylotriose complex

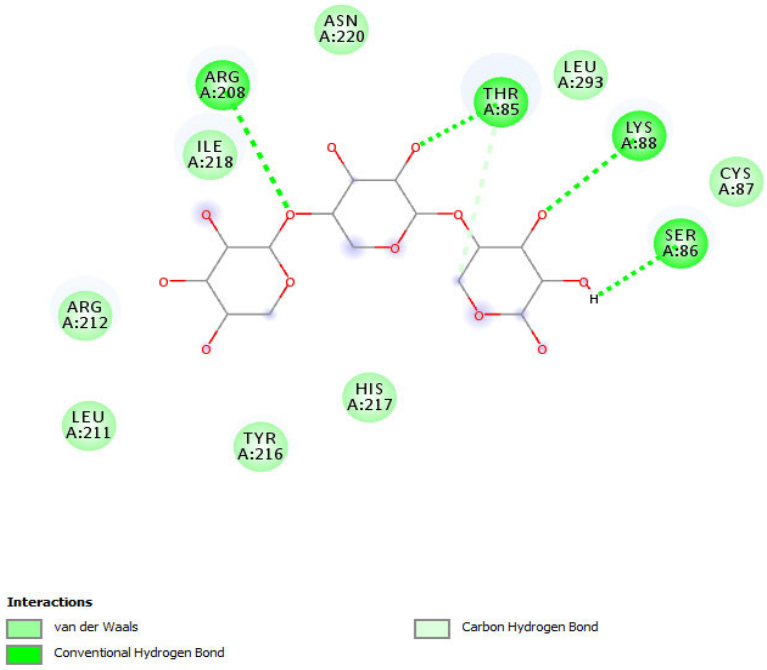

Figure 6.17: Interaction between xylotriose and the ligand sites of *B. bassiana* D1-5 xylanase.

The networking protein partners of the *B. bassiana* xylanase were predicted using the STRING server (Figure 6.18). The query protein was confirmed by STRING to be xylanase; however, it was also predicted to have significant polysaccharide deacetylase activity and was classified under the Polysaccharide deacetylase 1 family. The strong link between the degradation of xylan (and other hemicelluloses) and polysaccharide deacetylase such as acetyl xylan esterase has been shown in previous studies (Sista Kameshwar and Qin 2018; Hettiarachchi *et al.,* 2019). Proteins with the closest interaction with the xylanase include chitin synthase, endochitinase, glycosyltransferase, a putative esterase and other polysaccharide deacetylases. The putative esterase was predicted to possess the most significant interaction with *B. bassiana* xylanase. Esterases have been noted to deacetylate the O-acetyl in highly acetylated hemicellulose, making them more susceptible to further enzymatic attack and degradation (Beg *et al.,* 2001; Yang *et al.,* 2017).

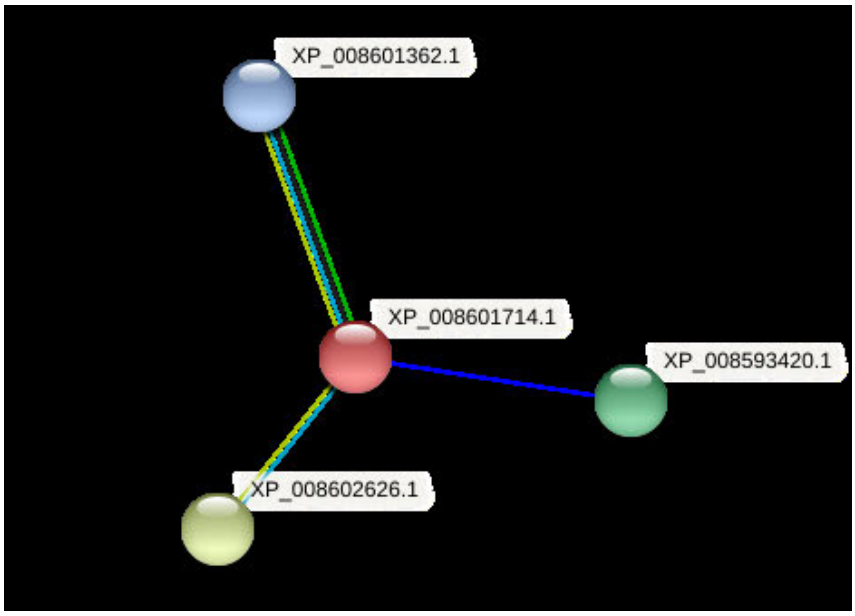

Figure 6.18: Protein-protein functional analysis of *B. bassiana* D1-5 xylanase

6.4 Conclusion

The *in silico* characterization revealed a remarkable variation amongst chitinases from different *B. bassiana* strains and gave significant insight into the structure of the selected xylanase. The lower GRAVY score and higher aliphatic index substantiated the hydrophilicity and thermostability of the chitinases. While the ExPasy-ProtParam predicted molecular weight and THMMM result of the xylanase was in accordance with wet-lab experimental results obtained earlier in this thesis. The 3D models of the representative enzymes created by homology modelling and validated by ERRAT, Verify 3D and MolProbity server revealed the high quality of both the selected chitinase and xylanase structures. In addition, some insights were gained into the probable active site of the enzymes by docking the selected *B. bassiana* chitinase and xylanase with allosamidin and xylotriose, respectively. This computational approach afforded some useful information about the carbohydrases from *B. bassiana*, which could help in future structural and biochemical characterization of the enzymes in vitro. This data would also help to understand the possible structure and functions of other hydrolytic enzymes produced by *B. bassiana*, thus increasing the potential of their industrial applicability.

CHAPTER SEVEN

Conclusion and Future Prospects

7.1 Conclusion

Recently, scientific inquiry into various classes of fungi, such as the entomopathogens and the endophytes, has risen with regards to production of industrially important enzymes and other fungal metabolites. Hence, this study was focused on exploiting the enzyme production potential of an entomopathogenic fungal endophyte, *Beauveria bassiana. B. bassiana*, isolated in its endophytic state from onion leaves, was demonstrated in pilot studies to possess remarkable biomass degradative ability. Preliminary results further revealed that the fungal strain produced various glycoside hydrolases at copious levels. However, it is believed that in exploring the fungus as a viable source of carbohydrases, it becomes imperative to investigate the changes occurring in the fungus at the molecular level, during its trophic transition from its natural endophytic state to its less known saprophytic/fermentation state. In this regard, some significant findings were recorded in this study and they are all summarised in this chapter.

The fungal isolate, which was subsequently referred to as *B. bassiana* SAN01, was confirmed to be a *B. bassiana* strain by the amplification and sequencing of its rDNA ITS sequence. In addition, phylogenetic analysis of the sequences highlighted the close relationship of *B. bassiana* SAN01 with other *B. bassiana* strains, other species of the *Beauveria* genus as well as other well-known entomopathogens. To further characterize the fungus, the carbon utilization profile of *B. bassiana* SAN01 was enumerated using the standard Biolog FF MicroPlate. The respiration rate and biomass growth of the fungus, as deduced from the phenotypic microarray, revealed its special preference for carbon sources such as polyols, pentoses, N-acetylglucosamine, etc. Hence, the metabolic versatility of the fungus, especially its ability to utilize nutritional substrates and its adaptability in different environments was demonstrated by the microarray experiments.

An in-depth analysis of *B. bassiana* SAN01 transcriptome under simulated endophytic, fermentation (saprophytic) and control (basal media) conditions revealed the genetic machinery underpinning the versatile nutrition mode of the fungus, observed earlier in the pilot studies. In this regard, significant differential gene expression patterns were observed in the fungus under the various evaluated trophic conditions. As earlier speculated, results from the RNA-seq affirmed that many genes involved in the deconstruction, transportation and assimilation of different carbohydrate polymers were remarkably upregulated under the fermentation condition. Prominent among these

upregulated genes are the genes coding for glycoside hydrolases such as alpha-glucosidase, amylases, beta-glucosidase, endoglucanase, beta-1,3, glucanases, chitinases, pectinases and xylanase. Furthermore, genes for some accessory enzymes involved in biomass degradation were also observed to be upregulated and these include the genes for catalases, feruloyl esterase, laccases, multi-copper oxidases, and peroxidase. Hence, the significant findings from this comparative transcriptomic analysis were able to clarify some fundamental questions about the versatility of the fungi. Firstly, it revealed that the interaction of *B. bassiana* SAN01 with its different environment and under its different nutritional states is quite dynamic in terms of transcriptional activity and secreted proteins. Secondly, the gene expression response of *B. bassiana* SAN01 under the endophytic conditions shared significant similarities with the fungus under the control condition (basal media). In contrast, the two aforementioned gene expression responses, both differed significantly from the gene response while under fermentation condition. Lastly, the basis for the lignocellulose-degrading capabilities of *B. bassiana* SAN01 was also established, as well as its substrate selection and utilization.

Thus, based on the gene expression profile, previous results, while also considering their industrial importance, four biomass-degrading enzymes were selected from *B. bassiana* SAN01 for optimization studies. The production parameters for the selected enzymes, *viz*., amylase, cellulase (endoglucanase), pectinase (polygalacturonase) and xylanase, were optimized using response surface methodology. At the end of the two-level optimization process, increased yields of 34.82 UmL^{-1}, 23.03 UmL^{-1}, 51.05 UmL^{-1} and 1061 UmL^{-1} were observed for the amylase, endoglucanase, polygalacturonase and xylanase, respectively. These production levels were found to be 1.79- (amylase), 1.35- (endoglucanase), 1.87- (polygalacturonase) and 3.44- (xylanase) folds higher than their initial yields prior to the optimization. In addition, it is also significant that these production levels are the highest ever reported for the four enzymes from any *B. bassiana* strain.

Subsequently, the enzymes were subjected to purification and biochemical characterization in order to enhance the feasibility of their prospective industrial applications. As protein purification is a highly expensive and onerous task, the scope of this study was limited to the complete purification of one of the enzymes, xylanase, while the other three enzymes were partially purified. *B. bassiana* SAN01 xylanase, which was purified to homogeneity, was found to have a specific activity of 324.2 Umg^{-1} and a

molecular mass of ~37 kDa. While the partial purification of the other enzymes led to specific activities of 2.9 Umg^{-1} (amylase), 2.72 Umg^{-1} (endoglucanase) and 3.1 Umg^{-1} (polygalacturonase), respectively. Expectedly, all of the carbohydrases were mesophilic in nature which is reflective of the physiological temperature of the fungus in its natural state. Similarly, the enzymes all performed optimally in the pH range of 6.0-7.0, which is the physiological pH range of the fungus, as well as the typical pH range for most fungal enzymes.

Afterwards, the potential of the *B. bassiana* SAN01 depolymerases in different industrial processes were evaluated and optimized. The purified xylanase was shown to effectively deink printed wastepaper as deduced from spectrophotometric analysis, FTIR analysis and scanning electron microscopy. In the same vein, significant saccharification of sugarcane bagasse was achieved by the hydrolytic action of the partially purified endoglucanase-xylanase enzyme cocktail. In the saccharification experiment, results showed that approximately 20% of the biomass was converted to reducing sugars at an optimum temperature of 30°C after 8 h incubation. The efficacy of the amylase-polygalacturonase cocktail in the clarification of pear juice was also highlighted in the study, with a 1.37-fold improvement in clarity demonstrated under optimized conditions. In addition, the enzyme cocktail also lowered the browning index, turbidity and viscosity of the juice samples. Similarly, the nutritional qualities of the fruit juice were also confirmed to be maintained after the enzyme treatment, as demonstrated by the antioxidant potential before and after the enzyme-assisted clarification.

The study was concluded by the structural characterization of chitinases and a xylanase from *B. bassiana* using computational techniques. This was necessitated by the fact that there is little or no information on the structure of *B. bassiana* chitinase despite the importance of chitinase isoforms in the physiology and industrial applications of *B. bassiana*. However, the selected xylanase was chosen for structural analysis based on the proximity of its computed molecular weight with the actual molecular weight of *B. bassiana* SAN01 xylanase, which had been established earlier in this study. The *in silico* analysis predicted that most of the enzymes were hydrophilic, thermostable and negatively charged with significant *in vivo* half-life. Results also revealed that the secondary structures of the chitinases and the selected xylanase were composed predominantly of random coils. In addition, the stereochemical quality of the modelled three-dimensional structures of a selected chitinase and the xylanase were validated using

the standard validation servers. The presence of ~ 90% of the amino acid residues of the two enzymes in the Ramachandran plot's favoured region confirmed the quality of both models. Finally, the binding site predictions and protein-ligand docking results suggested Asp-208, Gln-242, Gln-265 and Asn-268 as the most probable active site residues for the chitinase while it predicted Thr-85, Ser-86 and Asn-220 as the most probable active site residues for the xylanase.

7.2 Future Prospects

Building on the foundation laid by this study, future areas of research are thus recommended. As this study has highlighted many candidate genes and metabolites for further investigation, their detailed functional characterization will help verify their biological roles and gain more insights into the metabolic versatility of the fungus. The production of the selected *B. bassiana* SAN01 carbohydrases under solid-state fermentation conditions and with the application of other optimization techniques such as artificial neural network, ant colony colonization and differential evolution may yield interesting results with regards to the production levels. Furthermore, recombinant expression of *B. bassiana* SAN01 carbohydrases in appropriate host systems will not only lead to increased yield of the enzymes but also allow more efficient product recovery. In addition, the complete purification of the amylase, endoglucanase and polygalacturonase from *B. bassiana* SAN01 will facilitate further biochemical and kinetic characterization of these enzymes. It is also hoped that the tertiary structures of the *B. bassiana* SAN01 chitinase and xylanase will be determined experimentally using techniques such as cryo-electron microscopy, X-ray crystallography, etc. In addition to either authenticating/rebutting the current information gathered in this study using computational tools, these structural descriptions will go a long way in establishing the structure-function relationship of the enzymes. It is believed that the structural information from the wet-lab studies will also enhance future modification and control of the enzymes through protein engineering, directed evolution, etc., for improved catalytic efficiency. Finally, the economic and environmental feasibility of these enzymes are required to be well understood before possible industrial applications and commercialization. Techno-economic Analysis (TEA) of these biocatalysts and their highlighted applications would go a long way in evaluating the potential bottlenecks, economic feasibilities, operation targets for process improvement as well as identify

further research and development effort requirements during early stages of their different biobased applications. Similarly, the Life Cycle Assessment (LCA) of the *B. bassiana* carbohydrases and their potential industrial applications will also aid in assessing the potential environmental impacts and also in identifying potential environmental hotspots.

REFERENCES

Abd-Razak, N. H., Pihlajamäki, A., Virtanen, T., Chew, Y. J. and Bird, M. R. 2021. The influence of membrane charge and porosity upon the fouling and cleaning during the ultrafiltration of orange juice. *Food and Bioproducts Processing*, 126:184-194.

Abdella, A., Segato, F. and Wilkins, M. R. 2019. Optimization of nutrient medium components for production of a client endo-β-1, 4-xylanase from *Aspergillus fumigatus* var. niveus using a recombinant *Aspergillus nidulans* strain. *Biocatalysis and Agricultural Biotechnology*, 20: 101267.

Adedeji, O. E. and Ezekiel, O. O. 2020. Chemical composition and physicochemical properties of mango juice extracted using polygalacturonase produced by *Aspergillus awamori* CICC 2040 on pretreated orange peel. *LWT*, 132: 109891.

Adetunji, A. I. and Olaniran, A. O. 2020. Statistical modelling and optimization of protease production by an autochthonous *Bacillus aryabhattai* Ab15-ES: A response surface methodology approach. *Biocatalysis and Agricultural Biotechnology*, 24: 101528.

Adhikari, P. and Pandey, A. 2019. Phosphate solubilization potential of endophytic fungi isolated from *Taxus wallichiana* Zucc. roots. *Rhizosphere*, 9: 2-9.

Adhyaru, D. N., Bhatt, N. S. and Modi, H. A. 2014. Enhanced production of cellulase-free, thermo-alkali-solvent-stable xylanase from *Bacillus altitudinis* DHN8, its characterization and application in sorghum straw saccharification. *Biocatalysis and Agricultural Biotechnology*, 3 (2): 182-190.

Adigüzel, A. O. and Tunçer, M. 2016. Production, characterization and application of a xylanase from *Streptomyces* sp. AOA40 in fruit juice and bakery industries. *Food Biotechnology*, 30 (3): 189-218.

Adiguzel, G., Faiz, O., Sisecioglu, M., Sari, B., Baltaci, O., Akbulut, S., Genc, B. and Adiguzel, A. 2019. A novel endo-β-1,4-xylanase from *Pediococcus acidilactici* GC25;

purification, characterization and application in clarification of fruit juices. *International Journal of Biological Macromolecules*, 129: 571-578.

Afifah, L. and Saputro, N. 2020. Growth and viability of entomopathogenic fungus *Beauveria bassiana* (Balsamo) Vuillemin in different alternative media. *IOP Conference Series: Earth and Environmental Science* , 468 (1): 012037.

Aggarwal, R., Dutta, T. and Sheikh, J. 2020. Extraction of pectinase from *Candida* isolated from textile mill effluent and its application in bio-scouring of cotton. *Sustainable Chemistry and Pharmacy*, 17: 100291.

Ahmed, S. A., Abdella, M. A., El-Sherbiny, G. M., Ibrahim, A. M., El-Shamy, A. R., Atalla, S. M. and Hassan, M. E. 2020. Catalytic, kinetic and thermal properties of free andimmobilized *Bacillus subtilis* MK1 α-amylase on chitosan-magnetic nanoparticles. *Biotechnology Reports*, 26: e00443.

Ahmed, A., Batool, K. and Bibi, A. 2017. Microbial β-glucosidase: sources, production and applications. *Journal of Applied and Environmental Microbiology*, 5 (1): 31-46.

Ahmed, A. and Bibi, A. 2018. Fungal cellulase; production and applications: minireview. *LIFE: International Journal of Health and Life-Sciences*, 4 (1): 19-36.

Ahmed, A. and Sohail, M. 2020. Characterization of pectinase from *Geotrichum candidum* AA15 and its potential application in orange juice clarification. *Journal of King Saud University-Science*, 32 (1): 955-961.

Ahmed, I., Zia, M. A., Hussain, M. A., Akram, Z., Naveed, M. T. and Nowrouzi, A. 2016. Bioprocessing of citrus waste peel for induced pectinase production by *Aspergillus niger*; its purification and characterization. *Journal of Radiation Research and Applied Sciences*, 9 (2): 148-154.

Akello, J., Dubois, T., Coyne, D. and Kyamanywa, S. 2008. Endophytic *Beauveria bassiana* in banana (*Musa* spp.) reduces banana weevil (*Cosmopolites sordidus*) fitness and damage. *Crop Protection*, 27 (11): 1437-1441.

Akula, S. and Golla, N. 2018. Optimization of cellulase production by *Aspergillus niger* isolated from forest soil. *The Open Biotechnology Journal*, 12 (1): 256-269.

Al Khoury, C., Nemer, G., Guillot, J., Nour, A. A. and Nemer, N. 2019. Expression analysis of the genes involved in the virulence of *Beauveria bassiana*. *Agri Gene*, 14: 100094.

Alagesan, A., Padmanaban, B., Tharani, G., Jawahar, S. and Manivannan, S. 2019. An assessment of biological control of the banana pseudostem weevil *Odoiporus longicollis* (Olivier) by entomopathogenic fungi *Beauveria bassiana*. *Biocatalysis and Agricultural Biotechnology*, 20: 101262.

Alali, S., Mereghetti, V., Faoro, F., Bocchi, S., Al Azmeh, F. and Montagna, M. 2019. Thermotolerant isolates of *Beauveria bassiana* as potential control agent of insect pest in subtropical climates. *PLoS One*, 14 (2): e0211457.

Alalouf, O., Balazs, Y., Volkinshtein, M., Grimpel, Y., Shoham, G. and Shoham, Y. 2011. A new family of carbohydrate esterases is represented by a GDSL hydrolase/acetylxylan esterase from *Geobacillus stearothermophilus*. *Journal of Biological Chemistry*, 286 (49): 41993-42001.

Alfaro, M., Castanera, R., Lavín, J. L., Grigoriev, I. V., Oguiza, J. A., Ramírez, L. and Pisabarro, A. G. 2016. Comparative and transcriptional analysis of the predicted secretome in the lignocellulose-degrading basidiomycete fungus *Pleurotus ostreatus*. *Environmental Microbiology*, 18 (12): 4710-4726.

Ali, S., Duan, J., Charles, T. C. and Glick, B. R. 2014. A bioinformatics approach to the determination of genes involved in endophytic behavior in *Burkholderia* spp. *Journal of Theoretical Biology*, 343: 193-198.

Alsina, C., Sancho-Vaello, E., Aranda-Martínez, A., Faijes, M. and Planas, A. 2020. Auxiliary active site mutations enhance the glycosynthase activity of a GH18 chitinase for polymerization of chitooligosaccharides. *Carbohydrate Polymers*, 252: 117121.

Alvarez-Zúñiga, M. T., Santiago-Hernández, A., Rodríguez-Mendoza, J., Campos, J. E., Pavón-Orozco, P., Trejo-Estrada, S. and Hidalgo-Lara, M. E. 2017. Taxonomic identification of the thermotolerant and fast-growing fungus *Lichtheimia ramosa* H71D and biochemical characterization of the thermophilic xylanase LrXynA. *AMB Express*, 7 (1): 194.

Alves, E. A., Schmaltz, S., Tres, M. V., Zabot, G. L., Kuhn, R. C. and Mazutti, M. A. 2020. Process development to obtain a cocktail containing cell-wall degrading enzymes with insecticidal activity from *Beauveria bassiana*. *Biochemical Engineering Journal*, 156: 107484.

Amin, F., Bhatti, H. N., Bilal, M. and Asgher, M. 2017. Multiple parameter optimizations for enhanced biosynthesis of exo-polygalacturonase enzyme and its application in fruit juice clarification. *International Journal of Food Engineering*, 13 (2).

Amin, F., Mohsin, A., Bhatti, H. N. and Bilal, M. 2020. Production, thermodynamic characterization, and fruit juice quality improvement characteriztics of an exo-polygalacturonase from *Penicillium janczewskii*. *Biochimica et Biophysica Acta (BBA) - Proteins and Proteomics*, 1868 (5): 140379.

Amobonye, A., Singh, S. and Pillai, S. 2019. Recent advances in microbial glutaminase production and applications - a concise review. *Critical Reviews in Biotechnology*, 39 (7): 944-963.

Anand, G., Yadav, S. and Yadav, D. 2017a. Production, purification and biochemical characterization of an exo-polygalacturonase from *Aspergillus niger* MTCC 478 suitable for clarification of orange juice. *3 Biotech*, 7 (2): 122.

Anand, G., Yadav, S. and Yadav, D. 2017b. Purification and biochemical characterization of an exo-polygalacturonase from *Aspergillus flavus* MTCC 7589. *Biocatalysis and Agricultural Biotechnology*, 10: 264-269.

Andrioli, W., Lopes, A., Cavalcanti, B., Pessoa, C., Nanayakkara, N. and Bastos, J. 2017. Isolation and characterization of 2-pyridone alkaloids and alloxazines from *Beauveria bassiana. Natural Product Research*, 31 (16): 1920-1929.

Anfar, Z., Ait Ahsaine, H., Zbair, M., Amedlous, A., Ait El Fakir, A., Jada, A. and El Alem, N. 2020. Recent trends on numerical investigations of response surface methodology for pollutants adsorption onto activated carbon materials: A review. *Critical Reviews in Environmental Science and Technology*, 50 (10): 1043-1084.

Ardito, F., Giuliani, M., Perrone, D., Troiano, G. and Lo Muzio, L. 2017. The crucial role of protein phosphorylation in cell signaling and its use as targeted therapy. *International Journal of Molecular Medicine*, 40 (2): 271-280.

Armenteros, J. J. A., Tsirigos, K. D., Sønderby, C. K., Petersen, T. N., Winther, O., Brunak, S., von Heijne, G. and Nielsen, H. 2019. SignalP 5.0 improves signal peptide predictions using deep neural networks. *Nature Biotechnology*, 37 (4): 420-423.

Aronsson, A., Güler, F., Petoukhov, M. V., Crennell, S. J., Svergun, D. I., Linares-Pastén, J. A. and Karlsson, E. N. 2018. Structural insights of RmXyn10A–A prebiotic-producing GH10 xylanase with a non-conserved aglycone binding region. *Biochimica et Biophysica Acta (BBA)-Proteins and Proteomics*, 1866 (2): 292-306.

Artz, J. H., White, S. N., Zadvornyy, O. A., Fugate, C. J., Hicks, D., Gauss, G. H., Posewitz, M. C., Boyd, E. S. and Peters, J. W. 2015. Biochemical and structural properties of a thermostable mercuric ion reductase from *Metallosphaera sedula*. *Frontiers in Bioengineering and Biotechnology*, 3: 97.

Asgher, M., Ahmad, Z. and Iqbal, H. M. N. 2013. Alkali and enzymatic delignification of sugarcane bagasse to expose cellulose polymers for saccharification and bio-ethanol production. *Industrial Crops and Products*, 44: 488-495.

Atalla, S. M. and El Gamal, N. G. 2020. Production and characterization of xylanase from pomegranate peel by *Chaetomium globosum* and its application on bean under greenhouse condition. *Bulletin of the National Research Centre*, 44 (1): 1-11.

Atzeni, R., Moro, G., Marche, M. G., Uva, P. and Ruiu, L. 2020. Genome sequence of *Beauveria bassiana* Strain ATCC 74040, a widely employed insect pathogen. *Microbiology Resource Announcements*, 9 (23): e00446-20.

Augustyniuk-Kram, A. 2018. Relationships between host insect, enzymatic activity and virulence of isolates of the entomopathogenic fungus *Beauveria bassiana* (Bals.Criv.) Vuill.(Hypocreales). *Acta Zoologica Bulgarica,* 12: 3-10.

Ávila-Hernández, J. G., Carrillo-Inungaray, M. L., De, R., la Cruz-Quiroz, J. E. W., Paz, D. B. M.-M., Parra, R., Aguilar, C. N., Aguilar-Zárate, P., Huasteca, Z. and del Campo, R. 2020. *Beauveria bassiana* secondary metabolites: a review inside their production systems, biosynthesis, and bioactivities. *Mexican Journal of Biotechnology*, 5(4):1-33.

Azimi, S. Z., Hosseini, S. S. and Khodaiyan, F. 2021. Continuous clarification of grape juice using a packed bed bioreactor including pectinase enzyme immobilized on glass beads. *Food Bioscience*, 40: 100877.

Aziz, M. M. A., Elgammal, E. W. and Ghitas, R. G. 2020. Comparative study on modeling by neural networks and response surface methodology for better prediction and optimization of fermentation parameters: application on thermo-alkaline lipase production by *Nocardiopsis* sp. strain NRC/WN5. *Biocatalysis and Agricultural Biotechnology*: 101619.

Babu, C. R., Ketanapalli, H., Beebi, S. K. and Kolluru, V. C. 2018. Wheat bran-composition and nutritional quality: a review. *Advances in Biotechnology and Microbiology*, 9 (1): 1-7.

Bagewadi, Z. K., Mulla, S. I. and Ninnekar, H. Z. 2018. Optimization of endoglucanase production from *Trichoderma harzianum* strain HZN11 by central composite design under response surface methodology. *Biomass Conversion and Biorefinery*, 8 (2): 305-316.

Bailey, M. J., Biely, P. and Poutanen, K. 1992. Interlaboratory testing of methods for assay of xylanase activity. *Journal of Biotechnology*, 23 (3): 257-270.

Bailoni, L., Schiavon, S., Pagnin, G., Tagliapietra, F. and Bonsembiante, M. 2005. Quanti-qualitative evaluation of pectins in the dietary fibre of 24 foods. *Italian Journal of Animal Science*, 4 (1): 49-58.

Bajaj, B. K. and Manhas, K. 2012. Production and characterization of xylanase from *Bacillus licheniformis* P11(C) with potential for fruit juice and bakery industry. *Biocatalysis and Agricultural Biotechnology*, 1 (4): 330-337.

Bajpai, P. 2014. Purification of xylanases. In: Bajpai, P. ed. *Xylanolytic enzymes*. 1st ed. Amsterdam: Academic Press, 53-61.

Bakri, Y., Akeed, Y., Jawhar, M. and Arabi, M. 2020. Evaluation of xylanase production from filamentous fungi with different lifestyles. *Acta Alimentaria*, 49 (2): 197-203.

Balaji, L., Chittoor, J. T. and Jayaraman, G. 2020. Optimization of extracellular lipase production by halotolerant *Bacillus* sp. VITL8 using factorial design and applicability of enzyme in pretreatment of food industry effluents. *Preparative Biochemistry and Biotechnology*, 50(7): 708-716.

Bamisile, B. S., Senyo Akutse, K., Dash, C. K., Qasim, M., Ramos Aguila, L. C., Ashraf, H. J., Huang, W., Hussain, M., Chen, S. and Wang, L. 2020. Effects of seedling age on colonization patterns of citrus limon plants by endophytic *Beauveria bassiana* and *Metarhizium anisopliae* and their influence on seedlings growth. *Journal of Fungi*, 6 (1): 29.

Bara, G. T. and Laing, M. D. 2020. Entomopathogens: potential to control thrips in avocado, with special reference to *Beauveria bassiana*. *Horticultural Reviews*, 47: 325-368.

Barbero, F. 2016. Cuticular lipids as a cross-talk among ants, plants and butterflies. *International Journal of Molecular Sciences*, 17 (12): 1966.

Barman, S., Sit, N., Badwaik, L. S. and Deka, S. C. 2015. Pectinase production by *Aspergillus niger* using banana (Musa balbisiana) peel as substrate and its effect on

clarification of banana juice. *Journal of Food Science and Technology*, 52 (6): 3579-3589.

Barra-Bucarei, L., France Iglesias, A., Gerding González, M., Silva Aguayo, G., Carrasco-Fernández, J., Castro, J. F. and Ortiz Campos, J. 2020a. Antifungal activity of *Beauveria bassiana* endophyte against *Botrytis cinerea* in two Solanaceae crops. *Microorganisms*, 8 (1): 65.

Barra-Bucarei, L., González, M. G., Iglesias, A. F., Aguayo, G. S., Peñalosa, M. G. and Vera, P. V. 2020b. *Beauveria bassiana* multifunction as an endophyte: growth promotion and biologic control of *Trialeurodes vaporariorum* (westwood)(hemiptera: Aleyrodidae) in tomato. *Insects*, 11 (9): 591.

Basit, A., Liu, J., Miao, T., Zheng, F., Rahim, K., Lou, H. and Jiang, W. 2018. Characterization of two endo-β-1, 4-xylanases from *Myceliophthora thermophila* and their saccharification efficiencies, synergistic with commercial cellulase. *Frontiers in Microbiology* 14 (9): 233.

Beaugrand, J., Reis, D., Guillon, F., Debeire, P. and Chabbert, B. 2004. Xylanase-mediated hydrolysis of wheat bran: evidence for subcellular heterogeneity of cell walls. *International Journal of Plant Sciences*, 165 (4): 553-563.

Beer, B., Bartolome, M. J., Berndorfer, L., Bochmann, G., Guebitz, G. M. and Nyanhongo, G. S. 2020. Controlled enzymatic hydrolysis and synthesis of lignin cross-linked chitosan functional hydrogels. *International Journal of Biological Macromolecules*, 161: 1440-1446.

Beg, Q., Kapoor, M., Mahajan, L. and Hoondal, G. 2001. Microbial xylanases and their industrial applications: a review. *Applied Microbiology and Biotechnology*, 56 (3-4): 326-338.

Beg, Q. K., Bhushan, B., Kapoor, M. and Hoondal, G. S. 2000. Production and characterization of thermostable xylanase and pectinase from *Streptomyces* sp. QG-11-3. *Journal of Industrial Microbiology and Biotechnology*, 24 (6): 396-402.

Behie, S. W. and Bidochka, M. J. 2013. An additional branch of the soil nitrogen cycle: ubiquity of insect-derived nitrogen transfer to plants by endophytic insect pathogenic fungi. *Applied and Environmental Microbiology*, 80(5): 1553-1560.

Beier, S. and Bertilsson, S. 2013. Bacterial chitin degradation-mechanisms and ecophysiological strategies. *Frontiers in Microbiology*, 4: 149.

Belay, Y. C. and Tenkegna, T. A. 2017. Bioassay and pilot mass production of entomopathogenic fungus, *Beauveria bassiana* for the control of coffee berry borer (*Hypothenemus hampei*: Scolytidae), Ferrari. *Journal of Applied Biosciences*, 117: 11669-11683.

Benito, B., Garciadeblás, B., Schreier, P. and Rodríguez-Navarro, A. 2004. Novel P-type ATPases mediate high-affinity potassium or sodium uptake in fungi. *Eukaryotic Cell*, 3 (2): 359-368.

Berini, F., Katz, C., Gruzdev, N., Casartelli, M., Tettamanti, G. and Marinelli, F. 2018. Microbial and viral chitinases: attractive biopesticides for integrated pest management. *Biotechnology Advances*, 36 (3): 818-838.

Beveridge, T. and Wrolstad, R. E. 1997. Haze and cloud in apple juices. *Critical Reviews in Food Science & Nutrition*, 37 (1): 75-91.

Beygmoradi, A., Homaei, A., Hemmati, R., Santos-Moriano, P., Hormigo, D. and Fernández-Lucas, J. 2018. Marine chitinolytic enzymes, a biotechnological treasure hidden in the ocean? *Applied Microbiology and Biotechnology*, 102 (23): 9937-9948.

Bhagwat, P. K., Bhise, K. K., Bhuimbar, M. V. and Dandge, P. B. 2018. Use of statistical experimental methods for optimization of collagenolytic protease production by *Bacillus cereus* strain SUK grown on fish scales. *Environmental Science and Pollution Research*, 25 (28): 28226-28236.

Bharadwaj, V. S., Knott, B. C., Ståhlberg, J., Beckham, G. T. and Crowley, M. F. 2020. The hydrolysis mechanism of a GH45 cellulase and its potential relation to lytic transglycosylase and expansin function. *Journal of Biological Chemistry*, 295 (14): 4477-4487.

Bhardwaj, N., Verma, V. K., Chaturvedi, V. and Verma, P. 2020a. Cloning, expression and characterization of a thermo-alkali-stable xylanase from *Aspergillus oryzae* LC1 in *Escherichia coli* BL21 (DE3). *Protein Expression and Purification*, 168: 105551.

Bharate, S.S. and Bharate, S.B., 2014. Non-enzymatic browning in citrus juice: chemical markers, their detection and ways to improve product quality. *Journal of Food Science and Technology*, 51(10): 2271-2288.

Bhatt, B. M., Trivedi, U. B. and Patel, K. C. 2020. Extremophilic amylases: microbial production and applications. In: Kudus, M. ed. *Microbial enzymes: roles and applications in industries*. Singapore: Springer, 185-205.

Bhattacharjee, C., Saxena, V.K. and Dutta, S., 2017. Fruit juice processing using membrane technology: A review. *Innovative Food Science and Emerging Technologies*, 43:136-153.

Bhattacharjee, B., Pathaw, N., Chrungoo, N. K. and Bhattacharjee, A. 2017. Molecular modelling, dynamics simulation and characterization of antifungal chitinase from *Sechium edule*. *Gene*, 606: 39-46.

Biswas, P., Bharti, A. K., Kadam, A. and Dutt, D. 2019. Wheat bran as substrate for enzyme production and its application in the bio-deinking of mixed office waste (MOW) paper. *BioResources*, 14 (3): 5788-5806.

Blättel, V., Larisika, M., Pfeiffer, P., Nowak, C., Eich, A., Eckelt, J. and König, H. 2011. Beta-1,3-glucanase from *Delftia tsuruhatensis* strain MV01 and its potential application in vinification. *Applied and Environmental Microbiology*, 77 (3): 983-990.

Bonnin, E. and Pelloux, J. 2020. Pectin Degrading Enzymes. In: Kontogiorgos, V. ed. *Pectin: technological and physiological properties*. Switzerland: Springer, 37-60.

Bonturi, N., Crucello, A., Viana, A. J. C. and Miranda, E. A. 2017. Microbial oil production in sugarcane bagasse hemicellulosic hydrolysate without nutrient supplementation by a *Rhodosporidium toruloides* adapted strain. *Process Biochemistry*, 57: 16-25.

Bora, S. J., Handique, J. and Sit, N. 2017. Effect of ultrasound and enzymatic pre-treatment on yield and properties of banana juice. *Ultrasonics Sonochemistry*, 37: 445-451.

Borges, M. S., Barbosa, R. S., Rambo, M. K. D., Rambo, M. C. D. and Scapin, E. 2020. Evaluation of residual biomass produced in *Cerrado Tocantinense* as potential raw biomass for biorefinery. *Biomass Conversion and Biorefinery*, 2020.

Borgi, I., Dupuy, J.-W., Blibech, I., Lapaillerie, D., Lomenech, A.M., Rebai, A., Ksantini, M., Bonneu, M. and Gargouri, A. 2016. Hyper-proteolytic mutant of *Beauveria bassiana*, a new biological control agent against the tomato borer. *Agronomy for Sustainable Development*, 36 (4): 60.

Borgi, I. and Gargouri, A. 2016. A novel high molecular weight thermo-acidoactive β-glucosidase from *Beauveria bassiana*. *Applied Biochemistry and Microbiology*, 52 (6): 602-607.

Borglin, S., Joyner, D., DeAngelis, K. M., Khudyakov, J., D'haeseleer, P., Joachimiak, M. P. and Hazen, T. 2012. Application of phenotypic microarrays to environmental microbiology. *Current Opinion in Biotechnology*, 23 (1): 41-48.

Borin, G. P., Sanchez, C. C., de Santana, E. S., Zanini, G. K., Dos Santos, R. A. C., de Oliveira Pontes, A., de Souza, A. T., Dal, R. M. M. T. S., Riaño-Pachón, D. M. and Goldman, G. H. 2017. Comparative transcriptome analysis reveals different strategies for degradation of steam-exploded sugarcane bagasse by *Aspergillus niger* and *Trichoderma reesei*. *BMC Genomics*, 18 (1): 1-21.

Bortone, K., Monzingo, A. F., Ernst, S. and Robertus, J. D. 2002. The structure of an allosamidin complex with the *Coccidioides immitis* chitinase defines a role for a second acid residue in substrate-assisted mechanism. *Journal of Molecular Biology*, 320 (2): 293-302.

Botinestean, C., Hossain, M., Mullen, A. M., Auty, M. A., Kerry, J. P. and Hamill, R. M. 2020. Optimization of textural and technological parameters using response surface methodology for the development of beef products for older consumers. *Journal of Texture Studies*, 51 (2): 263-275.

Box, G. E. P. 1952. Multi-factor designs of first order. *Biometrika*, 39 (1-2): 49-57.

Brenelli, L. B., Persinoti, G. F., Cairo, J. P. L. F., Liberato, M. V., Gonçalves, T. A., Otero, I. V., Mainardi, P. H., Felby, C., Sette, L. D. and Squina, F. M. 2019. Novel redox-active enzymes for ligninolytic applications revealed from multiomics analyses of *Peniophora* sp. CBMAI 1063, a laccase hyper-producer strain. *Scientific Reports*, 9 (1): 1-15.

Brown, N. A., Ries, L. N. A., Reis, T. F., Rajendran, R., Corrêa dos Santos, R. A., Ramage, G., Riaño-Pachón, D. M. and Goldman, G. H. 2016. RNAseq reveals hydrophobins that are involved in the adaptation of *Aspergillus nidulans* to lignocellulose. *Biotechnology for Biofuels*, 9 (1): 145.

Bruder, M., Moo-Young, M., Chung, D. A. and Chou, C. P. 2015. Elimination of carbon catabolite repression in *Clostridium acetobutylicum*—a journey toward simultaneous use of xylose and glucose. *Applied Microbiology and Biotechnology*, 99 (18): 7579-7588.

Busk, P. K., Pilgaard, B., Lezyk, M. J., Meyer, A. S. and Lange, L. 2017. Homology to peptide pattern for annotation of carbohydrate-active enzymes and prediction of function. *BMC Bioinformatics*, 18 (1): 1-9.

Caicedo, N. H., Davalos, A. F., Puente, P. A., Rodríguez, A. Y. and Caicedo, P. A. 2019. Antioxidant activity of exo-metabolites produced by *Fusarium oxysporum*: an endophytic fungus isolated from leaves of *Otoba gracilipes*. *Microbiology Open*, 8 (10): e903.

Canassa, F., Esteca, F. C., Moral, R. A., Meyling, N. V., Klingen, I. and Delalibera, I. 2020. Root inoculation of strawberry with the entomopathogenic fungi *Metarhizium robertsii* and *Beauveria bassiana* reduces incidence of the twospotted spider mite and selected insect pests and plant diseases in the field. *Journal of Pest Science*, 93 (1): 261-274.

Canfora, L., Abu-Samra, N., Tartanus, M., Łabanowska, B., Benedetti, A., Pinzari, F. and Malusà, E. 2017. Co-inoculum of *Beauveria brongniartii* and *B. bassiana* shows in vitro different metabolic behaviour in comparison to single inoculums. *Scientific Reports*, 7 (1): 1-15.

Cao, W., Zhang, C., Ji, H. and Hao, J. 2012. Optimization of peptic hydrolysis parameters for the production of angiotensin I-converting enzyme inhibitory hydrolysate from *Acetes chinensis* through Plackett–Burman and response surface methodological approaches. *Journal of the Science of Food and Agriculture*, 92 (1): 42-48.

Carballeira, J., Quezada, M., Hoyos, P., Simeó, Y., Hernaiz, M., Alcantara, A. and Sinisterra, J. 2009. Microbial cells as catalysts for stereoselective redox reactions. *Biotechnology Advances*, 27 (6): 686-714.

Cardoso, W. S., Queiroz, P. V., Tavares, G. P., Santos, F. A., Soares, F. E. D. F., Kasuya, M. C. M. and Queiroz, J. H. D. 2018. Multi-enzyme complex of white rot fungi in saccharification of lignocellulosic material. *Brazilian Journal of Microbiology*, 49 (4): 879-884.

Carr, P. D. and Ollis, D. L. 2009. α/βHydrolase fold: an update. *Protein and Peptide Letters*, 16 (10): 1137-1148.

Carrasco, M., Rozas, J. M., Alcaíno, J., Cifuentes, V. and Baeza, M. 2019. Pectinase secreted by psychrotolerant fungi: identification, molecular characterization and heterologous expression of a cold-active polygalacturonase from *Tetracladium* sp. *Microbial Cell Factories*, 18 (1): 45.

Carrillo, N., Ceccarelli, E. A. and Roveri, O. A. 2010. Usefulness of kinetic enzyme parameters in biotechnological practice. *Biotechnology and Genetic Engineering Reviews*, 27 (1): 367-382.

Castro, D. R. G., Mar, J. M., da Silva, L. S., da Silva, K. A., Sanches, E. A., de Araújo Bezerra, J., Rodrigues, S., Fernandes, F. A. N. and Campelo, P. H. 2020. Improvement of the bioavailability of Amazonian juices rich in bioactive compounds using glow plasma technique. *Food and Bioprocess Technology*, 13: 670–679.

Cerreti, M., Liburdi, K., Benucci, I., Spinelli, S. E., Lombardelli, C. and Esti, M. 2017. Optimization of pectinase and protease clarification treatment of pomegranate juice. *LWT-Food Science and Technology*, 82: 58-65.

Chadha, B., Kaur, B., Basotra, N., Tsang, A. and Pandey, A. 2019. Thermostable xylanases from thermophilic fungi and bacteria: current perspective. *Bioresource Technology*, 277: 195-203.

Chand, S., Mahajan, R. V., Prasad, J. P., Sahoo, D. K., Mihooliya, K. N., Dhar, M. S. and Sharma, G. 2020. A comprehensive review on microbial L-asparaginase: Bioprocessing, characterization, and industrial applications. *Biotechnology and Applied Biochemistry*, 67: 619-647.

Chandra, M. R. G. S. and Yadav, P. S. 2021. Recent trends and future prospective of fungal cellulases for environmental management. In: Viswanath, B. ed. *Recent developments in applied microbiology and biochemistry*. Amsterdam: Elsevier, 247-256.

Chandra, P., Singh, R. and Arora, P. K. 2020. Microbial lipases and their industrial applications: a comprehensive review. *Microbial Cell Factories*, 19 (1): 1-42.

Chantasingh, D., Kitikhun, S., Eurwilaichitr, L., Uengwetwanit, T. and Pootanakit, K. 2011. Functional expression in *Beauveria bassiana* of a chitinase gene from *Ophiocordyceps unilateralis*, an ant-pathogenic fungus. *Biocontrol Science and Technology*, 21 (6): 677-686.

Chaturvedi, V., DeFiglio, H. and Chaturvedi, S. 2018. Phenotype profiling of white-nose syndrome pathogen *Pseudogymnoascus destructans* and closely-related *Pseudogymnoascus pannorum* reveals metabolic differences underlying fungal lifestyles. *F1000Research*, 7: 655.

Chauhan A., Ranjan A., Jindal T. 2018. Biological control agents for sustainable agriculture, safe water and soil health. In: Jindal T. ed. *Paradigms in pollution prevention.* Cham: Springer, 71-83.

Chen, A., Wang, Y., Shao, Y., Zhou, Q., Chen, S., Wu, Y., Chen, H. and Liu, E. 2018a. Genes involved in *Beauveria bassiana* infection to *Galleria mellonella*. *Archives of Microbiology*, 200 (4): 541-552.

Chen, J., Lai, Y., Wang, L., Zhai, S., Zou, G., Zhou, Z., Cui, C. and Wang, S. 2017. CRISPR/Cas9-mediated efficient genome editing via blastospore-based transformation in entomopathogenic fungus *Beauveria bassiana. Scientific Reports*, 7: 45763.

Chen, L., Wei, Y., Shi, M., Li, Z. and Zhang, S.-H. 2019a. An archaeal chitinase with a secondary capacity for catalyzing cellulose and its biotechnological applications in shell and straw degradation. *Frontiers in Microbiology*, 10: 1253.

Chen, X., Xu, F., Qin, W., Ma, L. and Zheng, Y. 2012. Optimization of enzymatic clarification of green asparagus juice using response surface methodology. *Journal of Food Science*, 77 (6): C665-C670.

Chen, Y., Cen, K., Lu, Y., Zhang, S., Shang, Y. and Wang, C. 2018b. Nitrogen-starvation triggers cellular accumulation of triacylglycerol in *Metarhizium robertsii*. *Fungal Biology*, 122 (6): 410-419.

Chen, Z., Liu, Y., Zaky, A. A., Liu, L., Chen, Y., Li, S. and Jia, Y. 2019b. Characterization of a novel xylanase from *Aspergillus flavus* with the unique properties in production of xylooligosaccharides. *Journal of Basic Microbiology*, 59 (4): 351-358.

Chen, Z., Zaky, A. A., Liu, Y., Chen, Y., Liu, L., Li, S. and Jia, Y. 2019c. Purification and characterization of a new xylanase with excellent stability from *Aspergillus flavus* and its application in hydrolyzing pretreated corncobs. *Protein Expression and Purification*, 154: 91-97.

Cheng, S.H., Khoo, H., Ismail, A., Abdul-Hamid, A. and Barakatun-Nisak, M. 2016. Influence of extraction solvents on *Cosmos caudatus* leaf antioxidant properties. *Iranian Journal of Science and Technology, Transactions A: Science*, 40 (1): 51-58.

Cheng, Y.S., Chen, C.C., Huang, J.W., Ko, T.P., Huang, Z. and Guo, R.T. 2015. Improving the catalytic performance of a GH11 xylanase by rational protein engineering. *Applied Microbiology and Biotechnology*, 99 (22): 9503-9510.

Cho, EM., Boucias, D. and Keyhani, N. O. 2006. EST analysis of cDNA libraries from the entomopathogenic fungus *Beauveria* (*Cordyceps*) *bassiana*. II. Fungal cells sporulating on chitin and producing oosporein. *Microbiology*, 152 (9): 2855-2864.

Cho, E.M., Liu, L., Farmerie, W. and Keyhani, N. O. 2006. EST analysis of cDNA libraries from the entomopathogenic fungus *Beauveria* (*Cordyceps*) *bassiana*. I. Evidence for stage-specific gene expression in aerial conidia, in vitro blastospores and submerged conidia. *Microbiology*, 152 (9): 2843-2854.

Chollom, M. N., Rathilal, S., Swalaha, F. M., Bakare, B. F. and Tetteh, E. K. 2020. Comparison of response surface methods for the optimization of an upflow anaerobic sludge blanket for the treatment of slaughterhouse wastewater. *Environmental Engineering Research*, 25 (1): 114-122.

Chu, X., Feng, M. and Ying, S. 2015. Transcriptomic analysis reveals the potential antioxidant pathways regulated by multiprotein bridging factor 1 (BbMBF1) in the fungal entomopathogen *Beauveria bassiana*. *Biocontrol Science and Technology*, 25 (11): 1346-1358.

Chutani, P. and Sharma, K. K. 2015. Biochemical evaluation of xylanases from various filamentous fungi and their application for the deinking of ozone treated newspaper pulp. *Carbohydrate Polymers*, 127: 54-63.

Cito, A., Barzanti, G. P., Strangi, A., Francardi, V., Zanfini, A. and Dreassi, E. 2016. Cuticle-degrading proteases and toxins as virulence markers of *Beauveria bassiana* (Balsamo) Vuillemin. *Journal of Basic Microbiology*, 56 (9): 941-948.

Cline, L. C., Schilling, J. S., Menke, J., Groenhof, E. and Kennedy, P. G. 2018. Ecological and functional effects of fungal endophytes on wood decomposition. *Functional Ecology*, 32 (1): 181-191.

Collins, T., Gerday, C. and Feller, G. 2005. Xylanases, xylanase families and extremophilic xylanases. *FEMS Microbiology Reviews*, 29 (1): 3-23.

Conejo-Saucedo, U., Cano-Camacho, H., Villa-Rivera, M. G., Lara-Márquez, A., López-Romero, E. and Zavala-Páramo, M. G. 2017. Protein homology modeling, docking, and phylogenetic analyses of an endo-1, 4-β-xylanase GH11 of *Colletotrichum lindemuthianum. Mycological Progress*, 16 (6): 577-591.

Confortin, T. C., Spannemberg, S. S., Todero, I., Luft, L., Brun, T., Alves, E. A., Kuhn, R. C. and Mazutti, M. A. 2019. Microbial enzymes as control agents of diseases and pests in organic agriculture. In: Gupta, V. K. and Pandey, A. eds. *New and Future Developments in Microbial Biotechnology and Bioengineering*. Amsterdam: Elsevier, 321-332.

Costa, E. M. d., Pimenta, F. C., Luz, C., Oliveira, V. d., Oliveira, M., Bueno, E. and Petrofeza, S. 2011. *Beauveria bassiana:* quercetinase production and genetic diversity. *Brazilian Journal of Microbiology*, 42 (1): 12-21.

Cytryńska, M., Wojda, I. and Jakubowicz, T. 2016. How insects combat infections. In: Ballarin. L and Cammarata, M. eds. *Lessons in Immunity*. New York: Elsevier, 117-128.

da Silva, W. J., Pilz-Júnior, H. L., Heermann, R. and da Silva, O. S. 2020. The great potential of entomopathogenic bacteria *Xenorhabdus* and *Photorhabdus* for mosquito control: a review. *Parasites & Vectors*, 13 (1): 1-14.

Dalvi, P. and Anthappan, P. 2007. Amylase and pectinase from single source for simultaneous desizing and scouring. *Indian Journal of Fibre and Textile Research* 32(4):459-465.

Dange, V. and Harke, S. 2018. Production and purification of pectinase by fungal strain in solid-state fermentation using agro-industrial bioproduct. *International Journal of Life Sciences Research* 6(4): 85-93.

Dannon, H. F., Dannon, A. E., Douro-Kpindou, O. K., Zinsou, A. V., Houndete, A. T., Toffa-Mehinto, J., Elegbede, I. M., Olou, B. D. and Manuele, T. 2020. Toward the efficient use of *Beauveria bassiana* in integrated cotton insect pest management. *Journal of Cotton Research*, 3 (1): 1-21.

Dar, R., Lotfy, D. and Moustafa, H. 2020. Field application of bio-insecticides on spiny bollworm, *Earias insulana* (Bosid.) on cotton by using recent low volume ground spraying equipment. *Egyptian Academic Journal of Biological Sciences. A, Entomology*, 13 (1): 47-57.

Das, A., Paul, T., Halder, S. K., Jana, A., Maity, C., Mohapatra, P. K. D., Pati, B. R. and Mondal, K. C. 2013. Production of cellulolytic enzymes by *Aspergillus fumigatus* ABK9 in wheat bran-rice straw mixed substrate and use of cocktail enzymes for deinking of waste office paper pulp. *Bioresource Technology*, 128: 290-296.

Das, K., Das, P., Parveen, A., Boro, R. C., Mudoi, A. and Roy, S. 2021. Molecular characterization of indigenous entomopathogenic fungus *Beauveria bassiana*, isolate and its virulence to *Corcyra cephalonica* (Stainton)(Lepidoptera: Pyralidae). *International Journal of Tropical Insect Science* 30 (96): 1-9.

De Beeck, M. O., Troein, C., Siregar, S., Gentile, L., Abbondanza, G., Peterson, C., Persson, P. and Tunlid, A. 2020. Regulation of fungal decomposition at single-cell level. *The ISME Journal*, 14 (4): 896-905.

de Carolina Sánchez-Pérez, L., Barranco-Florido, J. E., Rodríguez-Navarro, S. and Cervantes-Mayagoitia, J. F. 2014. Enzymes of entomopathogenic fungi, advances and insights. *Advances in Enzyme Research*, 02(02): 65-76.

de Cassia Pereira, J., Giese, E. C., de Souza Moretti, M. M., dos Santos Gomes, A. C., Perrone, O. M., Boscolo, M., da Silva, R., Gomes, E. and Martins, D. A. B. 2017. Effect of metal ions, chemical agents and organic compounds on lignocellulolytic enzymes activities. *Enzyme Inhibitors and Activators*, 29: 139-164.

de Castro, A. M., Castilho, L. R. and Freire, D. M. G. 2015. Multivariate optimization and supplementation strategies for the simultaneous production of amylases, cellulases, xylanases, and proteases by *Aspergillus awamori* under solid-state fermentation conditions. *Applied Biochemistry and Biotechnology*, 175 (3): 1588-1602.

de Faria, M. R. and Wraight, S. P. 2007. Mycoinsecticides and mycoacaricides: a comprehensive list with worldwide coverage and international classification of formulation types. *Biological Control*, 43 (3): 237-256.

deb Dutta, S., Tarafder, M., Islam, R. and Datta, B. 2018. Characterization of cellulolytic enzymes of *Fusarium* soil isolates. *Biocatalysis and Agricultural Biotechnology*, 14: 279-285.

Deepthi, B., Poornachandra Rao, K., Chennapa, G., Naik, M., Chandrashekara, K. and Sreenivasa, M. 2016. Antifungal attributes of *Lactobacillus plantarum* MYS6 against fumonisin producing *Fusarium proliferatum* associated with poultry feeds. *PLoS One*, 11 (6): e0155122.

Deng, Y., Xu, M., Ji, D. and Agyei, D. 2020. Optimization of β-galactosidase production by batch cultures of *Lactobacillus leichmannii* 313 (ATCC 7830™). *Fermentation*, 6 (1): 27.

Dereeper, A., Guignon, V., Blanc, G., Audic, S., Buffet, S., Chevenet, F., Dufayard, J.F., Guindon, S., Lefort, V. and Lescot, M. 2008. Phylogeny. fr: robust phylogenetic analysis for the non-specialist. *Nucleic Acids Research*, 36 (2): W465-W469.

Desai, D. I. and Iyer, B. D. 2016. Biodeinking of old newspaper pulp using a cellulase-free xylanase preparation of *Aspergillus niger* DX-23. *Biocatalysis and Agricultural Biotechnology*, 5: 78-85.

Devi, R., Madhavan Nampoothiri, K., Sukumaran, R. K., Sindhu, R. and Arumugam, M. 2020. Lipase of *Pseudomonas guariconesis* as an additive in laundry detergents and transesterification biocatalysts. *Journal of Basic Microbiology*, 60 (2): 112-125.

Deyhimi, F. and Nami, F. 2012. Peroxidase-catalyzed electrochemical assay of hydrogen peroxide: A ping–pong mechanism. *International Journal of Chemical Kinetics*, 44(10): 699-704.

Dhar, P. and Kaur, G. 2010. Effects of carbon and nitrogen sources on the induction and repression of chitinase enzyme from *Beauveria bassiana* isolates. *African Journal of Biotechnology*, 9 (47): 8092-8099.

Dhar, S., Jindal, V. and Gupta, V. 2016. Optimization of growth conditions and medium composition for improved conidiation of newly isolated *Beauveria bassiana* strains. *Indian Journal of Experimental Biology*, 54 (10): 634-643.

Dhar, S., Jindal, V., Jariyal, M. and Gupta, V. 2019. Molecular characterization of new isolates of the entomopathogenic fungus *Beauveria bassiana* and their efficacy against the tobacco caterpillar, *Spodoptera litura* (Fabricius)(Lepidoptera: Noctuidae). *Egyptian Journal of Biological Pest Control*, 29 (1): 8.

Dhawan, M. and Joshi, N. 2017. Enzymatic comparison and mortality of *Beauveria bassiana* against cabbage caterpillar *Pieris brassicae* LINN. *Brazilian Journal of Microbiology*, 48 (3): 522-529.

Ding, C., Li, M. and Hu, Y. 2018. High-activity production of xylanase by *Pichia stipitis*: Purification, characterization, kinetic evaluation and xylooligosaccharides production. *International Journal of Biological Macromolecules*, 117: 72-77.

Domingues, R. C., Junior, S. B., Silva, R. B., Madrona, G. S., Cardoso, V. L. and Reis, M. H. 2011. Evaluation of enzymatic pretreatment of passion fruit juice. *Chemical Engineering Transactions*, 24: 517-522.

Dong, W. X., Ding, J. L., Gao, Y., Peng, Y. J., Feng, M. G. and Ying, S. H. 2017. Transcriptomic insights into the alternative splicing-mediated adaptation of the entomopathogenic fungus *Beauveria bassiana* to host niches: autophagy-related gene 8 as an example. *Environmental Microbiology*, 19 (10): 4126-4139.

Doolotkeldieva, T., Bobusheva, S., Kulmanbetova, A., Zholdoshbekova, S. and Kyzy, A. A. 2019. Characterization of *Beauveria bassiana* isolates from Kyrgyzstan. *Journal of Invertebrate Pathology*, 167: 107243.

dos Reis, C. B. L., Sobucki, L., Mazutti, M. A., Guedes, J. V. C. and Jacques, R. J. S. 2018. Production of chitinase from *Metarhizium anisopliae* by solid-state fermentation using sugarcane bagasse as substrate. *Industrial Biotechnology*, 14 (4): 230-234.

Du, C. and van Wezel, G. P. 2018. Mining for microbial gems: integrating proteomics in the postgenomic natural product discovery pipeline. *Proteomics*, 18 (18): 1700332.

Du, F.Y., Li, X.M., Sun, Z.C., Meng, L.H. and Wang, B.G. 2020. Secondary metabolites with agricultural antagonistic potentials from *Beauveria felina*, a marine-derived entomopathogenic fungus. *Journal of Agricultural and Food Chemistry*, 68 (50): 14824-14831.

Du, R., Song, Q., Zhang, Q., Zhao, F., Kim, R.C., Zhou, Z. and Han, Y. 2018. Purification and characterization of novel thermostable and Ca-independent α-amylase produced by *Bacillus amyloliquefaciens* BH072. *International Journal of Biological Macromolecules*, 115: 1151-1156.

Dutra, T. R., Guimarães, V. M., Varela, E. M., da Silva Fialho, L., Milagres, A. M. F., Falkoski, D. L., Zanuncio, J. C. and de Rezende, S. T. 2017. A *Chrysoporthe cubensis* enzyme cocktail produced from a low-cost carbon source with high biomass hydrolysis efficiency. *Scientific Reports*, 7 (1): 1-9.

Dutt, D., Tyagi, C., Singh, R. and Kumar, A. 2012. Effect of enzyme concoctions on fiber surface roughness and deinking efficiency of sorted office paper. *Journal of Cellulose Chemical Technol*ogy, 46 (9-10): 611-623.

Dutta, B., Deska, J., Bandopadhyay, R. and Shamekh, S. 2021. *In silico* characterization of bacterial chitinase: illuminating its relationship with archaeal and eukaryotic cousins. *Journal of Genetic Engineering and Biotechnology*, 19 (1): 1-11.

Eide, K. B. and Sørlie, M. 2018. The effect of carbohydrate binding modules and linkers on inhibitor binding to family 18 glycoside hydrolases. *The Journal of Chemical Thermodynamics*, 125: 220-224.

Eisenthal, R., Danson, M. J. and Hough, D. W. 2007. Catalytic efficiency and $kcat/K_M$: a useful comparator? *Trends in Biotechnology*, 25 (6): 247-249.

Elawati, N., Pujiyanto, S. and Kusdiyantini, E. 2018. Production of extracellular chitinase *Beauveria bassiana* under submerged fermentation conditions. *In: Proceedings of Journal of Physics: Conference Series*. IOP Publishing, 012074.

Elkelawy, M., Bastawissi, H. A.E., Esmaeil, K. K., Radwan, A. M., Panchal, H., Sadasivuni, K. K., Suresh, M. and Israr, M. 2020. Maximization of biodiesel production from sunflower and soybean oils and prediction of diesel engine performance and emission characteriztics through response surface methodology. *Fuel*, 266: 117072.

Eneyskaya, E. V., Bobrov, K. S., Kashina, M. V., Borisova, A. S. and Kulminskaya, A. A. 2020. A novel acid-tolerant β-xylanase from *Scytalidium candidum* 3C for the synthesis of o-nitrophenyl xylooligosaccharides. *Journal of Basic Microbiology*, 60: 971-982.

Ern, K., Aron, H. A. H. and Eng, C. 2016. Comparison of total phenolic contents (tpc) and antioxidant activities of fresh fruit juices, commercial 100% fruit juices and fruit drinks. *Sains Malaysiana*, 45 (9): 1319-1327.

Espinoza, F., Vidal, S., Rautenbach, F., Lewu, F. and Nchu, F. 2019. Effects of *Beauveria bassiana* (Hypocreales) on plant growth and secondary metabolites of extracts of hydroponically cultivated chive (*Allium schoenoprasum* L. Amaryllidaceae). *Heliyon*, 5 (12): e03038.

Ezeilo, U. R., Wahab, R. A. and Mahat, N. A. 2020. Optimization studies on cellulase and xylanase production by *Rhizopus oryzae* UC2 using raw oil palm frond leaves as substrate under solid state fermentation. *Renewable Energy*, 156: 1301-1312.

Ezike, T. C., Udeh, J. O., Joshua, P. E., Ezugwu, A. L., Isiwu, C. V., Eze, S. O. and Chilaka, F. C. 2021. Substrate specificity of a new laccase from *Trametes polyzona* WRF03. *Heliyon*, 7 (1): e06080.

Fadel, M., AbdEl-Halim, S., Sharada, H., Yehia, A. and Ammar, M. 2020. Production of glucoamylase, α-amylase and cellulase by *Aspergillus oryzae* F-923 cultivated on wheat bran under solid state fermentation. *Journal of Advances in Biology and Biotechnology*, 23 (4): 8-22.

Fan, Y., Fang, W., Guo, S., Pei, X., Zhang, Y., Xiao, Y., Li, D., Jin, K., Bidochka, M. J. and Pei, Y. 2007a. Increased insect virulence in *Beauveria bassiana* strains overexpressing an engineered chitinase. *Applied Environmental Microbiolology*, 73 (1): 295-302.

Fan, Y., Zhang, Y., Yang, X., Pei, X., Guo, S. and Pei, Y. 2007b. Expression of a *Beauveria bassiana* chitinase (Bbchit1) in *Escherichia coli* and *Pichia pastoris*. *Protein Expression and Purification*, 56 (1): 93-99.

Fan, Y., Zhang, S., Kruer, N. and Keyhani, N. O. 2011. High-throughput insertion mutagenesis and functional screening in the entomopathogenic fungus *Beauveria bassiana. Journal of Invertebrate Pathology*, 106 (2): 274-279.

Fan, Y., Liu, X., Keyhani, N. O., Tang, G., Pei, Y., Zhang, W. and Tong, S. 2017. Regulatory cascade and biological activity of *Beauveria bassiana* oosporein that limits bacterial growth after host death. *Proceedings of the National Academy of Sciences*, 114 (9): E1578-E1586.

Fang, W., Leng, B., Xiao, Y., Jin, K., Ma, J., Fan, Y., Feng, J., Yang, X., Zhang, Y. and Pei, Y. 2005. Cloning of *Beauveria bassiana* chitinase gene Bbchit1 and its application to improve fungal strain virulence. *Applied Environmental Microbiolology*, 71 (1): 363-370.

Far, B. E., Ahmadi, Y., Khosroshahi, A. Y. and Dilmaghani, A. 2020. Microbial alpha-amylase production: progress, challenges and perspectives. *Advanced Pharmaceutical Bulletin*, 10 (3): 350.

Fargues, J., Goettel, M., Smits, N., Ouedraogo, A. and Rougier, M. 1997. Effect of temperature on vegetative growth of *Beauveria bassiana* isolates from different origins. *Mycologia*, 89 (3): 383-392.

Farooq, M. and Freed, S. 2018. Insecticidal activity of toxic crude proteins secreted by entomopathogenic fungi against *Musca domestica* L.(Diptera: Muscidae). *Kuwait Journal of Science*, 45 (2): 64-74.

Feng M, Ying S. 2002. Production of *Beauveria bassiana* amylase in liquid culture and activity influential facors. *Acta Microbiol Sinica*. 42:720–725.

Fernandes, E. G., Valério, H. M., Feltrin, T. and Sand, S. T. V. D. 2012. Variability in the production of extracellular enzymes by entomopathogenic fungi grown on different substrates. *Brazilian Journal of Microbiology*, 43 (2): 827-833.

Finn, R. D., Coggill, P., Eberhardt, R. Y., Eddy, S. R., Mistry, J., Mitchell, A. L., Potter, S. C., Punta, M., Qureshi, M. and Sangrador-Vegas, A. 2016. The Pfam protein families database: towards a more sustainable future. *Nucleic Acids Research*, 44 (D1): D279-D285.

Firouzbakht, H., Zibaee, A., Hoda, H. and Sohani, M. M. 2015. Purification and characterization of the cuticle-degrading proteases produced by an isolate of *Beauveria bassiana* using the cuticle of the predatory bug, *Andrallus spinidens* (Hemiptera: Pentatomidae). *Journal of Plant Protection Research*, 55 (2):179–186.

Fredriksen, L., Stokke, R., Jensen, M. S., Westereng, B., Jameson, J.-K., Steen, I. H. and Eijsink, V. G. H. 2019. Discovery of a thermostable GH10 xylanase with broad substrate specificity from the Arctic mid-ocean ridge vent system. *Applied and Environmental Microbiology*, 85 (6): e02970-02918.

Freour, P., Lahourcade, M. and Chomy, P. 1966. Les champignons *Beauveria* en pathologie humaine. A propos d'un cas alocalisation pulmonaire. *Press Med*, 74: 3317-3320.

Fu, L.H., Jiang, N., Li, C.X., Luo, X.-M., Zhao, S. and Feng, J.X. 2019. Purification and characterization of an endo-xylanase from *Trichoderma* sp., with xylobiose as the main product from xylan hydrolysis. *World Journal of Microbiology and Biotechnology*, 35 (11): 171.

Fuentes, M. E. and Quiñones, R. A. 2016. Carbon utilization profile of the filamentous fungal species *Fusarium fujikuroi*, *Penicillium decumbens,* and *Sarocladium strictum* isolated from marine coastal environments. *Mycologia*, 108 (6): 1069-1081.

Fuguet, R., Théraud, M. and Vey, A. 2004. Production in vitro of toxic macromolecules by strains of *Beauveria bassiana*, and purification of a chitosanase-like protein secreted by a melanizing isolate. *Comparative Biochemistry and Physiology Part C: Toxicology & Pharmacology*, 138 (2): 149-161.

Gafar, A., Khayat, M. E., Ahmad, S. A., Yasid, N. A. and Shukor, M. Y. 2020. Response surface methodology for the optimization of keratinase production in culture medium containing feathers by *Bacillus* sp. UPM-AAG1. *Catalysts*, 10 (8): 848.

Gama, A. R., Brito-Cunha, C. C. Q., Campos, I. T. N., de Souza, G. R. L., Carneiro, L. C. and Bataus, L. A. M. 2020. *Streptomyces thermocerradoensis* I3 secretes a novel

bifunctional xylanase/endoglucanase under solid-state fermentation. *Biotechnology Progress*, 36 (2): e2934.

Gamba, P. and Zenkin, N. 2018. Transcription fidelity and its roles in the cell. *Current Opinion in Microbiology*, 42: 13-18.

Gangwar, R., Rasool, S. and Mishra, S. 2020. Purified cellobiose dehydrogenase of *Termitomyces* sp. OE147 fuels cellulose degradation resulting in the release of reducing sugars. *Preparative Biochemistry and Biotechnology*: 1-9.

Gani, G., Naik, H., Jan, N., Bashir, O., Hussain, S. Z., Rather, A., Reshi, M. and Amin, T. 2020. Physicochemical and antioxidant properties of pear juice prepared through pectinase enzyme-assisted extraction from William Bartlett variety. *Journal of Food Measurement and Characterization*, 15: 743–757.

Gao, L., Gao, F., Zhang, D., Zhang, C., Wu, G. and Chen, S. 2013. Purification and characterization of a new β-glucosidase from *Penicillium piceum* and its application in enzymatic degradation of delignified corn stover. *Bioresource Technology*, 147: 658-661.

Gaur, R., Tiwari, S., Rai, P. and Srivastava, V. 2015. Isolation, production, and characterization of thermotolerant xylanase from solvent tolerant *Bacillus vallismortis* RSPP-15. *International Journal of Polymer Science*, 2015: 986324.

Gaviria, J., Parra, P. P. and Gonzales, A. 2020. Selection of strains of *Beauveria bassiana* and *Metarhizium anisopliae* (Ascomycota: Hypocreales) for endophytic colonization in coconut seedlings. *Chilean Journal of Agricultural & Animal Sciences*, 36 (1): 3-13.

Gelain, L., Pabst, M., da Cruz Pradella, J. G., da Costa, A. C., van der Wielen, L. and van Gulik, W. M. 2020. Analysis of the proteins secreted by *Trichoderma harzianum* P49P11 under carbon-limited conditions. *Journal of Proteomics*, 227: 103922.

Geourjon, C. and Deleage, G. 1995. SOPMA: significant improvements in protein secondary structure prediction by consensus prediction from multiple alignments. *Bioinformatics*, 11 (6): 681-684.

Ghafari, S., Aziz, H. A., Isa, M. H. and Zinatizadeh, A. A. 2009. Application of response surface methodology (RSM) to optimize coagulation–flocculation treatment of leachate using poly-aluminum chloride (PAC) and alum. *Journal of Hazardous Materials*, 163 (2-3): 650-656.

Ghosh, P. and Ghosh, U. 2019. Statistical optimization of laccase production by isolated strain *Aspergillus flavus* PUF5 utilising ribbed gourd peels as the substrate and enzyme application on apple juice clarification. *Indian Chemical Engineer*, 62:4, 427-438.

Ghosh, P., Pradhan, R. C. and Mishra, S. 2018. Clarification of jamun juice by centrifugation and microfiltration: analysis of quality parameters, operating conditions, and resistance. *Journal of Food Process Engineering*, 41 (1): e12603.

Gibson, D. M., Donzelli, B. G., Krasnoff, S. B. and Keyhani, N. O. 2014. Discovering the secondary metabolite potential encoded within entomopathogenic fungi. *Natural Product Reports*, 31 (10): 1287-1305.

Goettig, P. 2016. Effects of glycosylation on the enzymatic activity and mechanisms of proteases. *International Journal of Molecular Sciences*, 17 (12): 1969.

Gonçalves, E. C. S., Pérez, M. M., Vici, A. C., Salgado, J. C. S., de Souza Rocha, M., de Almeida, P. Z., da Conceição Infante, J., de Almeida Scarcella, A. S., de Lucas, R. C. and Vieira, A. T. 2020. Potential biodiesel production from Brazilian plant oils and spent coffee grounds by *Beauveria bassiana* lipase 1 expressed in *Aspergillus nidulans* A773 using different agroindustry inputs. *Journal of Cleaner Production*, 256: 120513.

Goughenour, K. D., Whalin, J., Slot, J. and Rappleye, C. A. 2020. Diversification of fungal chitinases and their functional differentiation in *Histoplasma capsulatum*. *Molecular Biology and Evolution*, (38) 4: 1339-1355.

Gouripur, G. C., Kaliwal, R. B. and Kaliwal, B. B. 2016. *In silico* characterization of beta-galactosidase using computational tools. *Journal of Bioinformatics and Sequence Analysis*, 8 (1): 1-11.

Gray, L. and Kernaghan, G. 2020. Fungal succession during the decomposition of ectomycorrhizal fine roots. *Microbial Ecology*, 79 (2): 271-284.

Grizanova, E. V., Coates, C. J., Dubovskiy, I. M. and Butt, T. M. 2019. *Metarhizium brunneum* infection dynamics differ at the cuticle interface of susceptible and tolerant morphs of *Galleria mellonella*. *Virulence*, 10 (1): 999-1012.

Grogan, G. J. and Holland, H. L. 2000. The biocatalytic reactions of *Beauveria* spp. *Journal of Molecular Catalysis B: Enzymatic*, 9 (1-3): 1-32.

Grosse-Holz, F., Kelly, S., Blaskowski, S., Kaschani, F., Kaiser, M. and van der Hoorn, R. A. 2018. The transcriptome, extracellular proteome and active secretome of agroinfiltrated *Nicotiana benthamiana* uncover a large, diverse protease repertoire. *Plant Biotechnology Journal*, 16 (5): 1068-1084.

Gryta, A., Frąc, M. and Oszust, K. 2020. Genetic and metabolic diversity of soil microbiome in response to exogenous organic matter amendments. *Agronomy*, 10 (4): 546.

Gu, C.X., Zhang, B.L., Bai, W.W., Liu, J., Zhou, W., Ling, Z.Q., Lu, Y., Xu, L. and Wan, Y.J. 2020. Characterization of the endothiapepsin-like protein in the entomopathogenic fungus *Beauveria bassiana* and its virulence effect on the silkworm, *Bombyx mori*. *Journal of Invertebrate Pathology*, 169: 107277.

Gu, Q., Duan, G. and Yu, X. 2019. Bioconversion of flavonoid glycosides from *Hippophae rhamnoides* leaves into flavonoid aglycones by *Eurotium amstelodami*. *Microorganisms*, 7 (5): 122.

Gu, X., Gui, Y., Li, J., Zhang, X. and Zilda, D. S. 2021. Identification and characterization of a novel alkali- and high temperature-tolerant lipase (Lip4346) from a macroalgae-associated bacterial strain. *Journal of Ocean University of China*, 20 (1): 181-188.

Gui, Y.J., Zhang, W.Q., Zhang, D.-D., Zhou, L., Short, D. P., Wang, J., Ma, X.F., Li, T.G., Kong, Z.Q. and Wang, B.-L. 2018. A *Verticillium dahliae* extracellular cutinase

modulates plant immune responses. *Molecular Plant-Microbe Interactions*, 31 (2): 260-273.

Guillaume, A., Thorigné, A., Carré, Y., Vinh, J. and Levavasseur, L. 2019. Contribution of proteases and cellulases produced by solid-state fermentation to the improvement of corn ethanol production. *Bioresources and Bioprocessing*, 6 (1): 7.

Guimarães, L. H. S., Peixoto-Nogueira, S. C., Michelin, M., Rizzatti, A. C. S., Sandrim, V. C., Zanoelo, F. F., Aquino, A. C. M., Junior, A. B. and Polizeli, M. D. L. 2006. Screening of filamentous fungi for production of enzymes of biotechnological interest. *Brazilian Journal of Microbiology*, 37 (4): 474-480.

Gupta, C. L., Akhtar, S. and Bajpai, P. 2014. *In silico* protein modeling: possibilities and limitations. *EXCLI journal*, 13: 513-515.

Gupta, M. N. 1992. Enzyme function in organic solvents. *European Journal of Biochemistry*, 203 (1-2): 25-32.

Gupta, V., Garg, S., Capalash, N., Gupta, N. and Sharma, P. 2015. Production of thermo-alkali-stable laccase and xylanase by co-culturing of *Bacillus* sp. and *B. halodurans* for biobleaching of kraft pulp and deinking of waste paper. *Bioprocess and Biosystems Engineering*, 38 (5): 947-956.

Haddad, Y., Adam, V. and Heger, Z. 2020. Ten quick tips for homology modeling of high-resolution protein 3D structures. *PLoS Computational Biology*, 16 (4): e1007449.

Hage, H. and Rosso, M.N., 2021. Evolution of fungal carbohydrate-active enzyme portfolios and adaptation to plant cell-wall polymers. *Journal of Fungi*, 7(3):185.

Hagspiel, K., Haab, D. and Kubicek, C. P. 1989. Protease activity and proteolytic modification of cellulases from a *Trichoderma reesei* QM 9414 selectant. *Applied Microbiology and Biotechnology*, 32 (1): 61-67.

Hamid, A. and Aftab, M. N. 2019. Cloning, purification, and characterization of recombinant thermostable β-xylanase Tnap_0700 from *Thermotoga naphthophila*. *Applied Biochemistry and Biotechnology*, 189 (4): 1274-1290.

Hammami, A., Bayoudh, A., Hadrich, B., Abdelhedi, O., Jridi, M. and Nasri, M. 2020. response-surface methodology for the production and the purification of a new H_2O_2-tolerant alkaline protease from *Bacillus invictae* AH1 strain. *Biotechnology Progress*, e2965.

Harith-Fadzilah, N., Abd Ghani, I. and Hassan, M., 2020. Omics-based approach in characterising mechanisms of entomopathogenic fungi pathogenicity: A case example of *Beauveria bassiana*. *Journal of King Saud University-Science*, 101332.

Hartree, E. 1972. Detennination of protein: A modification of the Lowry method. *Analytical Biochem*istry, 48: 422-427.

Hassan, M. A., Abol-Fotouh, D., Omer, A. M., Tamer, T. M. and Abbas, E. 2020. Comprehensive insights into microbial keratinases and their implication in various biotechnological and industrial sectors: a review. *International Journal of Biological Macromolecules*, 154: 567-583.

Hassan, N., Rafiq, M., Rehman, M., Sajjad, W., Hasan, F. and Abdullah, S. 2019. Fungi in acidic fire: a potential source of industrially important enzymes. *Fungal Biology Reviews*, 33 (1): 58-71.

Havukkala, I., Mitamura, C., Hara, S., Hirayae, K., Nishizawa, Y. and Hibi, T. 1993. Induction and purification of *Beauveria bassiana* chitinolytic enzymes. *Journal of Invertebrate Pathology*, 61 (1): 97-102.

Henke, M. O., de Hoog, G. S., Gross, U., Zimmermann, G., Kraemer, D. and Weig, M. 2002. Human deep tissue infection with an entomopathogenic *Beauveria* species. *Journal of Clinical Microbiology*, 40 (7): 2698-2702.

Herlet, J., Schwarz, W. H., Zverlov, V. V., Liebl, W. and Kornberger, P. 2018. Addition of β-galactosidase boosts the xyloglucan degradation capability of endoglucanase Cel9D from *Clostridium thermocellum*. *Biotechnology for Biofuels*, 11 (1): 1-6.

Hettiarachchi, S. A., Kwon, Y.K., Lee, Y., Jo, E., Eom, T.Y., Kang, Y.H., Kang, D.H., De Zoysa, M., Marasinghe, S. D. and Oh, C. 2019. Characterization of an acetyl xylan esterase from the marine bacterium *Ochrovirga pacifica* and its synergism with xylanase on beechwood xylan. *Microbial Cell Factories*, 18 (1): 122.

Holder, D. J. and Keyhani, N. O. 2005. Adhesion of the entomopathogenic fungus *Beauveria* (*Cordyceps*) *bassiana* to substrata. *Applied and Environmental Microbiology*, 71 (9): 5260-5266.

Holder, D. J., Kirkland, B. H., Lewis, M. W. and Keyhani, N. O. 2007. Surface characteriztics of the entomopathogenic fungus *Beauveria* (*Cordyceps*) *bassiana*. *Microbiology*, 153 (10): 3448-3457.

Hoog, G. D. 1972. The genera *Beauveria, Isaria, Tritirachium* and *Acrodontium* gen. nov. *Studies in Mycology*, 1: 1-41.

Hou, Q., Bourgeas, R., Pucci, F. and Rooman, M. 2018. Computational analysis of the amino acid interactions that promote or decrease protein solubility. *Scientific Reports*, 8 (1): 14661.

Houfani, A. A., Anders, N., Spiess, A. C., Baldrian, P. and Benallaoua, S. 2020. Insights from enzymatic degradation of cellulose and hemicellulose to fermentable sugars–a review. *Biomass and Bioenergy*, 134: 105481.

Hu, Q., Li, F. and Zhang, Y. 2016. Risks of mycotoxins from mycoinsecticides to humans. *BioMed Research International*, 2016: 3194321.

Huang, J., Ou, Y., Zhang, D., Zhang, G. and Pan, Y. 2018. Optimization of the culture condition of *Bacillus mucilaginous* using *Agaricus bisporus* industrial wastewater by

Plackett–Burman combined with Box–Behnken response surface method. *AMB Express*, 8 (1): 141.

Huang, P., Jiang, X., Wu, B. and Sun, J. 2020. *Aspergillus jilinensis* sp. nov. and its thermostable alkaline enzymes evaluation. *Mycoscience*, 61 (5): 205-211.

Huang, Q.S., Xie, X.L., Liang, G., Gong, F., Wang, Y., Wei, X.Q., Wang, Q., Ji, Z.L. and Chen, Q.X. 2011. The GH18 family of chitinases: their domain architectures, functions and evolutions. *Glycobiology*, 22 (1): 23-34.

Huang, X., Ge, J., Fan, J., Xu, X. C. X., Li, J., Zhang, Y. and Zhou, D. 2013. Characterization and optimization of xylanase and endoglucanase production by *Trichoderma viride* HG 623 using response surface methodology (RSM). *African Journal of Microbiology Research*, 7 (36): 4521-4532.

Huang, Y., Zheng, X., Pilgaard, B., Holck, J., Muschiol, J., Li, S. and Lange, L. 2019. Identification and characterization of GH11 xylanase and GH43 xylosidase from the chytridiomycetous fungus, *Rhizophlyctis rosea*. *Applied Microbiology and Biotechnology*, 103 (2): 777-791.

Ibrahim, H. M., Kusch, S., Didelon, M. and Raffaele, S. 2021. Genome-wide alternative splicing profiling in the fungal plant pathogen *Sclerotinia sclerotiorum* during the colonization of diverse host families. *Molecular Plant Pathology*, 22 (1): 31-47.

Ibrahim, R., Alahmadi, S., Binnaser, Y. S. and Shawer, D. 2019. Seasonal prevalence and histopathology of *Beauveria bassiana* infecting larvae of the leopard moth, *Zeuzera pyrina* L. (Lepidoptera: Cossidae). *Egyptian Journal of Biological Pest Control*, 29 (1): 65.

Idicula-Thomas, S. and Balaji, P. V. 2005. Understanding the relationship between the primary structure of proteins and its propensity to be soluble on overexpression in *Escherichia coli*. *Protein Science*, 14 (3): 582-592.

Iqbal, M., Dubey, M., Broberg, A., Viketoft, M., Jensen, D. F. and Karlsson, M. 2019. Deletion of the nonribosomal peptide synthetase gene nps1 in the fungus *Clonostachys rosea* attenuates antagonism and biocontrol of plant pathogenic *Fusarium* and Nematodes. *Phytopathology*, 109 (10): 1698-1709.

Iram, A., Cekmecelioglu, D. and Demirci, A. 2020. Screening of bacterial and fungal strains for cellulase and xylanase production using distillers' dried grains with solubles (DDGS) as the main feedstock. *Biomass Conversion and Biorefinery*, 2020.

Jaber, L. R. and Ownley, B. H. 2018. Can we use entomopathogenic fungi as endophytes for dual biological control of insect pests and plant pathogens? *Biological Control*, 116: 36-45.

Jami, M.S., García-Estrada, C., Barreiro, C., Cuadrado, A.A., Salehi-Najafabadi, Z. and Martín, J.F. 2010. The *Penicillium chrysogenum* extracellular proteome. conversion from a food-rotting strain to a versatile cell factory for white biotechnology. *Molecular and Cellular Proteomics*, 9 (12): 2729-2744.

Jaronski, S. and Mascarin, G. 2017. Mass production of fungal entomopathogens. In: Lacey, L. A. ed. *Microbial control of insect and mite pests*. New York: Elsevier, 141-155.

Jasni, A. B., Kamyab, H., Chelliapan, S., Arumugam, N., Krishnan, S. and Din, M. F. M. 2020. Treatment of wastewater using response surface methodology: a brief review. *Chemical Engineering Transactions*, 78: 535-540.

Jeffs, L. B. and Khachatourians, G. G. 1997. Toxic properties of *Beauveria* pigments on erythrocyte membranes. *Toxicon*, 35 (8): 1351-1356.

Jensen, R. E., Cabral, C., Enkegaard, A. and Steenberg, T. 2020. Influence of the plant interacting entomopathogenic fungus *Beauveria bassiana* on parasitoid host choice-behavior, development, and plant defense pathways. *PLoS One*, 15 (9): e0238943.

Jensen, R. E., Enkegaard, A. and Steenberg, T. 2019. Increased fecundity of *Aphis fabae* on *Vicia faba* plants following seed or leaf inoculation with the entomopathogenic fungus *Beauveria bassiana*. *PLoS One*, 14 (10): e0223616.

Jeon, J., Lee, G.W., Kim, K.T., Park, S.Y., Kim, S., Kwon, S., Huh, A., Chung, H., Lee, D.Y. and Kim, C.Y. 2020. Transcriptome profiling of the rice blast *fungus Magnaporthe oryzae* and its host *Oryza sativa* during infection. *Molecular Plant-Microbe Interactions*, 33 (2): 141-144.

Jiang, G.H., Kim, Y.M., Nam, S.H., Yim, S.H. and Eun, J.B. 2016. Enzymatic browning inhibition and antioxidant activity of pear juice from a new cultivar of asian pear (*Pyrus pyrifolia* Nakai cv. Sinhwa) with different concentrations of ascorbic acid. *Food Science and Biotechnology*, 25 (1): 153-158.

Jiménez, D. J., Maruthamuthu, M. and van Elsas, J. D. 2015. Metasecretome analysis of a lignocellulolytic microbial consortium grown on wheat straw, xylan and xylose. *Biotechnology for Biofuels*, 8 (1): 199.

John, J., Kaimal, K. K. S., Smith, M. L., Rahman, P. K. S. M. and Chellam, P. V. 2020. Advances in upstream and downstream strategies of pectinase bioprocessing: a review. *International Journal of Biological Macromolecules*, 162: 1086-1099.

Jović, J., Hao, J., Kocić-Tanackov, S. and Mojović, L. 2020. Improvement of lignocellulosic biomass conversion by optimization of fungal ligninolytic enzyme activity and molasses stillage supplementation. *Biomass Conversion and Biorefinery*: 1-17.

Juwon, A. D. and Emmanuel, O. F. 2012. Experimental investigations on the effects of carbon and nitrogen sources on concomitant amylase and polygalacturonase production by *Trichoderma viride* BITRS-1001 in submerged fermentation. *Biotechnology Research International*, 2012

Kamala Kumari, P., Sankar, G. G. and Prabhakar, T. 2015. Strain improvement studies for the production of L-asparaginase by *Beauveria bassiana* SS18/41. *International Journal Pharmaceutical Science and Research*, 31 (2): 173-176.

Kareem, S., Akpan, I., Popoola, T. and Sanni, L. 2011. Activated charcoal-a potential material in glucoamylase recovery. *Enzyme Research*, 2011: 483943.

Karthikeyan, A., Shanthi, V. and Nagasathya, A. 2008. Effect of different media and pH on the growth of *Beauveria bassiana* and its parasitism on leaf eating caterpillars. *Research Journal of Agriculture and Biological Sciences*, 4(2): 117-119.

Kaur, J., Duan, S. Y., Vaas, L. A., Penesyan, A., Meyer, W., Paulsen, I. T. and Nevalainen, H. 2015. Phenotypic profiling of *Scedosporium aurantiacum*, an opportunistic pathogen colonizing human lungs. *PLoS One*, 10 (3): e0122354.

Kaushal, J., Mehandia, S., Singh, G., Raina, A. and Arya, S. K. 2018. Catalase enzyme: application in bioremediation and food industry. *Biocatalysis and Agricultural Biotechnology*, 16: 192-199.

Kavuthodi, B. and Sebastian, D. 2018. Review on bacterial production of alkaline pectinase with special emphasis on *Bacillus* species. *Bioscience Biotechnology Research Communications*, 11 (1): 18-30.

Kawaguchi, H., Uematsu, K., Ogino, C., Teramura, H., Niimi-Nakamura, S., Tsuge, Y., Hasunuma, T., Oinuma, K.-I., Takaya, N. and Kondo, A. 2014. Simultaneous saccharification and fermentation of kraft pulp by recombinant *Escherichia coli* for phenyllactic acid production. *Biochemical Engineering Journal*, 88: 188-194.

Kawano, A., Matsumoto, Y., Nikaido, N., Tominaga, A., Tonozuka, T., Totani, K. and Yasutake, N. 2019. A novel α-glucosidase of the glycoside hydrolase family 31 from *Aspergillus sojae*. *Journal of Applied Glycoscience*, 66 (2): 73-81.

KC, S., Upadhyaya, J., Joshi, D. R., Lekhak, B., Kumar Chaudhary, D., Raj Pant, B., Raj Bajgai, T., Dhital, R., Khanal, S. and Koirala, N. 2020. Production, characterization, and industrial application of pectinase enzyme isolated from fungal strains. *Fermentation*, 6 (2): 59.

Keerthi, T., Suresh, P., Sabu, A., Rajeevkumar, S. and Chandrasekaran, M. 1999. Extracellular production of L-glutaminase by alkalophilic *Beauveria bassiana* BTMF S10 isolated from marine sediment. *World Journal of Microbiology and Biotechnology*, 15 (6): 751-752.

Keller, M. B., Sørensen, T. H., Krogh, K. B., Wogulis, M., Borch, K. and Westh, P. 2020. Activity of fungal β-glucosidases on cellulose. *Biotechnology for Biofuels*, 13 (1): 1-7.

Kepenekci, I., Saglam, H., Oksal, E., Yanar, D. and Yanar, Y. 2017. Nematicidal activity of *Beauveria bassiana* (Bals.-Criv.) Vuill. against root-knot nematodes on tomato grown under natural conditions. *Egyptian Journal of Biological Pest Control*, 27 (1): 117-120.

Keshk, S. M. 2016. Cellulase application in enzymatic hydrolysis of biomass. In: Gupta, V. *New and future developments in microbial biotechnology and bioengineering*. Amsterdam: Elsevier, 185-191.

Keswani, C., Singh, S. P. and Singh, H. B. 2013. *Beauveria bassiana*: status, mode of action, applications and safety issues. *Biotech Today*, 3 (1): 16-20.

Keyhani, N. O. 2018. Lipid biology in fungal stress and virulence: entomopathogenic fungi. *Fungal Biology*, 122 (6): 420-429.

Khamessan, A., Kermasha, S. and Marsot, P. 1994. Effects of polar organic solvents on the biocatalysis of chlorophyllase in a biphasic organic system. *Bioscience, Biotechnology and Biochemistry*, 58 (11): 1947-1952.

Khan, A., Khan, H., Faheem, M., Zeb, A., Badshah, M. and Chung, Y. R. 2021. Isolation and characterization of an acidic, salt-tolerant endoglucanase cel5a from a bacterial strain *Martelella endophytica* YC6887 genome. *Molecular Biotechnology*, 63(4): 305-315.

Khan, F. I., Govender, A., Permaul, K., Singh, S. and Bisetty, K. 2015. Thermostable chitinase II from *Thermomyces lanuginosus* SSBP: cloning, structure prediction and molecular dynamics simulations. *Journal of Theoretical Biology*, 374: 107-114.

Khonsanit, A., Luangsaard, J. J., Thanakitpipattana, D., Noisripoom, W., Chaitika, T. and Kobmoo, N. 2020. Cryptic diversity of the genus *Beauveria* with a new species from Thailand. *Mycological Progress*, 19 (4): 291-315.

Kidibule, P. E., Santos-Moriano, P., Plou, F. J. and Fernández-Lobato, M. 2020. Endo-chitinase Chit33 specificity on different chitinolytic materials allows the production of unexplored chitooligosaccharides with antioxidant activity. *Biotechnology Reports*, 27: e00500.

Kim, J., Clark, D. S. and Dordick, J. S. 2000. Intrinsic effects of solvent polarity on enzymic activation energies. *Biotechnology and Bioengineering*, 67 (1): 112-116.

Kim, J. C., Lee, M. R., Kim, S., Lee, S. J., Park, S. E., Baek, S., Gasmi, L., Shin, T. Y. and Kim, J. S. 2019. Long-term storage stability of *Beauveria bassiana* ERL836 granules as fungal biopesticide. *Journal of Asia-Pacific Entomology*, 22 (2): 537-542.

Kim, J. S. and Je, Y. H. 2010. A novel biopesticide production: attagel-mediated precipitation of chitinase from *Beauveria bassiana* SFB-205 supernatant for thermotolerance. *Applied Microbiology and Biotechnology*, 87 (5): 1639-1648.

Kim, J. S., Lee, Y. and Kim, T. H. 2016. A review on alkaline pretreatment technology for bioconversion of lignocellulosic biomass. *Bioresource Technology*, 199: 42-48.

Kim, S., Lee, S. J., Nai, Y.S., Yu, J. S., Lee, M. R., Yang, Y.T. and Kim, J. S. 2016. Characterization of T-DNA insertion mutants with decreased virulence in the entomopathogenic fungus *Beauveria bassiana* JEF-007. *Applied Microbiology and Biotechnology*, 100 (20): 8889-8900.

Kim, Y. J., Choi, S. Y., Kim, J., Jin, K. S., Lee, S. Y. and Kim, K. J. 2017. Structure and function of the N-terminal domain of *Ralstonia eutropha* polyhydroxyalkanoate synthase, and the proposed structure and mechanisms of the whole enzyme. *Biotechnology Journal*, 12 (1): 1600649.

Klibanov, A. M. 2001. Improving enzymes by using them in organic solvents. *Nature*, 409 (6817): 241-246.

Knob, A. and Carmona, E. C. 2010. Purification and characterization of two extracellular xylanases from *Penicillium sclerotiorum*: a novel acidophilic xylanase. *Applied Biochemistry and Biotechnology*, 162 (2): 429-443.

Kohli, I., Joshi, N. C. and Varma, A. 2020. Production, purification and applications of raw starch degrading and calcium-independent α-amylase from soil rich in extremophile. *International Journal of Biological Macromolecules*, 162: 873-881.

Konada, R. S. R., Krishnapati, L. S., Ashapogu, V., Lin, C.-H. and Nadimpalli, S. K. 2020. Comparative analysis of β-hexosaminidase and acid phosphatase from *Hydra vulgaris* Ind-Pune, *H. vulgaris* Naukuchiatal and *H. magnipapillata* sf-1: localization studies of acid phosphatase and β-hexosaminidase from *H. vulgaris* Ind-Pune. *Comparative Biochemistry and Physiology Part B: Biochemistry and Molecular Biology*, 239: 110365.

Kracher, D. and Ludwig, R. 2016. Cellobiose dehydrogenase: An essential enzyme for lignocellulose degradation in nature–A review/cellobiosedehydrogenase. *Journal of Land Management, Food and Environment*, 67 (3): 145-163.

Krause, A., Ramakumar, A., Bartels, D., Battistoni, F., Bekel, T., Boch, J., Böhm, M., Friedrich, F., Hurek, T. and Krause, L. 2006. Complete genome of the mutualistic, N 2-fixing grass endophyte *Azoarcus* sp. strain BH72. *Nature Biotechnology*, 24 (11): 1384-1390.

Krogh, A., Larsson, B., Von Heijne, G. and Sonnhammer, E. L. 2001. Predicting transmembrane protein topology with a hidden Markov model: application to complete genomes. *Journal of Molecular Biology*, 305 (3): 567-580.

Kubicek, C.P. and Kubicek, E.M., 2016. Enzymatic deconstruction of plant biomass by fungal enzymes. *Current Opinion in Chemical Biology*, 35: 51-57.

Kucharska, K., Rybarczyk, P., Hołowacz, I., Łukajtis, R., Glinka, M. and Kamiński, M. 2018. Pretreatment of lignocellulosic materials as substrates for fermentation processes. *Molecules*, 23 (11): 2937.

Kumar, D., Ladaniya, M. S., Gurjar, M., Mendke, S. and Kumar, S. 2020. Osmotic membrane distillation for retention of antioxidant potential in Nagpur mandarin (*Citrus reticulata* Blanco) fruit juice concentrate. *Journal of Food Process Engineering*, 43 (1): e13096.

Kumar, M., Verma, S., Gazara, R. K., Kumar, M., Pandey, A., Verma, P. K. and Thakur, I. S. 2018a. Genomic and proteomic analysis of lignin degrading and polyhydroxyalkanoate accumulating β-proteobacterium *Pandoraea* sp. ISTKB. *Biotechnology for Biofuels*, 11 (1): 154.

Kumar, N. V., Rani, M. E., Gunaseeli, R. and Kannan, N. 2018b. Paper pulp modification and deinking efficiency of cellulase-xylanase complex from *Escherichia coli* SD5. *International Journal of Biological Macromolecules*, 111: 289-295.

Kumar, V. and Satyanarayana, T. 2014. Production of endoxylanase with enhanced thermostability by a novel polyextremophilic *Bacillus halodurans* TSEV1 and its applicability in waste paper deinking. *Process Biochemistry*, 49 (3): 386-394.

Kuzhuppillymyal-Prabhakarankutty, L., Tamez-Guerra, P., Gomez-Flores, R., Rodriguez-Padilla, M. C. and Ek-Ramos, M. J. 2020. Endophytic *Beauveria bassiana* promotes drought tolerance and early flowering in corn. *World Journal of Microbiology and Biotechnology*, 36 (3): 1-10.

Kyamuhangire, W., Myhre, H., Sørensen, H. T. and Pehrson, R. 2002. Yield, characteriztics and composition of banana juice extracted by the enzymatic and mechanical methods. *Journal of the Science of Food and Agriculture*, 82 (4): 478-482.

Kyte, J. and Doolittle, R. F. 1982. A simple method for displaying the hydropathic character of a protein. *Journal of Molecular Biology*, 157 (1): 105-132.

Lacey, L. A. 2017. Entomopathogens used as microbial control agents. In: Lacey, L. A. (ed). *Microbial control of insect and mite pests*. 1st ed. London:Elsevier, 3-12.

Lachowicz, S., Oszmiański, J. and Kolniak-Ostek, J. 2018. Influence of different pectinolytic enzymes on bioactive compound content, antioxidant potency, colour and turbidity of chokeberry juice. *European Food Research and Technology*, 244 (11): 1907-1920.

Ladeira Ázar, R. I. S., da Luz Morales, M., Piccolo Maitan-Alfenas, G., Falkoski, D. L., Ferreira Alfenas, R. and Guimarães, V. M. 2020. Apple juice clarification by a purified polygalacturonase from *Calonectria pteridis*. *Food and Bioproducts Processing*, 119: 238-245.

Laemmli, U. 1979. Slab gel electrophoresis: SDS-PAGE with discontinuous buffers. *Nature*, 227: 680-685.

Lai, Y., Chen, H., Wei, G., Wang, G., Li, F. and Wang, S. 2017. *In vivo* gene expression profiling of the entomopathogenic fungus *Beauveria bassiana* elucidates its infection stratagems in anopheles mosquito. *Science China Life Sciences*, 60 (8): 839-851.

Lakshmidevi, R. and Muthukumar, K. 2010. Enzymatic saccharification and fermentation of paper and pulp industry effluent for biohydrogen production. *International Journal of Hydrogen Energy*, 35 (8): 3389-3400.

Lamounier, K. F., Rodrigues, P. O., Pasquini, D. and Baffi, M. A. 2018. Saccharification of sugarcane bagasse using an enzymatic extract produced by *Aspergillus fumigatus*. *Journal of Renewable Materials*, 6 (2): 169-175.

Lee, S. J., Lee, M. R., Kim, S., Kim, J. C., Park, S. E., Li, D., Shin, T. Y., Nai, Y.S. and Kim, J. S. 2018. Genomic analysis of the insect-killing fungus *Beauveria bassiana* JEF-007 as a biopesticide. *Scientific Reports*, 8 (1): 1-12.

Lee, S. R., Küfner, M., Park, M., Jung, W. H., Choi, S. U., Beemelmanns, C. and Kim, K. H. 2019. Beauvetetraones A–C, phomaligadione-derived polyketide dimers from the entomopathogenic fungus, *Beauveria bassiana*. *Organic Chemistry Frontiers*, 6 (2): 162-166.

Lee, S., Ricachenevsky, F.K. and Punshon, T., 2021. Functional overlap of two major facilitator superfamily transporter, ZIF1, and ZIFL1 in zinc and iron homeostasis. *Biochemical and Biophysical Research Communications*, 560: 7-13.

Lemoine, M., Engl, T. and Kaltenpoth, M. 2020. Microbial symbionts expanding or constraining abiotic niche space in insects. *Current Opinion in Insect Science*, 39: 14-20.

Leopold, J. and Samsˇinˇáková, A. 1970. Quantitative estimation of chitinase and several other enzymes in the fungus *Beauveria bassiana*. *Journal of Invertebrate Pathology*, 15 (1): 34-42.

Levetin, E., Horner, W. E., Scott, J. A., Barnes, C., Baxi, S., Chew, G. L., Grimes, C., Kennedy, K., Larenas-Linnemann, D. and Miller, J. D. 2016. Taxonomy of allergenic fungi. *The Journal of Allergy and Clinical Immunology: In Practice*, 4 (3): 375-385.

Li, J., Xu, X., Shi, P., Liu, B., Zhang, Y. and Zhang, W. 2017. Overexpression and characterization of a novel endo-β-1, 3 (4)-glucanase from thermophilic fungus *Humicola insolens* Y1. *Protein Expression and Purification*, 138: 63-68.

Li, Q., Loman, A. A., Callow, N. V., Islam, S. M. M. and Ju, L.K. 2018a. Leveraging pH profiles to direct enzyme production (cellulase, xylanase, polygalacturonase, pectinase, α-galactosidase, and invertase) by *Aspergillus foetidus*. *Biochemical Engineering Journal*, 137: 247-254.

Li, Q., Sun, B., Li, X., Xiong, K., Xu, Y., Yang, R., Hou, J. and Teng, C. 2018b. Improvement of the catalytic characteriztics of a salt-tolerant GH10 xylanase from *Streptomyce rochei* L10904. *International Journal of Biological Macromolecules*, 107: 1447-1455.

Li, Y. and Wilson, D. B. 2008. Chitin binding by *Thermobifida fusca* cellulase catalytic domains. *Biotechnology and Bioengineering*, 100 (4): 644-652.

Li, Z., Chen, S., Wang, Y., Liu, Z., Xia, Z., Zhang, M., Luo, X., Song, Y., Zhao, J. and Zhang, T. 2020. Biochemical characterization of a novel halo/organic-solvents/final-

products tolerant GH39 xylosidase from saline soil and its synergic action with xylanase. *International Journal of Biological Macromolecules*, 164: 184-192.

Lin, H., Sun, M.J., Li, J.H., Xu, Q.M., Yang, B., Wang, Q., Xie, W.J., Sun, S.J., Hu, K.H. and Zhang, L.Y. 2018. Purification and characterization of xylanase from spent mushroom compost and its application in saccharification of biomass wastes. *BioResources*, 13 (1): 220-230.

Lin, J., Ndlovu, L. M., Singh, S. and Pillay, B. 1999. Purification and biochemical characteriztics of β-D-xylanase from a thermophilic fungus, *Thermomyces lanuginosus* SSBP. *Biotechnology and Applied Biochemistry*, 30 (1): 73-79.

Litwin, A., Nowak, M. and Różalska, S. 2020b. Entomopathogenic fungi: unconventional applications. *Reviews in Environmental Science and BioTechnology*, 19 (1): 23-42.

Liu, Q., Ying, S.-H. and Feng, M.-G. 2011. Characterization of *Beauveria bassiana* neutral trehalase (BbNTH1) and recognition of crucial stress-responsive elements to control its expression in response to multiple stresses. *Microbiological Research*, 166 (4): 282-293.

Liu, S., Shao, S., Li, L., Cheng, Z., Tian, L., Gao, P. and Wang, L. 2015. Substrate-binding specificity of chitinase and chitosanase as revealed by active-site architecture analysis. *Carbohydrate Research*, 418: 50-56.

Liu, T., Wang, L., Duan, Y.-X. and Wang, X. 2008. Nematicidal activity of culture filtrate of *Beauveria bassiana* against *Meloidogyne hapla*. *World Journal of Microbiology and Biotechnology*, 24 (1): 113-118.

Liu, X., Liu, Y., Jiang, Z., Liu, H., Yang, S. and Yan, Q. 2018. Biochemical characterization of a novel xylanase from *Paenibacillus barengoltzii* and its application in xylooligosaccharides production from corncobs. *Food Chemistry*, 264: 310-318.

Liu, Y., Li, Y., Tong, S., Yuan, M., Wang, X., Wang, J. and Fan, Y. 2020a. Expression of a *Beauveria bassiana* chitosanase (BbCSN-1) in *Pichia pastoris* and enzymatic analysis of the recombinant protein. *Protein Expression and Purification*, 166: 105519.

Liu, Y., Luo, G., Ngo, H. H., Guo, W. and Zhang, S. 2020b. Advances in thermostable laccase and its current application in lignin-first biorefinery: a review. *Bioresource Technology*, 298: 122511.

Loesch, A., Hutwimmer, S. and Strasser, H. 2010. Carbon utilization pattern as a potential quality control criterion for virulence of *Beauveria brongniartii*. *Journal of Invertebrate Pathology*, 104 (1): 58-65.

Long, C., Liu, J., Gan, L., Zeng, B. and Long, M. 2019. Optimization of xylanase production by *Trichoderma orientalis* using corn cobs and wheat bran via statistical strategy. *Waste and Biomass Valorization*, 10 (5): 1277-1284.

Lopez, D. C. and Sword, G. A. 2015. The endophytic fungal entomopathogens *Beauveria bassiana* and *Purpureocillium lilacinum* enhance the growth of cultivated cotton (*Gossypium hirsutum*) and negatively affect survival of the cotton bollworm (*Helicoverpa zea*). *Biological Control*, 89: 53-60.

Łopusiewicz, Ł., Mazurkiewicz-Zapałowicz, K., Tkaczuk, C. and Bartkowiak, A. 2020. The influence of cobalt ions on growth and enzymatic activity of entomopathogenic fungi used in biological plant protection. *Journal of Plant Protection Research* 60 (1): 58-67.

Lord, J. C. 2005. Low humidity, moderate temperature, and desiccant dust favor efficacy of *Beauveria bassiana* (Hyphomycetes: Moniliales) for the lesser grain borer, *Rhyzopertha dominica* (Coleoptera: Bruchidae). *Biological Control*, 34 (2): 180-186.

Lovera, A., Belaich, M., Villamizar, L., Patarroyo, M. A. and Barrera, G. 2020. Enhanced virulence of *Beauveria bassiana* against *Diatraea saccharalis* using a soluble recombinant enzyme with endo- and exochitinase activity. *Biological Control*, 144: 104211.

Lu, Z., Deng, J., Wang, H., Zhao, X., Luo, Z., Yu, C. and Zhang, Y. 2021. Multifunctional role of a fungal pathogen-secreted laccase 2 in evasion of insect immune defense. *Environmental Microbiology*, 23: 1256-1274.

Luo, F., Wang, Q., Yin, C., Ge, Y., Hu, F., Huang, B., Zhou, H., Bao, G., Wang, B. and Lu, R. 2015. Differential metabolic responses of *Beauveria bassiana* cultured in pupae extracts, root exudates and its interactions with insect and plant. *Journal of Invertebrate Pathology*, 130: 154-164.

Luo, Z., Zhang, T., Liu, P., Bai, Y., Chen, Q., Zhang, Y. and Keyhani, N. O. 2018. The *Beauveria bassiana* Gas3 β-glucanosyltransferase contributes to fungal adaptation to extreme alkaline conditions. *Applied and Environmental Microbiology*, 84 (15): e01086-18.

MacPherson, J. and Khachatourians, G. 1991. Partial purification and characterization of beta-galactosidase produced by *Beauveria bassiana*. *Biotechnology and Applied Biochemistry,* 13: 217-230.

Magara, E., Nankinga, C., Gold, C., Kyamanywa, S., Ragama, P., Tushemereirwe, W., Moore, D. and Gowen, S. 2004. Efficacy of *Beauveria bassiana* substrates and formulations for the control of banana weevil. *Uganda Journal of Agricultural Sciences*, 9 (1): 900-905.

Magdeldin, S., Yoshida, Y., Li, H., Maeda, Y., Yokoyama, M., Enany, S., Zhang, Y., Xu, B., Fujinaka, H. and Yaoita, E. 2012. Murine colon proteome and characterization of the protein pathways. *BioData Mining*, 5 (1): 1-14.

Maibam, P. D. and Maiti, S. K. 2020. A strategy for simultaneous xylose utilization and enhancement of cellulase enzyme production by *Trichoderma reesei* cultivated on liquid hydrolysate followed by induction with feeding of solid sugarcane bagasse. *Waste and Biomass Valorization*, 11 (7): 3151-3160.

Malgas, S., Mafa, M. S. and Pletschke, B. I. 2020. The effects of xylanase synergistic interactions during lignocellulose degradation and their significance for industry. In:

Shrivastava S. ed. *Industrial Applications of Glycoside Hydrolases*.. Singapore: Springer, 229-246.

Mallebrera, B., Prosperini, A., Font, G. and Ruiz, M. J. 2018. *In vitro* mechanisms of Beauvericin toxicity: a review. *Food and Chemical Toxicology*, 111: 537-545.

Mamat, S., Shah, U. K. M., Remli, N. A. M., Shaari, K., Laboh, R. and Rahman, N. A. A. 2018. Characterization of antifungal activity of endophytic *Penicillium oxalicum* T 3.3 for anthracnose biocontrol in dragon fruit (Hylocereus sp). *International Journal of Environmental and Agriculture Research*, 4 (1): 65-76.

Manavalan, T., Manavalan, A., Thangavelu, K. P. and Heese, K. 2015. Characterization of a novel endoglucanase from *Ganoderma lucidum*. *Journal of Basic Microbiology*, 55 (6): 761-771.

Mancillas-Paredes, J. M., Hernández-Sánchez, H., Jaramillo-Flores, M. E. and García-Gutiérrez, C. 2019. Proteases and chitinases induced in *Beauveria bassiana* during infection by *Zabrotes subfasciatus*. *Southwestern Entomologist*, 44 (1): 125-137.

Mandal, S. and Banerjee, D. 2019. Proteases from endophytic fungi with potential industrial applications. In: Yadav A., Mishra S., Singh S., Gupta A. eds. *Recent advancement in white biotechnology through fungi*. Cham: Springer, 319-359.

Mandalari, G., Bennett, R. N., Kirby, A. R., Lo Curto, R. B., Bisignano, G., Waldron, K. W. and Faulds, C. B. 2006. Enzymatic hydrolysis of flavonoids and pectic oligosaccharides from bergamot (*Citrus bergamia* Risso) peel. *Journal of Agricultural and Food Chemistry*, 54 (21): 8307-8313.

Manojkumar, N., Muthukumaran, C. and Sharmila, G. 2020. A comprehensive review on the application of response surface methodology for optimization of biodiesel production using different oil sources. *Journal of King Saud University-Engineering Sciences*, In Press.

Mantilla, J. G., Galeano, N. F., Gaitan, A. L., Cristancho, M. A., Keyhani, N. O. and Gongora, C. E. 2012. Transcriptome analysis of the entomopathogenic fungus *Beauveria bassiana* grown on cuticular extracts of the coffee berry borer (*Hypothenemus hampei*). *Microbiology*, 158 (7): 1826-1842.

Mantzoukas, S. and Eliopoulos, P. A. 2020. Endophytic entomopathogenic fungi: a valuable biological control tool against plant pests. *Applied Sciences*, 10 (1): 360.

Manyes, L., Escrivá, L., Ruiz, M. and Juan-García, A. 2018. Beauvericin and enniatin B effects on a human lymphoblastoid Jurkat T-cell model. *Food and Chemical Toxicology*, 115: 127-135.

Mao, H., Wang, K., Wang, Z., Peng, J. and Ren, N. 2020. Metabolic function, trophic mode, organics degradation ability and influence factor of bacterial and fungal communities in chicken manure composting. *Bioresource Technology*, 302: 122883.

Marangoni, A. G. 2003. *Enzyme kinetics: a modern approach*. New Jersey: John Wiley & Sons.

Marcondes, N. R., Taira, C. L., Vandresen, D. C., Svidzinski, T. I. E., Kadowaki, M. K. and Peralta, R. M. 2008. New feather-degrading filamentous fungi. *Microbial Ecology*, 56 (1): 13-17.

Marino, G., Eckhard, U. and Overall, C. M. 2015. Protein termini and their modifications revealed by positional proteomics. *ACS Chemical Biology*, 10 (8): 1754-1764.

Marques, G. L., dos Santos Reis, N., Silva, T. P., Ferreira, M. L. O., Aguiar-Oliveira, E., de Oliveira, J. R. and Franco, M. 2018. Production and characterization of xylanase and endoglucanases produced by *Penicillium roqueforti* ATCC 10110 through the solid-state fermentation of rice husk residue. *Waste and Biomass Valorization*, 9 (11): 2061-2069.

Martin, K., McDougall, B. M., McIlroy, S., Chen, J. and Seviour, R. J. 2007. Biochemistry and molecular biology of exocellular fungal β-(1, 3)-and β-(1, 6)-glucanases. *FEMS Microbiology Reviews*, 31 (2): 168-192.

Martins, F., Pereira, J. A. and Baptista, P. 2014. Oxidative stress response of *Beauveria bassiana* to Bordeaux mixture and its influence on fungus growth and development. *Pest Management Science*, 70 (8): 1220-1227.

Mascarin, G., Kobori, N., Jackson, M., Dunlap, C. and Delalibera Jr, Í. 2018. Nitrogen sources affect productivity, desiccation tolerance and storage stability of *Beauveria bassiana* blastospores. *Journal of Applied Microbiology*, 124 (3): 810-820.

Mascarin, G. M. and Jaronski, S. T. 2016. The production and uses of *Beauveria bassiana* as a microbial insecticide. *World Journal of Microbiology and Biotechnology*, 32 (11): 177.

Mattoo, A. J. and Nonzom, S. 2021. Endophytic fungi: understanding complex cross-talks. *Symbiosis*: 1-28.

Mchunu, N. P., Permaul, K., Alam, M. and Singh, S. 2013. Carbon utilization profile of a thermophilic fungus, *Thermomyces lanuginosus* using phenotypic microarray. *Advances in Bioscience and Biotechnology,* 4 (9A):24-32.

McKinnon, A. C., Saari, S., Moran-Diez, M. E., Meyling, N. V., Raad, M. and Glare, T. R. 2017. *Beauveria bassiana* as an endophyte: a critical review on associated methodology and biocontrol potential. *BioControl*, 62 (1): 1-17.

Meena, R. K. and Mishra, P. 2020. Bio-pesticides for agriculture and environment sustainability. In: Kumar S., Meena R.S., Jhariya M.K. eds. *Resources Use Efficiency in Agriculture*. Singapore: Springer, 85-107.

Mehmood, A., Hussain, A., Irshad, M., Hamayun, M., Iqbal, A. and Khan, N. 2019. *In vitro* production of IAA by endophytic fungus *Aspergillus awamori* and its growth promoting activities in *Zea mays*. *Symbiosis*, 77 (3): 225-235.

Melnichuk, N., Braia, M. J., Anselmi, P. A., Meini, M.R. and Romanini, D. 2020. Valorization of two agroindustrial wastes to produce alpha-amylase enzyme from *Aspergillus oryzae* by solid-state fermentation. *Waste Management*, 106: 155-161.

Merali, Z., Collins, S. R., Elliston, A., Wilson, D. R., Käsper, A. and Waldron, K. W. 2015. Characterization of cell wall components of wheat bran following hydrothermal pretreatment and fractionation. *Biotechnology for Biofuels*, 8 (1): 1-13.

Mhiri, S., Bouanane-Darenfed, A., Jemli, S., Neifar, S., Ameri, R., Mezghani, M., Bouacem, K., Jaouadi, B. and Bejar, S. 2020. A thermophilic and thermostable xylanase from *Caldicoprobacter algeriensis*: Recombinant expression, characterization and application in paper biobleaching. *International Journal of Biological Macromolecules*, 164: 808-817.

Miao, J., Wang, M., Ma, L., Li, T., Huang, Q., Liu, D. and Shen, Q. 2019. Effects of amino acids on the lignocellulose degradation by *Aspergillus fumigatus* Z5: insights into performance, transcriptional, and proteomic profiles. *Biotechnology for Biofuels*, 12 (1): 1-19.

Michalski, R. 2018. Ion chromatography applications in wastewater analysis. *Separations*, 5 (1): 16.

Michelin, M., Silva, T. M., Jorge, J. A. and Polizeli, M. D. L. T. M. 2014. Purification and biochemical properties of multiple xylanases from *Aspergillus ochraceus* tolerant to Hg^{2+} ion and a wide range of pH. *Applied Biochemistry and Biotechnology*, 174 (1): 206-220.

Mishra, A., Pandey, B., Tyagi, C., Chakraborty, O., Kumar, A. and Jain, A. 2015. Structural and functional analysis of chitinase gene family in wheat (*Triticum aestivum*). *Indian Journal of Biochemistry and Biophysics,* 52 (2): 169-178.

Mishra, S., Kumar, P. and Malik, A. 2013. Effect of process parameters on the enzyme activity of a novel *Beauveria bassiana* isolate. *International Journal of Current Microbiology and Applied Sciences*, 2 (9): 49-56.

Mishra, S., Kumar, P. and Malik, A. 2015. Effect of temperature and humidity on pathogenicity of native *Beauveria bassiana* isolate against *Musca domestica* L. *Journal of Parasitic Diseases*, 39 (4): 697-704.

Mistry, J., Chuguransky, S., Williams, L., Qureshi, M., Salazar, G. A., Sonnhammer, E. L., Tosatto, S. C., Paladin, L., Raj, S. and Richardson, L. J. 2021. Pfam: The protein families database in 2021. *Nucleic Acids Research*, 49 (D1): D412-D419.

Mondal, S., Baksi, S., Koris, A. and Vatai, G. 2016. Journey of enzymes in entomopathogenic fungi. *Pacific Science Review A: Natural Science and Engineering*, 18 (2): 85-99.

Moran, G. P., Anderson, M. Z., Myers, L. C. and Sullivan, D. J. 2019. Role of mediator in virulence and antifungal drug resistance in pathogenic fungi. *Current Genetics*, 65 (3):621-630.

More, S. V., Chavan, S. and Prabhune, A. A. 2018. Silk degumming and utilization of silk sericin by hydrolysis using alkaline protease from *Beauveria* sp.(MTCC 5184): a green approach. *Journal of Natural Fibers*, 15 (3): 373-383.

Mudrončeková, S., Mazáň, M., Nemčovič, M. and Šalamon, I. 2019. Entomopathogenic fungus species *Beauveria bassiana* (Bals.) and *Metarhizium anisopliae* (Metsch.) used as mycoinsecticide effective in biological control of Ips typographus (L.). *Journal of Microbiology, Biotechnology and Food Sciences*, 2019: 2469-2472.

Mullowney, M. W., McClure, R. A., Robey, M. T., Kelleher, N. L. and Thomson, R. J. 2018. Natural products from thioester reductase containing biosynthetic pathways. *Natural Product Reports*, 35 (9): 847-878.

Munir, M., Abdullah, R., Haq, I., Kaleem, A., Iqtedar, M. and Ashraf, S. 2020. Purification, characterization, kinetics and thermodynamic analysis of polygalacturonase from *Aspergillus tamarii* for industrial applications. *Revista Mexicana de Ingeniería Química*, 19 (1): 293-304.

Mustafa, U. and Kaur, G. 2009. Effects of carbon and nitrogen sources and ratio on the germination, growth and sporulation characteriztics of *Metarhizium anisopliae* and *Beauveria bassiana* isolates. *African Journal of Agricultural Research*, 4 (10): 922-930.

Muthukrishnan, S. 2017. Optimization and production of industrial important cellulase enzyme from *Penicillium citrinum* in Western Ghats of Sathuragiri Hills soil sample isolate. *Journal of Microbiology Research*, 5: 7-16.

Mwamburi, L. A. 2021. Endophytic fungi, *Beauveria bassiana* and *Metarhizium anisopliae*, confer control of the fall armyworm, *Spodoptera frugiperda* (JE Smith)(Lepidoptera: Noctuidae), in two tomato varieties. *Egyptian Journal of Biological Pest Control*, 31 (1): 1-6.

Myers, R. H. 1999. Response surface methodology-current status and future directions. *Journal of Quality Technology*, 31 (1): 30-44.

Nageswara, S., Guntuku, G. and Tadimalla, P. 2014. Production of L-asparaginase by solid state fermentation using marine fungus. *BioMed Res* 1 (1): 1-9.

Naik, B. S. 2019. Potential roles for endophytic fungi in biotechnological processes: a review. In: Ozturk M., Hakeem K. eds. *Plant and Human Health*. Cham: Springer, 327-344.

Namatame, I., Tomoda, H., Ishibashi, S. and Ōmura, S. 2004. Antiatherogenic activity of fungal beauveriolides, inhibitors of lipid droplet accumulation in macrophages. *Proceedings of the National Academy of Sciences*, 101 (3): 737-742.

Naranjo-Ortiz, M. A. and Gabaldón, T. 2019. Fungal evolution: major ecological adaptations and evolutionary transitions. *Biological Reviews*, 94 (4): 1443-1476.

Nardelli, A., Vecchi, M., Mandrioli, M. and Manicardi, G. C. 2019. The evolutionary history and functional divergence of trehalase (treh) genes in insects. *Frontiers in Physiology*, 10: 62.

Naveed, M., Nadeem, F., Mehmood, T., Bilal, M., Anwar, Z. and Amjad, F. 2020. Protease-a versatile and ecofriendly biocatalyst with multi-industrial applications: an updated review. *Catalysis Letters*, 151: 307–323.

Neelamathi, E., Vasumathi, E., Bagyalakshmi, S. and Kannan, R. 2009. *In silico* prediction of structure and functional aspects of a hypothetical protein of *Neurospora crassa*. *Journal of Cell and Tissue Research*, 9 (3): 1989.

Nene, S. N. and Joshi, K. S. 2020. A comparative study of production of hydrophobin like proteins (HYD-LPs) in submerged liquid and solid state fermentation from white rot fungus *Pleurotus ostreatus*. *Biocatalysis and Agricultural Biotechnology*, 23: 101440.

Nianios, D., Thierbach, S., Steimer, L., Lulchev, P., Klostermeier, D. and Fetzner, S. 2015. Nickel quercetinase, a "promiscuous" metalloenzyme: metal incorporation and metal ligand substitution studies. *BMC Biochemistry*, 16 (1): 10.

Nicoletti, R. and Becchimanzi, A. 2020. Endophytism of *Lecanicillium* and *Akanthomyces*. *Agriculture*, 10 (6): 205.

Niere, B., Athman, S., Viljoen, A., Gold, C., Dubois, T., Ragama, P., Coyne, D. and Labuschagne, N. 2006. *In vitro* antagonism of endophytic *Fusarium oxysporum* isolates against the burrowing nematode *Radopholus similis*. *Nematology*, 8 (4): 627-636.

Ninawe, S., Kapoor, M. and Kuhad, R. C. 2008. Purification and characterization of extracellular xylanase from *Streptomyces cyaneus* SN32. *Bioresource Technology*, 99 (5): 1252-1258.

Nishi, O., Sushida, H., Higashi, Y. and Iida, Y. 2020. Epiphytic and endophytic colonisation of tomato plants by the entomopathogenic fungus *Beauveria bassiana* strain GHA. *Mycology*, , 12 (1): 39-47.

Nithya, K., Muthukumar, C., Kadaikunnan, S., Alharbi, N. S., Khaled, J. M. and Dhanasekaran, D. 2017. Purification, characterization, and statistical optimization of a thermostable α-amylase from desert actinobacterium *Streptomyces fragilis* DA7-7. *3 Biotech*, 7 (5): 350.

Niveditha, P., Simon, S., Reddy, R. N. and Lal, A. A. 2019. Effect of *Beauveria bassiana* with botanicals on root knot nematode population (*Meloidogyne graminicola*) in rice

seedlings. *International Journal of Current Microbiology and Applied Sciences,* 8 (10): 442-448.

Nouadri, T., Meraihi, Z., Shahrazed, D.-D. and Leila, B. 2010. Purification and characterization of the-amylase isolated from *Penicillium camemberti* PL21. *African Journal of Biochemistry Research*, 4 (6): 155-162.

Nouri, H., Azin, M. and Mousavi, S. L. 2018. Enhanced ethanol production from sugarcane bagasse hydrolysate with high content of inhibitors by an adapted *Barnettozyma californica*. *Environmental Progress and Sustainable Energy*, 37 (3): 1169-1175.

Nsa, I. Y., Kareem, R. O., Aina, O. T. and Akinyemi, B. T. 2020. Isolation of an emerging thermotolerant medically important Fungus, *Lichtheimia ramosa* from soil. *African Journal of Microbiology Research*, 14 (6): 237-241.

Ntsobi, N., Etsassala, N. G., Akinpelu, E. A. and Nchu, F. 2020. Assessment of the effects of *Beauveria bassiana* (Hypocreales) inoculum on the composting of vegetable wastes. *In: Proceedings of South Africa International Conference on Agricultural, Chemical, Biological & Environmental Sciences,* 249-254.

Nuñez-Gaona, O., Saucedo-Castañeda, G., Alatorre-Rosas, R. and Loera, O. 2010. Effect of moisture content and inoculum on the growth and conidia production by *Beauveria bassiana* on wheat bran. *Brazilian Archives of Biology and Technology*, 53 (4): 771-777.

Ohshiro, T., Kobayashi, K., Ohba, M., Matsuda, D., Rudel, L. L., Takahashi, T., Doi, T. and Tomoda, H. 2017. Selective inhibition of sterol O-acyltransferase 1 isozyme by beauveriolide III in intact cells. *Scientific Reports*, 7 (1): 1-9.

Oide, S., Tanaka, Y., Watanabe, A. and Inui, M. 2019. Carbohydrate-binding property of a cell wall integrity and stress response component (WSC) domain of an alcohol oxidase from the rice blast pathogen *Pyricularia oryzae*. *Enzyme and Microbial Technology*, 125: 13-20.

Oikawa, A., Itoh, E., Ishihara, A. and Iwamura, H. 2003. Purification and characterization of β-N-acetylhexosaminidase from maize seedlings. *Journal of Plant Physiology*, 160 (9): 991-999.

Olofsson, K., Bertilsson, M. and Lidén, G. 2008. A short review on SSF–an interesting process option for ethanol production from lignocellulosic feedstocks. *Biotechnology for Biofuels*, 1 (1): 7.

Onipe, O. O., Jideani, A. I. and Beswa, D. 2015. Composition and functionality of wheat bran and its application in some cereal food products. *International Journal of Food Science & Technology*, 50 (12): 2509-2518.

Oppert, B., Perkin, L. C., Lorenzen, M. and Dossey, A. T. 2020. Transcriptome analysis of life stages of the house cricket, *Acheta domesticus*, to improve insect crop production. *Scientific Reports*, 10 (1): 1-13.

Ortiz, J., Soto, J., Fuentes, A., Herrera, H., Meneses, C. and Arriagada, C. 2019. The endophytic fungus *Chaetomium cupreum* regulates expression of genes involved in the tolerance to metals and plant growth promotion in *Eucalyptus globulus* roots. *Microorganisms*, 7 (11): 490.

Oshoma, C., Okonkwo, P. and Obasuyi, C. 2019. Influence of nitrogen sources on the production of single cell protein and amylase by *Aspergillus niger* using wheat bran. *SAU Science-Tech Journal*, 4 (1): 75-84.

Oumer, O. J. and Abate, D. 2018. Comparative studies of pectinase production by *Bacillus subtilis* strain Btk 27 in submerged and solid-state fermentations. *BioMed Research International*, 2018: 1514795.

Ownley, B. H., Griffin, M. R., Klingeman, W. E., Gwinn, K. D., Moulton, J. K. and Pereira, R. M. 2008. *Beauveria bassiana*: endophytic colonization and plant disease control. *Journal of Invertebrate Pathology*, 98 (3): 267-270.

Ozdemir, S., Fincan, S. A., Karakaya, A. and Enez, B. 2018. A novel raw starch hydrolyzing thermostable α-amylase produced by newly isolated *Bacillus mojavensis* SO-10: purification, characterization and usage in starch industries. *Brazilian Archives of Biology and Technology*, 61: e18160399.

Pachauri, P., V, A., More, S., Sullia, S. B. and Deshmukh, S. 2020. Purification and characterization of cellulase from a novel isolate of *Trichoderma longibrachiatum*. *Biofuels*, 11 (1): 85-91.

Padmavathi, J., Devi, K. U. and Rao, C. U. M. 2003. The optimum and tolerance pH range is correlated to colonial morphology in isolates of the entomopathogenic fungus *Beauveria bassiana*–a potential biopesticide. *World Journal of Microbiology and Biotechnology*, 19 (5): 469-477.

Pal, S. and Ghosh, S. K. 2017. Extracellular protease production by entomopathogenic fungus *Beauveria bassiana* and its compatibility test against detergent and surfactant. *Plant Cell Biotechnology and Molecular Biology*, 18 (7-8): 366-372.

Palavesam, A. 2015. Investigation on lignocellulosic saccharification and characterization of haloalkaline solvent tolerant endo-1,4 β-d-xylanase from *Halomonas meridiana* APCMST-KS4. *Biocatalysis and Agricultural Biotechnology*, 4 (4): 761-766.

Pande, R. and Mishra, H. 2018. Efficacy of non formulated entomopathogenic fungi (*Beauveria bassiana*) to control the storage insect pests of green gram (*Vigna radiata*) seeds. *Indian Journal of Agricultural Research*, 52 (3): 295-299.

Pandya, J. J. and Gupte, A. 2012. Production of xylanase under solid-state fermentation by *Aspergillus tubingensis* JP-1 and its application. *Bioprocess and Biosystems Engineering*, 35 (5): 769-779.

Pariseau, B., Nehls, S., Ogawa, G. S., Sutton, D. A., Wickes, B. L. and Romanelli, A. M. 2010. *Beauveria* keratitis and biopesticides: case histories and a random amplification of polymorphic DNA comparison. *Cornea*, 29 (2): 152-158.

Park, E.S., Song, G.H., Kim, S.H., Lee, S.-M., Kim, Y.G., Lim, Y.I., Kang, S. A. and Park, K.Y. 2018. *Rumex crispus* and *Cordyceps militaris* mixture ameliorates production of pro-inflammatory cytokines induced by lipopolysaccharide in C57BL/6 mice splenocytes. *Preventive Nutrition and Food Science*, 23 (4): 374–381.

Patel, H., Divecha, J. and Shah, A. 2017. Microwave assisted alkali treated wheat straw as a substrate for co-production of (hemi) cellulolytic enzymes and development of balanced enzyme cocktail for its enhanced saccharification. *Journal of the Taiwan Institute of Chemical Engineers*, 71: 298-306.

Pathare, P. B., Opara, U. L. and Al-Said, F. A.J. 2013. Colour measurement and analysis in fresh and processed foods: a review. *Food and Bioprocess Technology*, 6 (1): 36-60.

Patocka, J. 2016. Bioactive metabolites of entomopathogenic fungi *Beauveria bassiana*. *Military Medical Sciience Letters,* 85 (2): 80-88.

Patriarca, A., Larumbe, G., Buera, M. P. and Vaamonde, G. 2011. Stimulating effect of sorbitol and xylitol on germination and growth of some xerophilic fungi. *Food Microbiology*, 28 (8): 1463-1467.

Pawlik, A., Mazur, A., Wielbo, J., Koper, P., Żebracki, K., Kubik-Komar, A. and Janusz, G. 2019. RNA sequencing reveals differential gene expression of *Cerrena unicolor* in response to variable lighting conditions. *International Journal of Molecular Sciences*, 20 (2): 290.

Pawłowska, J., Okrasińska, A., Kisło, K., Aleksandrzak-Piekarczyk, T., Szatraj, K., Dolatabadi, S. and Muszewska, A. 2019. Carbon assimilation profiles of mucoralean fungi show their metabolic versatility. *Scientific Reports*, 9 (1): 1-8.

Pedrini, N., Juárez, M. P., Crespo, R. and de Alaniz, M. J. 2006. Clues on the role of *Beauveria bassiana* catalases in alkane degradation events. *Mycologia*, 98 (4): 528-534.

Pedrolli, D. B. and Carmona, E. C. 2010. Purification and characterization of the exopolygalacturonase produced by *Aspergillus giganteus* in submerged cultures. *Journal of Industrial Microbiology and Biotechnology*, 37 (6): 567-573.

Pemberton, R. W. 1999. Insects and other arthropods used as drugs in Korean traditional medicine. *Journal of Ethnopharmacology*, 65 (3): 207-216.

Permadi, M., Samosir, B., Siregar, D. and Wayni, M. 2020. Physiology characterization of entomopathogenic fungi *Beauveria bassiana* and *Metarhizium anisopliae* on different carbohydrate sources. In: *Proceedings of Journal of Physics Conference Series*. 072007.

Perreault, V., Gouin, N., Bérubé, A., Villeneuve, W., Pouliot, Y. and Doyen, A. 2021. Effect of pectinolytic enzyme pretreatment on the clarification of cranberry juice by ultrafiltration. *Membranes*, 11 (1): 55.

Petlamul, W. and Boukaew, S. 2019. Optimization and stabilisation of cellulase and xylanase production by *Beauveria bassiana*. *Environment Asia*, 12 (1): 11-19.

Petlamul, W., Sripornngam, T., Buakwan, N., Buakaew, S. and Mahamad, K. 2017. The capability of *Beauveria bassiana* for cellulase enzyme production. In: *Proceedings of the 7th International Conference on Bioscience, Biochemistry and Bioinformatics*. 62-66.

Petruzzi, L., Campaniello, D., Speranza, B., Corbo, M. R., Sinigaglia, M. and Bevilacqua, A. 2017. Thermal treatments for fruit and vegetable juices and beverages: a literature overview. *Comprehensive Reviews in Food Science and Food Safety*, 16 (4): 668-691.

Petry, A. L. and Patience, J. F. 2020. Xylanase supplementation in corn-based swine diets: a review with emphasis on potential mechanisms of action. *Journal of Animal Science*, 98 (11): skaa318.

Pieterse, C. M., Zamioudis, C., Berendsen, R. L., Weller, D. M., Van Wees, S. C. and Bakker, P. A. 2014. Induced systemic resistance by beneficial microbes. *Annual Review of Phytopathology*, 52: 347-75.

Pilgaard, B., Wilkens, C., Herbst, F.-A., Vuillemin, M., Rhein-Knudsen, N., Meyer, A. S. and Lange, L. 2019. Proteomic enzyme analysis of the marine fungus *Paradendryphiella salina* reveals alginate lyase as a minimal adaptation strategy for brown algae degradation. *Scientific Reports*, 9 (1): 1-13.

Podestá, M. V., Morilla, E. A., Allasia, M. B., Woitovich Valetti, N., Tubio, G. and Boggione, M. J. 2019. An eco-friendly method of purification for xylanase from *Aspergillus niger* by polyelectrolyte precipitation. *Journal of Polymers and the Environment*, 27 (12): 2895-2905.

Podzimek, T., Přerovská, T., Šantrůček, J., Kovaľ, T., Dohnálek, J., Matoušek, J. and Lipovová, P. 2018. N-glycosylation of tomato nuclease TBN1 produced in *N. benthamiana* and its effect on the enzyme activity. *Plant Science*, 276: 152-161.

Pommier, J.C., Goma, G., Fuentes, J.L. and Rousset, C. 1990. Using enzymes to improve the process and the product quality in the recycled paper industry. 2. Industrial applications. *TAPPI Journal,* 72: 187-191.

Poutanen, K. and Sundberg, M. 1988. An acetyl esterase of *Trichoderma reesei* and its role in the hydrolysis of acetyl xylans. *Applied Microbiology and Biotechnology*, 28 (4): 419-424.

Pradhan, D., Abdullah, S. and Pradhan, R. C. 2020. Optimization of pectinase assisted extraction of chironji (*Buchanania Lanzan*) fruit juice using response surface methodology and artificial neural network. *International Journal of Fruit Science*, 20(1): 1-19.

Prajapati, B. P., Jana, U. K., Suryawanshi, R. K. and Kango, N. 2020. Sugarcane bagasse saccharification using *Aspergillus tubingensis* enzymatic cocktail for 2G bio-ethanol production. *Renewable Energy*, 152: 653-663.

Pramanik, K., Saren, S., Mitra, S., Ghosh, P. K. and Maiti, T. K. 2018. Computational elucidation of phylogenetic, structural and functional characteriztics of *Pseudomonas* lipases. *Computational Biology and Chemistry*, 74: 190-200.

Przybysz Buzała, K., Przybysz, P., Kalinowska, H. and Derkowska, M. 2016. Effect of cellulases and xylanases on refining process and kraft pulp properties. *PLoS One*, 11 (8): e0161575.

Punia, G., Tondan, N., Kumar, A. and Prasad, C. 2019. Identification and molecular characterization of an isolate of entomopathogenic fungus *Beauveria bassiana* from Meerut (UP, India) using RAPD-PCR. *The Pharma Innovation Journal*, 8(2): 459-463.

Qin, X., Zhao, X., Huang, S., Deng, J., Li, X., Luo, Z. and Zhang, Y. 2020. Pest management via endophytic colonization of tobacco seedlings by the insect fungal pathogen *Beauveria bassiana*. *Pest Management Science*, 33342046.

Quesada-Moraga, E. and Alain, V. 2004. Bassiacridin, a protein toxic for locusts secreted by the entomopathogenic fungus *Beauveria bassiana*. *Mycological Research*, 108 (4): 441-452.

Radha, A., Sneha, R., Kiruthiga, R., Priyadharshini, P. and Prabhu, N. 2019. A Review on production of polygalacturonase using various organisms and its applications. *Asian Journal of Biotechnology and Bioresource Technology*, 5 (3): 1-12.

Rahimnahal, S., Shams, M., Tarrahimofrad, H. and Mohammadi, Y. 2020. Analysis to describe the catalytic critical residue of keratinase mojavensis using peptidase inhibitors: A docking-based bioinformatics study. *Journal of Basic Research in Medical Sciences*, 7 (2): 13-28.

Rahman, A., Ulven, C. A., Johnson, M. A., Durant, C. and Hossain, K. G. 2017. Pretreatment of wheat bran for suitable reinforcement in biocomposites. *Journal of Renewable Materials*, 5 (1): 62-67.

Ramakuwela, T., Hatting, J., Bock, C., Vega, F. E., Wells, L., Mbata, G. N. and Shapiro-Ilan, D. 2020. Establishment of *Beauveria bassiana* as a fungal endophyte in pecan (*Carya illinoinensis*) seedlings and its virulence against pecan insect pests. *Biological Control*, 140: 104102.

Rameshthangam, P., Solairaj, D., Arunachalam, G. and Ramasamy, P. 2018. Chitin and chitinases: biomedical and environmental applications of chitin and its derivatives. *Journal of Enzymes*, 1 (1): 20-43..

Randhawa, A., Ogunyewo, O. A., Eqbal, D., Gupta, M. and Yazdani, S. S. 2018. Disruption of zinc finger DNA binding domain in catabolite repressor Mig1 increases growth rate, hyphal branching, and cellulase expression in hypercellulolytic fungus *Penicillium funiculosum* NCIM1228. *Biotechnology for Biofuels*, 11 (1): 1-22.

Rao, F. V., Houston, D. R., Boot, R. G., Aerts, J. M., Sakuda, S. and Van Aalten, D. M. 2003. Crystal structures of allosamidin derivatives in complex with human macrophage chitinase. *Journal of Biological Chemistry*, 278 (22): 20110-20116.

Rao, Y. K., Lu, S.C., Liu, B.L. and Tzeng, Y.M. 2006. Enhanced production of an extracellular protease from *Beauveria bassiana* by optimization of cultivation processes. *Biochemical Engineering Journal*, 28 (1): 57-66.

Ravichandran, A., Kolte, A. P., Dhali, A., Gopinath, S. M. and Sridhar, M. 2020. Transcriptomic analysis of *Lentinus squarrosulus* to provide insights into its biodegradation ability. *BioRxiv*. In Press.

Razeq, F. M., Jurak, E., Stogios, P. J., Yan, R., Tenkanen, M., Kabel, M. A., Wang, W. and Master, E. R. 2018. A novel acetyl xylan esterase enabling complete deacetylation of substituted xylans. *Biotechnology for Biofuels*, 11 (1): 74.

Reddy, S. and Bhardwaj, S. 2020. Apple pomace as effective substrate for growth and spore production of entomopathogenic fungi, *Lecanicillium lecanii, Beauveria bassiana* and *Paecilomyces fumosoroseus*, 58: 138-142.

Regnault-Roger, C. 2020. Trends for commercialization of biocontrol agents (biopesticide). In: Ramawat K. ed. *Plant defence: biological control*. Dordrecht :Springer, 445-471.

Reinhold-Hurek, B., Maes, T., Gemmer, S., Van Montagu, M. and Hurek, T. 2006. An endoglucanase is involved in infection of rice roots by the not-cellulose-metabolizing endophyte *Azoarcus* sp. strain BH72. *Molecular Plant-Microbe Interactions*, 19 (2): 181-188.

Ren, A., Li, C. and Gao, Y. 2011. Endophytic fungus improves growth and metal uptake of *Lolium arundinaceum* Darbyshire ex. Schreb. *International Journal of Phytoremediation*, 13 (3): 233-243.

Requião, R. D., Fernandes, L., de Souza, H. J. A., Rossetto, S., Domitrovic, T. and Palhano, F. L. 2017. Protein charge distribution in proteomes and its impact on translation. *PLoS Computational Biology*, 13 (5): e1005549.

Reverberi, M., Punelli, M., Scala, V., Scarpari, M., Uva, P., Mentzen, W. I., Dolezal, A. L., Woloshuk, C., Pinzari, F. and Fabbri, A. A. 2013. Genotypic and phenotypic versatility of *Aspergillus flavus* during maize exploitation. *PLoS One*, 8 (7): e68735.

Ribas-Agustí, A., Martín-Belloso, O., Soliva-Fortuny, R. and Elez-Martínez, P. 2018. Food processing strategies to enhance phenolic compounds bioaccessibility and bioavailability in plant-based foods. *Critical Reviews in Food Science and Nutrition*, 58 (15): 2531-2548.

Riou, C., Freyssinet, G. and Fevre, M. 1992. Purification and characterization of extracellular pectinolytic enzymes produced by *Sclerotinia sclerotiorum*. *Applied and Environmental Microbiology*, 58 (2): 578-583.

Rizwan, M., Atta, B., Rizwan, M., Sabir, A. M., Shah, Z. U. and Hussain, M. 2019. Effect of the entomopathogenic fungus, *Beauveria bassiana*, combined with diatomaceous earth on the red flour beetle, *Tribolium castaneum* (Herbst)(Tenebrionidae: Coleoptera). *Egyptian Journal of Biological Pest Control*, 29 (1): 27.

Rodrigues, I. D. S. V., Barreto, J. T., Moutinho, B. L., Oliveira, M. M. G., da Silva, R. S., Fernandes, M. F. and Fernandes, R. P. M. 2020. Production of xylanases by *Bacillus*

sp. TC-DT13 in solid state fermentation using bran wheat. *Preparative Biochemistry and Biotechnology*, 50 (1): 91-97.

Rodriguez, P., Gonzalez, D. and Rodríguez Giordano, S. 2016. Endophytic microorganisms: a source of potentially useful biocatalysts. *Journal of Molecular Catalysis B: Enzymatic*, 133: S569-S581.

Rodríguez-Mendoza, J., Santiago-Hernández, A., Alvarez-Zúñiga, M. T., Gutiérrez-Antón, M., Aguilar-Osorio, G. and Hidalgo-Lara, M. E. 2019. Purification and biochemical characterization of a novel thermophilic exo-β-1, 3-glucanase from the thermophile biomass-degrading fungus *Thielavia terrestris* Co3Bag1. *Electronic Journal of Biotechnology*, 41: 60-71.

Rojas-Osnaya, J., Rocha-Pino, Z., Nájera, H., González-Márquez, H. and Shirai, K. 2020. Novel transglycosylation activity of β-N-acetylglucosaminidase of *Lecanicillium lecanii* produced by submerged culture. *International Journal of Biological Macromolecules*, 145: 759-767.

Romero-González, J., Ah-Hen, K. S., Lemus-Mondaca, R. and Muñoz-Fariña, O. 2020. Total phenolics, anthocyanin profile and antioxidant activity of maqui, *Aristotelia chilensis* (Mol.) Stuntz, berries extract in freeze-dried polysaccharides microcapsules. *Food Chemistry*, 313: 126115.

Rondot, Y. and Reineke, A. 2018. Endophytic *Beauveria bassiana* in grapevine Vitis vinifera (L.) reduces infestation with piercing-sucking insects. *Biological Control*, 116: 82-89.

Roth, C., Moroz, O. V., Turkenburg, J. P., Blagova, E., Waterman, J., Ariza, A., Ming, L., Tianqi, S., Andersen, C. and Davies, G. J. 2019. Structural and functional characterization of three novel fungal amylases with enhanced stability and pH tolerance. *International Journal of Molecular Sciences*, 20 (19): 4902.

Russo, M. L., Scorsetti, A. C., Vianna, M. F., Allegrucci, N., Ferreri, N. A., Cabello, M. N. and Pelizza, S. A. 2019. Effects of endophytic *Beauveria bassiana* (Ascomycota:

Hypocreales) on biological, reproductive parameters and food preference of the soybean pest *Helicoverpa gelotopoeon*. *Journal of King Saud University-Science*, 31 (4): 1077-1082.

Ryali, S. L., Shiv S., Sneha,l V. M., Harish B. K., Chandra B. K. N., Saravanan P., Padmanabhan B. 2020. Fungal strain *Beauveria* sp. MTCC 5184 and a process for the preparation of enzymes therefrom. U.S. Patent 10,544,473.

Rytioja, J., Hildén, K., Di Falco, M., Zhou, M., Aguilar-Pontes, M. V., Sietiö, O. M., Tsang, A., de Vries, R. P. and Mäkelä, M. R. 2017. The molecular response of the white-rot fungus *Dichomitus squalens* to wood and non-woody biomass as examined by transcriptome and exoproteome analyses. *Environmental Microbiology*, 19 (3): 1237-1250.

Saad, A. M., Mohamed, A. S. and Ramadan, M. F. 2020. Storage and heat processing affect flavors of cucumber juice enriched with plant extracts. *International Journal of Vegetable Science*: 1-11.

Saad, W. F., Othman, A. M., Abdel-Fattah, M. and Ahmad, M. S. 2021. Response surface methodology as an approach for optimization of α-amylase production by the new isolated thermotolerant *Bacillus licheniformis* WF67 strain in submerged fermentation. *Biocatalysis and Agricultural Biotechnology*: 101944.

Sabu, A., Keerthi, T., Kumar, S. R. and Chandrasekaran, M. 2000. L-Glutaminase production by marine *Beauveria* sp. under solid state fermentation. *Process Biochemistry*, 35 (7): 705-710.

Saldarriaga-Hernández, S., Velasco-Ayala, C., Flores, P.L.I., de Jesús Rostro-Alanis, M., Parra-Saldivar, R., Iqbal, H.M. and Carrillo-Nieves, D., 2020. Biotransformation of lignocellulosic biomass into industrially relevant products with the aid of fungi-derived lignocellulolytic enzymes. *International Journal of Biological Macromolecules*, 161: 1099-1116.

Sahab, A. F. 2012. Antimicrobial efficacy of secondary metabolites of *Beauveria bassiana* against selected bacteria and phytopathogenic fungi. *Journal of Applied Sciences Research,* 8 (3): 1441-1444.

Sahnoun, M., Bejar, S., Sayari, A., Triki, M. A., Kriaa, M. and Kammoun, R. 2012. Production, purification and characterization of two α-amylase isoforms from a newly isolated *Aspergillus oryzae* strain S2. *Process Biochemistry*, 47 (1): 18-25.

Saini, R., Saini, H. S. and Dahiya, A. 2017. Amylases: characteriztics and industrial applications. *Journal of Pharmacognosy and Phytochemistry*, 6 (4): 1865-1871.

Saini, S., Chutani, P., Kumar, P. and Sharma, K. K. 2020. Development of an eco-friendly deinking process for the production of bioethanol using diverse hazardous paper wastes. *Renewable Energy*, 146: 2362-2373.

Sakaguchi, M. 2020. Diverse and common features of trehalases and their contributions to microbial trehalose metabolism. *Applied Microbiology and Biotechnology*, 104 (5): 1837-1847.

Saleem, A., Waris, S., Ahmed, T. and Tabassum, R. 2021. Biochemical characterization and molecular docking of cloned xylanase gene from *Bacillus subtilis* RTS expressed in *E. coli*. *International Journal of Biological Macromolecules*, 168: 310-321.

Salehi, F. 2020. Physicochemical characteriztics and rheological behaviour of some fruit juices and their concentrates. *Journal of Food Measurement and Characterization,* 14: 2472–2488.

Sánchez-Rodríguez, A. R., Del Campillo, M. C. and Quesada-Moraga, E. 2015. *Beauveria bassiana*: An entomopathogenic fungus alleviates Fe chlorosis symptoms in plants grown on calcareous substrates. *Scientia Horticulturae*, 197: 193-202.

Sánchez-Rodríguez, A. R., Raya-Díaz, S., Zamarreño, Á. M., García-Mina, J. M., del Campillo, M. C. and Quesada-Moraga, E. 2018. An endophytic *Beauveria bassiana* strain increases spike production in bread and durum wheat plants and effectively controls cotton leafworm (*Spodoptera littoralis*) larvae. *Biological Control*, 116: 90-102.

Sand, M., Rodrigues, M., González, J. M., de Crécy-Lagard, V., Santos, H., Müller, V. and Averhoff, B. 2015. Mannitol-1-phosphate dehydrogenases/phosphatases: a family of novel bifunctional enzymes for bacterial adaptation to osmotic stress. *Environmental Microbiology*, 17 (3): 711-719.

Sandri, I. G. and Silveira, M. M. d. 2018. Production and application of pectinases from *Aspergillus niger* obtained in solid state cultivation. *Beverages*, 4 (3): 48.

Sanghvi, G. V., Koyani, R. D. and Rajput, K. S. 2010. Thermostable xylanase production and partial purification by solid-state fermentation using agricultural waste wheat straw. *Mycology*, 1 (2): 106-112.

Sansen, S., De Ranter, C. J., Gebruers, K., Brijs, K., Courtin, C. M., Delcour, J. A. and Rabijns, A. 2004. Structural basis for inhibition of *Aspergillus niger* xylanase by *Triticum aestivum* xylanase inhibitor-I. *Journal of Biological Chemistry*, 279 (34): 36022-36028.

Santa, H. S. D., Santa, O. R. D., Brand, D., Vandenberghe, L. P. D. S. and Soccol, C. R. 2005. Spore production of *Beauveria bassiana* from agro-industrial residues. *Brazilian Archives of Biology and Technology*, 48 (SPE): 51-60.

Santana, M. L., Bispo, J. A. C., de Sena, A. R., Teshima, E., de Brito, A. R., Costa, F. S., Franco, M. and de Assis, S. A. 2020. Clarification of tangerine juice using cellulases from *Pseudoyma* sp. *Journal of Food Science and Technology*, 58: 44-51.

Santi, L., Coutinho-Rodrigues, C. J., Berger, M., Klein, L. A., De Souza, E. M., Rosa, R. L., Guimarães, J. A., Yates, J. R., Perinotto, W. M. and Bittencourt, V. R. 2019. Secretomic analysis of *Beauveria bassiana* related to cattle tick, *Rhipicephalus microplus*, infection. *Folia Microbiologica*, 64 (3): 361-372.

Sarkar, S., Banerjee, A., Chakraborty, N., Soren, K., Chakraborty, P. and Bandopadhyay, R. 2020. Structural-functional analyses of textile dye degrading azoreductase, laccase and peroxidase: a comparative in silico study. *Electronic Journal of Biotechnology*, 43: 48-54.

Sassá, D. C., Varéa-Pereira, G., Miyagui, D. T., Neves, P. M. D. O. J., Wu, J. I., Sugahara, V. H., Mita, C. and Kamogawa, E. 2008. Evaluation of kinetic parameters of chitinases produced by *Beauveria bassiana* (Bals.) Vuill. *Semina: Ciências Agrárias*, 29 (4): 807-814.

Sassi, A. H., Tounsi, H., Trigui-Lahiani, H., Bouzouita, R., Romdhane, Z. B. and Gargouri, A. 2016. A low-temperature polygalacturonase from *P. occitanis*: characterization and application in juice clarification. *International Journal of Biological Macromolecules*, 91: 158-164.

Satti, S. M., Abbasi, A. M., Marsh, T. L., Auras, R., Hasan, F., Badshah, M., Farman, M. and Shah, A. A. 2019. Statistical optimization of lipase production from *Sphingobacterium* sp. strain S2 and evaluation of enzymatic depolymerization of poly (lactic acid) at mesophilic temperature. *Polymer Degradation and Stability*, 160: 1-13.

Saxena, D., Sabikhi, L., Chakraborty, S. K. and Singh, D. 2014. Process optimization for enzyme aided clarification of watermelon juice. *Journal of Food Science and Technology*, 51 (10): 2490-2498.

Sayed, S., Elarrnaouty, S.-A., AlOtaibi, S. and Salah, M. 2021. Pathogenicity and side effect of indigenous *Beauveria bassiana* on *Coccinella undecimpunctata* and *Hippodamia variegata* (Coleoptera: Coccinellidae). *Insects*, 12 (1): 42.

Scazzocchio, C. 2000. The fungal GATA factors. *Current Opinion in Microbiology*, 3 (2): 126-131.

Scheiner, S., Kar, T. and Pattanayak, J. 2002. Comparison of various types of hydrogen bonds involving aromatic amino acids. *Journal of the American Chemical Society*, 124 (44): 13257-13264.

Schieber, A., Keller, P. and Carle, R. 2001. Determination of phenolic acids and flavonoids of apple and pear by high-performance liquid chromatography. *Journal of Chromatography A*, 910 (2): 265-273.

Schmaltz, S., Aita, B. C., Alves, E. A., Fochi, A., Bolson, V. F., Navarro-Díaz, H. J., Kuhn, R. C. and Mazutti, M. A. 2021. Ultrasound-assisted fermentation for production of β-1, 3-glucanase and chitinase by *Beauveria bassiana*. *Journal of Chemical Technology & Biotechnology*, 96 (1): 88-98.

Segel, I. H. 1975. *Biochemical calculations*. 2nd ed. London: Wiley.

Seger, C., Erlebach, D., Stuppner, H., Griesser, U. J. and Strasser, H. 2005. Physicochemical properties of oosporein, the major secreted metabolite of the entomopathogenic fungus *Beauveria brongniartii*. *Helvetica Chimica Acta*, 88 (4): 802-810.

Seid, A. M., Fredensborg, B. L., Steinwender, B. M. and Meyling, N. V. 2019. Temperature-dependent germination, growth and co-infection of *Beauveria* spp. isolates from different climatic regions. *Biocontrol Science and Technology*, 29 (5): 411-426.

Sena, A. R., Júnior, G. L., Góes Neto, A., Taranto, A. G., Pirovani, C. P., Cascardo, J., Zingali, R. B., Bezerra, M. A. and Assis, S. A. 2011. Production, purification and characterization of a thermostable β-1, 3-glucanase (laminarinase) produced by *Moniliophthora perniciosa*. *Anais da Academia Brasileira de Ciências*, 83 (2): 599-609.

Senthilraja, G., Anand, T., Durairaj, C., Kennedy, J., Suresh, S., Raguchander, T. and Samiyappan, R. 2010. A new microbial consortia containing entomopathogenic fungus, *Beauveria bassiana* and plant growth promoting rhizobacteria, *Pseudomonas fluorescens* for simultaneous management of leafminers and collar rot disease in groundnut. *Biocontrol Science and Technology*, 20 (5): 449-464.

Senthilraja, G., Anand, T., Mohankumar, S., Raguchander, T. and Samiyappan, R. 2018. Analysis of variation in virulence of *Beauveria bassiana* against insect pests of pigeonpea using qPCR. *Journal of Basic Microbiology*, 58 (3): 277-282.

Serrano, A., Carro, J. and Martínez, A. T. 2020. Reaction mechanisms and applications of aryl-alcohol oxidase. *The Enzymes*, 47: 167-192.

Sethi, S., Joshi, A., Arora, B., Bhowmik, A., Sharma, R. and Kumar, P. 2020. Significance of FRAP, DPPH, and CUPRAC assays for antioxidant activity determination in apple fruit extracts. *European Food Research and Technology*, 246 (3): 591-598.

Shah, N.N.A.K., Rahman, R.A., Shamsuddin, R. and Adzahan, N.M., 2015. Effects of pectinase clarification treatment on phenolic compounds of pummelo (*Citrus grandis* l. Osbeck) fruit juice. *Journal of Food Science and Technology*, 52(8): 5057-5065.

Shahabazuddin, M., Chandra, T. S., Meena, S., Sukumaran, R., Shetty, N. and Mudliar, S. 2018. Thermal assisted alkaline pretreatment of rice husk for enhanced biomass deconstruction and enzymatic saccharification: physico-chemical and structural characterization. *Bioresource Technology*, 263: 199-206.

Shahaf, N., Pappalardo, M., Basile, L., Guccione, S. and Rayan, A. 2016. How to choose the suitable template for homology modelling of GPCRs: 5-HT7 receptor as a test case. *Molecular Informatics*, 35 (8-9): 414-423.

Shahriari, M., Zibaee, A., Khodaparast, S. A. and Fazeli-Dinan, M. 2021. Screening and virulence of the entomopathogenic fungi associated with *Chilo suppressalis* Walker. *Journal of Fungi*, 7 (1): 34.

Shahryari, Z., Fazaelipoor, M. H., Ghasemi, Y., Lennartsson, P. R. and Taherzadeh, M. J. 2019. Amylase and xylanase from edible fungus *Neurospora intermedia*: production and characterization. *Molecules*, 24 (4): 721.

Shankar, S. and Laxman, R. S. 2015. Biophysicochemical characterization of an alkaline protease from *Beauveria* sp. MTCC 5184 with multiple applications. *Applied Biochemistry and Biotechnology*, 175 (1): 589-602.

Shankar, S., Rao, M. and Laxman, R. S. 2011. Purification and characterization of an alkaline protease by a new strain of *Beauveria* sp. *Process Biochemistry*, 46 (2): 579-585.

Sharma A., Srivastava A., Shukla A.K., Srivastava K., Srivastava A.K., Saxena A.K. 2020. Entomopathogenic fungi: a potential source for biological control of insect pests. In: Solanki M., Kashyap P., Kumari B. eds. *Phytobiomes: current insights and future vistas*. Singapore: Springer, 225-250.

Sharma, D., Garlapati, V. K. and Goel, G. 2016. Bioprocessing of wheat bran for the production of lignocellulolytic enzyme cocktail by *Cotylidia pannosa* under submerged conditions. *Bioengineered*, 7 (2): 88-97.

Sharma, H. P., Patel, H. and Sugandha. 2017. Enzymatic added extraction and clarification of fruit juices-a review. *Critical Reviews in Food Science and Nutrition*, 57 (6): 1215-1227.

Sharma K., Thakur A., Goyal A. 2019. Xylanases for food applications. In: Parameswaran B., Varjani S., Raveendran S. eds. Green Bio-processes, energy, environment, and sustainability. Singapore: Springer, 99-118.

Sharma, V., Salwan, R., Sharma, P. and Kanwar, S. 2016. Molecular cloning and characterization of ech46 endochitinase from *Trichoderma harzianum*. *International Journal of Biological Macromolecules*, 92: 615-624.

Sharma, V., Salwan, R. and Shanmugam, V. 2018. Molecular characterization of β-endoglucanase from antagonistic *Trichoderma saturnisporum* isolate GITX-Panog (C) induced under mycoparasitic conditions. *Pesticide Biochemistry and Physiology*, 149: 73-80.

Shehata, M. G., Badr, A. N., El Sohaimy, S. A., Asker, D. and Awad, T. S. 2019. Characterization of antifungal metabolites produced by novel lactic acid bacterium and their potential application as food biopreservatives. *Annals of Agricultural Sciences*, 64 (1): 71-78.

Sheng, K., Zhang, S., Liu, J., Shuang, E., Jin, C., Xu, Z. and Zhang, X. 2019. Hydrothermal carbonization of cellulose and xylan into hydrochars and application on glucose isomerization. *Journal of Cleaner Production*, 237: 117831.

Shikano, K., Bessho, Y., Kato, M., Iwakoshi-Ukena, E., Taniuchi, S., Furumitsu, M., Tachibana, T., Bentley, G. E., Kriegsfeld, L. J. and Ukena, K. 2018. Localization and function of neurosecretory protein GM, a novel small secretory protein, in the chicken hypothalamus. *Scientific Reports*, 8 (1): 6235.

Shin, T. Y., Bae, S. M. and Woo, S. D. 2016. Screening and characterization of antimicrobial substances originated from entomopathogenic fungi. *Journal of Asia-Pacific Entomology*, 19 (4): 1053-1059.

Shoseyov, O., Shani, Z. and Levy, I. 2006. Carbohydrate binding modules: biochemical properties and novel applications. *Microbiology and Molecular Biology Reviews*, 70 (2): 283-295.

Shrivastava, G., Ownley, B. H., Augé, R. M., Toler, H., Dee, M., Vu, A., Köllner, T. G. and Chen, F. 2015. Colonization by arbuscular mycorrhizal and endophytic fungi enhanced terpene production in tomato plants and their defense against a herbivorous insect. *Symbiosis*, 65 (2): 65-74.

Sibi, G. 2015. Low cost carbon and nitrogen sources for higher microalgal biomass and lipid production using agricultural wastes. *Journal of Environmental Science and Technology*, 8 (3): 113-121.

Sigler, L. 2002. Miscellaneous opportunistic fungi: Microascaceae and other Ascomycetes, Hyphomycetes, Coelomycetes, and Basidiomycetes. *Mycology Series*, 16: 637-676.

Silva, A. C. L., Silva, G. A., Abib, P. H. N., Carolino, A. T. and Samuels, R. I. 2020. Endophytic colonization of tomato plants by the entomopathogenic fungus *Beauveria bassiana* for controlling the South American tomato pinworm, *Tuta absoluta*. *CABI Agriculture and Bioscience*, 1 (1): 1-9.

Silva, D., Martins, E. S., Leite, R. S. R., Da Silva, R., Ferreira, V. and Gomes, E. 2007. Purification and characterization of an exo-polygalacturonase produced by *Penicillium viridicatum* RFC3 in solid-state fermentation. *Process Biochemistry*, 42 (8): 1237-1243.

Silva, C., Martins, M., Jing, S., Fu, J. and Cavaco-Paulo, A. 2018. Practical insights on enzyme stabilization. *Critical Reviews in Biotechnology*, 38 (3): 335-350.

Silva, T. P., de Albuquerque, F. S., dos Santos, C. W. V., Franco, M., Caetano, L. C. and Pereira, H. J. V. 2018b. Production, purification, characterization and application of a new halotolerant and thermostable endoglucanase of *Botrytis ricini* URM 5627. *Bioresource Technology*, 270: 263-269.

Sindhu, R., Binod, P., Madhavan, A., Beevi, U. S., Mathew, A. K., Abraham, A., Pandey, A. and Kumar, V. 2017. Molecular improvements in microbial α-amylases for enhanced stability and catalytic efficiency. *Bioresource Technology*, 245: 1740-1748.

Singh, D., Raina, T. K. and Singh, J. 2017. Entomopathogenic fungi: An effective biocontrol agent for management of insect populations naturally. *Journal of Pharmaceutical Sciences and Research*, 9 (6): 830-839.

Singh, D., Son, S. Y. and Lee, C. H. 2016. Perplexing metabolomes in fungal-insect trophic interactions: a *Terra incognita* of mycobiocontrol mechanisms. *Frontiers in Microbiology*, 7: 1678.

Singh, S. and Tiwari, A. J. R. 2021. Performance of *Beauveria bassiana* and *Metarhizium anisopliae* against Pyrilla (*Pyrilla perpusilla*) in sugarcane. *Journal of Pharmacognosy and Phytochemistry*, 10 (1): 1467-1474.

Singh, V., Jawandha, S. and Gill, P. 2020. Effect of exogenous putrescine treatment on internal browning and colour retention of pear fruit. *Journal of Food Measurement and Characterization*, 15: 905–913.

Sinha, S., Chand, S. and Tripathi, P. 2016. Recent progress in chitosanase production of monomer-free chitooligosaccharides: bioprocess strategies and future applications. *Applied Biochemistry and Biotechnology*, 180 (5): 883-899.

Sista Kameshwar, A. K. and Qin, W. 2018. Understanding the structural and functional properties of carbohydrate esterases with a special focus on hemicellulose deacetylating acetyl xylan esterases. *Mycology*, 9 (4): 273-295.

Soares, L., Bonan, C., Biazi, L., Dionísio, S., Bonatelli, M., Andrade, A., Renzano, E., Costa, A. and Ienczak, J. 2020. Investigation of hemicellulosic hydrolysate inhibitor resistance and fermentation strategies to overcome inhibition in non-saccharomyces species. *Biomass and Bioenergy*, 137: 105549.

Somboon, C., Boonrung, S., Katekaew, S., Ekprasert, J., Aimi, T. and Boonlue, S. 2020. Purification and characterization of low molecular weight alkali stable xylanase from *Neosartorya spinosa* UZ-2-11. *Mycoscience*, 61 (3): 128-135.

Sorrivas, V., Genovese, D. and Lozano, J. 2006. Effect of pectinolytic and amylolytic enzymes on apple juice turbidity. *Journal of Food Processing and Preservation*, 30 (2): 118-133.

Souza, L. O., de Brito, A. R., Bonomo, R. C. F., Santana, N. B., Almeida Antunes Ferraz, J. L. D., Aguiar-Oliveira, E., Araújo Fernandes, A. G. D., Ferreira, M. L. O., de Oliveira, J. R. and Franco, M. 2018. Comparison of the biochemical properties between the xylanases of *Thermomyces lanuginosus* and excreted by *Penicillium roqueforti* ATCC 10110 during the solid state fermentation of sugarcane bagasse. *Biocatalysis and Agricultural Biotechnology*, 16: 277-284.

Sparks, M. E., Nelson, D. R., Haber, A. I., Weber, D. C. and Harrison, R. L. 2020. Transcriptome sequencing of the striped cucumber beetle, *Acalymma vittatum* (F.), reveals numerous sex-specific transcripts and xenobiotic detoxification genes. *BioTech*, 9 (4): 21.

Sridevi, A., Sandhya, A., Ramanjaneyulu, G., Narasimha, G. and Devi, P. S. 2016. Biocatalytic activity of *Aspergillus niger* xylanase in paper pulp biobleaching. *3 Biotech*, 6 (2): 165.

Srivastava, A., Murugaiyan, J., Garcia, J. A., De Corte, D., Hoetzinger, M., Eravci, M., Weise, C., Kumar, Y., Roesler, U. and Hahn, M. W. 2020. Combined methylome, transcriptome and proteome analyses document rapid acclimatization of a bacterium to environmental changes. *Frontiers in Microbiology*, 11: 2197.

St. Leger, R. J. and Wang, J. B. 2020. *Metarhizium*: jack of all trades, master of many. *Open Biology*, 10 (12): 200307.

Stark, R., Grzelak, M. and Hadfield, J. 2019. RNA sequencing: the teenage years. *Nature Reviews Genetics*, 20 (11): 631-656.

Staszczak, M. 2008. The role of the ubiquitin-proteasome system in the response of the ligninolytic fungus *Trametes versicolor* to nitrogen deprivation. *Fungal Genetics Biology*, 45 (3): 328-337.

Steiner, E. and Margesin, R. 2020. Production and partial characterization of a crude cold-active cellulase (CMCase) from *Bacillus mycoides* AR20-61 isolated from an Alpine forest site. *Annals of Microbiology*, 70 (1): 1-8.

Stephenie, S., Chang, Y. P., Gnanasekaran, A., Esa, N. M. and Gnanaraj, C. 2020. An insight on superoxide dismutase (SOD) from plants for mammalian health enhancement. *Journal of Functional Foods*, 68: 103917.

Strasser H., Hutwimmer S., Burgstaller W. 2011. Metabolite toxicology of fungal biocontrol agents. In: Ehlers R.U. ed. *Regulation of biological control agents*. Dordrecht : Springer, 191-213.

Sudan, R. and Bajaj, B. K. 2007. Production and biochemical characterization of xylanase from an alkalitolerant novel species *Aspergillus niveus* RS2. *World Journal of Microbiology and Biotechnology*, 23 (4): 491-500.

Sun, J., Wang, W., Ying, Y. and Hao, J. 2020. A novel glucose-tolerant GH1 β-glucosidase and improvement of its glucose tolerance using site-directed mutation. *Applied Biochemistry and Biotechnology*, 192 (3): 999-1015.

Sun, X., Liu, Z., Qu, Y. and Li, X. 2008. The effects of wheat bran composition on the production of biomass-hydrolyzing enzymes by *Penicillium decumbens*. *Applied Biochemistry and Biotechnology*, 146(1-3):119-128.

Sundarram, A. and Murthy, T. P. K. 2014. α-amylase production and applications: a review. *Journal of Applied and Environmental Microbiology*, 2 (4): 166-175.

Suresh, P. V. and Chandrasekaran, M. 1998. Utilization of prawn waste for chitinase production by the marine fungus *Beauveria bassiana* by solid state fermentation. *World Journal of Microbiology and Biotechnology*, 14 (5): 655-660.

Sützl, L., Foley, G., Gillam, E. M., Bodén, M. and Haltrich, D. 2019. The GMC superfamily of oxidoreductases revisited: analysis and evolution of fungal GMC oxidoreductases. *Biotechnology for Biofuels*, 12 (1): 1-18.

Svedese, V. M., Tiago, P. V., Bezerra, J. D. P., Paiva, L. M., Lima, E. Á. D. L. A. and Porto, A. L. F. 2013. Pathogenicity of *Beauveria bassiana* and production of cuticle-degrading enzymes in the presence of *Diatraea saccharalis* cuticle. *African Journal of Biotechnology*, 12 (46): 6491-6497.

Tadakittisarn, S., Haruthaithanasan, V., Chompreeda, P. and Suwonsichon, T. 2007. Optimization of pectinase enzyme liquefaction of banana 'Gros Michel'for banana syrup production. *Agriculture and Natural Resources*, 41 (4): 740-750.

Taghavi, S., Van Der Lelie, D., Hoffman, A., Zhang, Y.B., Walla, M. D., Vangronsveld, J., Newman, L. and Monchy, S. 2010. Genome sequence of the plant growth promoting endophytic bacterium *Enterobacter* sp. 638. *PLoS Genetics*, 6 (5): e1000943.

Tai, W. Y., Tan, J. S., Lim, V. and Lee, C. K. 2019. Comprehensive studies on optimization of cellulase and xylanase production by a local indigenous fungus strain via solid state fermentation using oil palm frond as substrate. *Biotechnology Progress*, 35 (3): e2781.

Tall, S. and Meyling, N. V. 2018. Probiotics for plants? Growth promotion by the entomopathogenic fungus *Beauveria bassiana* depends on nutrient availability. *Microbial Ecology*, 76 (4): 1002-1008.

Tanaka, Y., Konno, N., Suzuki, T. and Habu, N. 2020. Starch-degrading enzymes from the brown-rot fungus *Fomitopsis palustris*. *Protein Expression and Purification*, 170: 105609.

Tang, N., Chen, N., Hu, N., Deng, W., Chen, Z. and Li, Z. 2018. Comparative metabolomics and transcriptomic profiling reveal the mechanism of fruit quality deterioration and the resistance of citrus fruit against *Penicillium digitatum*. *Postharvest Biology and Technology*, 145: 61-73.

Tarrsini, M., Ng, Q., Teoh, Y., Kunasundari, B., Ang, W., Shuit, S., Ooi, Z. and Hoo, P. 2020. Optimization of on-site xylanase production from *Aspergillus niger* via central composite design (CCD*). In: Proceedings* of *IOP Conference Series: Materials Science and Engineering*. IOP Publishing, 012005.

Tartar, A. and Boucias, D. G. 2004. A pilot-scale expressed sequence tag analysis of *Beauveria bassiana* gene expression reveals a tripeptidyl peptidase that is differentially expressed in vivo. *Mycopathologia*, 158 (2): 201-209.

Taylor, M. E. and Drickamer, K. 2011. *Introduction to glycobiology*. 3rd ed. Oxford: Oxford University Press.

Terrone, C. C., de Freitas Nascimento, J. M., Terrasan, C. R. F., Brienzo, M. and Carmona, E. C. 2020a. Salt-tolerant α-arabinofuranosidase from a new specie *Aspergillus hortai* CRM1919: production in acid conditions, purification, characterization and application on xylan hydrolysis. *Biocatalysis and Agricultural Biotechnology*, 23: 101460.

Terrone, C. C., Freitas, C. d., Terrasan, C. R. F., Almeida, A. F. d. and Carmona, E. C. 2018. Agroindustrial biomass for xylanase production by *Penicillium chrysogenum*:

purification, biochemical properties and hydrolysis of hemicelluloses. *Electronic Journal of Biotechnology*, 33: 39-45.

Terrone, C. C., Montesino de Freitas Nascimento, J., Fanchini Terrasan, C. R., Brienzo, M. and Carmona, E. C. 2020b. Salt-tolerant α-arabinofuranosidase from a new specie *Aspergillus hortai* CRM1919: production in acid conditions, purification, characterization and application on xylan hydrolysis. *Biocatalysis and Agricultural Biotechnology*, 23: 101460.

Thadathil, N. and Velappan, S. P. 2014. Recent developments in chitosanase research and its biotechnological applications: a review. *Food Chemistry*, 150: 392-399.

Thakur P., Mukherjee G. 2021. Utilization of agro-waste in pectinase production and its industrial applications. In: Prasad R., Kumar V., Singh J., Upadhyaya C.P. eds. *Recent developments in microbial technologies, environmental and microbial biotechnology*. Springer, Singapore, 145-162.

Theander, O., Åman, P., Westerlund, E., Andersson, R. and Pettersson, D. 1995. Total dietary fiber determined as neutral sugar residues, uronic acid residues, and Klason lignin (the Uppsala method): collaborative study. *Journal of AOAC International*, 78 (4): 1030-1044.

Thite, V. S., Nerurkar, A. S. and Baxi, N. N. 2020. Optimization of concurrent production of xylanolytic and pectinolytic enzymes by *Bacillus safensis* M35 and *Bacillus altitudinis* J208 using agro-industrial biomass through response surface methodology. *Scientific Reports*, 10 (1): 1-12.

Thomas, L., Parameswaran, B. and Pandey, A. 2016. Hydrolysis of pretreated rice straw by an enzyme cocktail comprising acidic xylanase from *Aspergillus* sp. for bioethanol production. *Renewable Energy*, 98: 9-15.

Thomas, L., Ushasree, M. V. and Pandey, A. 2014. An alkali-thermostable xylanase from *Bacillus pumilus* functionally expressed in *Kluyveromyces lactis* and evaluation of its deinking efficiency. *Bioresource Technology*, 165: 309-313.

Tjalsma, H., Bolhuis, A., Jongbloed, J. D., Bron, S. and van Dijl, J. M. 2000. Signal peptide-dependent protein transport in *Bacillus subtilis*: a genome-based survey of the secretome. *Microbiology and Molecular Biology Reviews,* 64 (3): 515-547.

Toghueo, R., Zabalgogeazcoa, I., de Aldana, B. V. and Boyom, F. 2017. Enzymatic activity of endophytic fungi from the medicinal plants *Terminalia catappa*, *Terminalia mantaly* and *Cananga odorata*. *South African Journal of Botany*, 109: 146-153.

Tsai, C.Y., Wang, K.T., Wu, Y.S., Yeh, S.P. and Wu, T.M. 2019. Secretory expression and characterization of xylanase isolated from *Bacillus subtilis* E20 increase the utilization of plant ingredients in tilapia feed. *Aquaculture Research*, 50 (8): 2240-2250.

Tu, E. Y. and Park, A. J. 2007. Recalcitrant *Beauveria bassiana* keratitis: confocal microscopy findings and treatment with posaconazole (Noxafil). *Cornea*, 26 (8): 1008-1010.

Tucker, D., Beresford, C., Sigler, L. and Rogers, K. 2004. Disseminated *Beauveria bassiana* infection in a patient with acute lymphoblastic leukemia. *Journal of Clinical Microbiology*, 42 (11): 5412-5414.

Uçan, F., Ağçam, E. and Akyildiz, A. 2016. Bioactive compounds and quality parameters of natural cloudy lemon juices. *Journal of Food Science and Technology*, 53 (3): 1465-1474.

Uday, U. S. P., Majumdar, R., Tiwari, O. N., Mishra, U., Mondal, A., Bandyopadhyay, T. K. and Bhunia, B. 2017. Isolation, screening and characterization of a novel extracellular xylanase from *Aspergillus niger* (KP874102.1) and its application in orange peel hydrolysis. *International Journal of Biological macromolecules*, 105 (1): 401-409.

Ullah, S., Irfan, M., Sajjad, W., Rana, Q. U. A., Hasan, F., Khan, S., Badshah, M. and Ali Shah, A. 2019. Production of an alkali-stable xylanase from *Bacillus pumilus* K22 and its application in tomato juice clarification. *Food Biotechnology*, 33 (4): 353-372.

Urtz, B. and Rice, W. 2000. Purification and characterization of a novel extracellular protease from *Beauveria bassiana*. *Mycological Research*, 104 (2): 180-186.

Uzuner, S. 2018. Effect of crude pectinase on apple juice quality characteriztics by desirability approach. *GIDA*, 43 (4): 558-568.

Valero-Jimenez, C. A., Faino, L., Spring, D., Smit, S., Zwaan, B. J. and van Kan, J. A. 2016. Comparative genomics of *Beauveria bassiana*: uncovering signatures of virulence against mosquitoes. *BMC Genomics*, 17 (1): 986.

Varland, S., Osberg, C. and Arnesen, T. 2015. N-terminal modifications of cellular proteins: the enzymes involved, their substrate specificities and biological effects. *Proteomics*, 15 (14): 2385-2401.

Vázquez-Montoya, E. L., Castro-Ochoa, L. D., Maldonado-Mendoza, I. E., Luna-Suárez, S. and Castro-Martínez, C. 2020. Moringa straw as cellulase production inducer and cellulolytic fungi source. *Revista Argentina de Microbiología*, 52 (1): 4-12.

Veloz Villavicencio, E., Mali, T., Mattila, H. K. and Lundell, T. 2020. Enzyme activity profiles produced on wood and straw by four fungi of different decay strategies. *Microorganisms*, 8 (1): 73.

Vertyporokh, L., Hułas-Stasiak, M. and Wojda, I. 2020. Host–pathogen interaction after infection of *Galleria mellonella* with the filamentous fungus *Beauveria bassiana*. *Insect Science*, 27 (5): 1079-1089.

Vestergaard S., Cherry A., Keller S., Goettel M. 2003. Safety of hyphomycete fungi as microbial control agents. In: Hokkanen H.M.T., Hajek A.E. eds. *Environmental impacts of microbial insecticides. progress in biological control*. Dordrecht: Springer, 35-62.

Viaud, M., Couteaudier, Y., Levis, C. and Riba, G. 1996. Genome Organization in *Beauveria bassiana*: electrophoretic karyotype, gene mapping, and telomeric fingerprint. *Fungal Genetics and Biology*, 20 (3): 175-183.

Vici, A. C., da Cruz, A. F., Facchini, F. D., de Carvalho, C. C., Pereira, M. G., Fonseca-Maldonado, R., Ward, R. J., Pessela, B. C., Fernandez-Lorente, G. and Torres, F. A. 2015. *Beauveria bassiana* lipase A expressed in *Komagataella* (*Pichia*) *pastoris* with potential for biodiesel catalysis. *Frontiers in Microbiology*, 6: 1083.

Waghmare, P. R., Khandare, R. V., Jeon, B.-H. and Govindwar, S. P. 2018. Enzymatic hydrolysis of biologically pretreated sorghum husk for bioethanol production. *Biofuel Research Journal*, 5 (3): 846-853.

Walker, S. P., Yallapragada, V. V. and Tangney, M. 2020. Arming yourself for the *in silico* protein design revolution. *Trends in Biotechnology*, In Press.

Wang, C., Hu, G. and Leger, R. J. S. 2005. Differential gene expression by *Metarhizium anisopliae* growing in root exudate and host (*Manduca sexta*) cuticle or hemolymph reveals mechanisms of physiological adaptation. *Fungal Genetics and Biology*, 42 (8): 704-718.

Wang, C.Y., Hsieh, Y.R., Ng, C.C., Chan, H., Lin, H.T., Tzeng, W.S. and Shyu, Y.T. 2009. Purification and characterization of a novel halostable cellulase from *Salinivibrio* sp. strain NTU-05. *Enzyme and Microbial Technology*, 44 (6): 373-379.

Wang, Z.L., Ying, S.H. and Feng, M.G. 2010. Gene cloning and catalysis features of a new mannitol-1-phosphate dehydrogenase (BbMPD) from *Beauveria bassiana*. *Carbohydrate Research*, 345 (1): 50-54.

Wang, S., Lin, C., Liu, Y., Shen, Z., Jeyaseelan, J. and Qin, W. 2016. Characterization of a starch-hydrolyzing α-amylase produced by *Aspergillus niger* WLB42 mutated by ethyl methanesulfonate treatment. *International Journal of Biochemistry and Molecular Biology*, 7 (1): 1-10.

Wang, H., Wang, J., Li, L., Hsiang, T., Wang, M., Shang, S. and Yu, Z. 2016a. Metabolic activities of five botryticides against *Botrytis cinerea* examined using the Biolog FF MicroPlate. *Scientific Reports*, 6 (1): 1-11.

Wang, D., Li, L., Wu, G., Vasseur, L., Yang, G. and Huang, P. 2017a. De novo transcriptome sequencing of *Isaria cateniannulata* and comparative analysis of gene expression in response to heat and cold stresses. *PLoS One*, 12 (10): e0186040.

Wang, J.J., Bai, W.W., Zhou, W., Liu, J., Chen, J., Liu, X.Y., Xiang, T.T., Liu, R.H., Wang, W.H. and Zhang, B.L. 2017b. Transcriptomic analysis of two *Beauveria bassiana* strains grown on cuticle extracts of the silkworm uncovers their different metabolic response at early infection stage. *Journal of Invertebrate Pathology*, 145: 45-54.

Wang, J., Li, Y. and Lu, F. 2018. Molecular cloning and biochemical characterization of an α-amylase family from *Aspergillus niger*. *Electronic Journal of Biotechnology*, 32: 55-62.

Wang, H., He, Z., Luo, L., Zhao, X., Lu, Z., Luo, T., Li, M. and Zhang, Y. 2018a. An aldo-keto reductase, Bbakr1, is involved in stress response and detoxification of heavy metal chromium but not required for virulence in the insect fungal pathogen, *Beauveria bassiana. Fungal Genetics and Biology*, 111: 7-15.

Wang, Y., Branicky, R., Noë, A. and Hekimi, S. 2018b. Superoxide dismutases: Dual roles in controlling ROS damage and regulating ROS signaling. *Journal of Cell Biology*, 217 (6): 1915-1928.

Wang, H., Hart, D. J. and An, Y. 2019. Functional metagenomic technologies for the discovery of novel enzymes for biomass degradation and biofuel production. *BioEnergy Research*, 12 (3): 457-470.

Wang, K., Cao, R., Wang, M., Lin, Q., Zhan, R., Xu, H. and Wang, S. 2019a. A novel thermostable GH10 xylanase with activities on a wide variety of cellulosic substrates from a xylanolytic *Bacillus* strain exhibiting significant synergy with commercial Celluclast 1.5 L in pretreated corn stover hydrolysis. *Biotechnology for Biofuels*, 12 (1): 48.

Wang, X., Zeng, J., Gao, W., Chen, K., Wang, B. and Xu, J. 2019b. Endoglucanase recycling for disintegrating cellulosic fibers to fibrils. *Carbohydrate Polymers*, 223: 115052.

Wang, C. and Zhuang, W.Y. 2020. Carbon metabolic profiling of *Trichoderma* strains provides insight into potential ecological niches. *Mycologia*, 112 (2): 213-223.

Wang, S. C., Davejan, P., Hendargo, K. J., Javadi-Razaz, I., Chou, A., Yee, D. C., Ghazi, F., Lam, K. J. K., Conn, A. M. and Madrigal, A. 2020a. Expansion of the Major Facilitator Superfamily (MFS) to include novel transporters as well as transmembrane-acting enzymes. *Biochimica et Biophysica Acta (BBA)-Biomembranes*, 1862 (9): 183277.

Wang, Y.C., Hu, H.F., Ma, J.W., Yan, Q.J., Liu, H.J. and Jiang, Z.Q. 2020b. A novel high maltose-forming α-amylase from *Rhizomucor miehei* and its application in the food industry. *Food Chemistry*, 305: 125447.

Westwood, G. S., Huang, S.-W. and Keyhani, N. O. 2006. Molecular and immunological characterization of allergens from the entomopathogenic fungus *Beauveria bassiana*. *Clinical and Molecular Allergy*, 4 (1): 12.

White, R. J., Collins, J. E., Sealy, I. M., Wali, N., Dooley, C. M., Digby, Z., Stemple, D. L., Murphy, D. N., Billis, K. and Hourlier, T. 2017. A high-resolution mRNA expression time course of embryonic development in zebrafish. *ELIFE*, 6: e30860.

White, T. J., Bruns, T., Lee, S. and Taylor, J. 1990. Amplification and direct sequencing of fungal ribosomal RNA genes for phylogenetics. In: Innis A.M., Gelfand H.D. eds. *PCR protocols: a guide to methods and applications*. Cambridge: Academic Press, 315-322.

Williams, C. J., Headd, J. J., Moriarty, N. W., Prisant, M. G., Videau, L. L., Deis, L. N., Verma, V., Keedy, D. A., Hintze, B. J. and Chen, V. B. 2018. MolProbity: more and better reference data for improved all-atom structure validation. *Protein Science*, 27 (1): 293-315.

Wu, H., Cheng, X., Zhu, Y., Zeng, W., Chen, G. and Liang, Z. 2018a. Purification and characterization of a cellulase-free, thermostable endo-xylanase from *Streptomyces griseorubens* LH-3 and its use in biobleaching on eucalyptus kraft pulp. *Journal of Bioscience and Bioengineering*, 125 (1): 46-51.

Wu, X., Wang, Y., Tong, B., Chen, X. and Chen, J. 2018b. Purification and biochemical characterization of a thermostable and acid-stable alpha-amylase from *Bacillus licheniformis* B4-423. *International Journal of Biological Macromolecules*, 109: 329-337.

Wu, Q., Patocka, J. and Kuca, K. 2019. Beauvericin, a *Fusarium* mycotoxin: anticancer activity, mechanisms, and human exposure risk assessment. *Mini Reviews in Medicinal Chemistry*, 19 (3): 206-214.

Wu, L., Yu, Z., Jia, Q., Zhang, X., Ma, E., Li, S., Zhu, K. Y., Feyereisen, R. and Zhang, J. 2020a. Knockdown of LmCYP303A1 alters cuticular hydrocarbon profiles and increases the susceptibility to desiccation and insecticides in *Locusta migratoria*. *Pesticide Biochemistry and Physiology*, 168: 104637.

Wu, M., Wang, M., Zhang, Y., Zhou, J., Xu, L., Xia, G., Yan, Z., Shen, Y. and Yang, H. 2020b. Efficient and clean preparation of rare prosaikogenin d by enzymatic hydrolysis of saikosaponin b2 and response surface methodology optimization. *Enzyme and Microbial Technology*, 142: 109690.

Xiao, G., Ying, S.-H., Zheng, P., Wang, Z.L., Zhang, S., Xie, X.Q., Shang, Y., St. Leger, R. J., Zhao, G.P., Wang, C. and Feng, M.G. 2012. Genomic perspectives on the evolution of fungal entomopathogenicity in *Beauveria bassiana*. *Scientific Reports*, 2 (1): 483.

Xie, X.Q., Wang, J., Huang, B.-F., Ying, S.-H. and Feng, M.G. 2010. A new manganese superoxide dismutase identified from *Beauveria bassiana* enhances virulence and stress tolerance when overexpressed in the fungal pathogen. *Applied Microbiology and Biotechnology*, 86 (5): 1543-1553.

Xu, M., Lu, Z., Lu, Y.Y., Balusu, R. R., Ajayi, O. S., Fadamiro, H. Y., Appel, A. G. and Chen, L. 2018. Cuticular hydrocarbon chemistry, an important factor shaping the current distribution pattern of the imported fire ants in the USA. *Journal of Insect Physiology*, 110: 34-43.

Xu, Y., Zhan, J., Wijeratne, E. K., Burns, A. M., Gunatilaka, A. L. and Molnár, I. 2007. Cytotoxic and antihaptotactic beauvericin analogues from precursor-directed biosynthesis with the insect pathogen *Beauveria bassiana* ATCC 7159. *Journal of Natural Products*, 70 (9): 1467-1471.

Yadav, A., Ali, A. A. M., Ingawale, M., Raychaudhuri, S., Gantayet, L. and Pandit, A. 2020. Enhanced co-production of pectinase, cellulase and xylanase enzymes from *Bacillus subtilis* ABDR01 upon ultrasonic irradiation. *Process Biochemistry*, 92; 197-201.

Yamada-Okabe, T., Sakamori, Y., Mio, T. and Yamada-Okabe, H. 2001. Identification and characterization of the genes for N-acetylglucosamine kinase and N-acetylglucosamine-phosphate deacetylase in the pathogenic fungus *Candida albicans*. *European Journal of Biochemistry*, 268 (8): 2498-2505.

Yamazaki, H., Rotinsulu, H., Kaneko, T., Murakami, K., Fujiwara, H., Ukai, K. and Namikoshi, M. 2012. A new dibenz [b, e] oxepine derivative, 1-hydroxy-10-methoxy-dibenz [b, e] oxepin-6, 11-dione, from a marine-derived fungus, *Beauveria bassiana* TPU942. *Marine Drugs*, 10 (12): 2691-2697.

Yan, R., Wang, X., Huang, L., Tian, Y. and Cai, W. 2017. Transmembrane region prediction by using sequence-derived features and machine learning methods. *RSC Advances*, 7 (46): 29200-29211.

Yang, M., Yu, X.W., Zheng, H., Sha, C., Zhao, C., Qian, M. and Xu, Y. 2015. Role of N-linked glycosylation in the secretion and enzymatic properties of *Rhizopus chinensis* lipase expressed in *Pichia pastoris*. *Microbial Cell Factories*, 14 (1): 1-14.

Yang, Y.T., Lee, S. J., Nai, Y.S., Kim, S. and Kim, J. S. 2016. Up-regulation of carbon metabolism-related glyoxylate cycle and toxin production in *Beauveria bassiana* JEF-007 during infection of bean bug, *Riptortus pedestris* (Hemiptera: Alydidae). *Fungal Biology*, 120 (10): 1236-1248.

Yang, Y., Zhu, N., Yang, J., Lin, Y., Liu, J., Wang, R., Wang, F. and Yuan, H. 2017. A novel bifunctional acetyl xylan esterase/arabinofuranosidase from *Penicillium chrysogenum* P33 enhances enzymatic hydrolysis of lignocellulose. *Microbial Cell Factories*, 16 (1): 166.

Yang, S. Q., Dai, X. Y., Wei, X. Y., Zhu, Q. and Zhou, T. 2019. Co-immobilization of pectinase and glucoamylase onto sodium aliginate/graphene oxide composite beads and its application in the preparation of pumpkin–hawthorn juice. *Journal of Food Biochemistry*, 43 (3): e12741.

Yang, J.I., Stadler, M., Chuang, W.Y., Wu, S. and Ariyawansa, H. A. 2020. *In vitro* inferred interactions of selected entomopathogenic fungi from Taiwan and eggs of *Meloidogyne graminicola*. *Mycological Progress*, 19 (1): 97-109.

Yazici, S. O., Sahin, S., Biyik, H. H., Geroglu, Y. and Ozmen, I. 2020. Optimization of fermentation parameters for high-activity inulinase production and purification from *Rhizopus oryzae* by Plackett–Burman and Box–Behnken. *Journal of Food Science and Technology*, 58: 739–751.

Yildiz, S., Pokhrel, P. R., Unluturk, S. and Barbosa-Cánovas, G. V. 2021. Shelf life extension of strawberry juice by equivalent ultrasound, high pressure, and pulsed electric fields processes. *Food Research International*, 140: 110040.

Yin, Y.R., Li, T., Sang, P., Yang, R.F., Liu, H.Y., Xiao, M., Li, S., Yang, L.Q. and Li, W.J. 2020. Characterization of an alkali-tolerant, thermostable, and multifunctional GH5 family endoglucanase from *Thermoactinospora rubra* YIM 77501 T for prebiotic production. *Biomass Conversion and Biorefinery*: 1-10.

Yolmeh, M. and Jafari, S. M. 2017. Applications of response surface methodology in the food industry processes. *Food and Bioprocess Technology*, 10 (3): 413-433.

Younus, H. 2018. Therapeutic potentials of superoxide dismutase. *International Journal of Health Sciences*, 12 (3): 88.

Youssef, M. M., El-Nagdi, W. M. and Lotfy, D. E. 2020. Evaluation of the fungal activity of *Beauveria bassiana, Metarhizium anisopliae* and *Paecilomyces lilacinus* as biocontrol agents against root-knot nematode, *Meloidogyne incognita* on cowpea. *Bulletin of the National Research Centre*, 44 (1): 1-11.

Yu, C. S., Chen, Y. C., Lu, C. H. and Hwang, J. K. 2006. Prediction of protein subcellular localization. *Proteins: Structure, Function, and Bioinformatics*, 64 (3): 643-651.

Yuan, Z., Li, G. and Hegg, E. L. 2018. Enhancement of sugar recovery and ethanol production from wheat straw through alkaline pre-extraction followed by steam pretreatment. *Bioresource Technology*, 266: 194-202.

Zeng, J., Yang, N., Li, X.M., Shami, P. J. and Zhan, J. 2010. 4′-O-methylglycosylation of curcumin by *Beauveria bassiana*. *Natural Product Communications*, 5 (1): 1934578X1000500119.

Zeng, Y., Xu, J., Fu, X., Tan, M., Liu, F., Zheng, H. and Song, H. 2019. Effects of different carbohydrate-binding modules on the enzymatic properties of pullulanase. *International Journal of Biological Macromolecules*, 137: 973-981.

Zhang, J., Cai, J., Wu, K., Jin, S., Pan, R. and Fan, M. 2004. Production and properties of chitinase from *Beauveria bassiana* Bb174 in solid state fermentation. *The Journal of Applied Ecology*, 15 (5): 863-866.

Zhang, J., Fu, B., Lin, Q., Riley, I. T., Ding, S., Chen, L., Cui, J., Yang, L. and Li, H. 2020. Colonization of *Beauveria bassiana* 08F04 in root-zone soil and its biocontrol of cereal cyst nematode (*Heterodera filipjevi*). *PLoS One*, 15 (5): e0232770.

Zhang, S., Widemann, E., Bernard, G., Lesot, A., Pinot, F., Pedrini, N. and Keyhani, N. O. 2012. CYP52X1, representing new cytochrome P450 subfamily, displays fatty acid hydroxylase activity and contributes to virulence and growth on insect cuticular substrates in entomopathogenic fungus *Beauveria bassiana*. *Journal of Biological Chemistry*, 287 (16): 13477-13486.

Zhang, X., Lei, Z., Reitz, S. R., Wu, S. and Gao, Y. 2019a. Laboratory and greenhouse evaluation of a granular formulation of *Beauveria bassiana* for control of western flower thrips, *Frankliniella occidentalis*. *Insects*, 10 (2): 58.

Zhang, Z., Lu, Y., Xu, W., Du, Q., Sui, L., Zhao, Y. and Li, Q. 2019b. RNA sequencing analysis of *Beauveria bassiana* isolated from *Ostrinia furnacalis* identifies the pathogenic genes. *Microbial Pathogenesis*, 130: 190-195.

Zhao, D., Liu, B., Wang, Y., Zhu, X., Duan, Y. and Chen, L. 2013. Screening for nematicidal activities of *Beauveria bassiana* and associated fungus using culture filtrate. *African Journal of Microbiology Research*, 7 (11): 974-978.

Zhen, W., Du, L.X., Cao, W.P., Wang, R.Y., Song, J., Wang, J.Y. And Feng, S.L. 2010. Cloning and analysis of a chitinase gene from *Beauveia bassiana* HFW-05. *Acta Agriculturae Boreali-Sinica*, 25 (1) : 3 6-39.

Zheng, F., Song, L., Basit, A., Liu, J., Miao, T., Wen, J., Cao, Y. and Jiang, W. 2020. An endoxylanase rapidly hydrolyzes xylan into major product xylobiose via transglycosylation of xylose to xylotriose or xylotetraose. *Carbohydrate Polymers*: 116121.

Zheng, H.C., Sun, M.Z., Meng, L.C., Pei, H.S., Zhang, X.Q., Yan, Z., Zeng, W.H., Zhang, J.S., Hu, J.R. And Lu, F.P. 2014. Purification and characterization of a thermostable xylanase from *Paenibacillus* sp. NF1 and its application in xylooligosaccharides production. *Journal of Microbiology and Biotechnology*, 24 (4): 489-496.

Zhou, J., Li, X., Huang, P.W. and Dai, C.C. 2018. Endophytism or saprophytism: decoding the lifestyle transition of the generalist fungus *Phomopsis liquidambari*. *Microbiological Research*, 206: 99-112.

Zhou, J., Li, Z., Wu, J., Li, L., Li, D., Ye, X., Luo, X., Huang, Y., Cui, Z. and Cao, H. 2017. Functional analysis of a novel β-(1,3)-Glucanase from *Corallococcus* sp. strain EGB containing a fascin-like module. *Applied and Environmental Microbiology*, 83 (16): e01016-01017.

Zhou, J., Liu, X., Yuan, F., Deng, B. and Yu, X. 2020. Biocatalysis of heterogenously-expressed chitosanase for the preparation of desirable chitosan oligosaccharides applied against phytopathogenic fungi. *ACS Sustainable Chemistry and Engineering*, 8 (12): 4781-4791.

Zhou, Q., Shao, Y., Chen, A., Li, W., Wang, J. and Wang, Y. 2019. In vivo transcriptomic analysis of *Beauveria bassiana* reveals differences in infection strategies in *Galleria mellonella* and *Plutella xylostella*. *Pest Management Science*, 75 (5): 1443-1452.

Zhu, T., Li, R., Sun, J., Cui, Y. and Wu, B. 2020. Characterization and efficient production of a thermostable, halostable and organic solvent-stable cellulase from an oil reservoir. *International Journal of Biological Macromolecules*, 159: 622-629.

Zhuo, R., Yu, H., Qin, X., Ni, H., Jiang, Z., Ma, F. and Zhang, X. 2018. Heterologous expression and characterization of a xylanase and xylosidase from white rot fungi and their application in synergistic hydrolysis of lignocellulose. *Chemosphere*, 212: 24-33.

Zi, J., Gladstone, S. G. and Zhan, J. 2012. Specific 5-hydroxylation of piperlongumine by *Beauveria bassiana* ATCC 7159. *Bioscience, Biotechnology, and Biochemistry*, 76 (8): 1565-1567.

Zibaee, A. and Bandani, A. R. 2009. Purification and characterization of the cuticle-degrading protease produced by the entomopathogenic fungus, *Beauveria bassiana* in the presence of Sunn pest, *Eurygaster integriceps* (Hemiptera: Scutelleridae) cuticle. *Biocontrol Science and Technology*, 19 (8): 797-808.

Zibaee, A. and Ramzi, S. 2018. Cuticle-degrading proteases of entomopathogenic fungi: from biochemistry to biological performance. *Archives of Phytopathology and Plant Protection*, 51 (13-14): 779-794.

Zibaee, A., Sadeghi-Sefidmazgi, A. and Fazeli-Dinan, M. 2011. Properties of a lipase produced by *Beauveria bassiana*: purification and biochemical studies. *Biocontrol Science and Technology*, 21 (3): 317-331.

Zimmermann, G. 2007. Review on safety of the entomopathogenic fungi *Beauveria bassiana* and *Beauveria brongniartii*. *Biocontrol Science and Technology*, 17 (6): 553-596.

APPENDICES

Appendix 1

NCBI accession numbers for ITS gene sequence used in this study

Fungal strain	NCBI Accession no
Akanthomyces muscarius IMI 068689	NR_111096.1
Akanthomyces waltergamsii TBRC 7252	NR_164417.1
Beauveria amorpha ARSEF 2641	NR_111601.1
Beauveria asiatica ARSEF 4850	NR_111596.1
Beauveria australis ARSEF 4598	NR_111597.1
Beauveria brongniartii ARSEF 617	NR_111595.1
Beauveria bassiana ARSEF 1564	NR_111594.1
B. bassiana SBI-Bb01	MT584878.1
B. bassiana SF_661	MT529937.1
B. bassiana SBI-Bb02	MT584882.1
B. bassiana SF_676	MT529952.1
B. bassiana SF_807	MT530083.1
B. bassiana SF_684	MT529960.1
Beauveria caledonica BCRC 32867	NR_077147.1
Beauveria kipukae ARSEF 7032	NR_111600.1
Beauveria lii ARSEF 11741	NR_111678.1
Beauveria malawiensis IMI 228343	NR_136979.1

Beauveria majiangensis GZAC GZU1214	NR_158356.1
Beauveria pseudobassiana ARSEF 3405	NR_111598.1
Beauveria sungii ARSEF 1685	NR_111602.1
Beauveria varroae ARSEF 8257	NR_111599.1
Beauveria vermiconia ARSEF 2922	NR_151832.1
Blackwellomyces cardinalis	NR_159788.1
Cordyceps cateniannulata CBS 152.83	NR_111169.1
Cordyceps javanica CBS 134.22	NR_111172.1
Cordyceps ningxiaensis HMJAU 25074	NR_137117.1
Gibellula shennongjiaensis GZAC SNJ2012	NR_158478.1
Lecanicillium araneicola NBRC 105407	NR_121208.1
Lecanicillium fungicola CBS 992.69	NR_119653.1
Lecanicillium kalimantanense BTCC F23	NR_121200.1
Lecanicillium longisporum IMI 021167	NR_111095.1
Lecanicillium saksenae IMI 179841	NR_111102.1
Samsoniella hepiali CGMCC 3.17103	NR_160318.1
Samsoniella inthanonensis TBRC 7915	NR_164420.1

A1 Water	A2 Tween 80	A3 N-Acetyl-D-Galactosamine	A4 N-Acetyl-D-Glucosamine	A5 N-Acetyl-D-Mannosamine	A6 Adonitol	A7 Amygdalin	A8 D-Arabinose	A9 L-Arabinose	A10 D-Arabitol	A11 Arbutin	A12 D-Cellobiose
B1 α-Cyclodextrin	B2 β-Cyclodextrin	B3 Dextrin	B4 i-Erythritol	B5 D-Fructose	B6 L-Fucose	B7 D-Galactose	B8 D-Galacturonic Acid	B9 Gentiobiose	B10 D-Gluconic Acid	B11 D-Glucosamine	B12 α-D-Glucose
C1 Glucose-1-Phosphate	C2 Glucuronamide	C3 D-Glucuronic Acid	C4 Glycerol	C5 Glycogen	C6 m-Inositol	C7 2-Keto-D-Gluconic Acid	C8 α-D-Lactose	C9 Lactulose	C10 Maltitol	C11 Maltose	C12 Maltotriose
D1 D-Mannitol	D2 D-Mannose	D3 D-Melezitose	D4 D-Melibiose	D5 α-Methyl-D-Galactoside	D6 β-Methyl-D-Galactoside	D7 α-Methyl-D-Glucoside	D8 β-Methyl-D-Glucoside	D9 Palatinose	D10 D-Psicose	D11 D-Raffinose	D12 L-Rhamnose
E1 D-Ribose	E2 Salicin	E3 Sedoheptulosan	E4 D-Sorbitol	E5 L-Sorbose	E6 Stachyose	E7 Sucrose	E8 D-Tagatose	E9 D-Trehalose	E10 Turanose	E11 Xylitol	E12 D-Xylose
F1 γ-Amino-butyric Acid	F2 Bromosuccinic Acid	F3 Fumaric Acid	F4 β-Hydroxy-butyric Acid	F5 γ-Hydroxy-butyric Acid	F6 p-Hydroxyphenyl-acetic Acid	F7 α-Keto-glutaric Acid	F8 D-Lactic Acid Methyl Ester	F9 L-Lactic Acid	F10 D-Malic Acid	F11 L-Malic Acid	F12 Quinic Acid
G1 D-Saccharic Acid	G2 Sebacic Acid	G3 Succinamic Acid	G4 Succinic Acid	G5 Succinic Acid Mono-Methyl Ester	G6 N-Acetly-L-Glutamic Acid	G7 Alaninamide	G8 L-Alanine	G9 L-Alanyl-Glycine	G10 L-Asparagine	G11 L-Aspartic Acid	G12 L-Glutamic Acid
H1 Glycyl-L-Glutamic Acid	H2 L-Ornithine	H3 L-Phenylalanine	H4 L-Proline	H5 L-Pyroglutamic Acid	H6 L-Serine	H7 L-Threonine	H8 2-Amino Ethanol	H9 Putrescine	H10 Adenosine	H11 Uridine	H12 Adenosine-5'-Monophosphate

Appendix 2

Distribution of utilizable carbon sources in the Biolog FF MicroPlate used in this study.

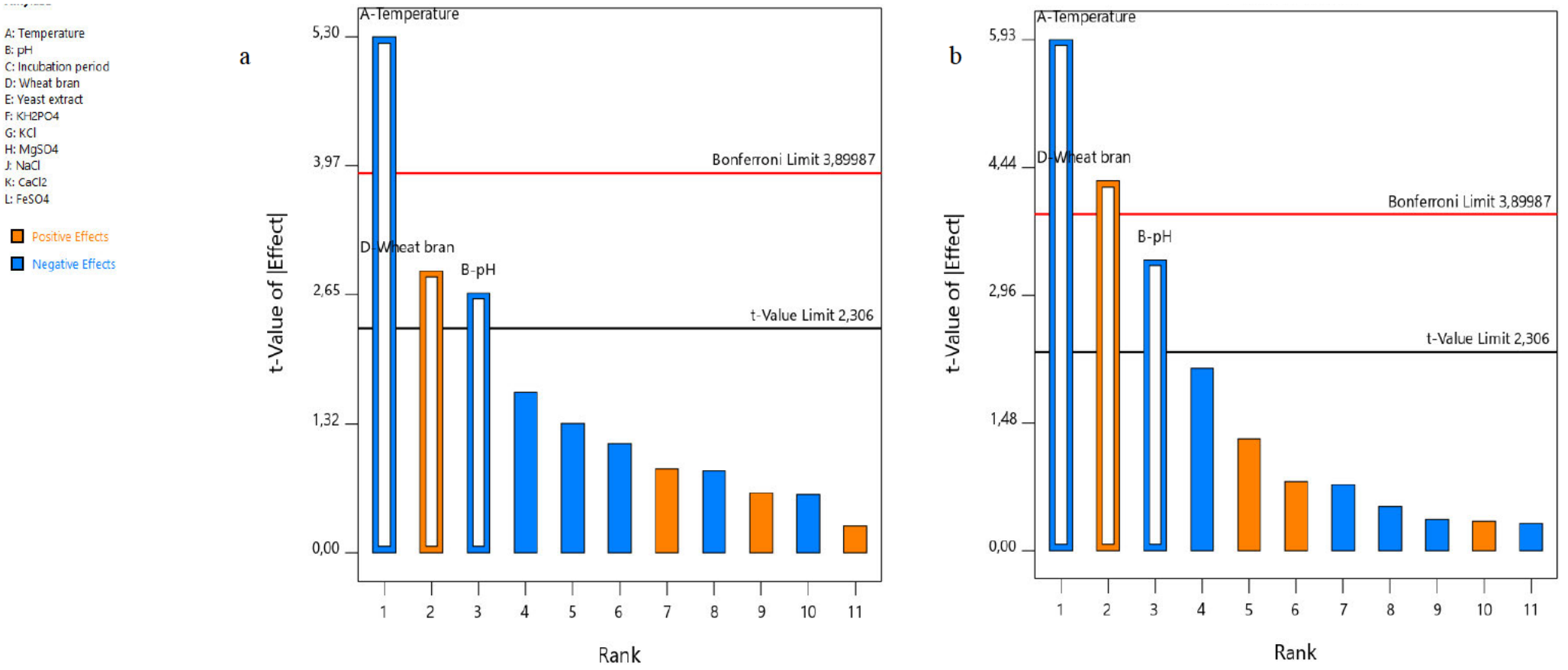

Appendix 3

Pareto chart identifying significant parameters through Plackett–Burman design (a) amylase (b) polygalacturonase

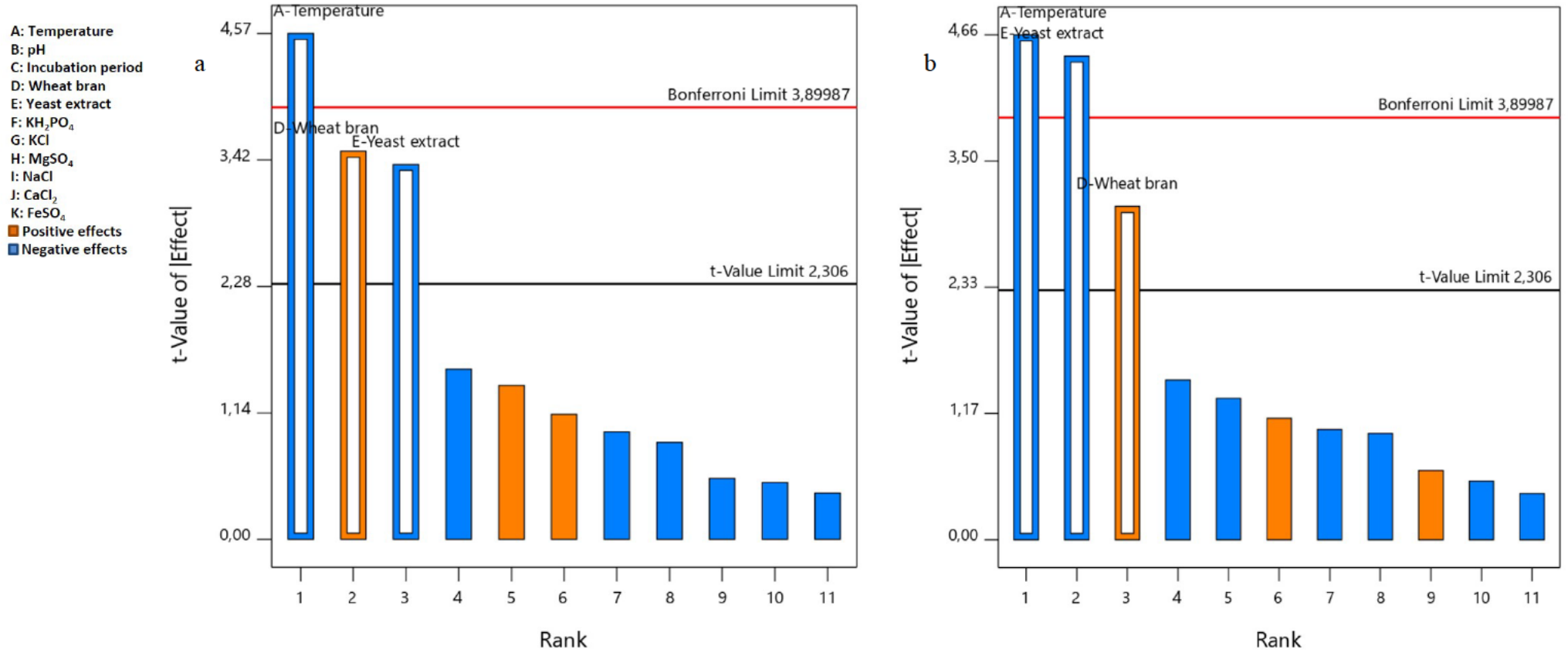

Appendix 4

Pareto chart identifying significant parameters through Plackett–Burman design (a) endoglucanase (b) xylanase

Appendix 5a

ANOVA for factorial models for *B. bassiana* SAN01 amylase and polygalacturonase production

	Amylase					Polygalacturonase				
	Sum of Squares	**df**	**Mean Square**	**F-value**	**p-value**	**Sum of Squares**	**df**	**Mean Square**	**F-value**	**p-value**
Model	387.22	3	129.07	14.52	0.0013	315.44	3	105.15	21.63	0.0003
Temperature	249.52	1	249.52	28.08	0.0007	170.71	1	170.71	35.11	0.0004
pH	63.3	1	63.3	7.12	0.0284	55.3	1	55.3	11.37	0.0097
Wheat bran	74.4	1	74.4	8.37	0.0201	89.43	1	89.43	18.4	0.0027
Residual	71.09	8	8.89			38.89	8	4.86		
Cor Total	458.31	11				354.33	11			

degree of freedom *Significant p- values at $P \leq 0.1$

Appendix 5b

ANOVA for factorial models for *B. bassiana* SAN01 xylanase and endoglucanase production

	Xylanase					Endoglucanase				
	Sum of Squares	**df**	**Mean Square**	**F-value**	**p-value**	**Sum of Squares**	**df**	**Mean Square**	**F-value**	**p-value**
Model	55970.49	3	18656.83	17.05	0.0008*	42.58	3	14.19	14.85	0.0012*
Temperature	23787.04	1	23787.04	21.74	0.0016*	19.92	1	19.92	20.84	0.0018*
pH	10361.15	1	10361.15	9.47	0.0152*	11.72	1	11.72	12.27	0.0081*
Wheat bran	21822.3	1	21822.3	19.94	0.0021*	10.94	1	10.94	11.45	0.0096*
Residual	8753.59	8	1094.2			7.65	8	0.9557		
Cor Total	64724.08	11				50.23	11			

degree of freedom *Significant p- values at $P \leq 0.1$

Appendix 6a
Coefficient estimates for amylase and polygalacturonase PBD models

	Amylase		Polygalacturonase	
Factor	**Coefficient Estimate**	**Standard Error**	**Coefficient Estimate**	**Standard Error**
Intercept	17.76	0.8605	24.87	0.6365
A-Temperature	-4.56	0.8605	-3.77	0.6365
B-pH	-2.3	0.8605	-2.15	0.6365
D-Wheat bran	2.49	0.8605	2.73	0.6365

Appendix 6b
Coefficient estimates for endoglucanase and xylanase PBD models

	Endoglucanase		Xylanase	
Factor	**Coefficient Estimate**	**Standard Error**	**Coefficient Estimate**	**Standard Error**
Intercept	10.33	0.2822	109.57	9.55
A-Temperature	-1.29	0.2822	-44.52	9.55
D-Wheat bran	0.9883	0.2822	29.38	9.55
E-Yeast extract	-0.955	0.2822	-42.64	9.55

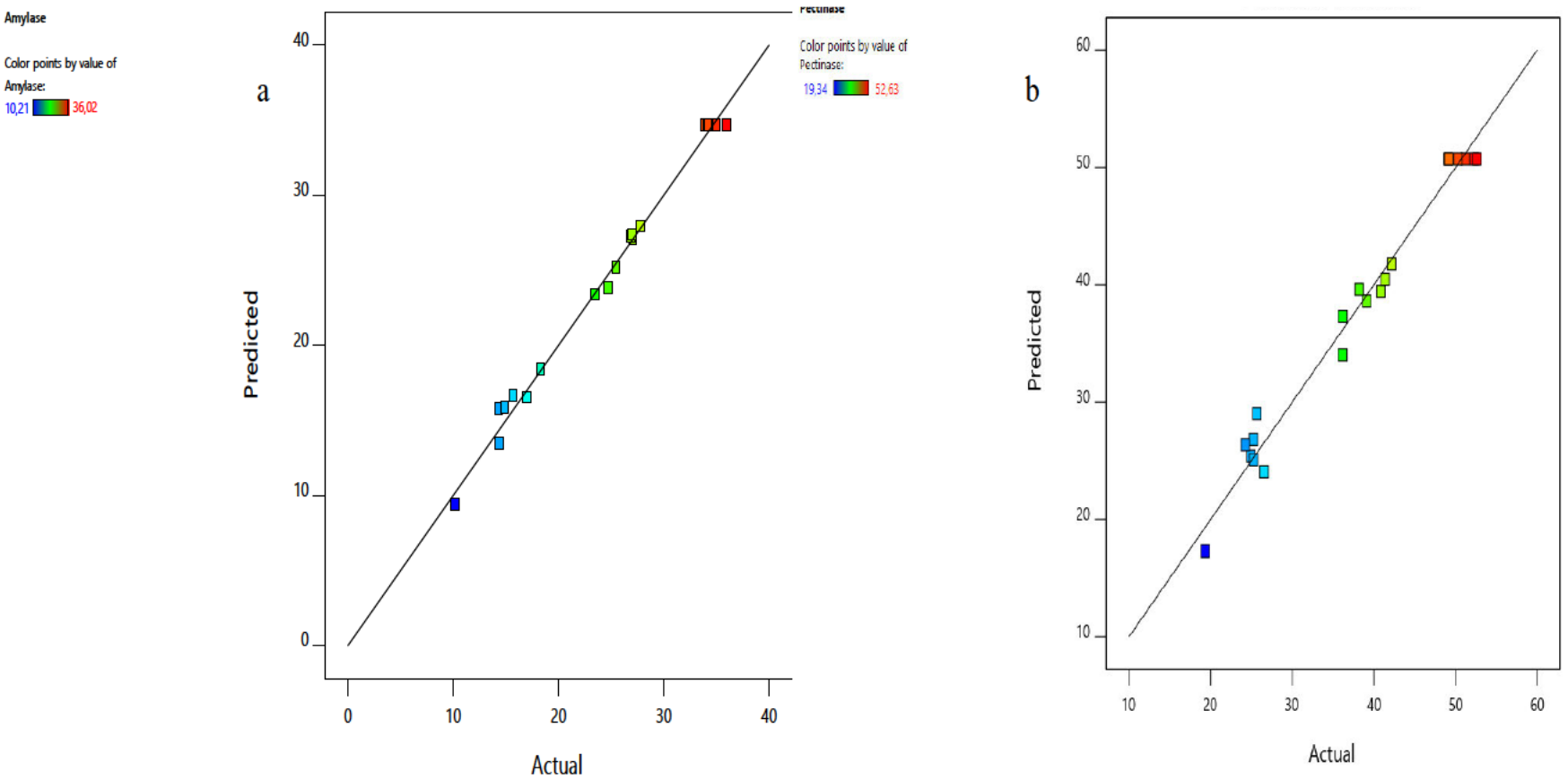

Appendix 7

Predicted vs actual plot of *B. bassiana* SAN01 enzyme production outputs (a) amylase (b) polygalacturonase

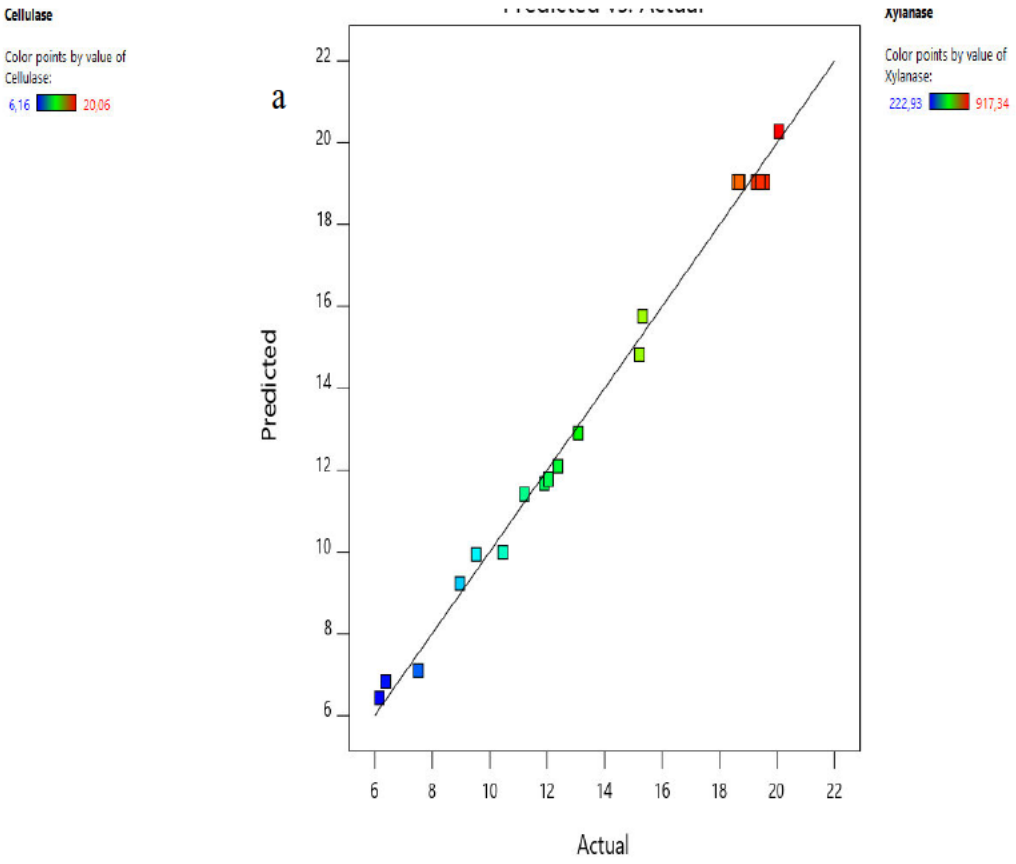

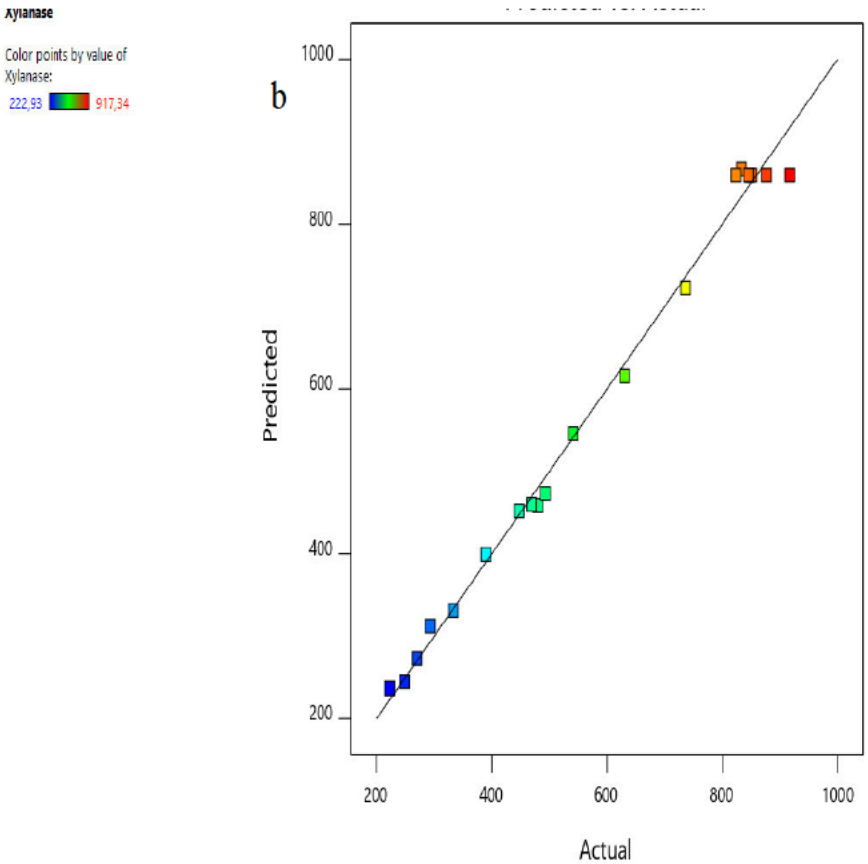

Appendix 8

Predicted vs actual plot of *B. bassiana* SAN01 enzyme production outputs (a) endoglucanase (b) xylanase

Appendix 9a

Coefficient estimate for the amylase production CCD model

Factor	Coefficient Estimate	df	Standard Error	95% CI Low	95% CI High	VIF
Intercept	34.67	1	0.4044	33.77	35.57	
A-Temperature	2.26	1	0.2683	1.66	2.86	1.0000
B-pH	3.40	1	0.2683	2.80	3.99	1.0000
C-Wheat bran	3.18	1	0.2683	2.59	3.78	1.0000
AB	-3.14	1	0.3505	-3.92	-2.36	1.0000
AC	1.83	1	0.3505	1.05	2.61	1.0000
BC	-0.6837	1	0.3505	-1.46	0.0973	1.0000
A^2	-5.34	1	0.2612	-5.92	-4.76	1.02
B^2	-4.64	1	0.2612	-5.22	-4.06	1.02
C^2	-4.48	1	0.2612	-5.06	-3.90	1.02

Appendix 9b

Coefficient estimate for the polygalacturonase production CCD model

Factor	Coefficient Estimate	df	Standard Error	95% CI Low	95% CI High	VIF
Intercept	50.73	1	0.9256	48.66	52.79	
A-Temperature	1.49	1	0.6141	0.1183	2.85	1.0000
B-pH	4.19	1	0.6141	2.82	5.56	1.0000
C-Wheat bran	4.30	1	0.6141	2.94	5.67	1.0000
AB	-4.96	1	0.8023	-6.75	-3.18	1.0000
AC	2.40	1	0.8023	0.6148	4.19	1.0000
BC	-1.48	1	0.8023	-3.27	0.3102	1.0000
A^2	-6.78	1	0.5978	-8.11	-5.45	1.02
B^2	-6.11	1	0.5978	-7.44	-4.78	1.02
C^2	-6.49	1	0.5978	-7.82	-5.16	1.02

Appendix 9c

Coefficient estimate for the endoglucanase production CCD model

Factor	Coefficient Estimate	df	Standard Error	95% CI Low	95% CI High	VIF
Intercept	19.05	1	0.2028	18.60	19.50	
A-Temperature	-0.8517	1	0.1345	-1.15	-0.5519	1.0000
B-Wheat bran	0.9418	1	0.1345	0.6420	1.24	1.0000
C-Yeast extract	-2.53	1	0.1345	-2.83	-2.23	1.0000
AB	-0.5400	1	0.1758	-0.9317	-0.1483	1.0000
AC	0.6525	1	0.1758	0.2608	1.04	1.0000
BC	1.02	1	0.1758	0.6258	1.41	1.0000
A^2	-2.97	1	0.1310	-3.26	-2.68	1.02
B^2	-3.76	1	0.1310	-4.05	-3.47	1.02
C^2	-1.07	1	0.1310	-1.36	-0.7737	1.02

Appendix 9d

Coefficient estimate for the xylanase production CCD model

Factor	Coefficient Estimate	df	Standard Error	95% CI Low	95% CI High	VIF
Intercept	859.56	1	11.92	832.99	886.12	
A-Temperature	-69.33	1	7.91	-86.96	-51.70	1.0000
B-Wheat bran	48.40	1	7.91	30.77	66.03	1.0000
C-Yeast extract	-120.96	1	7.91	-138.58	-103.33	1.0000
AB	-23.08	1	10.34	-46.10	-0.0454	1.0000
AC	32.28	1	10.34	9.25	55.31	1.0000
BC	17.93	1	10.34	-5.10	40.96	1.0000
A^2	-152.12	1	7.70	-169.27	-134.96	1.02
B^2	-191.33	1	7.70	-208.49	-174.17	1.02
C^2	-69.44	1	7.70	-86.60	-52.29	1.02

Appendix 10

ANOVA of quadratic models for pear juice clarification

Source	Sum of Squares	df	Mean Square	F-value	p-value*
Model	4926.40	6	821.07	41.06	< 0.0001
A	1220.67	1	1220.67	61.05	< 0.0001
B	275.42	1	275.42	13.77	0.0059
C	551.45	1	551.45	27.58	0.0008
AB	85.41	1	85.41	4.27	0.0726
AC	1250.65	1	1250.65	62.54	< 0.0001
BC	0.7909	1	0.7909	0.0396	0.8473
A^2	159.97	8	20.00		
B^2	121.15	4	30.29	3.12	0.1481
C^2	4926.40	6	821.07	41.06	< 0.0001
Residual	1220.67	1	1220.67	61.05	< 0.0001
Lack of Fit	275.42	1	275.42	13.77	0.0059

R^2 = 0.9685, Adjusted R^2 = 0.945, Predicted R^2 = 0.9061, Adequate precision AP= 23.291
*Significant p- values at P ≤ 0.1

Appendix 11

ANOVA of quadratic models for xylanase-assisted printed paper deinking

Source	Sum of Squares	df	Mean Square	F-value	p-value
Model	4823.68	9	535.96	123.02	< 0.0001
A-Incubation temperature	32.16	1	32.16	7.38	0.0419
B-Time	381.43	1	381.43	87.55	0.0002
C-Enzyme load	1299.99	1	1299.99	298.39	< 0.0001
AB	0.1376	1	0.1376	0.0316	0.8659
AC	121.99	1	121.99	28.00	0.0032
BC	144.69	1	144.69	33.21	0.0022
A^2	285.84	1	285.84	65.61	0.0005
B^2	129.81	1	129.81	29.80	0.0028
C^2	1,86	1	1.86	0.4258	0.5429
Residual	21.78	5	4.36		
Lack of Fit	0.2758	1	0.2758	0.0513	0.8319

R^2 = 0.9955, Adjusted R^2 = 0.9874, Predicted R^2 = 0.9872, Adequate precision AP= 42.089. df; degree of freedom. *Significant p- values at P ≤ 0.1

Appendix 12

UniProt entry numbers and NCBI accession numbers of *B. bassiana* chitinases and xylanase amino acid sequence used in this study

S/N	Strain	UniProt Entry No	NCBI Accession no
Chitinase			
1	*B. bassiana* ARSEF 2860	A0A2N6NDL2	AIT18882.1
2	*B. bassiana* ARSEF 2860	A0A097F8M1	AIT18885.1
3	*B. bassiana* ARSEF 2860	A0A097F8I5	AIT18879.1
4	*B. bassiana* ARSEF 2860	A0A097F8I9	\AIT18873.1
5	*B. bassiana* ARSEF 2860	A0A097F8L2	AIT18872.1
6	*B. bassiana* ARSEF 2860	J4UK12	EJP64367.1
7	*B. bassiana* ARSEF 2860	J4UI73	EJP63137.1
8	*B. bassiana* ARSEF 2860	A0A097F8J9	AIT18883.1
9	*B. bassiana* ARSEF 2860	A0A097F8H5	AIT18869.1
10	*B. bassiana* D1-5	A0A0A2VZR1	KGQ11645.1
11	*B. bassiana* D1-5	A0A0A2VHD9	KGQ07286.1
12	*B. bassiana* D1-5	A0A0A2VUZ7	KGQ10005.1
13	*B. bassiana* JEF-007	A0A2N6NEI6	PMB65707.1
14	*B. bassiana* JEF-007	A0A2N6N925	PMB63785.1
15	*B. bassiana* JEF-007	A0A2N6NDL2	PMB65373.1
Xylanase			
1	*B. bassiana* D1-5	A0A0A2W4W0	KGQ08014.1

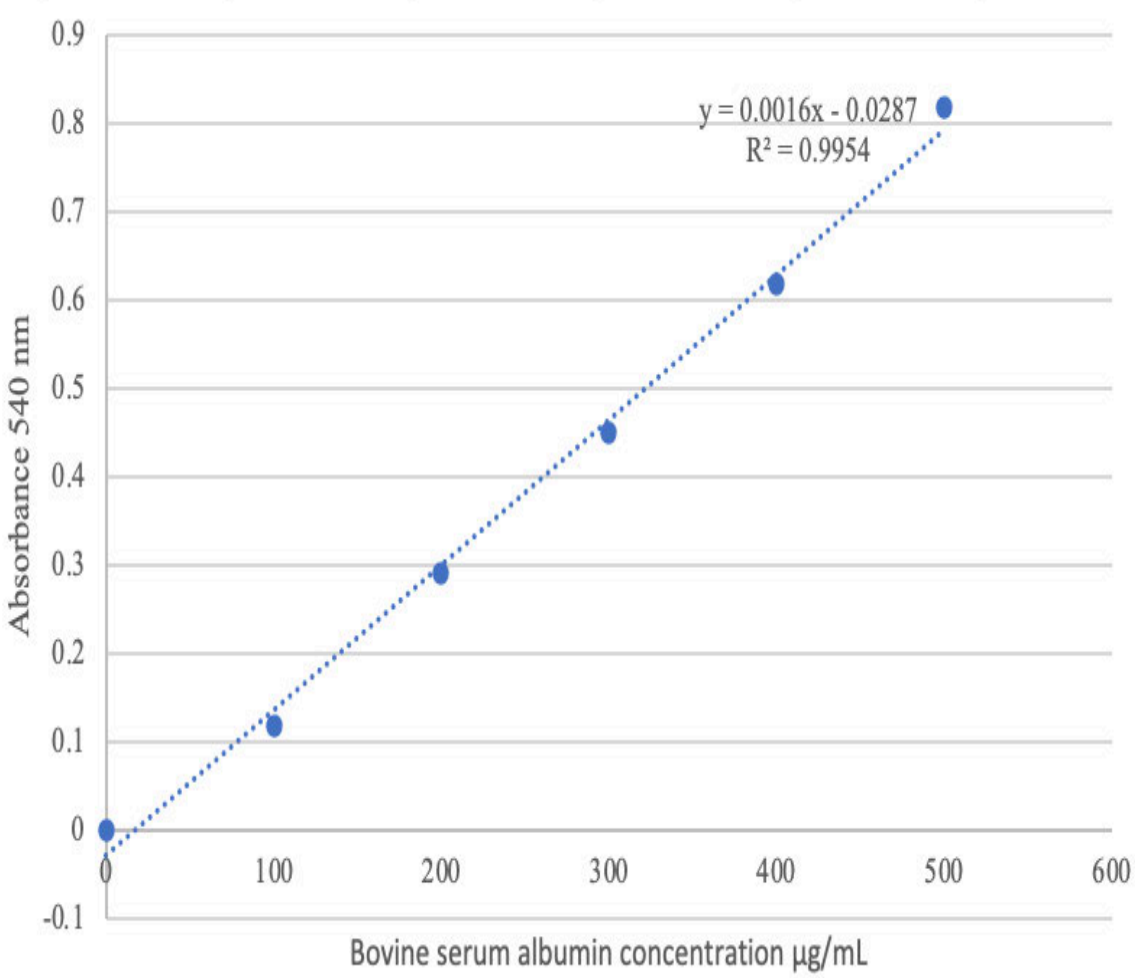

Appendix 13

Bovine serum albumin standard curve for Protein estimation (Lowry-Hartree method)

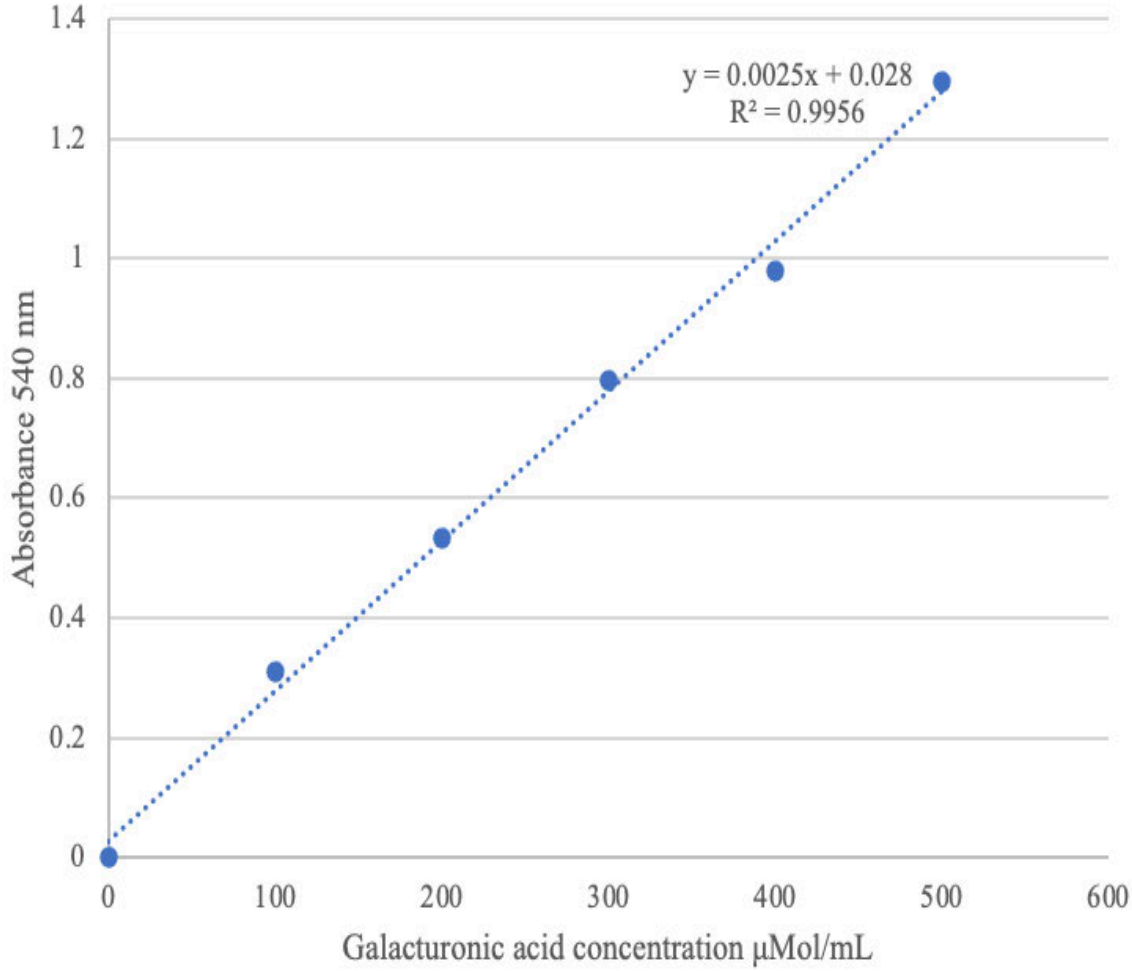

Appendix 14

Galacturonic acid standard for Polygalacturonase enzyme activity (DNS method)

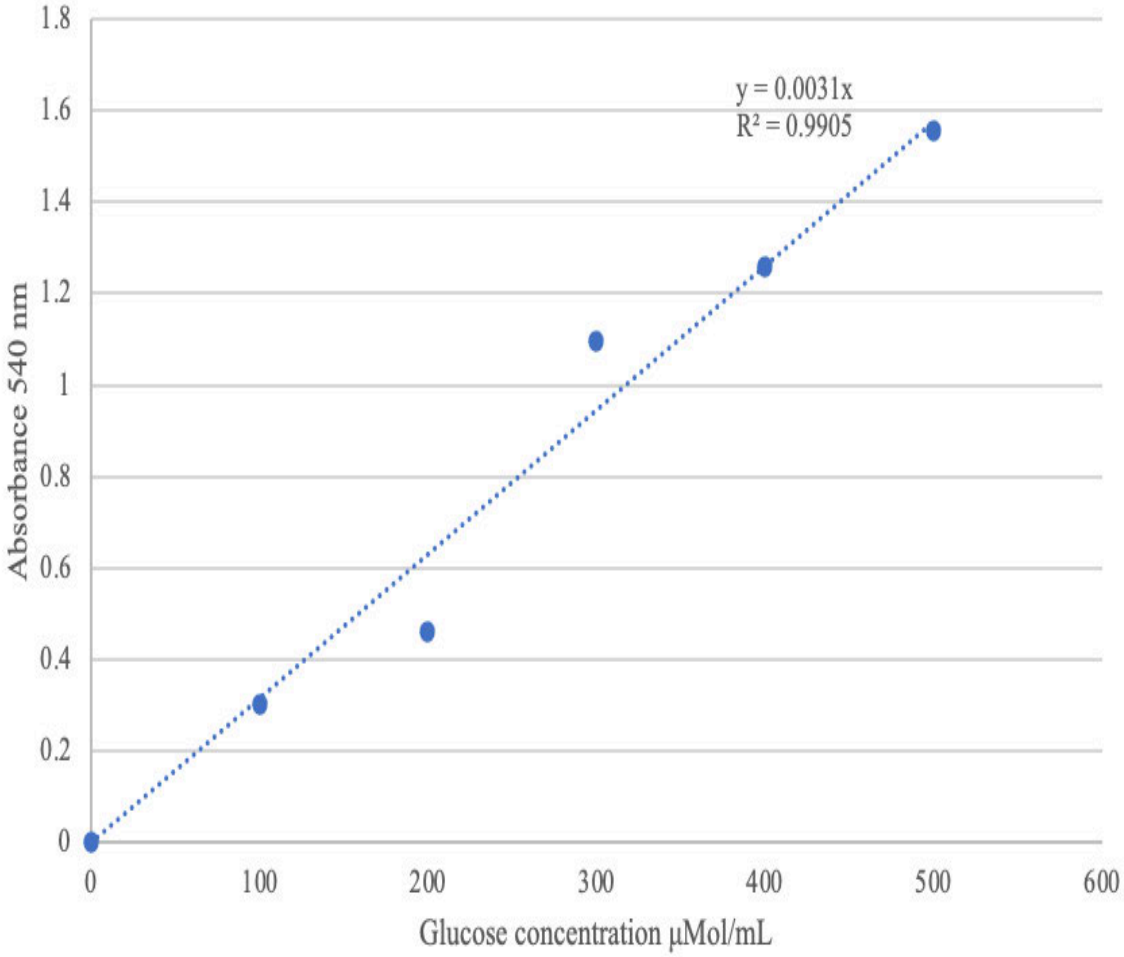

Appendix 15

Glucose standard for Amylase and Endoglucanase enzymes activity (DNS method)

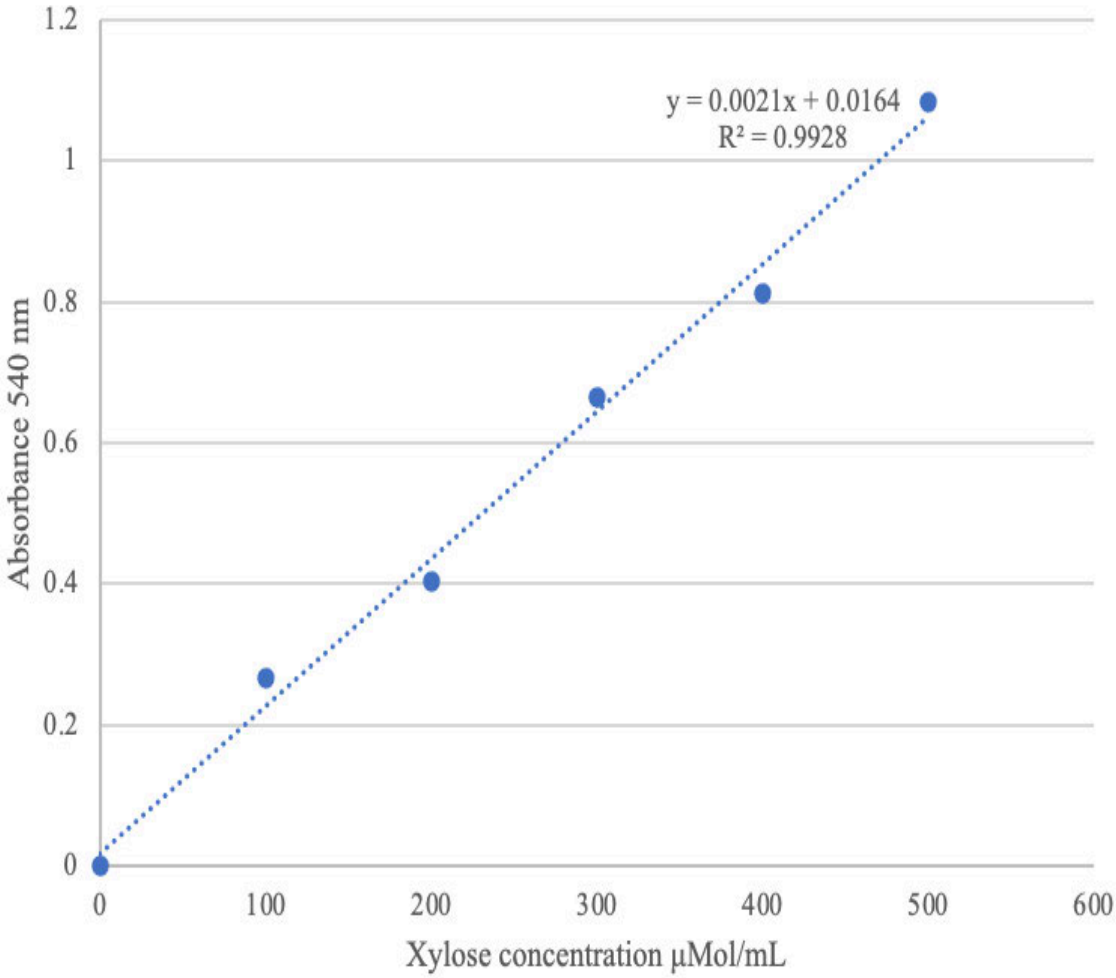

Appendix 16

Xylose standard for Xylanase and Endoglucanase enzymes activity (DNS method)